

PB98145451



# The Loma Prieta, California, Earthquake of October 17, 1989—Landslides

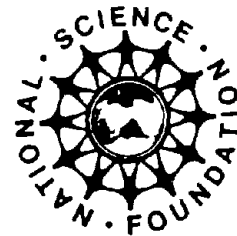
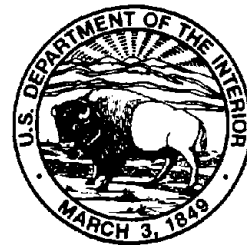
DAVID K. KEEFER, *Editor*

STRONG GROUND MOTION AND GROUND FAILURE

THOMAS L. HOLZER, *Coordinator*

---

U.S. GEOLOGICAL SURVEY PROFESSIONAL PAPER 1551-C



---

UNITED STATES GOVERNMENT PRINTING OFFICE, WASHINGTON : 1998

REPRODUCED BY: **NTIS**  
U.S. Department of Commerce  
National Technical Information Service  
Springfield, Virginia 22161

**DEPARTMENT OF THE INTERIOR**

**BRUCE BABBITT, *Secretary***

**U.S. GEOLOGICAL SURVEY**

**MARK SCHAFFER, *Acting Director***

Any use of trade, product, or firm names in this publication  
is for descriptive purposes only and does not imply endorsement  
by the U.S. Government

Manuscript approved for publication,  
February 28, 1997

---

Library of Congress catalog-card No. 92-32287

---

For sale by the  
U.S. Geological Survey  
Information Services  
Box 25286  
Federal Center  
Denver, CO 80225

## CONTENTS

---

	Page
Synopsis -----	C1
By David K. Keefer	
Regional distribution and characteristics of landslides generated by the earthquake -----	7
By David K. Keefer and Michael W. Manson	
Coastal-bluff failures in northern Monterey Bay induced by the earthquake -----	33
By Gary B. Griggs and Nathaniel Plant	
Landslide dams in Santa Cruz County, California, resulting from the earthquake -----	51
By Robert L. Schuster, Gerald F. Wieczorek, and David G. Hope II	
Large landslides near the San Andreas fault in the Summit Ridge area, Santa Cruz Mountains, California -----	71
By David K. Keefer, Gary B. Griggs, and Edwin L. Harp	
Origin of fractures triggered by the earthquake in the Summit Ridge and Skyland Ridge areas and their relation to landslides -----	129
By Edwin L. Harp	
Evaluation of coseismic ground cracking accompanying the earthquake: Trenching studies and case histories -----	145
By Jeffrey M. Nolan and Gerald E. Weber	
Analysis of earthquake-reactivated landslides in the epicentral region, central Santa Cruz Mountains, California -----	165
By William F. Cole, Dale R. Marcum, Patrick O. Shires, and Bruce R. Clark	

REFERENCED PLATES

NOT AVAILABLE FROM

N. T. I. S.



THE LOMA PRIETA, CALIFORNIA, EARTHQUAKE OF OCTOBER 17, 1989:  
STRONG GROUND MOTION AND GROUND FAILURE

LANDSLIDES

SYNOPSIS

By David K. Keefer,  
U.S. Geological Survey

CONTENTS

	Page
Introduction .....	C1
Overall distribution and characteristics of landslides .....	2
Coastal landslides .....	2
Landslide dams .....	2
Large landslides near the fault rupture in the Summit Ridge area .....	4
Characterization .....	4
Relation of landslide cracks to other, earthquake-generated cracks .....	4
Trenching investigations .....	4
Seismic slope-stability analysis .....	4
Concluding remarks .....	5
References cited .....	5

INTRODUCTION

Central California, in the vicinity of San Francisco and Monterey Bays, has a history of fatal and damaging landslides, triggered by heavy rainfall, coastal and stream erosion, construction activity, and earthquakes. The great 1906 San Francisco earthquake ( $M_S=8.2-8.3$ ) generated more than 10,000 landslides throughout an area of 32,000 km<sup>2</sup> (Keefer, 1984); these landslides killed at least 11 people and caused substantial damage to buildings, roads, railroads, and other civil works. Smaller numbers of landslides, which caused more localized damage, have also been reported from at least 20 other earthquakes that have occurred in the San Francisco Bay-Monterey Bay region since 1838 (Youd and Hoose, 1978; Keefer, 1984; Wicczorek and Keefer, 1987; D.K. Keefer, unpub. data, 1992). Conditions that make this region particularly susceptible to landslides include steep and rugged topography, weak rock and soil materials, seasonally heavy rainfall, and active seismicity.

Given these conditions and history, it was no surprise that the 1989 Loma Prieta earthquake generated thousands of landslides throughout the region. Landslides caused one fatality and damaged at least 200 residences, numerous roads, and many other structures. Direct damage from landslides probably exceeded \$30 million; additional, indirect

economic losses were caused by long-term landslide blockage of two major highways and by delays in rebuilding brought about by concern over the potential long-term instability of some earthquake-damaged slopes.

The 1989 Loma Prieta earthquake provided the first relatively complete data set on landslides generated by an earthquake of this size ( $M=7.0$ ,  $M_S=7.1$ ) in central California. Previous landslide-producing earthquakes in the region, except for the 1906 event, were either much smaller or too poorly documented to accurately assess landslide effects. The papers in this chapter discuss many aspects of earthquake-induced landsliding, ranging from determinations of the overall distribution of landslides to detailed analyses of individual slope failures. Many of these aspects are consistent with the results of previous analyses based largely on data from other regions. Therefore, many of the slopes that failed during the earthquake could have been identified as susceptible to landsliding by using existing criteria and techniques (for example, Keefer, 1984; Wicczorek and others, 1985; Wilson and Keefer, 1985; Keefer and Wilson, 1989).

Several other aspects of the landsliding, however, had few, if any, historical analogs and thus lead to new conclusions concerning the generation of landslides by seismic events. Among these new conclusions are that (1) many ground cracks throughout the epicentral region were caused by incipient landslide movement, (2) seismically generated landslides may be important contributors to long-term coastal erosion, (3) areas of ground cracking adjacent to some fault ruptures may produce landslides substantially larger and more complex than those produced at greater distances from the fault by shaking alone, (4) many ground cracks associated with landslides near fault ruptures show evidence of previous movement and thus may be detectable by subsurface investigations, and (5) slope-stability analyses based on material strengths measured on small-diameter samples may underestimate actual earthquake-induced landslide displacements.

The first three papers in this chapter discuss various facets of the regional distribution of landslides: overall distribution and characteristics, coastal landslides, and generation of landslide dams. The next four papers discuss large, complex landslides that were generated near the

rupture zone, including their overall characterization, analysis of their relation to ground cracks produced by processes other than landsliding, subsurface investigations documenting previous movement histories, and use of these well-documented features to calibrate methods of dynamic slope-stability analysis. Other chapters in this volume also discuss topics closely related to landslides: soil liquefaction, which produces types of landslides not described here (see O'Rourke, 1992; Holzer, in press); and ground cracks near the rupture zone (Ponti, in press).

### OVERALL DISTRIBUTION AND CHARACTERISTICS OF LANDSLIDES

The landslides produced by the 1989 Loma Prieta earthquake occurred throughout an area of 15,000 km<sup>2</sup>, including most of the heavily populated San Francisco Bay region (fig. 1). Landslides damaged hundreds of residences and other structures, some as far from the epicenter as San Francisco (fig. 1), and blocked major highways for periods as long as weeks to months, but they caused only one fatality. The overall distribution and characteristics of these earthquake-generated landslides (except for those caused by soil liquefaction) are discussed by Keefer and Manson (this chapter).

Landslides were most abundant in an area of about 2,000 km<sup>2</sup> in the southern Santa Cruz Mountains (fig. 1). Despite its rugged topography, this mountainous area is populated, and the landslides caused substantial damage. At least 1,050 and, possibly, as many as about 3,000 landslides occurred. The most common types of landslides were rock falls, rock slides, and disrupted soil slides, types that also are most common in earthquakes worldwide (Keefer, 1984). Deeper seated and more coherent slumps and block slides were moderately common.

Most landslides were in materials that previous studies had identified as highly susceptible to earthquake-induced failure, including weakly cemented rocks, artificial fills, uncemented alluvial materials, and preexisting landslide deposits (Keefer, 1984; Wieczorek and others, 1985; Wilson and Keefer, 1985; Keefer and Wilson, 1989). In fact, many of the same geologic units that produced abundant landslides in this earthquake had previously been identified as highly susceptible to seismic slope failure in a study of San Mateo County, immediately to the north (Wieczorek and others, 1985). More than 85 percent of the earthquake-induced landslides occurred southwest of the fault rupture, almost certainly because the fault separated groups of rocks with significantly different properties.

In addition to cracks associated with clearly defined landslides, the earthquake opened cracks in hundreds of ridgetops and hillsides throughout the southern Santa Cruz

Mountains. Analysis of the locations and characteristics of these cracks leads to the conclusion that many of the cracks were, in fact, produced by incipient landslides. Keefer and Manson (this chapter) conclude that if conditions had been wetter at the time of the earthquake or if shaking had been more severe, many of these sites probably would have produced fully developed landslides, and so the total landslide damage would have been much greater.

### COASTAL LANDSLIDES

Outside the Santa Cruz Mountains, landslides occurred along a 240-km-long stretch of the central California coast (fig. 1), which is characterized in most places by steep, high bluffs. Griggs and Plant (this chapter) discuss these coastal landslides, with emphasis on the northern Monterey Bay area, where these landslides were most abundant. Coastal landslides damaged or imperiled residences and other structures both on bluff tops and in beach areas at the bases of bluffs. In addition to fully developed landslides, the earthquake generated cracks on bluff tops as much as 10 m inland from bluff faces, raising questions about the long-term stability of many sites.

Griggs and Plant (this chapter) note that seismic failure of coastal bluffs may be a hazard not widely recognized during planning for construction in coastal areas. This absence of recognition derives from the common practice of basing construction setbacks or other hazard-mitigation procedures on calculated long-term average rates of bluff erosion. Because the period of recorded data may be too short to include major, well-documented earthquakes, the contribution of earthquake-induced failure may not be taken into account. Our experience in the 1989 Loma Prieta earthquake thus can be used to improve recognition and mitigation of hazards in the coastal area.

### LANDSLIDE DAMS

Another effect of the earthquake-triggered landslides was the formation of landslide dams in the Santa Cruz Mountains, as described by Schuster and others (this chapter). Such landslide dams can pose delayed or long-term hazards because these dams are prone to fail from buildup of water behind them. Historical failures of landslide dams and consequent flooding events have killed as many as 100,000 people. The 1989 Loma Prieta earthquake produced five documented landslide dams, all within about 10 km of the epicenter (fig. 1). These dams were small, ranging from 200 to 50,000 m<sup>3</sup> in volume, and impounded lake volumes ranging from 150 to 6,000 m<sup>3</sup>. Two of the dams were removed by human excavation, and three failed

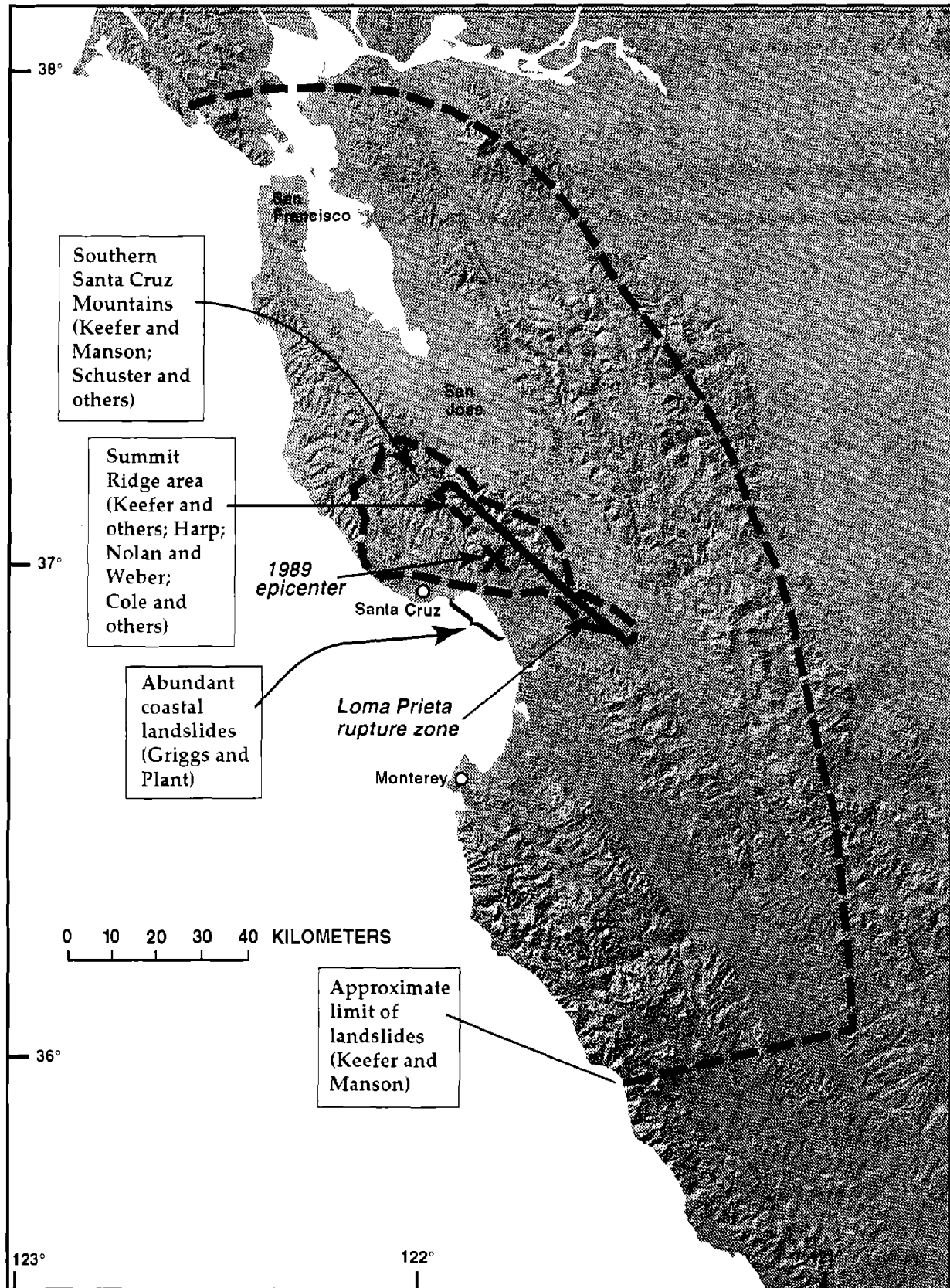


Figure 1.—San Francisco Bay-Monterey Bay region, Calif., showing approximate limit of area affected by earthquake-generated landslides and locations of study areas of papers in this chapter. Base map from Edwards and Batson (1990).

naturally, producing only minor flooding that did not exceed channel capacity. Schuster and others conclude that the generation of landslide dams by the earthquake was limited by the uncommonly dry conditions in the San Francisco-Monterey Bay region at the time of the event.

## **LARGE LANDSLIDES NEAR THE FAULT RUPTURE IN THE SUMMIT RIDGE AREA**

### **CHARACTERIZATION**

The most unusual slope-failure effects generated by the earthquake were the large, complex, deep-seated landslides that occurred in and around Summit Ridge, near the rupture zone (fig. 1; see Keefer and others, this chapter). Initial recognition of these landslides was hindered by their occurrence in an area of pervasive ground cracks, many of which originated from mechanisms other than landsliding (Ponti and Wells, 1991; Ponti, in press). Detailed mapping (Spittler and Harp, 1990) and analysis of ground-surface features in the Summit Ridge area eventually delineated 20 landslides, each with surface areas of more than 10,000 m<sup>2</sup>. The largest individual landslide, which had a surface area of 680,000 m<sup>2</sup> and an estimated volume of 27 million m<sup>3</sup>, encompassed about 165 homes, many of which were severely damaged. An unusual feature of the landslides in the Summit Ridge area, in addition to their size and complexity, was the discontinuity of the surface features defining their boundaries. Keefer and others conclude that these discontinuous boundary features probably resulted from the small landslide displacements, ranging from 0.25 to 2.44 m.

According to Keefer and others (this chapter), the close association of these landslides with other, earthquake-generated ground cracks, the historical record of landslides in the Summit Ridge area, and analytical slope-stability modeling all suggest that future reactivation of the landslides is unlikely except during earthquakes. Although two possible analogs of these landslides, generated by previous earthquakes, are discussed by Harp (this chapter), such landslides are extremely rare in the historical record. Thus, the landslides in the Summit Ridge area represent a newly recognized type of landslide hazard along fault traces.

### **RELATION OF LANDSLIDE CRACKS TO OTHER, EARTHQUAKE-GENERATED CRACKS**

Differentiation of landslide-generated ground cracks from other cracks in the Summit Ridge area is detailed by Harp (this chapter), who concludes that the locations and orientations of most nonlandslide ground cracks were con-

trolled by elements of the regional geologic structure, such as bedding planes and local faults. Harp shows how these structurally related cracks interacted with downslope movement to produce the unusually complex structure of the landslides in the Summit Ridge area.

### **TRENCHING INVESTIGATIONS**

Trenching investigations designed to determine the subsurface characteristics and movement histories of ground cracks are described by Nolan and Weber (this chapter). Their study includes detailed analyses of the features observed in two postearthquake trenches and a synthesis of data from 24 previous (both preearthquake and postearthquake) trenching investigations in the Summit Ridge area. One of the trenches studied in detail was excavated across the well-defined main scarp of a large landslide; the other was excavated across a ground crack that could be related to landsliding, tectonic deformation, or both. Both trenches revealed features indicative of at least four displacement events, including the 1989 Loma Prieta earthquake. These events occurred within a time period of approximately 3,200 years in one place and of approximately 2,000 years in the other. One movement event on one crack was probably associated with the 1906 San Francisco earthquake.

From their analysis of these and the 24 other trenching investigations, Nolan and Weber (this chapter) conclude that most ground cracks showing more than 3 to 5 cm of extension and (or) more than 1 to 3 cm of vertical displacement attributable to the 1989 Loma Prieta earthquake also showed clear subsurface evidence of previous movement. They also found that although not all ground cracks with previous displacements were reactivated by the earthquake, most cracks with previous displacements were associated with recognizable surface topographic features. The results of their study thus indicate that careful subsurface investigation before construction can minimize the potential hazard from earthquake-induced ground cracking in such areas.

### **SEISMIC SLOPE-STABILITY ANALYSIS**

The landslides in the Summit Ridge area presented a rare opportunity to calibrate existing techniques for analyzing potential slope displacements under seismic conditions. The study by Cole and others (this chapter) involved sampling, material testing, and seismic slope-stability analysis of two of these landslides. Cole and others conclude that slope-stability analyses conducted by measuring material strengths in the laboratory on small-diameter samples may underestimate actual landslide displacements. They also found that calculated landslide displacements



are highly sensitive to predicted ground-water levels within the analyzed slopes and to the ground-motion record used as input to the analysis. Their study shows that seismic slope-stability analysis may be made more accurate if material strengths can be estimated from backanalysis of previous slope failures.

## CONCLUDING REMARKS

The 1989 Loma Prieta earthquake was the most important seismic event in a major U.S. urban area since 1906. As such, it provided both a significant test of existing hazard-reduction techniques and a case study for improving those techniques. In the areas of landsliding, techniques for identifying slopes susceptible to failure, developed largely during the past 10 years, were largely proved correct: Most slopes that failed in the earthquake could have been accurately characterized with sufficiently detailed preearthquake mapping and analysis. Postearthquake studies, however, have also led to the recognition of types of landslide hazards not fully appreciated in the past, including the potential for particularly large and complex landslides along fault traces, pervasive ridgetop and hillside cracking due to incipient landslide movement, and the contribution of earthquake-induced failure to coastal erosion. In addition, the earthquake provided an opportunity for the calibration and improvement of site-specific numeric methods, used to estimate potential earthquake-induced slope displacements.

The landslide damage and loss of life associated with the earthquake were fortuitously light, given the high population density and geologic conditions in the Loma Prieta region. However, the damage that did occur, the long-term disruption of transportation by landslides along roads, and the delays in recovery due to possible continuing instability of earthquake-damaged slopes all illustrate the types of problems that landslides can create as a result of earthquakes, both in this region and in other regions of the United States and the rest of the world. Minimizing the potential damage and loss of life from landslides in future earthquakes will require continued application and enhancement of the techniques of hazard reduction. The

1989 Loma Prieta earthquake has provided both a warning about the need for these efforts and significant new information with which to improve them.

## REFERENCES CITED

- Edwards, Kathleen, and Batson, R.M., 1990, Experimental digital shaded-relief maps of California: U.S. Geological Survey Miscellaneous Investigations Series Map I-1848, scale 1:1,000,000, 2 sheets.
- Holzer, T.L., ed., in press, The Loma Prieta, California, earthquake of October 17, 1989—liquefaction: U.S. Geological Survey Professional Paper 1551-B.
- Keefer, D.K., 1984, Landslides caused by earthquakes: Geological Society of America Bulletin, v. 95, no. 4, p. 406-421.
- Keefer, D.K., and Wilson, R.C., 1989, Predicting earthquake-induced landslides, with emphasis on arid and semi-arid environments, in Sadler, P.M., and Morton, D.M., eds., Landslides in a semi-arid environment with emphasis on the Inland Valleys of Southern California: Riverside, Calif., Inland Geological Society of Southern California Publications, v. 2, no. 1, p. 118-149.
- O'Rourke, T.D., ed., 1992, The Loma Prieta, California, earthquake of October 17, 1989—Marina District: U.S. Geological Survey Professional Paper 1551-F, p. F1-F215.
- Ponti, D.J., ed., in press, The Loma Prieta, California, earthquake of October 17, 1989—ground ruptures: U.S. Geological Survey Professional Paper 1551-D.
- Ponti, D.J., and Wells, R.E., 1991, Off-fault ground ruptures in the Santa Cruz Mountains, California; ridge-top spreading versus tectonic extension during the 1989 Loma Prieta earthquake: Seismological Society of America Bulletin, v. 81, no. 5, p. 1480-1510.
- Spittler, T.E., and Harp, E.L., compilers, 1990, Preliminary map of landslide features and coseismic fissures in the Summit Road area of the Santa Cruz Mountains triggered by the Loma Prieta earthquake of October 17, 1989: U.S. Geological Survey Open-File Report 90-688, 53 p., scale 1:4,800, 3 sheets.
- Wieczorek, G.F., and Keefer, D.K., 1987, Earthquake triggered landslide at La Honda, California, in Hoose, S.N., ed., The Morgan Hill, California, earthquake of April 24, 1984: U.S. Geological Survey Bulletin 1639, p. 73-79.
- Wieczorek, G.F., Wilson, R.C., and Harp, E.L., 1985, Map showing slope stability during earthquakes in San Mateo County, California: U.S. Geological Survey Miscellaneous Investigations Series Map I-1257-E, scale 1:62,500.
- Wilson, R.C., and Keefer, D.K., 1985, Predicting areal limits of earthquake-induced landsliding, in Ziony, J.I., ed., Evaluating earthquake hazards in the Los Angeles region—an earth-science perspective: U.S. Geological Survey Professional Paper 1360, p. 317-345.
- Youd, T.L., and Hoose, S.N., 1978, Historic ground failures in northern California triggered by earthquakes: U.S. Geological Survey Professional Paper 993, 177 p.



THE LOMA PRIETA, CALIFORNIA, EARTHQUAKE OF OCTOBER 17, 1989:  
STRONG GROUND MOTION AND GROUND FAILURE

LANDSLIDES

REGIONAL DISTRIBUTION AND CHARACTERISTICS OF  
LANDSLIDES GENERATED BY THE EARTHQUAKE

By David K. Keefer,  
U.S. Geological Survey;  
and  
Michael W. Manson,  
California Division of Mines and Geology

CONTENTS

Abstract .....	Page C7
Introduction .....	7
Setting of the earthquake .....	8
Climate, vegetation, and population .....	8
Geology .....	8
Seismicity .....	10
Previous landslide activity .....	10
Distribution and characteristics of landslides generated by the earthquake .....	11
General characteristics and classification of earthquake- induced landslides .....	11
Identification and mapping of landslides after the earthquake .....	11
Southern Santa Cruz Mountains .....	12
Disrupted slides and falls (category I landslides) .....	12
Coherent slides (category II landslides) .....	15
Ground cracks .....	18
Estimated total number of landslides in the southern Santa Cruz Mountains .....	19
Landslides in other areas .....	20
Coastal landslides .....	20
Peripheral area .....	23
Discussion and conclusions .....	24
Acknowledgments .....	28
References cited .....	29

ABSTRACT

The 1989 Loma Prieta earthquake generated thousands of landslides, most of which occurred within an area of approximately 2,000 km<sup>2</sup> in the rugged, heavily vegetated southern Santa Cruz Mountains, but also along a 240-km stretch of the central California coast and throughout another 13,000 km<sup>2</sup> of the San Francisco Bay-Monterey Bay region. Landslides triggered by the earthquake damaged or destroyed more than 100 residences and other struc-

tures, blocked roads throughout the affected region, and caused one fatality.

Near the rupture zone itself, the earthquake generated several large, complex landslides with surface areas as great as 85 ha and depths possibly exceeding 100 m. Throughout the rest of the southern Santa Cruz Mountains, the most abundant landslides were shallow, internally disrupted rock falls, rock slides, and soil slides, although more coherent and deeper seated landslides also were moderately common. In addition to landslides, the earthquake opened ground cracks at hundreds of localities throughout the Santa Cruz Mountains. Many of these cracks almost certainly marked incipient landslides, which would have developed more fully had ground conditions been wetter or the earthquake shaking more severe.

The shallow, internally disrupted landslides were most common in weakly to moderately cemented sedimentary rocks, whereas the more coherent landslides were most abundant in artificial fill and preexisting landslide deposits. All types of landslides were more abundant southwest of the San Andreas fault than to the northeast, probably owing to the widespread distribution of relatively weakly consolidated rocks in the area southwest of the fault. Along the coastal cliffs bordering the Pacific Ocean, large landslides occurred out to relatively great distances from the rupture zone, indicating that these seacliffs are especially susceptible to seismically induced failure.

INTRODUCTION

The  $M=7.0$  Loma Prieta earthquake triggered thousands of landslides throughout approximately 15,000 km<sup>2</sup> of central California, including most of the San Francisco Bay-Monterey Bay region (fig. 1). These landslides were

of several different types, occurred in various geologic environments, and locally caused significant damage to public infrastructure and private property. As part of an effort to document the effects of this earthquake, the largest in the region since 1906, mapping of landslides and related ground-failure features was begun the day after the earthquake. The mapping was carried out by more than 50 individuals from Government agencies, universities, and private firms; landslide localities and detailed descriptions from the area most heavily affected by landslides were compiled by Manson and others (1992). This paper uses these and other data to summarize general characteristics of the landslides generated by the earthquake and to compare these landslides with those generated by other historical earthquakes.

## SETTING OF THE EARTHQUAKE

The region affected by the 1989 Loma Prieta earthquake stretches inland from the Pacific coast, through the broad lowlands around San Francisco Bay and Monterey Bay, to parts of the Coast Ranges of central California (fig. 1).

## CLIMATE, VEGETATION, AND POPULATION

The affected region has a Mediterranean climate, characterized by warm, dry summers and cool, rainy winters. Virtually all precipitation occurs as rain, 90 percent of which falls during the winter months of November through April. Mean annual precipitation ranges from about 300 to about 2,000 mm throughout the region; coastal mountains generally receive the most precipitation, and inland valleys the least (Rantz, 1971). Precipitation varies widely from year to year. The 1989 Loma Prieta earthquake occurred during the fourth year of drought conditions, when rainfall was only about 50 to 70 percent of normal, and at the end of the dry summer season—a combination of circumstances that made ground conditions especially dry.

The San Francisco Bay-Monterey Bay region (fig. 1) is heavily urbanized, with a population of almost 6 million people. Vegetation varies throughout the nonurbanized parts of the region, with areas of marsh, grassland, coastal scrub, chaparral, oak, evergreen, redwood, and mixed forests (Thomas, 1961).

Most of the landslides produced by the earthquake occurred in the southern Santa Cruz Mountains, through which the rupture zone passes (fig. 1). Topography in this area ranges from gently rolling hills to steep, rugged ridges separated by narrow canyons; altitudes range from near sea level to 1,155 m. Much of the area is covered by dense redwood or oak forest or chaparral, and the dense

vegetation precluded systematic mapping of landslides from aerial photographs or airborne observations. Mean annual precipitation in the area ranges from about 500 to 1,500 mm (Rantz, 1971).

## GEOLOGY

The Coast Ranges and intervening lowlands (fig. 1) are underlain by a wide variety of sedimentary, igneous, and metamorphic rocks and unconsolidated sedimentary deposits, most of which range in age from Jurassic through Holocene. The rocks vary greatly in composition, degree of consolidation, amount of deformation, and depth of weathering. Shale, siltstone, sandstone, and volcanic rocks predominate. Colluvium of varying depth and composition mantles most hillslopes.

In the southern Santa Cruz Mountains, the geologic conditions and bedrock units southwest of the San Andreas fault differ significantly from those to the northeast. Southwest of the fault, the predominant bedrock units are Tertiary sedimentary rocks—primarily sandstone, siltstone, mudstone, and shale—and smaller bodies of intrusive, volcanic, and metamorphic rocks (Brabb, 1989). The most widespread sedimentary units are the Purisima Formation (siltstone with sandstone interbeds), the Butano Sandstone (sandstone, siltstone, and minor conglomerate), the Santa Cruz Mudstone (mudstone), the Monterey Formation (mudstone and siltstone), the San Lorenzo Formation (sandstone, mudstone, and shale), the Vaqueros Sandstone (sandstone with interbeds of mudstone and shale), and the Santa Margarita Sandstone (sandstone). These rocks, which typically strike northwest, are poorly to moderately consolidated, variably weathered, intensely folded, and locally sheared and faulted. They are commonly covered by colluvial and residual soils, as much as several meters thick. Near the coast and in the southern part of the area, near Pajaro Valley (see pl. 1), these rocks are overlain by poorly consolidated to unconsolidated Quaternary alluvial and terrace deposits.

Northeast of the San Andreas fault, large parts of the area are underlain by rocks of the Central Belt of the Franciscan Complex (Upper Cretaceous to Lower Eocene?). Although these rocks are more indurated than those southwest of the fault, they are intensely and pervasively sheared. The predominant unit is melange, composed of resistant blocks of different sizes and rock types enclosed in a less resistant matrix of penetratively sheared argillite, tuff, and sandstone (McLaughlin and others, 1991). Other types of Franciscan rocks include limestone, chert, basalt, and metasandstone (McLaughlin and others, 1988, 1991). Also present in the area northeast of the fault are rocks of the Coast Range ophiolite (Middle? to Late Jurassic), made up of serpentinite, ultramafic rocks, gabbro, diabase, igneous dikes and sills, and volcanic

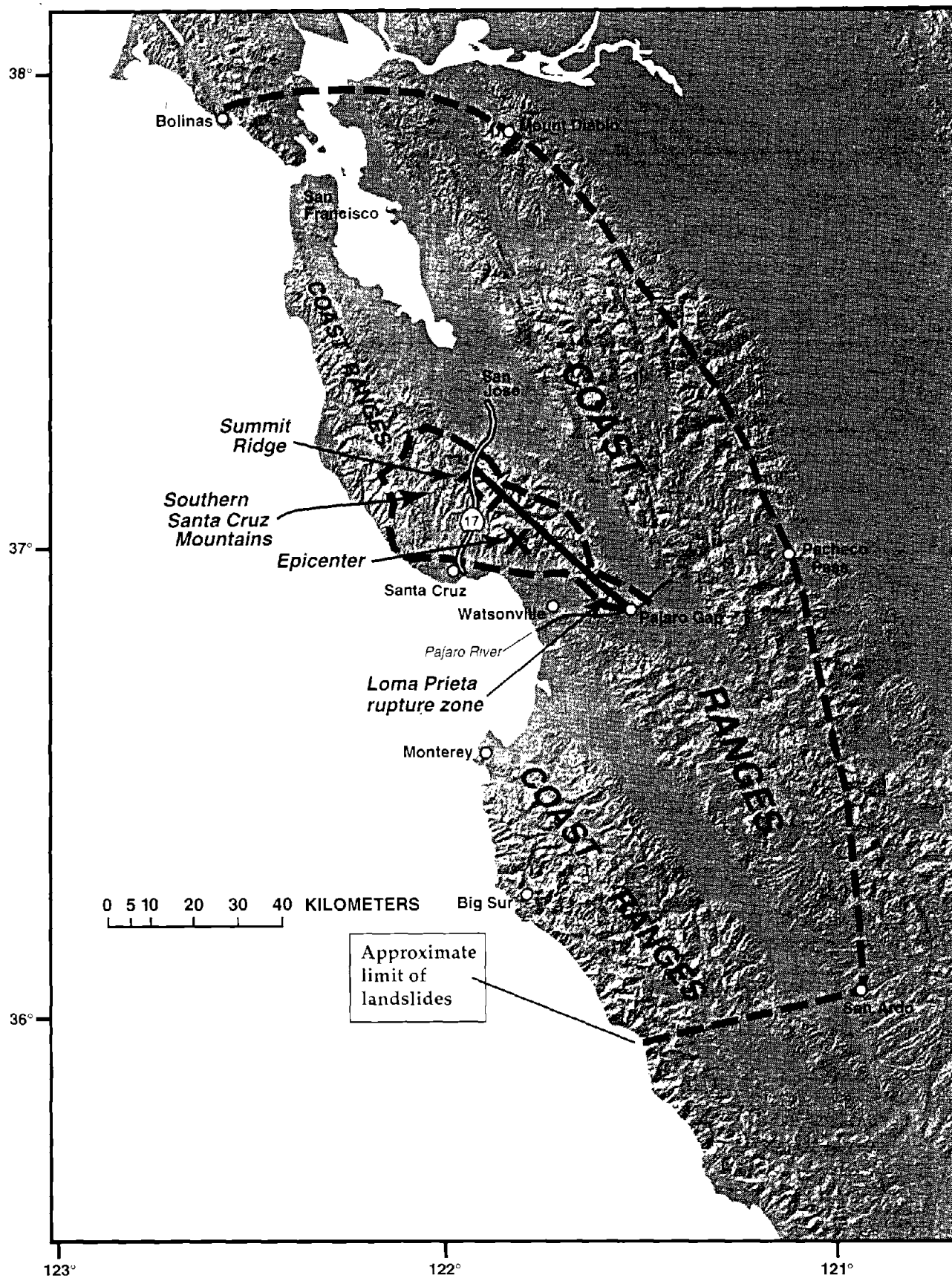


Figure 1.—San Francisco Bay-Monterey Bay region, showing geographic limit of landslides generated by 1989 Loma Prieta earthquake and locations of landslide zones discussed in text in relation to epicenter and rupture zone. Base map from Edwards and Batson (1990).

rocks (McLaughlin and others, 1988, 1991; Clark and others, 1989).

The areas immediately northeast of the San Andreas fault is underlain by sedimentary rocks that range in age from Upper Jurassic through Tertiary. These rocks vary widely in degree of induration, but on average they are more indurated than the sedimentary rocks in the area southwest of the fault. Predominant rock types are conglomerate, sandstone, mudstone, and shale. These rocks also are intensely folded and locally sheared and faulted.

### SEISMICITY

The region affected by the 1989 Loma Prieta earthquake lies along the boundary between the North American and Pacific plates. This region contains many active and potentially active faults, including the plate-bounding San Andreas fault. In addition to myriad small and moderate historical earthquakes, 23 earthquakes of  $M \geq 6.0$  have occurred in the region since 1836 (Wesnousky, 1986; U.S. Geological Survey, 1990), two of which were as large as the 1989 Loma Prieta earthquake ( $M=7.0$  in 1838 and  $M=7.0$  in 1868) and one substantially larger ( $M=8.2-8.3$  in 1906) (U.S. Geological Survey, 1990).

The earthquake occurred at 5:04 p.m. P.d.t. on October 17, 1989, and had a Richter surface-wave magnitude ( $M_S$ ) of 7.1 (Plafker and Galloway, 1989) and a moment magnitude ( $M$ ) of 7.0 (Hanks and Krawinkler, 1991). The hypocenter was at approximately 18-km depth and was located at lat  $37^{\circ}02'$  N., long  $121^{\circ}53'$  W., in the Santa Cruz Mountains (fig. 1; Plafker and Galloway, 1989). The earthquake is inferred to have ruptured a 40-km-long segment of either the San Andreas or a nearby fault (Plafker and Galloway, 1989; Working Group on California Earthquake Probabilities, 1990; Hanks and Krawinkler, 1991); the rupture zone extended from near the Pajaro Gap, east of Watsonville, northwestward to near California Highway 17 (fig. 1; Plafker and Galloway, 1989; Working Group on California Earthquake Probabilities, 1990).

No throughgoing surface fault rupture was found. Instead, areas of the ground surface adjacent to the trace of the San Andreas fault exhibited complex patterns of coseismic fissures (U.S. Geological Survey staff, 1989; Spittler and Harp, 1990; Ponti and Wells, 1991; Aydin and others, in press). Geodetic surveys showed that the fault slip caused as much as 173 mm of subsidence in a zone mostly northeast of the mapped trace of the San Andreas fault, and as much as 592 mm of uplift in a zone mostly southwest of the mapped fault trace (Marshall and others, 1991).

### PREVIOUS LANDSLIDE ACTIVITY

Prehistoric landslide deposits are widespread in the mountains of the San Francisco Bay-Monterey Bay region (for example, Brabb and others, 1972 and Cooper-Clark and Associates, 1975), and abundant historical landslides have occurred there in association with earthquakes (Lawson, 1908; Youd and Hoose, 1978; Keefer, 1984; Marshall, 1990), storms (Keefer and others, 1987; Ellen and Wieczorek, 1988), and other events, such as construction activity and coastal erosion. These landslides have caused several deaths and significant property damage, and landsliding is a common and recurring hazard in the region.

Landslides are known to have occurred during the October 8, 1865, earthquake ( $M=6.5$ ) on the San Andreas fault and the October 21, 1868, earthquake ( $M=7.0$ ) on the Hayward fault. These earthquakes, however, were poorly documented, and the available historical information is fragmentary (Youd and Hoose, 1978; Marshall, 1990).

Documentation of landslides caused by the much larger April 18, 1906, San Francisco earthquake ( $M=8.2-8.3$ ), though incomplete, was substantially more extensive (Lawson, 1908; Youd and Hoose, 1978; Keefer, 1984; Marshall, 1990). This earthquake probably generated more than 10,000 landslides throughout an area of 32,000 km<sup>2</sup> (Keefer, 1984; Keefer and Wilson, 1989). In addition to causing many shallow, highly disrupted landslides of the types most common in earthquakes (Keefer, 1984), the 1906 earthquake triggered or reactivated many deep-seated rotational slumps in the Coast Ranges (Lawson, 1908). In addition to being larger than the 1989 earthquake, the 1906 earthquake occurred when the region was relatively wet as a result of recent precipitation (Lawson, 1908; Youd and Hoose, 1978; Schuster and others, this chapter).

More recent seismic events in the region for which landslides have been documented were smaller than the 1989 Loma Prieta earthquake. They include the 1957 Daly City earthquake ( $M_L=5.3$ ), the 1979 Coyote Lake earthquake ( $M_L=5.4$ ), the 1980 Greenville-Mount Diablo earthquake sequence (max  $M_L=5.8$ ), and the 1984 Morgan Hill earthquake ( $M_S=6.1$ ), each of which triggered a few dozen to a few hundred landslides (predominantly shallow rock falls, soil falls, and disrupted soil slides) within areas of about 10 to 500 km<sup>2</sup> around the epicenters (Keefer, 1984; D.K. Keefer, unpub. data, 1992). In addition, the 1984 Morgan Hill earthquake triggered a large, deep-seated landslide at an anomalously large distance of 53 km from the epicenter (Wieczorek and Keefer, 1987).

Substantial landslide activity due to precipitation in the region has been documented during the rainfall seasons of 1949-50, 1955-56, 1961-62, 1962-63, 1964-65, 1966-67, 1968-69, 1969-70, 1972-73, 1974-75, 1977-78, 1982-

83, 1983–84, and 1986–87 (Keefer and others, 1987; Brown, 1988; Ellen and Wieczorek, 1988). The greatest documented landslide activity was associated with the storm of January 3–5, 1982, which produced as much as 610 mm of rain within 34 hours and caused more than 18,000 landslides and more than \$66 million in landslide-related damage (Ellen and others, 1988).

## DISTRIBUTION AND CHARACTERISTICS OF LANDSLIDES GENERATED BY THE EARTHQUAKE

### GENERAL CHARACTERISTICS AND CLASSIFICATION OF EARTHQUAKE-INDUCED LANDSLIDES

Earthquake-induced landslides were classified into three major categories and 14 individual types by Keefer (1984), on the basis of the landslide terminology defined by Varnes (1978). Landslides in the first major category—called “disrupted slides and falls” by Keefer (1984) and “category I landslides” by Keefer and Wilson (1989)—include landslides with a high degree of internal disruption that typically originate on steep slopes and travel at high velocities of several meters per hour to 100 km/h or more. The six individual types of landslides in this category include falls, slides, and avalanches in both soil and rock. Rock falls and soil falls move by falling, bouncing, and rolling; rock slides and soil slides move by translational sliding on discrete basal shear surfaces; and rock avalanches and soil avalanches move by complex mechanisms involving both sliding and fluidlike flow. Except for rock avalanches, most category I landslides are less than 3 m thick; rock avalanches, which have volumes of more than  $0.5 \times 10^6 \text{ m}^3$ , are typically thicker.

Category II landslides, or “coherent slides,” include five individual types that move primarily by sliding on discrete basal shear surfaces. These landslides are more coherent than those in category I and typically consist of one to several moving blocks; they also are relatively deep seated, typically more than 3 m thick. Included in this category are rock slumps and soil slumps, which move on concave-upward basal shear surfaces with significant headward rotation, and rock block slides, soil block slides, and slow earth flows, all of which move primarily by translational sliding on planar or gently curved basal shear surfaces. Typical velocities of landslides in this category range from a few millimeters per hour to several meters per hour.

Category III landslides, or “lateral spreads and flows,” include soil lateral spreads, rapid soil flows, and

subaqueous landslides, all of which move primarily by fluidlike flow. Most category III landslides are associated with soil liquefaction. Soil liquefaction caused by the 1989 Loma Prieta earthquake is the subject of other chapters of this volume (O'Rourke, 1992; Holzer, in press), and so category III landslides are not discussed further here.

### IDENTIFICATION AND MAPPING OF LANDSLIDES AFTER THE EARTHQUAKE

Landslide identification and mapping began the day after the earthquake. Initial observations from fixed-wing aircraft and preliminary examination of postearthquake aerial photographs showed that because of the dense vegetation cover in much of the epicentral region, mapping of landslide distribution from the air was not feasible. Therefore, subsequent mapping was conducted primarily on the ground, consisting of traverses in vehicles along all primary and many secondary roads throughout this region, and on foot through selected areas. Additional data on landslides in Santa Cruz County was provided from reports by building inspectors, who noted instances of building damage after the earthquake. Landslide localities were compiled on U.S. Geological Survey 1:24,000-scale 7.5-minute topographic quadrangles, and data on landslide types and other characteristics were compiled from field notes (Manson and others, 1992).

In the southern Santa Cruz Mountains, where most of the landslides occurred, landslide localities were digitized, and maps and accompanying field-locality descriptions were published by Manson and others (1992); these 1:48,000-scale maps cover 15 7.5-minute quadrangles (Manson and others, 1992). In this paper, those data were used to determine the numbers and characteristics of landslides in categories I and II. The data include some localities where multiple landslides were reported, at a few of which the number of landslides was estimated from the field descriptions because it was not reported directly. For each landslide locality, the geologic unit was determined from either the field description or a geologic map. In addition, each landslide source was classified according to geomorphic environment (ridgecrest, midslope, streambank, artificial cut or artificial fill), using either the field description or a topographic map.

In addition to this regional mapping, more detailed mapping, involving closely spaced traverses on foot, was carried out in the Summit Ridge area (fig. 1; Spittler and Harp, 1990) and in Forest of Nisene Marks State Park (see pl. 1), immediately around the epicenter (Weber and Nolan, 1989). In these two areas, most earthquake-induced landslides were probably identified. In other areas, however, the number of landslides that occurred was

probably higher than that reported, because of heavy vegetation, remoteness of some areas, and lack of access to some private property. As discussed below, the detailed mapping in Forest of Nisene Marks State Park was used to estimate the total number of landslides that occurred throughout the affected region.

The next subsection discusses the characteristics, abundance, and geologic environments of landslides that occurred in the southern Santa Cruz Mountains, followed by data on coastal landslides (discussed in more detail by Griggs and Plant, this chapter) and on landslides that occurred at widely scattered localities throughout the rest of the San Francisco Bay-Monterey Bay region. Finally, we discuss these results and compare the landslides generated by the 1989 Loma Prieta earthquake with those generated by other historical earthquakes.

### SOUTHERN SANTA CRUZ MOUNTAINS

After the earthquake, a total of about 1,280 landslides from 1,046 different sources were mapped within in an area of approximately 2,000 km<sup>2</sup> in the southern Santa Cruz Mountains (see pls. 1, 2; fig. 1): about 1,050 landslides were mapped during the general reconnaissance; 210 in Forest of Nisene Marks State Park, immediately around the epicenter (Weber and Nolan, 1989); and 20, particularly large, in the Summit Ridge area (see Keefer and others, this chapter). Altogether, these landslides damaged more than 160 homes (Seed and others, 1990; Spittler and Harp, 1990; Manson and others, 1992); damaged other structures, such as retaining walls and water-supply pipes and tanks (Manson and others, 1992); damaged and blocked numerous roads (Manson and others, 1992); and dammed creeks at five localities (see Schuster and others, this chapter). In addition to landslides, ground cracks were reported in another 300 localities (see pls. 1, 2; Weber and Nolan, 1989; Manson and others, 1992), as well as in the Summit Ridge area, where coseismic ground cracking was pervasive throughout an area of about 30 km<sup>2</sup> (Spittler and Harp, 1990; Ponti and Wells, 1991). As discussed below, many of the ground cracks in the southern Santa Cruz Mountains were probably caused by incipient landslide movement.

#### DISRUPTED SLIDES AND FALLS (CATEGORY I LANDSLIDES)

Of all the landslides identified in the southern Santa Cruz Mountains, 950 (74 percent) were disrupted slides and falls (category I landslides), primarily rock falls, rock slides, and disrupted soil slides. Deposits of those landslides typically consisted of shallow, highly disrupted masses of soil and rock (figs. 2, 3), some containing boulders more than 1 m in diameter (fig. 4). These landslides

occurred on steep roadcuts, streambanks, and ridge flanks. A third (33 percent) of the landslides were adjacent to roads, and most of these landslides involved artificial cuts. Of the remaining category I landslides, 31 percent originated low on slopes, along streambanks; 6 percent near ridgecrests; and 62 percent in midslope localities.

Most of the rock falls, rock slides, and soil slides had volumes of less than 100 m<sup>3</sup>, but about 90 were larger, ranging in volume from 100 m<sup>3</sup> to several thousand cubic meters. These larger landslides were restricted to localities within about 10 km of the rupture zone (fig. 1), mostly in the drainages of Bear Creek, Zayante Creek, Lyndon Canyon, Corralitos Creek, Rider Creek, Browns Creek, Hinckley Creek, or Soquel Creek (see pls. 1, 2). Four rock falls and rock slides, ranging in volume from 200 to 3,500 m<sup>3</sup>, dammed creeks in this area (see Schuster and others, this chapter).

One of the largest rock falls (fig. 5), with an estimated volume of 5,000 to 8,000 m<sup>3</sup>, blocked both northbound lanes of California Highway 17, the main road between Santa Cruz and the San Francisco Bay region, for 33 days after the earthquake, necessitating \$1.8 million in repairs (Spittler and others, 1990). This rock fall originated from two source areas in moderately cemented sandstone of the Purisima Formation on a steep roadcut, 15 m high. One source was in highly fractured rock with three conspicuous, orthogonal joint sets; the other source was in rock that was both highly fractured and intensely weathered. Between these two sources, the rock was relatively unweathered massive sandstone, with an average joint spacing of about 1 m.

Another complex of rock falls and rock slides, which resulted from failures of cut slopes on both sides of California Highway 17, temporarily blocked that highway at the Santa Cruz-Santa Clara County line (fig. 2). The landslide source was a sequence of steeply dipping beds of sandstone and shale of the Vaqueros Sandstone, which were massive but locally closely fractured. Rock falls were generated only within the shale beds, and open fissures on the ridgecrest above the source west of the highway indicated that these rock falls were related to an incipient slope failure which was much larger and deeper. Together, the rock falls and rock slides at this locality contained an estimated several hundred cubic meters of material.

The bedrock units in which rock falls, rock slides, and soil slides occurred in the southern Santa Cruz Mountains are listed in table 1 in decreasing order of landslide abundance. Whereas 32 different geologic units produced category I landslides, only 7 units produced more than 24 landslides each (table 1). Five of these seven units were Tertiary sedimentary rocks southwest of the San Andreas fault, one was a sedimentary unit northeast of the fault, and another was composed of preexisting landslide deposits (table 1). The Purisima Formation produced far more landslides than any other unit (more than 25 percent of





Figure 2.—Part of deposit from complex of rock falls and rock slides along California Highway 17 at Santa Cruz-Santa Clara County line (see pl. 1 for location). Landslide source was in intensely fractured rock.



Figure 3.—Rock fall from near-vertical cut along Old San Jose Road, about 0.9 km northwest of Sugarloaf Mountain (see pl. 2 for location). Source rock is weakly to moderately cemented sandstone, broken by conspicuous, through-going joints. Estimated volume of deposit is 500 to 1,000 m<sup>3</sup>.

the total), consistent with the generally poor consolidation of its rocks (Clark and others, 1989) and their widespread distribution near the rupture zone (fig. 1; Brabb, 1989). Where observed in outcrop, the sources of cat-

egory I landslides in all units were typically in materials that were weakly cemented, closely fractured, intensely weathered, and (or) broken by conspicuous, throughgoing joints.



Figure 4.—Boulder, approximately 1.5 m in maximum diameter, from earthquake-induced rock fall near conference ground about 2.5 km north of Soquel (see pl. 2 for location). Several boulders of nearly comparable size bounced and rolled into gently sloping field from steep slope above.



Figure 5.—Part of rock-fall deposit from cut slope above California Highway 17 in Glenwood area (see pl. 2 for location).

More indurated igneous rocks, southwest of the San Andreas fault, and Franciscan Complex rocks, northeast of the fault, produced few category I landslides (table 1); in all, 85 percent of the category I landslides occurred southwest of the San Andreas fault.

To compare the landslide susceptibility of the various units, we calculated the number of landslides per unit area (table 1). Data on the areas of occurrence of the various units were derived from digitized U.S. Geological Survey geologic maps (Brabb, 1989; Clark and others, 1989; McLaughlin and others, 1988, 1991). The results of this comparison showed that sedimentary rocks, primarily southwest of the fault and primarily of Tertiary age, were most susceptible to generating category I landslides. (Some Quaternary units, particularly alluvium, artificial fill, and preexisting landslide deposits, were incompletely represented on these maps and so were omitted from the calculations.)

Many of the units that produced more than 10 reported category I landslides had been identified as highly susceptible to earthquake-induced slope failure in San Mateo County, just north of the southern Santa Cruz Mountains, by Wieczorek and others (1985). Those high-susceptibility units included the Purisima Formation, the San Lorenzo Formation, preexisting landslide deposits, the Monterey Formation, and the Lambert Shale.

#### COHERENT SLIDES (CATEGORY II LANDSLIDES)

In the southern Santa Cruz Mountains, 330 (26 percent) of the mapped landslides were slumps or block slides (category II landslides; fig. 6). These landslides typically were deeper and more coherent than the category I landslides and consisted of one or a few blocks of displaced material. Commonly, the category II landslides were bounded at their heads by distinct scarps or fissures, and many contained internal fissures and compressional features as well.

The slumps and block slides triggered by the earthquake ranged in size from small features, a few meters long and a few meters wide, to the large, complex landslides in the Summit Ridge area, as much as 980 m long by 1,300 m wide (see Keefer and others, this chapter). Measured displacements on category II landslides ranged from less than 1 to more than 300 cm, and most displacements were from 10 to 100 cm. Of these landslides, 30 percent involved roadcuts, fills, or embankments; 15 percent originated on ridgecrests; 33 percent occurred in midslope localities; and 22 percent were along ridge flanks. Average slopes where these landslides occurred ranged from about 12° to near vertical.

Probably the most common category II landslides were small slumps in roadfill (fig. 7), which were typically characterized by arcuate, concave-downslope main scarps

and several subsidiary fissures that disrupted the road surface and continued into underlying material. Such slumps were common on both paved and unpaved roads throughout the southern Santa Cruz Mountains.

Many larger, more complex slumps also occurred, both in the Summit Ridge area and elsewhere in the southern Santa Cruz Mountains. One of the largest of these slumps outside the Summit Ridge area, with an estimated volume of 50,000 m<sup>3</sup>, dammed the west branch of Soquel Creek (see Schuster and others, this chapter). Another large slump occurred in the Rebecca Drive area of the community of Boulder Creek, where five residences were heavily damaged by a combination of earthquake shaking and landslide movement (fig. 8).

The Rebecca Drive landslide originated near the crest of a long, broad ridge. The main scarp (fig. 9), which passed under two houses, was 150 m long, and discontinuous small scarps and cracks continued along its strike for an additional 90 m. Maximum measured displacement across the main scarp was 57 cm. Subsidiary cracks were present both upslope from the main scarp and within the body of the landslide. Material exposed at the surface in the head of the landslide was a slightly cohesive, fine-sand fill, but the landslide almost certainly extended downward into the underlying soil and Santa Margarita Sandstone bedrock.

No compressional feature marking the landslide toe was found, but because the ridge flank was heavily vegetated, small compressional features may have been present but not observed. No indications of landslide displacement, however, were found along a roadcut into the ridge about 150 m downslope from the main scarp, and so the slump was probably less than 150 m long from crown to toe.

Several large block slides in bedrock occurred from the ends of prominent ridges in the southern Santa Cruz Mountains. These landslides had distinctive shapes and were recognized primarily by displacements in road surfaces and adjacent roadcuts. Their features typically consisted of (1) zones of linear or arcuate, concave-downslope scarps and cracks above the roads, which marked the main scarps and heads of the block slides (figs. 10, 11); (2) flank cracks trending perpendicular to the long axes of the roads and exhibiting displacements consistent with downslope movement (figs. 10, 12); and (3) small rock falls or soil slides dislodged where flank cracks intersected steep cuts above the roads (figs. 10, 12). The block slides typically were several tens to a few hundreds of meters wide and moved from a few to a few tens of centimeters. Because these landslides did not develop visible compressional features marking their toes, their lengths could not be determined.

Most category II landslides were in unconsolidated Quaternary deposits (especially artificial fill, preexisting landslide deposits, or alluvium) or in poorly to moderately indurated Tertiary sedimentary rocks (especially the

Table 1.—Geologic units that produced category I landslides

[Predominant lithologies from Dibblee and Brabb (1978), Brabb and Dibblee (1979), Brabb and Pampeyan (1983), McLaughlin and others (1988, 1991), Brabb (1989), Clark and others (1989), and E.E. Brabb (oral commun., 1992). Ages: K, Cretaceous; J, Jurassic; Mz, Mesozoic; Pz, Paleozoic; Q, Quaternary; T, Tertiary. n.d., not determined]

Unit	Predominant lithology	Age	Direction from San Andreas Fault	Average number of landslides per square kilometer
<b>More than 200 landslides reported</b>				
Purísima Formation	Weakly consolidated sandstone and siltstone	T	SW	1.62
<b>50 to 100 landslides reported</b>				
Vaqueros Sandstone	Sandstone, shale, and mudstone	T	SW	1.67
San Lorenzo Formation	Mudstone, sandstone, and shale	T	SW	1.68
Preexisting landslide deposits-- Sierra Azul unit (sandstone and shale).	Colluvium and various rocks, displaced downslope-- Sandstone and argillite	Q K	Both NE	n.d. 2.18
<b>25 to 49 landslides reported</b>				
Butano Sandstone	Sandstone and siltstone	T	SW	.44
Monterey Formation	Organic mudstone and sandy siltstone	T	SW	.39
<b>10 to 24 landslides reported</b>				
Highland Way unit	Carbonaceous shale and minor sandstone	T	NE	2.52
Lambert Shale	Organic mudstone	T	SW	1.26
Santa Cruz Mudstone	Siliceous organic mudstone	T	SW	.19
Aromas Sand	Semiconsolidated fluvial clay, silt, sand, and gravel	Q	SW	.43
Franciscan Complex (sandstone and argillite).	Intensely sheared sandstone and argillite	T, K	NE	.60
Quartz diorite	Quartz diorite, grading to granodiorite	K	SW	.11
<b>5 to 9 landslides reported</b>				
Alluvium	Unconsolidated fluvial silt and sand with local clay and gravel	Q	Both	n.d.
Lompico Sandstone	Calcareous arkosic sandstone	T	SW	.42
Mount Chual unit	Mudstone and minor sandstone and conglomerate	T	NE	.83
Santa Margarita Sandstone	Friable arkosic sandstone	T	SW	.15
Granite and adamellite	Granite and adamellite	K	SW	.88
Older alluvium	Unconsolidated gravel, sand, and silt	Q	Both	n.d.
<b>1 to 5 landslides reported</b>				
Nonmarine deposits	Fluvial sand and silt	Q, T	SW	1.89
Marine sandstone and shale	Sandstone, silty sandstone, and silty mudstone	T	NE	.15
Sierra Azul unit (conglomerate).	Pebbly to bouldery conglomerate	K	NE	.25
Zayante Sandstone	Arkosic sandstone with interbedded siltstone and conglomerate	T	SW	.26
Franciscan Complex (basalt and tuff).	Basalt flow breccia with minor flows and tuff	T, K	NE	.18
Franciscan Complex (metasandstone).	Complexly folded metasandstone	T, K	NE	.10
Franciscan Complex (sheared rocks).	Sheared and faulted rocks	T, K	NE	.05
Metasedimentary rocks	Pelitic schist and quartzite	Mz, Pz	SW	.13
Ultramafic rocks	Partially to completely serpentized, sheared ultramafic rocks	J	NE	.41
Great Valley Sequence, lower part	Cherty shale, commonly sheared, and minor sandstone	K, J	NE	.71
Santa Clara Formation	Coarse fluvial gravel and conglomerate	Q, T	NE	.15
Locatelli Formation	Micaceous siltstone	T	SW	.34
Basalt	Basalt	T	SW	.60

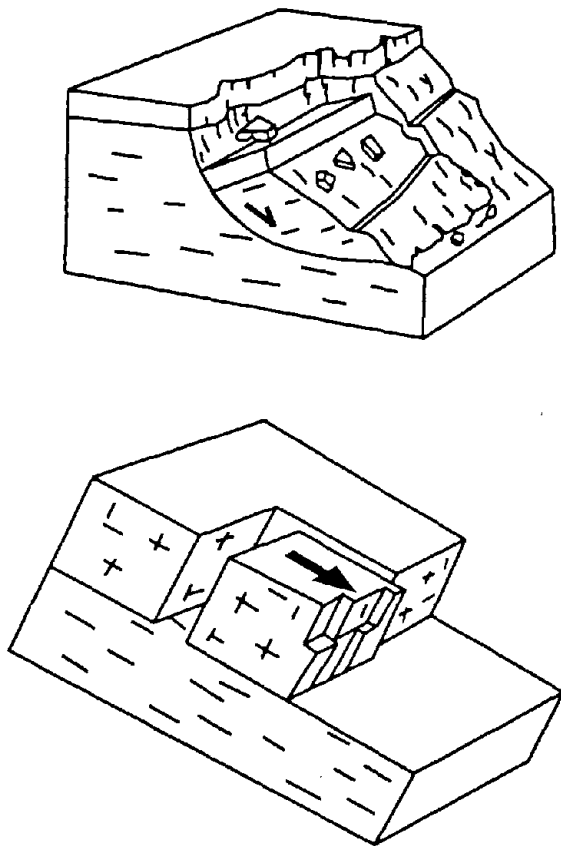


Figure 6.—Block diagrams showing idealized coherent (category II) landslides. *A*, Slump, consisting of single coherent block, showing movement with significant headward rotation on curved basal shear surface. *B*, Block slide, consisting of single coherent block, showing translational movement on planar basal shear surface. Adapted from Varnes (1978, fig. 2.1); copyright © U.S. National Academy of Sciences, used with permission.

*A* Purisima Formation, Vaqueros Sandstone, or San Lorenzo Formation) (table 2). All of these units except the Vaqueros Sandstone were identified by Wieczorek and others (1985) as highly susceptible to slope failure in earthquakes. The more indurated Franciscan Complex rocks northeast of the San Andreas fault produced only one reported landslide of this type, whereas the intrusive rocks southwest of the fault produced none. Approximately 95 percent of these landslides occurred in the area southwest of the San Andreas fault.

*B* At least 20 particularly large and complex category II landslides and landslide complexes with distinctive characteristics occurred in an area of about 30 km<sup>2</sup>, on and around Summit Ridge, immediately southwest of the rupture zone (fig. 1). These landslides are described by Keefer and others (this chapter), and various aspects of them are discussed by Cole and others (this chapter), Harp (this chapter), and Nolan and Weber (this chapter). These landslides occurred in an area that also contained the greatest abundance of earthquake-induced ground cracks (Spittler and Harp, 1990; Ponti and Wells, 1991), and the landslides and ground cracks in this area destroyed or damaged more than 100 residences (Spittler and Harp, 1990).

The landslides and landslide complexes ranged in surface area from 1 to 85 ha. Drilling and other evidence indicated that the landslides were at least 27, and possibly more than 100 m, deep (William Cotton and Associates, Inc., 1990; Cole and others, 1991, this chapter; Keefer, 1991; Keefer and others, this chapter). The maximum estimated volume of an individual landslide was  $27 \times 10^6$  m<sup>3</sup> (see Keefer and others, this chapter). In addition to their large sizes, the landslides were characterized by



Figure 7.—Small slump in road fill near Bean Hill (see pl. 2 for location). Note arcuate, concave-downslope main scarp nearly parallel to long axis of road. Slumps in fill were most common type of category II landslides in the southern Santa Cruz Mountains. Photograph by David M. Peterson, U.S. Geological Survey.

highly irregular shapes and boundaries marked by discontinuous sets of ground cracks and other surficial features.

These landslides occurred on moderate slopes, typically ranging from 12° to 30°, in an area underlain by poorly to moderately cemented Tertiary sandstone, siltstone, mudstone, and shale, varying weathered and sheared and covered by colluvial and residual soils, more than 20 m thick. The rocks are tightly folded and locally faulted, and most of the largest landslides were along the southwest flank of Summit Ridge, where the folding is tightest and faults and coseismic ground cracks most numerous (See Keefer and others, this chapter). Virtually all of the large landslides and landslide complexes also contained material from preexisting landslide deposits that had been identified before the 1989 Loma Prieta earthquake (Cooper-Clark and Associates, 1975).

#### GROUND CRACKS

In addition to landslides, the earthquake generated numerous ground cracks throughout the southern Santa Cruz Mountains. During the general reconnaissance, such fissures were identified at about 220 localities (see pl. 1), and the intensive mapping in Forest of Nisene

Marks State Park identified about 80 more localities (Weber and Nolan, 1989). In addition, ground cracks were pervasive throughout the Summit Ridge area, as noted above.

Earthquake-induced ground cracks throughout the southern Santa Cruz Mountains evidently were caused by several different processes, including differential settlement, particularly in roadfills and embankments; local adjustments to the tectonic uplift that occurred southwest of the rupture zone (fig. 1); and incipient landsliding. Ground cracks interpreted as marking incipient landslides commonly occurred along or near ridgecrests and (or) upslope from either preexisting landslide deposits or earthquake-generated landslides. These ground cracks typically were also nearly parallel to slope contours, were linear or concave downslope in plan view, and exhibited displacements consistent with downslope movement. An example of a ground crack interpreted as an incipient landslide feature is shown in figure 13. Reported ground cracks were most common in artificial fill, preexisting landslide deposits, and the Tertiary sedimentary rocks southwest of the San Andreas fault, especially in the Purisima Formation, Vaqueros Sandstone, Lambert Shale, Butano Sandstone, and San Lorenzo Formation.



Figure 8.—Severely damaged house on Rebecca Drive landslide (see pl. 1 for location). Main scarp of landslide passes under house. Note ground cracks in foreground.

### ESTIMATED TOTAL NUMBER OF LANDSLIDES IN THE SOUTHERN SANTA CRUZ MOUNTAINS

An extrapolation to the total number of landslides in the southern Santa Cruz Mountains may be obtained by comparing the landslide concentration in Forest of Nisene Marks State Park with that in adjacent areas, as determined by regional reconnaissance mapping. That study was designed to map all earthquake-induced landslides in the rugged, heavily vegetated terrain of the park through extensive traverses on foot (Weber and Nolan, 1989). The bedrock units in Forest of Nisene Marks State Park are the same as those that are extensive throughout adjacent areas and consist largely of folded Tertiary sedimentary rocks, including the Purisima Formation, Vaqueros Sandstone, San Lorenzo Formation, Butano Sandstone, Lambert Shale, and Zayante Sandstone.

Within the study area of 38.85 km<sup>2</sup>, intensive mapping identified 210 earthquake-induced landslides, and so the average landslide concentration was 5.4 landslides per square kilometer. Throughout the rest of the Laurel and Loma Prieta 7.5-minute topographic quadrangles, in which Forest of Nisene Marks is located, 559 landslides were

mapped by the general reconnaissance (see pls. 1, 2). The total area of these two quadrangles outside the park is 269.3 km<sup>2</sup>, and so the landslide concentration in this area is 2.1 landslides per square kilometer. Thus, the average, mapped landslide concentration within the park is 2.6 times the average concentration throughout the rest of the two quadrangles. If (1) geologic conditions in the park were the same as throughout the rest of the two quadrangles and (2) the difference in landslide concentration is assumed to be due entirely to the more intensive mapping effort within the park, then the total number of landslides in the southern Santa Cruz Mountains outside the park may be about 2.6 times greater than the 1,050 actually mapped, or a total of 2,730. In addition to the 210 landslides mapped inside the park, then, the total number of earthquake-generated landslides in the southern Santa Cruz Mountains may be as many as 3,000. Because Forest of Nisene Marks State Park surrounds the epicenter (see pl. 2) and rocks that predominate there are among the most susceptible to landsliding (table 1), this estimate probably represents an upper limit to the actual number of landslides that occurred in the southern Santa Cruz Mountains.



Figure 9.—Part of main scarp of Rebecca Drive landslide (see pl. 1 for location). Notebook (circled) is 20 by 27 cm. Approximate downslope displacement at this locality was 40 cm; maximum measured displacement across scarp was 57 cm.

## LANDSLIDES IN OTHER AREAS

### COASTAL LANDSLIDES

The earthquake also generated many landslides on the steep seacliffs, dunes, and terraces that border the Pacific Ocean. The San Francisco Bay-Monterey Bay region has an emergent, actively eroding coastline; typically, behind the beach, the coastal area contains a steep, rugged seacliff that in many places is topped with a gently sloping terrace surface. In some places, such as along the Big Sur coast, south of Monterey (fig. 1), the seacliff directly borders steep mountain slopes, hundreds of meters high. In a few other areas, such as along Sunset State Beach near the mouth of the Pajaro River (fig. 1), the beach is bordered by dunes.

Earthquake-induced landslides occurred along the coast from Marin County, north of San Francisco, to the Big Sur area south of Monterey, a distance of about 240 km

(fig. 14). Coastal landslides caused several million dollars in damage and killed one person (see Griggs and Plant, this chapter). The seacliff along much of this stretch of coast is composed largely of Tertiary sedimentary rocks, capped in many places by Quaternary terrace deposits, but also locally includes granitic or metamorphic rocks, Franciscan Complex materials, and semiconsolidated Quaternary sedimentary deposits.

The greatest concentration of coastal landslides was between Seabright State Beach in Santa Cruz and Sunset State Beach near the Santa Cruz-Monterey County line (fig. 14; Plant and Griggs, 1990; Sydnor and others, 1990; Griggs and Plant, this chapter). The predominant seacliff materials along this stretch of coast are (1) siltstone, mudstone, and fine-grained sandstone of the Purisima Formation, capped by unconsolidated terrace deposits; (2) weakly cemented, eolian Aromas Sand; and (3) Pleistocene dune deposits. This stretch of coast produced 80 mapped land-

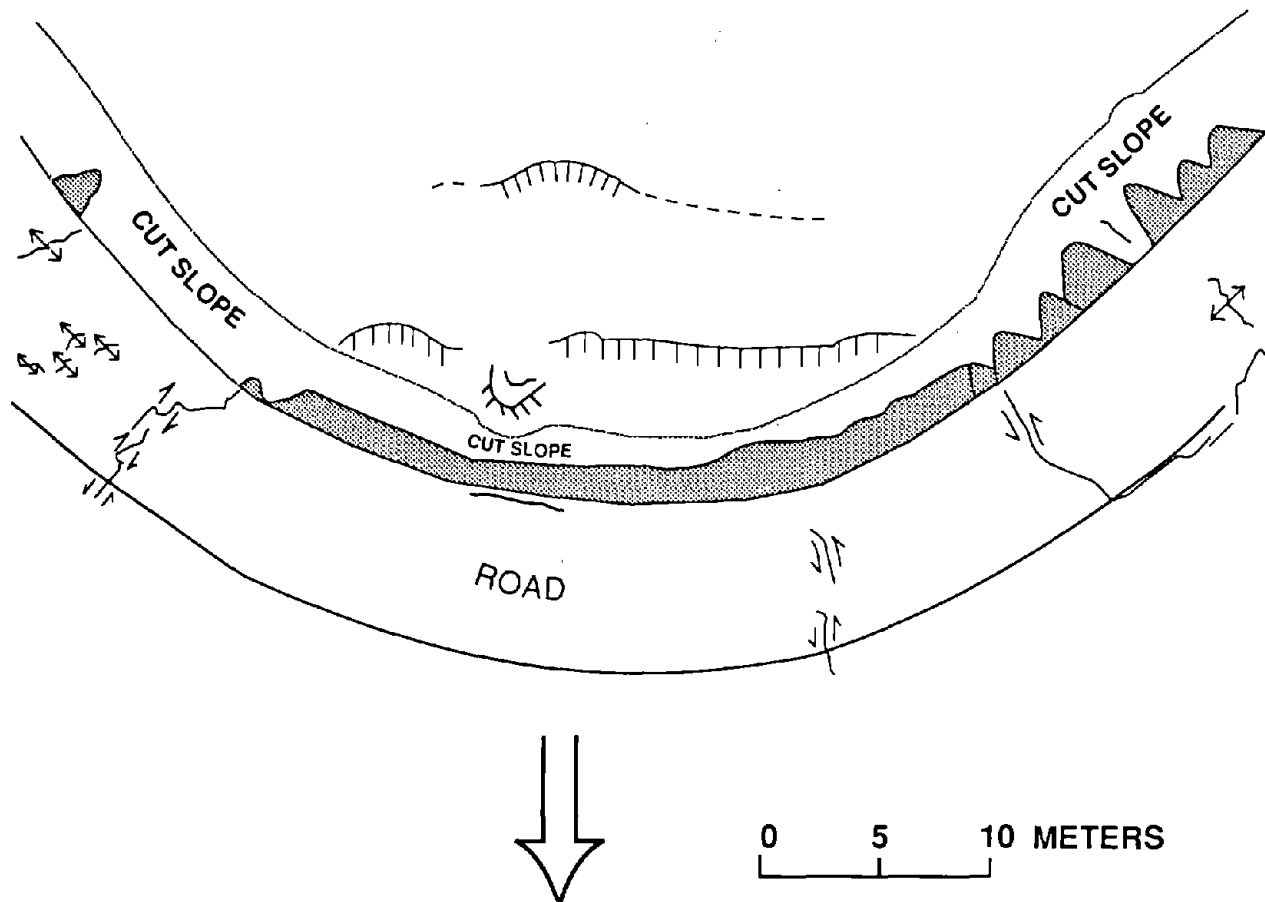


Figure 10.—Sketch map showing rock fall and block slide from end of ridge in Big Basin Redwoods State Park (see pl. 1 for location). Road curves around end of ridge in midslope position. Prominent scarps on ridgecrest above road (hachured on downdropped side, dashed where approximately located) showed as much as 6 cm of downslope displacement. Small arrows denote relative senses of motion on cracks in road, which typically trend perpendicular to long axis of roadway. Maximum local lateral displacement was 1.5 cm. Large arrow indicates approximate, inferred direction of movement of slide. No compressional features were found in heavily vegetated area downslope from road. Rock and soil falls (shaded areas) occurred on cut slope above road.





Figure 11.—Part of main scarp of rock block slide on end of ridge near Laurel (see pl. 2 for location). Notebook is 20 by 27 cm.



Figure 12.—Lateral margin (left flank) of block slide near Laurel (see pl. 2 for location) defined by crack across road, showing left-lateral movement. Note small rock fall where crack intersects steep cut slope across road.

slides: 69 disrupted slides and falls and 11 coherent slides (Plant and Griggs, 1990; Manson and others, 1992). At least 13 of the disrupted slides and falls had volumes greater than  $1,000 \text{ m}^3$ , and another 22 had volumes greater than  $100 \text{ m}^3$  (see pl. 1; Manson and others, 1992).

North of Seabright State Beach landslides along the seacliffs were moderately common as far north as Lake Merced in San Francisco (fig. 14); many of these landslides also were relatively large (fig. 15), with reported volumes of as much as  $40,000 \text{ m}^3$ . The landslides along this stretch of coast were most common in Santa Cruz Mudstone, Purisima Formation, Pigeon Point Formation, and the terrace deposits that locally cap these rocks. In the Lake Merced area, landslides occurred in weakly cemented sand, silt, and clay of the Merced Formation—the same materials that produced several landslides in the 1906 San Francisco earthquake ( $M_S=8.2-8.3$ ) (Lawson, 1908) and the 1957 Daly City earthquake ( $M_L=5.3$ ) (Bonilla, 1960).

North of the Lake Merced area, small landslides triggered by the 1989 Loma Prieta earthquake were observed as far north as Bolinas, in Marin County (fig. 14), and one large landslide reactivation was reported between Muir Beach and Stinson Beach (Seed and others, 1990). This reactivated landslide, approximately 300 m wide by 30 m deep, involved highly weathered and sheared sandstone and shale of the Franciscan Complex. Since previously activated as a result of severe storms in winter 1982, this landslide had been moving relatively continuously at a rate of less than 30 cm/yr. This rate increased significantly immediately after the earthquake, and between 2 and 3 weeks after the earthquake, the coastal highway

Table 2.—*Geologic units that produced category II landslides*

[Predominant lithologies from Dibblee and Brabb (1978), Brabb and Dibblee (1979), Brabb and Pampeyan (1983), McLaughlin and others (1988, 1991), Brabb (1989), Clark and others (1989), and E.E. Brabb (oral commun., 1992) Ages: K, Cretaceous; Q, Quaternary; T, Tertiary. n.d., not determined]

Unit	Predominant lithology	Age	Direction from San Andreas Fault	Average number of landslides per square kilometer
<b>More than 50 landslides</b>				
Artificial fill	Artificial fill, composed of various mixtures of clay, silt, sand, gravel, and coarser material.	Q	Both	n.d.
<b>25 to 50 landslides</b>				
Preexisting landslide deposits--	Colluvium and various rocks, displaced downslope	Q	Both	n.d.
Purísima Formation-----	Weakly consolidated sandstone and siltstone-----	T	SW	.25
Vaqueros Sandstone-----	Sandstone, shale, and mudstone-----	T	SW	.60
<b>10 to 24 landslides</b>				
San Lorenzo Formation-----	Mudstone, sandstone, and shale-----	T	SW	.62
Alluvium-----	Unconsolidated fluvial silt and sand with local clay and gravel-----	Q	Both	n.d.
<b>5 to 9 landslides</b>				
Santa Margarita Sandstone-----	Friable arkosic sandstone-----	T	SW	.56
Aromas Sand-----	Semiconsolidated fluvial clay, silt, sand, gravel and eolian sand.-----	Q	SW	.64
Butano Sandstone-----	Sandstone and siltstone-----	T	SW	.05
Sierra Azul unit----- (sandstone and shale).	Sandstone and argillite-----	K	NE	.21
<b>1 to 4 landslides</b>				
Highland Way unit----- (sandstone and shale).	Carbonaceous shale and minor sandstone-----	T	NE	.38
Lambert Shale-----	Organic mudstone-----	T	SW	.20
Monterey Formation-----	Organic mudstone and sandy siltstone-----	T	SW	.05
Sierra Azul unit----- (conglomerate).	Pebbly to bouldery conglomerate-----	K	NE	.17
Older alluvium-----	Unconsolidated gravel, sand, and silt-----	Q	Both	n.d.
Nonmarine deposits-----	Fluvial sand and silt-----	Q, T	SW	.76
Marine sandstone and shale-----	Sandstone, silty sandstone, and silty mudstone-----	T	NE	.06
Lompico Sandstone-----	Calcareous, arkosic sandstone-----	T	SW	.09
Franciscan Complex----- (sheared rocks).	Sheared and faulted rocks-----	T, K	NE	.05
Dune sands-----	Dune sand-----	Q	SW	1.96
Santa Cruz Mudstone-----	Siliceous organic mudstone-----	T	SW	.01
Zayante Sandstone-----	Arkosic sandstone with interbedded siltstone and conglomerate-----	T	SW	.01

(California Highway 1) was closed at this locality pending repairs, which were estimated by the California Department of Transportation to involve the excavation of 460,000 m<sup>3</sup> of material (Seed and others, 1990).

South of Sunset State Beach (see pl. 1), along the Monterey County coast, small landslides were observed along the seacliffs as far south as the Big Sur area (figs. 1, 14). The southernmost landslide, a small rock fall, was

reported from a locality known locally as Raining Rocks Point (Edwin L. Harp, oral commun., 1989), in an apparent reference to the common occurrence of rock falls there.

#### PERIPHERAL AREA

Outside the southern Santa Cruz Mountains and the coastal area, landslides occurred at widely separated localities throughout an additional 13,000 km<sup>2</sup> of the San Francisco Bay-Monterey Bay region. Several dozen landslides, mostly small rock falls, rock slides, or soil slides less than 100 m<sup>3</sup> in volume, were mapped. However, the mapping in this area was not as thorough as in the Santa Cruz Mountains, and extrapolating from available observations, several hundred landslides may actually have occurred in this area. The east limit of the landslide-affected area was determined as a line through reported landslide

localities near San Ardo, at Pacheco Pass, near Livermore, and through Mount Diablo (fig. 1). A few landslides in this peripheral area were rotational slumps.

One large, particularly destructive landslide was reported in central San Francisco, along Eighth Avenue between Ortega and Moraga Streets (Seed and others, 1990; J.J. Lienkaemper, unpub. data, 1990). The slope on which the landslide occurred was approximately 22°–38° and was composed of dry, loose to weakly cemented dune sand. The landslide formed a zone of cracks about 350 m long, with estimated maximum displacements of 10 to 20 cm. These cracks were near the top of the slope, which was about 20 to 35 m high. At least 30 residences were destroyed or heavily damaged by the landslide displacement (Seed and others, 1990). Indications of slope instability had been reported since the first houses were built there, approximately 50 years before the earthquake (Seed and others, 1990).



A

Figure 13.—Ridgecrest fissure and associated landslide along Robinwood Way (see pl. 2 for location). *A*, Ground crack, also breaking pavement and foundation slab. Crack is nearly linear, trends parallel to long axis of steep, high, narrow ridge, and is immediately upslope from slump shown in figure 13*B*. Downslope direction is toward right. *B*, Rotational slump originating on edge of ridgecrest, immediately below ground crack shown in figure 13*A*. Position and orientation of crack and relation to slump indicate that crack is an incipient landslide feature.

## DISCUSSION AND CONCLUSIONS

The 1989 Loma Prieta earthquake generated landslides throughout an area of about 15,000 km<sup>2</sup>. Category I landslides occurred as far as 133 km from the epicenter and 100 km from the rupture zone (fig. 1); category II landslides occurred as far as 111 km from the epicenter and 99 km from the rupture zone. These area and maximum distance values are within the ranges of similar data compiled from other historical earthquakes (figs. 16–18). However, most of the landslides triggered by the 1989 Loma Prieta earthquake (75–85 percent of estimated total; see below) were within a comparatively small area of about 2,000 km<sup>2</sup> in the southern Santa Cruz Mountains and within 25 km of the fault zone. Similar concentrations of landslides relatively close to a fault rupture were noted in the 1980 Mammoth Lakes, Calif., earthquake ( $M_S=6.1$ ) and the 1980 Mount Diablo, Calif., earthquake ( $M_S=5.8$ ),

two of the only three other earthquakes for which such data have been reported (Keefer and Wilson, 1989).

Estimates of the total number of landslides generated by the earthquake (exclusive of those caused by soil liquefaction) range from the approximately 1,500 actually mapped (1,280 in the southern Santa Cruz Mountains, 80 along the coast, and several dozen elsewhere) to approximately 4,000 (3,000 in the southern Santa Cruz Mountains, as extrapolated from mapping in Forest of Nisene Marks State Park, and a few hundred elsewhere).

Studies of other historical earthquakes have shown that the total number of landslides generated by an earthquake of a given magnitude varies widely, depending on the geologic conditions in the affected region and the characteristics of the ground motion (Keefer, 1984; Keefer and Wilson, 1989). Keefer and Wilson, who presented data from eight previous earthquakes of  $M_S=7.0-7.2$ , estimated that the numbers of landslides generated by those earth-



B

Figure 13.—Continued.

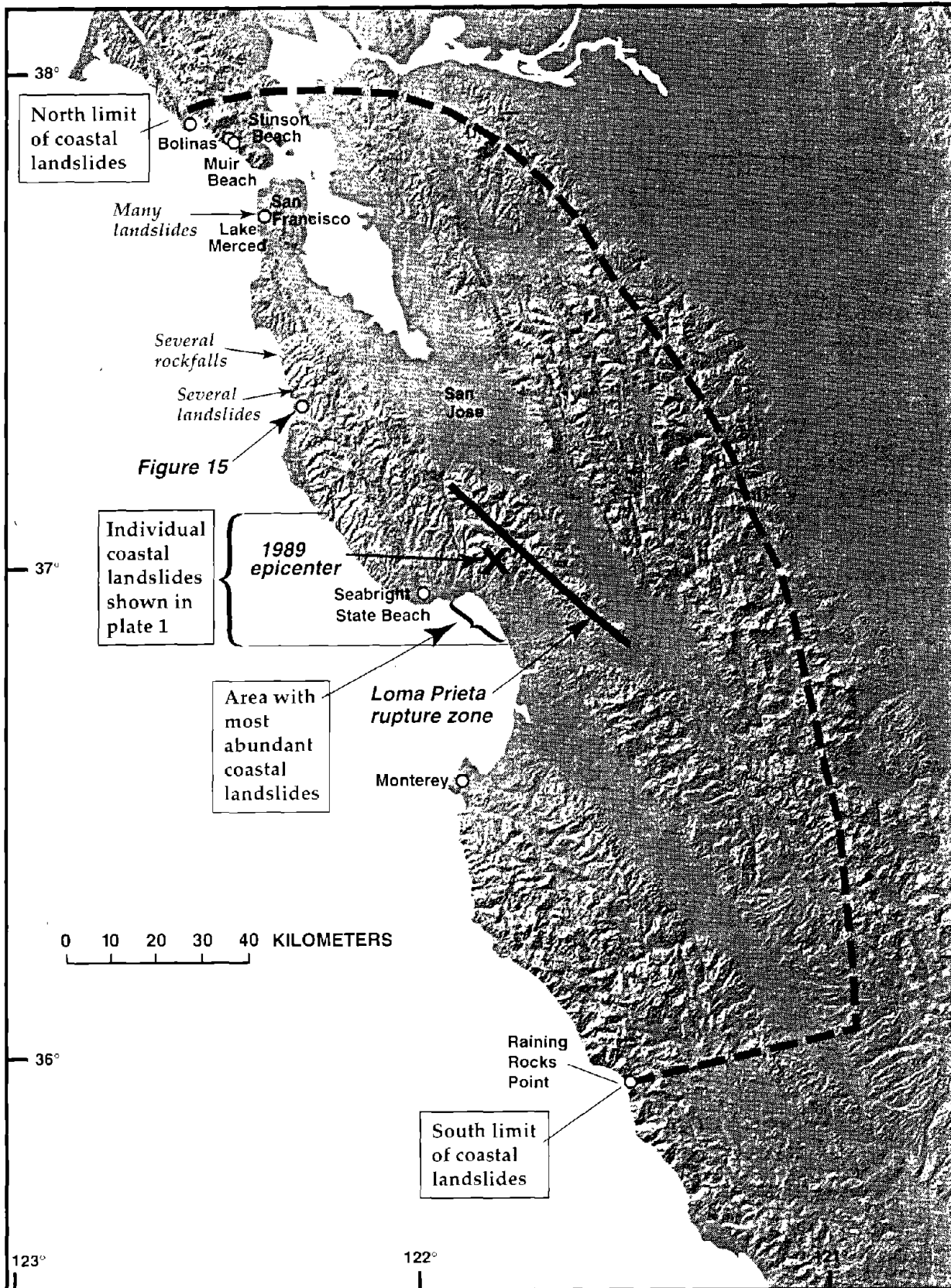


Figure 14.—San Francisco Bay-Monterey Bay region, showing limits of coastal landslides and areas of abundant coastal landslides. Base map from Edwards and Batson (1990).

quakes ranged from less than 100 to 20,000. The number of landslides generated by the 1989 Loma Prieta earthquake falls in about the middle of this range. The high proportion of category I landslides generated by the earthquake (74 percent of those in the southern Santa Cruz Mountains and most of those elsewhere) is also consistent with data from other historical earthquakes (Keefer, 1984; Keefer and Wilson, 1989).

Most category I landslides generated by the 1989 Loma Prieta earthquake involved weakly to moderately cemented rocks that locally were deeply weathered, closely fractured, and (or) broken by conspicuous, throughgoing joints. A significant number also occurred in preexisting landslide deposits. Preexisting landslide deposits and rocks with such characteristics have been identified as highly to extremely highly susceptible to slope failure, on the basis



Figure 15.—Coastal landslide about 0.8 km south of mouth of San Gregorio Creek (see fig. 14 for location). Toe of deposit is approximately 60 m wide. Photograph by Mary M. Donato, U.S. Geological Survey.

of studies of other earthquakes (Keefer, 1984, 1993); many of the specific geologic units that produced abundant landslides had also been previously identified as particularly susceptible to failure (Wieczorek and others, 1985). Similarly, category II landslides were mostly in materials previously identified as highly susceptible to failure, especially uncemented to poorly cemented artificial fills, alluvium, and many of the same rock types that produced category I landslides (Keefer, 1984).

The distribution of landslides generated by the earthquake was significantly asymmetric with respect to the rupture zone (fig. 1): In the southern Santa Cruz Mountains, 85 percent of the category I landslides and 95 percent of the category II landslides were southwest of the San Andreas fault. This asymmetry probably is due mostly to differences in geologic conditions on the two sides of the fault: Relatively weakly consolidated rocks (primarily Tertiary sedimentary rocks) are significantly more abundant southwest of the fault than to the northeast. The southwest side of the fault, however, was also the hanging-wall block above a high-angle reverse fault and underwent tectonic ground-surface deformation as well;

thus, the asymmetry could also be partly due to this condition.

Outside the southern Santa Cruz Mountains, the slopes most susceptible to failure, as indicated by the number and size of landslides, were the seacliffs along the Pacific coast. This high susceptibility also conforms to findings in other historical earthquakes, including the 1906 San Francisco earthquake (Lawson, 1908).

Three aspects of the landsliding that were anomalous relative to other earthquakes were (1) the occurrence of large, complex landslides in the Summit Ridge area (fig. 1); (2) the generation of large, deep-seated block slides from the ends of prominent ridges; and (3) the occurrence of ground cracks at hundreds of localities in the southern Santa Cruz Mountains. The large, complex landslides in the Summit Ridge area are described in more detail by Keefer and others (this chapter). These landslides were restricted to an area of pervasive ground cracking adjacent to the San Andreas fault, and their generation probably is directly related to that ground cracking. Descriptions of similar landslides are rare in reports on previous earthquakes (see Harp, this chapter), and so the

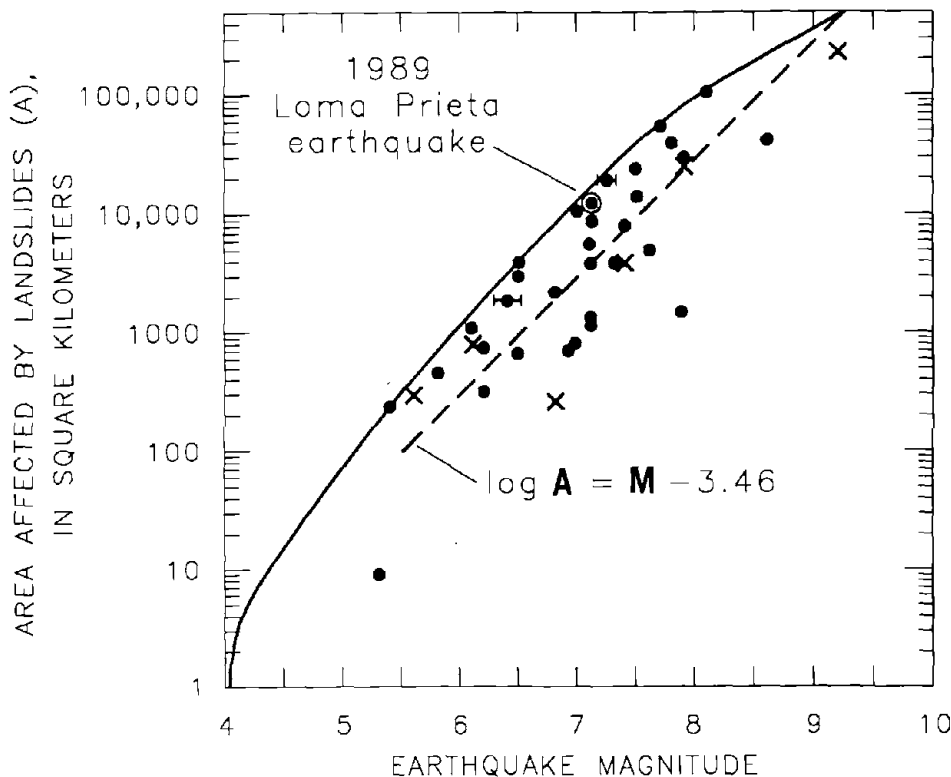


Figure 16.—Area of landslides generated by 1989 Loma Prieta earthquake,  $A$ , as a function of earthquake magnitude,  $M$ , in comparison with other historical earthquakes with epicenters onshore (dots) and offshore (x's). Most data points and upper-bound curve (solid line) from Keefer (1984); additional data points and log-linear mean (dashed line) from Keefer and Wilson (1989).

Summit Ridge landslides are manifestations of a newly recognized, probably recurrent hazard in areas adjacent to some fault traces.

The generation of large, deep-seated block slides from the ends of prominent ridges was also an occurrence not recognized in reports on previous earthquakes, although previous studies had identified the ends of ridges as susceptible to shallow rock falls (for example, Harp and others, 1981). The block slides in the Santa Cruz Mountains were marked by the occurrence of small rock falls along their flanks, and other earthquake-induced rock falls in similar environments might also indicate the presence of larger, deeper seated landslides. The ends of prominent ridges in the Santa Cruz Mountains thus are also environments subject to a newly recognized, probably recurrent hazard.

Finally, the earthquake generated ground cracks at hundreds of localities in the southern Santa Cruz Mountains. Many of these ground cracks showed characteristics consistent with the formation of incipient landslides. In similar environments, the 1906 San Francisco earthquake,

which occurred when ground conditions were comparatively wet, generated abundant deep-seated landslides (Lawson, 1908). Under wetter conditions and (or) more severe ground shaking during the Loma Prieta earthquake, many of these zones of ground cracks probably would have developed into large, deep-seated landslides, and so the magnitude of landslide damage could have been much greater.

## ACKNOWLEDGMENTS

We gratefully acknowledge the following people who mapped the landslides generated by the earthquake: A.G. Barrows, R.L. Baum, T.L. Bedrossian, K. Boyle, R. Brumbaugh, W.A. Bryant, J. Bussman, R.H. Campbell, M.C. Carey, S. Carson, K.H. Custis, M.M. Donato, G. Dunfield, R. Gibson, C. Giovannoni, T. Goddard, G.B. Griggs, S. Guiney, K.M. Haller, J. Hayes, R. Haltenhoff, E.L. Harp, D. Hope, J.K. Howard, P. Irvine, R.W. Jibson, D. Johnston, M. Jordan, P. Levine, H.H. Majmundar, M.A. McKittrick, D. Murray, J.M. Nolan, S.F. Personius, D.M.

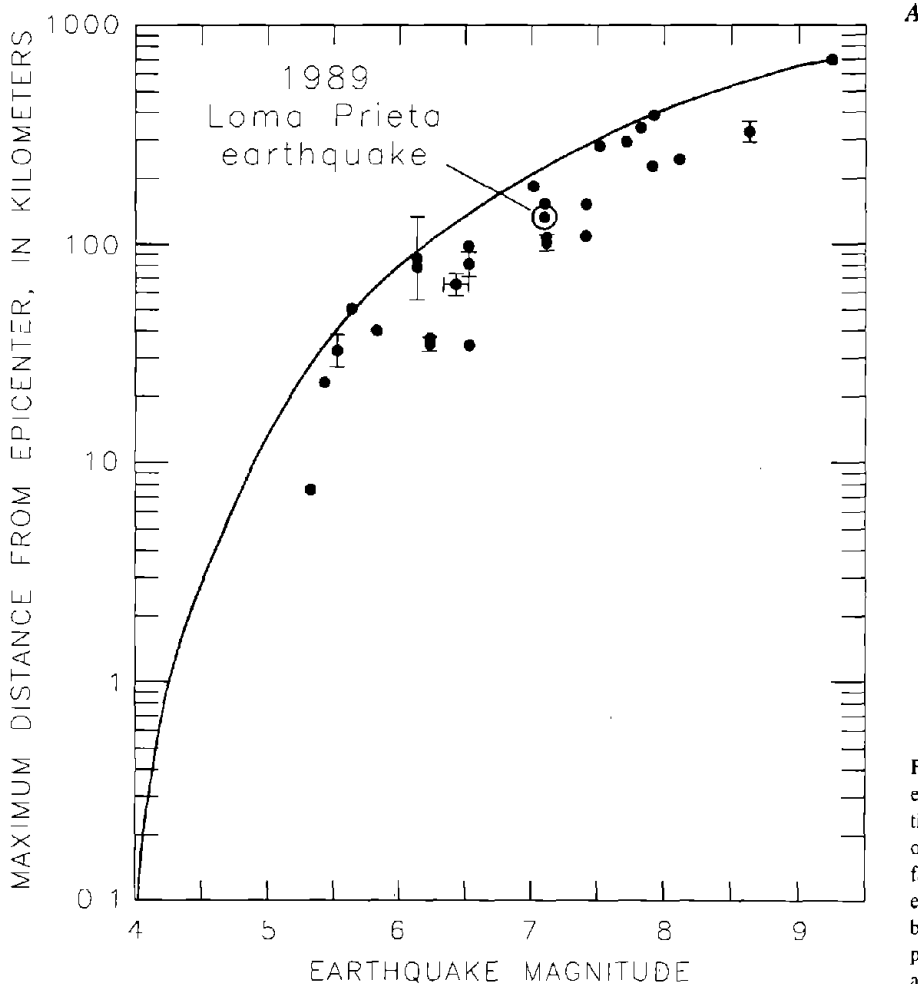


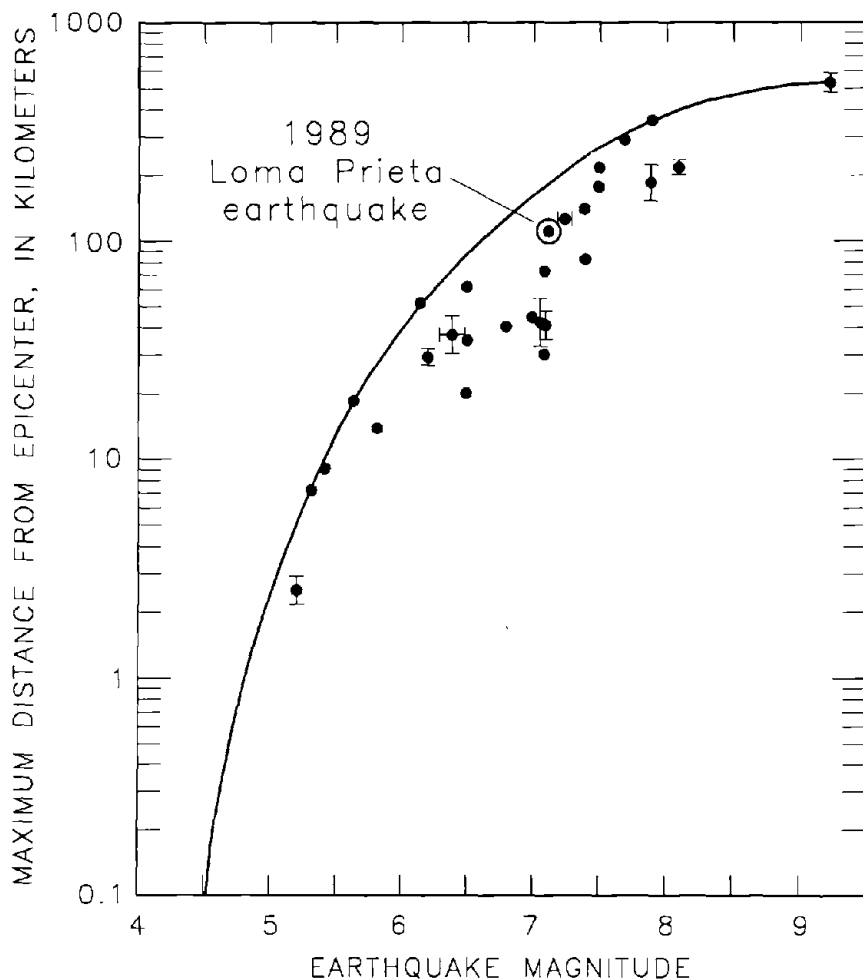
Figure 17.—Maximum distance of landslides from epicenter of 1989 Loma Prieta earthquake as a function of earthquake magnitude, in comparison with other historical earthquakes. *A*. Disrupted slides and falls (category I landslides). *B*. Coherent slides (category II landslides). Most data points and upper-bound lines from Keefer (1984); additional data points from Wiczorek and Keefer (1987) and Harp and Keefer (1990).



Peterson, N.G. Plant, R. Powers, J. Rigby, J.P. Schlosser, K.M. Schmidt, R.L. Schuster, J.E. Slosson, R. Smith-Evernden, J.A. Sowma, T.E. Spittler, J.G. Staude, L.R. Stevens, R.H. Sydnor, S. Tan, J. Thornberg, J.C. Tinsley, J. Treiman, J. Van Velsor, B.V. Vassil, D.L. Wagner, G.E. Weber, G.F. Wiczorek, C.J. Wills, and R.C. Wilson. Sarah Christian, Monique Jaasma, Donna Knifong, and Carl Wentworth helped with the analysis of digital data. The manuscript was improved by the thoughtful reviews of Gerald Wiczorek and Raymond Wilson.

### REFERENCES CITED

- Alger, C.S., and Brabb, E.E., 1985, Bibliography of United States landslide maps and reports: U.S. Geological Survey Open-File Report 85-585, 119 p.
- Aydin, Atilla, Johnson, A.M., and Fleming, R.W., in press, Coseismic right-lateral and left-lateral surface rupture and landsliding along the San Andreas and Sargent fault zones during the earthquake. in Ponti, D.J., ed., *The Loma Prieta, California, earthquake of October 17, 1989—ground ruptures*: U.S. Geological Survey Professional Paper 1551-D.
- Bonilla, M.G., 1960, Landslides in the San Francisco south quadrangle, California: U.S. Geological Survey Open-File Report, 44 p.
- Brabb, E.E., 1989, Geologic Map of Santa Cruz County, California: U.S. Geological Survey Miscellaneous Investigations Series Map I-1905, scale 1:62,500.
- Brabb, E.E., and Dibblee, T.W., Jr., 1979, Preliminary geologic map of the Castle Rock Ridge quadrangle, Santa Cruz and Santa Clara Counties, California: U.S. Geological Survey Open-File Report 79-659, scale 1:24,000.
- Brabb, E.E., and Pampeyan, E.H., compilers, 1983, Geological map of San Mateo County, California: U.S. Geological Survey Miscellaneous Investigations Series Map I-1257-A, scale 1:62,500.
- Brabb, E.E., Pampeyan, E.H., and Bonilla, M.G., 1972, Landslide susceptibility in San Mateo County, California: U.S. Geological Survey Miscellaneous Field Studies Map MF-360, scale 1:62,500.
- Brown, W.M., III, 1988, Historical setting of the storm; perspectives on population, development, and damaging rainstorms in the San Francisco Bay region, chap. 1 of Ellen, S.D., and Wiczorek, G.F., eds.,



**B**

Figure 17.—Continued.

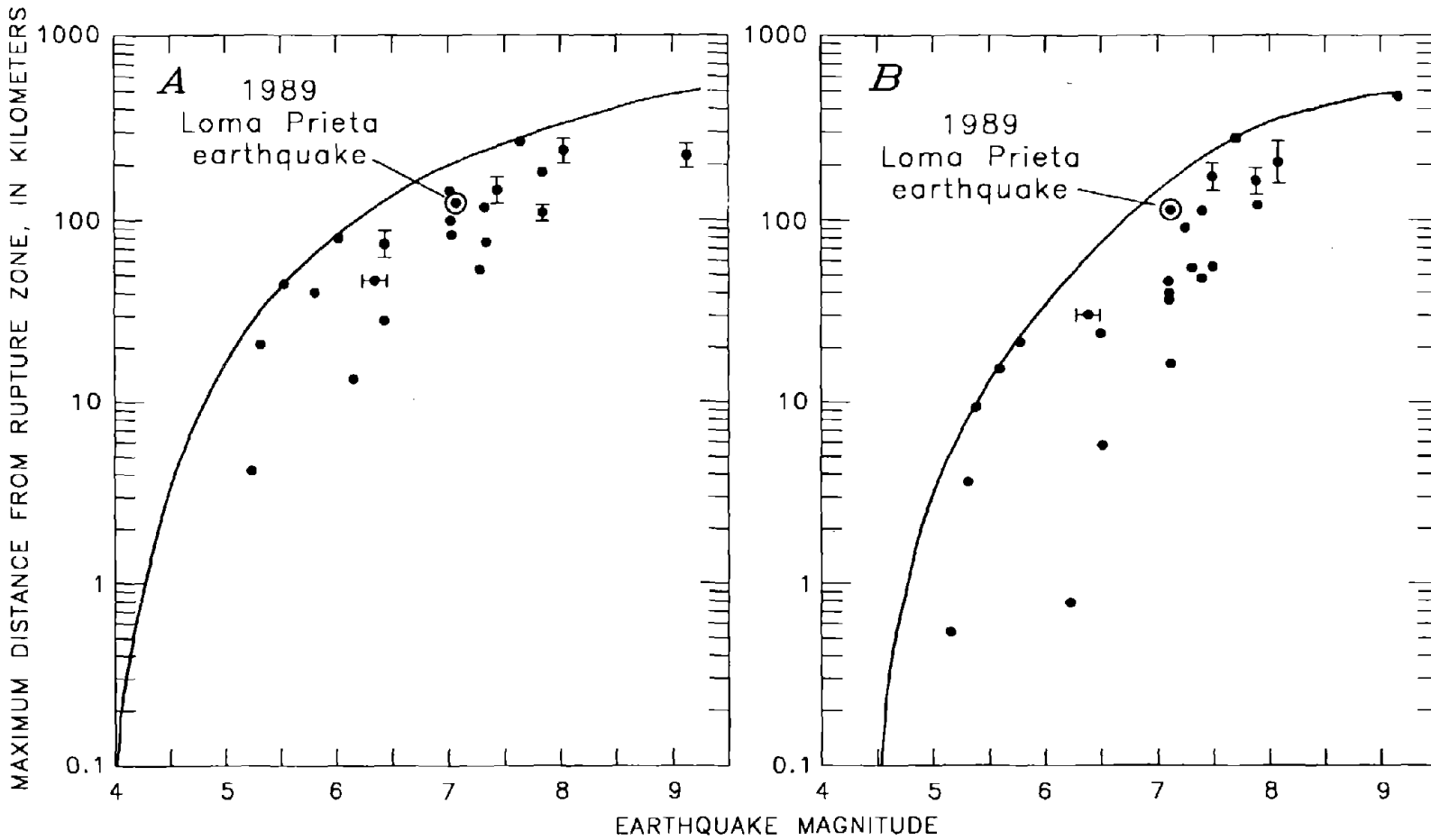


Figure 18. Maximum distance of landslides from rupture zone of 1989 Loma Prieta earthquake (fig. 1) as a function of earthquake magnitude, in comparison with other historical earthquakes. A, Disrupted slides and falls (category I landslides). B, Coherent slides (category II landslides). Most data points and upper-bound lines from Keefer (1984); additional data points from Keefer and Wilson (1989).

- 1988, Landslides, floods, and marine effects of the storm of January 3-5, 1982, in the San Francisco Bay region, California: U.S. Geological Survey Professional Paper 1434, p. 7-15.
- Clark, J.C., Brabb, E.E., and McLaughlin, R.J., 1989, Geologic map and structure sections of the Laurel 7 1/2' Quadrangle, Santa Clara and Santa Cruz counties, California: U.S. Geological Survey Open-File Map 89-676, 31 p., scale 1:24,000, 2 sheets.
- Cole, W.J., Marcum, D.R., Shires, P.O., and Clark, B.R., 1991, Investigation of landsliding triggered by the Loma Prieta earthquake and evaluation of analysis methods: final technical report to U.S. Geological Survey under contract 14-08,001-G1860, 33 p.
- Cooper-Clark and Associates, 1975, Preliminary map of landslide deposits in Santa Cruz County, California, in *Seismic safety element: Santa Cruz, Calif.* Santa Cruz County Planning Department, scale 1:62,500.
- Dibblee, T.W., Jr. and Brabb, E.E., 1978, Preliminary geologic maps of the Chittenden, Los Gatos, and Watsonville East quadrangles, California: U.S. Geological Survey Open-File Report 78-453, scale 1:24,000, 3 sheets.
- Edwards, Kathleen, and Batson, R.M., 1990, Experimental digital shaded-relief maps of California: U.S. Geological Survey Miscellaneous Investigations Series Map 1-1848, scale 1:1,000,000, 2 sheets.
- Ellen, S.D., and Wieczorek, G.F., eds., 1988, Landslides, floods, and marine effects of the storm of January 3-5, 1982, in the San Francisco Bay region, California: U.S. Geological Survey Professional Paper 1434, 310 p.
- Ellen, S.D., Wieczorek, G.F., Brown, W.M., III, and Herd, D.G., 1988, Introduction, in Ellen, S.D., and Wieczorek, G.F., eds., 1988, Landslides, floods, and marine effects of the storm of January 3-5, 1982, in the San Francisco Bay region, California: U.S. Geological Survey Professional Paper 1434, p. 1-5.
- Hanks, T.C., and Krawinkler, Helmut, 1991, The 1989 Loma Prieta, California, earthquake and its effects; introduction to the special issue: *Seismological Society of America Bulletin*, v. 81, no. 5, p. 1415-1423.
- Harp, E.L., and Keefer, D.K., 1990, Landslides triggered by the earthquake, in Rymer, M.J., and Ellsworth, W.L., eds., *The Coalinga, California, earthquake sequence of May 2, 1983*: U.S. Geological Survey Professional Paper 1487, p. 335-348.
- Harp, E.L., Wilson, R.C., and Wieczorek, G.F., 1981, Landslides from the February 4, 1976, Guatemala earthquake: U.S. Geological Survey Professional Paper 1204-A, 35 p.
- Holzer, T.L., ed., in press, *The Loma Prieta, California, earthquake of October 17, 1989—liquefaction*: U.S. Geological Survey Professional Paper 1551-B.
- Keefer, D.K., 1984, Landslides caused by earthquakes: *Geological Society of America Bulletin*, v. 95, no. 4, p. 406-421.
- , 1993, The susceptibility of rock slopes to earthquake-induced failure: *Association of Engineering Geologists Bulletin*, v. 30, no. 3, p. 353-361.
- , ed., 1991, Geologic hazards in the Summit Ridge area of the Santa Cruz Mountains, Santa Cruz County, California, evaluated in response to the October 17, 1989, Loma Prieta earthquake; report of the Technical Advisory Group: U.S. Geological Survey Open-File Report 91-618, 427 p.
- Keefer, D.K., and Wilson, R.C., 1989, Predicting earthquake-induced landslides, with emphasis on arid and semi-arid environments, in Sadler, P.M., and Morton, D.M., eds., *Landslides in a semi-arid environment with emphasis on the Inland Valleys of Southern California*: Riverside, Calif., Inland Geological Society of Southern California Publications, v. 2, pt. 1, p. 118-149.
- Keefer, D.K., Wilson, R.C., Mark, R.K., Brabb, E.E., Brown, W.M., III, Ellen, S.D., Harp, E.L., Wieczorek, G.F., Alger, C.S., and Zatkun, R.S., 1987, Real-time landslide warning during heavy rainfall: *Science*, v. 238, no. 4829, p. 921-925.
- Lawson, A. C., chairman, 1908, *The California earthquake of April 18, 1906*; report of the State Earthquake Investigation Commission: Carnegie Institution of Washington Publication 87, 2 v.
- Manson, M.W., Keefer, D.K., and McKittrick, M.A., compilers, 1992, *Landslides and other geologic features in the Santa Cruz Mountains, California, resulting from the Loma Prieta earthquake of October 17, 1989*: California Division of Mines and Geology Open-File Report 91-08, 45 p.
- Marshall, G.A., Stein, R.S., and Thatcher, Wayne, 1991, Faulting geometry and slip from coseismic elevation changes; the 18 October, 1989 Loma Prieta, California, earthquake: *Seismological Society of America Bulletin*, v. 81, no. 5, p. 1660-1693.
- Marshall, J.S., 1990, History of landsliding associated with prior earthquakes in the Santa Cruz Mountains, app. C of Griggs, G.B., Rosenbloom, N.A., and Marshall, J.S., 1990, Investigation and monitoring of ground cracking and landslides initiated by the October 17, 1989 Loma Prieta earthquake: Santa Cruz, Calif., Gary B. Griggs and Associates, unpaginated.
- McLaughlin, R.J., Clark, J.C., and Brabb, E.E., 1988, Geologic map and structure sections of the Loma Prieta 7 1/2' Quadrangle, Santa Clara and Santa Cruz counties, California: U.S. Geological Survey Open-File Map 88-752, 32 p., scale 1:24,000, 2 sheets.
- McLaughlin, R.J., Clark, J.C., Brabb, E.E., and Helley, E.J., 1991, Geologic map and structure sections of the Los Gatos 7 1/2' Quadrangle, Santa Clara and Santa Cruz counties, California: U.S. Geological Survey Open-File Report 91-593, 48 p., scale 1:24,000, 3 sheets.
- O'Rourke, T.D., ed., 1992, *The Loma Prieta, California, earthquake of October 17, 1989—Marina District*: U.S. Geological Survey Professional Paper 1551-F, p. F1-F215.
- Plafker, George, and Galloway, J.P., eds., 1989, *Lessons learned from the Loma Prieta, California, earthquake of October 17, 1989*: U.S. Geological Survey Circular 1045, 48 p.
- Plant, Nathaniel, and Griggs, G.B., 1990, Coastal landslides caused by the October 17, 1989 earthquake Santa Cruz County, California: *California Geology*, v. 43, no. 4, p. 75-84.
- Ponti, D.J., and Wells, R.E., 1991, Off-fault ground ruptures in the Santa Cruz Mountains, California: ridge-top spreading versus tectonic extension during the 1989 Loma Prieta earthquake: *Seismological Society of America Bulletin*, v. 81, no. 5, p. 1480-1510.
- Rantz, S.E., 1971, Mean annual precipitation and precipitation depth-duration-frequency data for the San Francisco Bay region, California: U.S. Geological Survey Open-File Report, 23 p.
- Seed, R.B., Dickenson, S.E., Reimer, M.F., Bray, J.D., Sitar, Nicholas, Mitchell, J.K., Idriss, I.M., Kayen, R.E., Kropp, Alan, Harder, L.F., Jr., and Power, M.S., 1990, Preliminary report on the principal geotechnical aspects of the October 17, 1989 Loma Prieta earthquake: Berkeley, University of California, Earthquake Engineering Research Center Report UCB/EERC-90/05, 137 p.
- Spittler, T.E., and Harp, E.L., compilers, 1990, Preliminary map of landslide features and coseismic fissures, in the Summit Road area of the Santa Cruz Mountains, triggered by the Loma Prieta earthquake of October 17, 1989: U.S. Geological Survey Open-File Report 90-688, 31 p., scale 1:4,800, 3 sheets.
- Spittler, T.E., Harp, E.L., Keefer, D.K., Wilson, R.C., and Sydnor, R.H., 1990, Landslide features and other coseismic fissures triggered by the Loma Prieta earthquake, central Santa Cruz Mountains, California, in McNutt, S.R., and Sydnor, R.H., eds., *The Loma Prieta (Santa Cruz Mountains), California earthquake of 17 October 1989*: California Division of Mines and Geology Special Publication 104, p. 59-66.
- Sydnor, R.H., Griggs, G.B., Weber, G.E., McCarthy, R.J., and Plant, Nathaniel, 1990, Coastal bluff landslides in Santa Cruz County resulting from the Loma Prieta earthquake of 17 October 1989, in McNutt, S.R., and Sydnor, R.H., eds., *The Loma Prieta (Santa Cruz Mountains), California earthquake of 17 October 1989*:

- California Division of Mines and Geology Special Publication 104, p. 67-82.
- Thomas, J.H., 1961, *Flora of the Santa Cruz Mountains of California; a manual of the vascular plants*: Stanford, Calif., Stanford University Press, 434 p.
- U.S. Geological Survey, 1990, *The next big earthquake in the Bay Area may come sooner than you think*: Menlo Park, Calif., 23 p.
- U.S. Geological Survey staff, 1989, *Preliminary map of fractures formed in the Summit Road-Skyland Ridge area during the Loma Prieta, California, earthquake of October 17, 1989*: U.S. Geological Survey Open-File Report 89-686, scale 1:12,000.
- Varnes, D. J., 1978, *Slope movement types and processes*, in Schuster, R.L., and Krizek, R.J., eds., *Landslides—analysis and control*: U.S. National Academy of Sciences, Transportation Research Board Special Report 176, p. 11-33.
- Weber, G.E., and Nolan, J.M., 1989, *Landslides and associated ground failure in the epicentral region of the October 17, 1989, Loma Prieta earthquake*: final technical report to U.S. Geological Survey under contract 14-08-0001-G1861, 26 p.
- Wesnowsky, S.G., 1986, *Earthquakes, Quaternary faults, and seismic hazards of California*: *Journal of Geophysical Research*, v. 91, no. B12, p. 12587-12631.
- Wieczorek, G.F., and Keefer, D.K., 1987, *Earthquake-triggered landslide at La Honda, California*, in Hoose, S.N., ed., *The Morgan Hill, California, earthquake of April 24, 1984*, U.S. Geological Survey Bulletin 1639, p. 73-79.
- Wieczorek, G.F., Wilson, R.C., and Harp, E.L., 1985, *Map showing slope stability during earthquakes in San Mateo County, California*: U.S. Geological Survey Miscellaneous Investigations Series Map I-1257-E, scale 1:62,500.
- William Cotton and Associates, Inc., 1990, *Schultheis Road and Villa Del Monte areas geotechnical exploration Santa Cruz County, California*: Los Gatos, Calif., report to U.S. Army Corps of Engineers, 2 v.
- Working Group on California Earthquake Probabilities, 1990, *Probabilities of large earthquakes in the San Francisco Bay region, California*: U.S. Geological Survey Circular 1053, 51 p.
- Youd, T.L., and Hoose, S.N., 1978, *Historic ground failures in northern California triggered by earthquakes*: U.S. Geological Survey Professional Paper 993, 177 p.

THE LOMA PRIETA, CALIFORNIA, EARTHQUAKE OF OCTOBER 17, 1989:  
STRONG GROUND MOTION AND GROUND FAILURE

LANDSLIDES

COASTAL-BLUFF FAILURES IN NORTHERN MONTEREY BAY  
INDUCED BY THE EARTHQUAKE

By Gary B. Griggs,  
University of California, Santa Cruz;  
and  
Nathaniel Plant,  
Oregon State University

CONTENTS

INTRODUCTION

	Page
Abstract .....	C33
Introduction .....	33
The 1989 Loma Prieta earthquake .....	37
Coastal-bluff failures in northern Monterey Bay .....	37
Summary and implications for land-use planning .....	41
Recommendations .....	43
References cited .....	50

ABSTRACT

The 1989 Loma Prieta earthquake caused bluff failures along 240 km of coastline between Marin County and the Big Sur coast of Monterey County, in various rock types and under varying slope conditions. Peak accelerations of 0.54 g horizontal and 0.60 g vertical were measured 10 km from the epicenter on the coast at Capitola. Coastal-bluff failures were most common nearest the epicenter, where extensive blufftop cracking and collapse led ultimately to the demolition of three homes and six apartment units. One death and several million dollars in damage were attributed to coastal landslides. Three types of coastal bluff failures were documented: (1) block falls in well-consolidated sedimentary rocks, (2) translational slides in more friable sandstone, and (3) sandflows in Quaternary dune deposits. Long-term stability of the central-coast bluffs, which underwent tensional cracking as far as 10 m inland from the bluff edge, is uncertain. The potential for earthquake-induced bluff failures exists along virtually the entire coastline of California, owing to the presence of active faults throughout the region. To date, however, this hazard has not been widely recognized.

At least 86 percent of California's 1,750 km of shoreline is actively eroding, while 80 percent of the State's population now live within 50 km of the coast. The conflict between the population growth and the inherent instability of much of the shoreline has become increasingly apparent in recent years, with \$150 million in coastal storm damage during the decade 1978-88 alone.

Coastal erosion along the California shoreline is dominated by episodic events, typically the simultaneous occurrence of large storm waves and high tides. Although coastal-bluff erosion is commonly perceived as primarily a wave-induced phenomenon, seacliff failure is also a sub-aerial process. Landslides, slumps, and debris flows occur in response to elevated pore pressures resulting from either intense rainfall or elevated ground-water conditions, or overloading or oversteepening of a coastal bluff. Another significant process affecting coastal-cliff retreat is seismic shaking during large earthquakes. Although coastal-protection structures have slowed erosion of the coastline by wave action in some areas, failures continue to take place along both protected and unprotected bluffs, owing to terrestrial processes (fig. 1).

The potential for earthquakes that can affect coastal bluffs is significant along the entire length of the State's coastline (fig. 2). Of principal concern in northern California is the active San Andreas fault system, which follows the shoreline from Cape Mendocino to the San Francisco peninsula. Along the central California coast, the active San Gregorio-Hosgri fault extends from north of San Francisco southwesterly along the shoreline of San Mateo and northern Santa Cruz counties, across Monterey Bay, and along the coast of Monterey, San Luis Obispo, and northern Santa Barbara Counties. The Santa Ynez,

More Ranch, Mesa, Arroyo Parida, and Oakridge faults extend along or intersect the shoreline between Point Conception and Ventura. The Malibu Coast, Palos Verdes, and Newport-Inglewood faults traverse or intersect the shoreline of Los Angeles County and the northern part of Orange County. Finally, the Rose Canyon Fault parallels the coast of much of San Diego County. No part of the coastline of California is more than 20 or 30 km from an active fault (Jennings, 1975), and most areas are considerably closer.

The effects of large earthquakes on coastal-bluff stability in central and northern California have generally been poorly documented, partly because of the infrequency of these events, the relatively short historical record in the region, the relatively low population densities along this part of the California coast at the time of previous large earthquakes, and, therefore, the absence of observations.

During the October 8, 1865, Santa Cruz Mountains earthquake ( $M=6.5$ ), the Santa Cruz *Sentinel* reported that "below Soquel the high cliffs crumbled into the sea" and "a continuous cloud of dust rose along the cliffs between Castro's Landing [now called Rio Del Mar] and Santa Cruz." One of us (N.P.) was on the beach at Rio Del Mar during the 1989 Loma Prieta earthquake and noted the same phenomenon: A continuous cloud of dust rose along the coastal bluffs as loose surficial material broke loose and cascaded downslope. During the great 1906 San Francisco earthquake ( $M=8.3$ ), "much earth fell from bluffs near the town [of Capitola]" (Lawson, 1908). Lawson documented bluff failures in 1906 extending from Capitola on the south to Eureka on the north, a distance of about 500 km. These few accounts constitute the extent of the readily available, published information describing historical earthquake-induced bluff failures along the

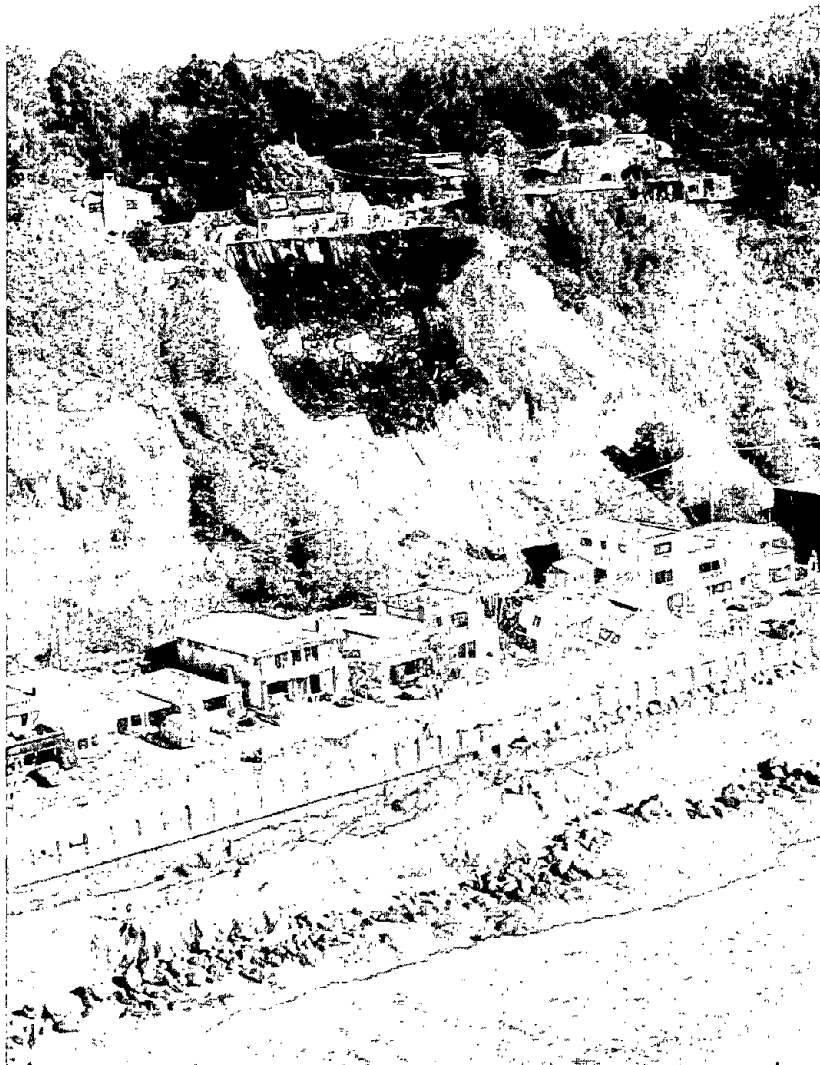


Figure 1.—Coastal-bluff failure in Rio Del Mar (see fig. 4 for location) during a 100-yr 24-hour rainstorm in January 1982.

Monterey Bay shoreline and lead to the following conclusions:

1. Large earthquakes apparently can cause instantaneous cliff retreat and weaken seacliffs through seismic shaking and the formation of cracks and fissures, which increase the seacliffs' susceptibility to failure. In addition to the hazards to structures or utilities at the top of a cliff, a risk also exists at the base of the seacliff, owing to the downslope movement, impact, and deposition of rock or soil from the adjacent cliff.

2. The intensity of development along the outer edge of the present seacliff along most of the California coast (fig. 3), relative to the location of coastal fault zones (fig. 2), indicates that the potential for cliff failures from seismic shaking was probably not considered when geologic or geotechnical evaluations were carried out, permits were issued, and construction took place.

A recent statewide evaluation of the coastal-bluff setbacks required by local governments for new construction indicates that a wide variety of approaches to this hazard

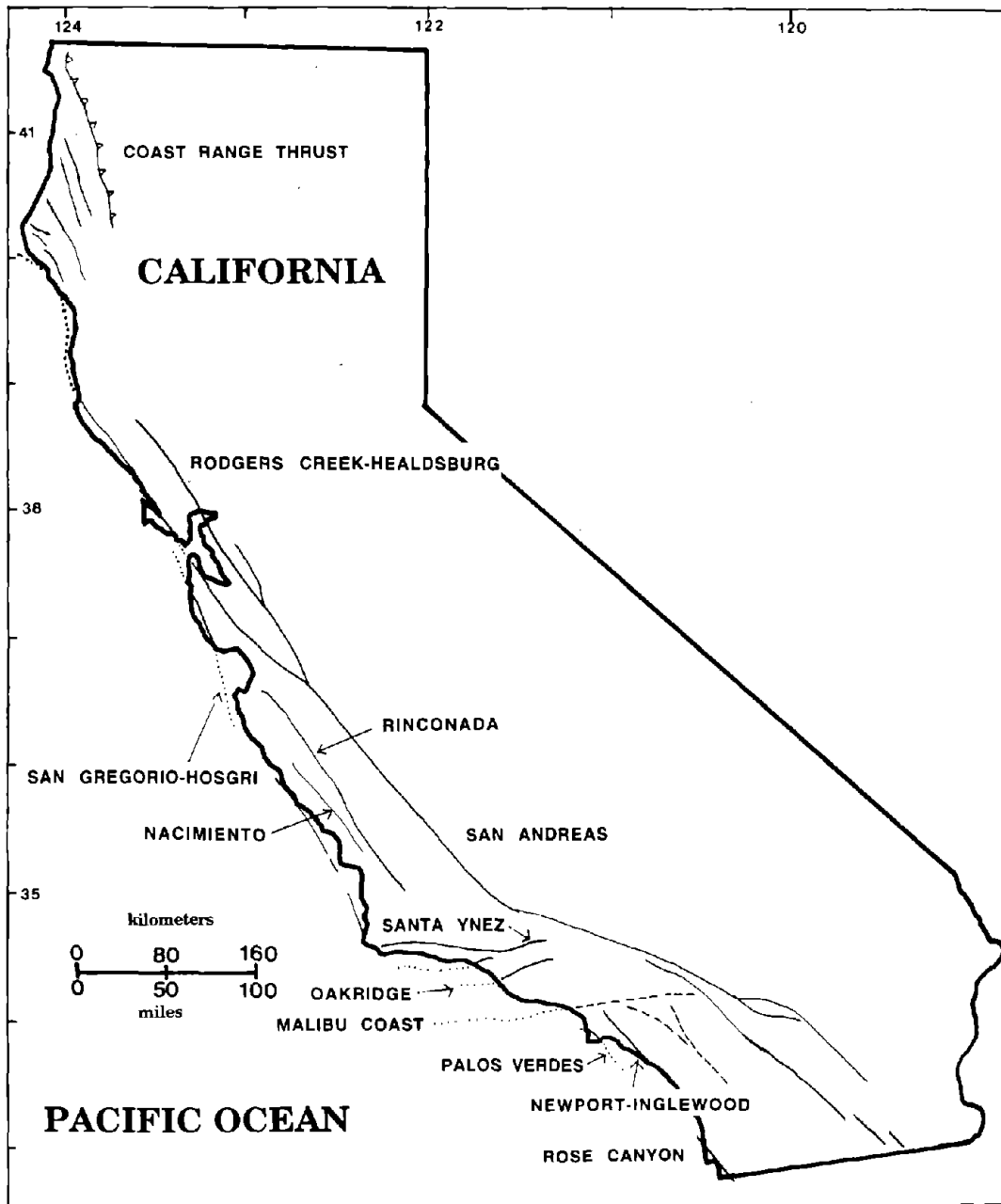


Figure 2.—California, showing locations of active faults (irregular thin lines, dashed where approximately located, dotted where concealed) and thrust faults (sawteeth on upper plate) with potential to affect coastal bluffs.

exist (Griggs and others, 1991). Some municipalities require a complete geologic report, written according to specific guidelines and subject to peer review, and a minimum setback of 16 to 48 m (50–150 ft) but also use a 50- to 75-year structural lifetime to calculate a precise setback. At the other end of the spectrum, one coastal city has a minimum 6-m (20-ft) setback and does not require a geologic report.

Several approaches have been used to analyze the potential for bluff failures during the lifetime of a proposed new development. A standard approach is to use aerial photography and maps to determine an average long-term cliff-recession rate, typically based on 25 to 50 years of data. Using an average erosional rate in combination with a structural lifetime, a safe setback distance can be established. The assumption with this approach is that the timeframe covered by available maps and photographs is representative of long-term conditions (that is, rainfall, storm frequency, sea level, and so on). The longer the data base, the more representative the calculated erosional rates should be.

Along the central California coast, all of the recent (past 150 years) historical earthquakes large enough to have potentially induced bluff failures took place before aerial photography. Evaluations of bluff stability under seismic

conditions, therefore, have had to rely on a combination of historical accounts, interpretation of more recent aerial photographs, existing bluff topography, and slope-stability analyses. These analyses have typically incorporated seacliff topography, strength parameters from blufftop or bluff-face borings, and peak accelerations based on a maximum probable earthquake. Slope-stability analysis is a common geotechnical tool; disruption of soil fabric during sampling, lateral and vertical variations in the strength of soil or rock, uncertainties in the peak horizontal accelerations at the site, and the role of ground water are important variables that affect the analysis. Whereas the strength values of the bedrock and overlying soils are used in the analysis, failure typically occurs along joint surfaces or other planes of weakness, such that the strength of the materials themselves may not be the critical factor affecting failure.

A key question in the evaluation of the potential for seismically induced bluff failures along this stretch of coast is whether historical failures are recognizable on older aerial photographs. For example, if deep-seated bluff failure took place during the 1906 San Francisco earthquake, should geomorphic evidence still be present 22 years later (1928) when the first aerial photographs were taken? The Monterey Bay region also sustained two  $M=6$  earthquakes



Figure 3.—Intense blufftop development along coast of San Diego County, showing use of seawalls and gunnite to reduce bluff failure.



in October 1926 (presumably located on the offshore San Gregorio-Hosgri fault zone), just 2 years before these first aerial photographs. Site-specific analysis of several coastal-bluff sites around the northern margin of Monterey Bay through interpretation of aerial photographs indicates no evidence of large-scale or deep-seated failures. Although shallow or surficial failures have taken place repeatedly, primarily during winter months of prolonged or intense rainfall (fig. 1), deep-seated or large-scale landsliding or slumping does not appear to have been common, at least during earthquakes in the 20th century.

### THE 1989 LOMA PRIETA EARTHQUAKE

The 1989 Loma Prieta earthquake ( $M=7.1$ ) ruptured a 40-km-long segment of the San Andreas fault zone in the Santa Cruz Mountains about 85 km south of San Francisco (fig. 4). This earthquake, which was the largest to strike the central California coast since 1906, was felt over an area of 1 million km<sup>2</sup>, from Los Angeles in the south to the California-Oregon State line in the north. Within 15 to 20 s, the earthquake resulted in 67 known deaths, 3,757 injuries, more than 18,000 homes and 2,500 businesses damaged, and more than 12,000 people homeless, as well as more than \$6 billion in damage (U.S. Geological Survey, 1989). The earthquake ruptured a segment of the San Andreas fault beneath the Santa Cruz Mountains that had been recognized as having the greatest probability (30 percent for the next 30 years) for producing an  $M=6.5-7$  earthquake of any fault segment north of the Mojave Desert in southern California (Plafker and Galloway, 1989).

The epicenter was about 8 km from the nearest segment of coastline. The most populous, densely developed section of coastal bluffs in Santa Cruz County sustained the most intense shaking. Four strong-motion-recording stations operated by the California Division of Mines and Geology provided quantitative records of shaking (Sydnor and others, 1990). At Capitola (fig. 4), about 13.5 km from the epicenter, the peak horizontal ground acceleration was 0.60 g, and the peak vertical acceleration was 0.54 g. These peak accelerations offer a unique opportunity to compare actual peak ground-motion data with seismic coefficients typically used in slope-stability analyses by geotechnical engineers.

Coastal-bluff failures resulting from the earthquake occurred along approximately 240 km of coastline between the town of Bolinas in the north to the Big Sur coast in the south, in various rock types and under varying slope conditions (Plant and Griggs, 1989). Failures were most prevalent closest to the epicenter between Seabright Beach to the northwest and Sunset Beach to the southeast (figs. 4, 5).

The bluff failures at Daly City, south of San Francisco (fig. 6), are significant because of their size, the proxim-

ity of many homes precariously close to the cliff edge, and the epicentral distance of about 80 km at this site. The materials exposed in the 100- to 150-m-high bluffs consist of weakly cemented sandstone and siltstone. On the basis of the strong-motion data recorded within 5 km of the site, peak accelerations were about 0.10 to 0.14 g. Considering the height of the bluff, the failure was relatively thin (4.5–6 m). The 1957 Daly City earthquake ( $M=5.7$ ), which generated similar accelerations, also produced significant landsliding along these bluffs, as well as apparent tension cracks landward of the crest of the bluffs (Sitar, 1990). However, the blufftop was not developed at that time.

The peninsular section of the San Andreas fault lies only a few hundred meters inland from these steep landslide-prone but intensively developed coastal cliffs. The most recent assessment of earthquake probabilities in the San Francisco Bay region (Working Group on California Earthquake Probabilities, 1990) concluded that there is a 67-percent probability for at least one earthquake of  $M\geq 7$  between 1990 and 2020. One of the fault segments most likely to rupture is the peninsular section of the San Andreas fault (fig. 4), which has been assessed as having a 23-percent probability of rupturing within the next 30 years. Depending on which of the San Francisco Bay region faults rupture, the intensity of future ground shaking within the area of figure 5 is estimated at 2 to 7 times greater than that sustained during the 1989 Loma Prieta earthquake (U.S. Geological Survey, 1990). The coastal bluffs along the Daly City shoreline probably will be severely disrupted during such an event.

### COASTAL-BLUFF FAILURES IN NORTHERN MONTEREY BAY

The type and extent of failures that took place along the seacliffs and bluffs of northern Monterey Bay were closely tied to the lithologies of the cliff-forming materials. Three general types of seismically induced landslides occurred in the coastal bluffs: rockfalls, translational slides, and sandflows (figs. 7–9). Sedimentary bedrock cliffs are particularly susceptible to earthquake-induced landslides where they are closely jointed or where the bedrock is unconsolidated or weakly cemented, and where the base of the cliff is unprotected from wave attack.

Between Seabright Beach and Capitola (fig. 4), seacliffs are cut into a marine terrace that is as much as 25 m high. The lower part of the cliff consists of thick-bedded to massive siltstone, mudstone, and very fine grained sandstone of the Purisima Formation. Even though this bedrock is well indurated, it is extensively jointed and susceptible to failure and toppling along joint surfaces. The coastline in this area parallels the most pronounced

set of joints, which typically dip steeply seaward. Overlying the sedimentary bedrock is as much as 6 m of unconsolidated terrace deposits consisting of marine cobbles, sand, and, commonly, a more cohesive, clay-rich soil horizon. The near-vertical seacliffs in this area are actively eroding where they are not protected by seawalls or riprap.

Seismic shaking during the earthquake initiated numerous rockfalls and block slides along this section of the coast (fig. 10). Undercut bedrock and fractured promonto-

ries toppled downslope, blufftop terrace deposits collapsed, and weakened bedrock failed. Horizontal and downslope separation along joint surfaces allowed large blocks to separate from more intact rock (fig. 7). The size of these failures was a function of joint spacing and orientation, frictional or cohesive strength along the joint surface, cliff height, and toe support. High cliffs with widely spaced, subvertical joints and poor toe support sustained the largest instantaneous and incipient failures in weakened or undercut sedimentary rocks.

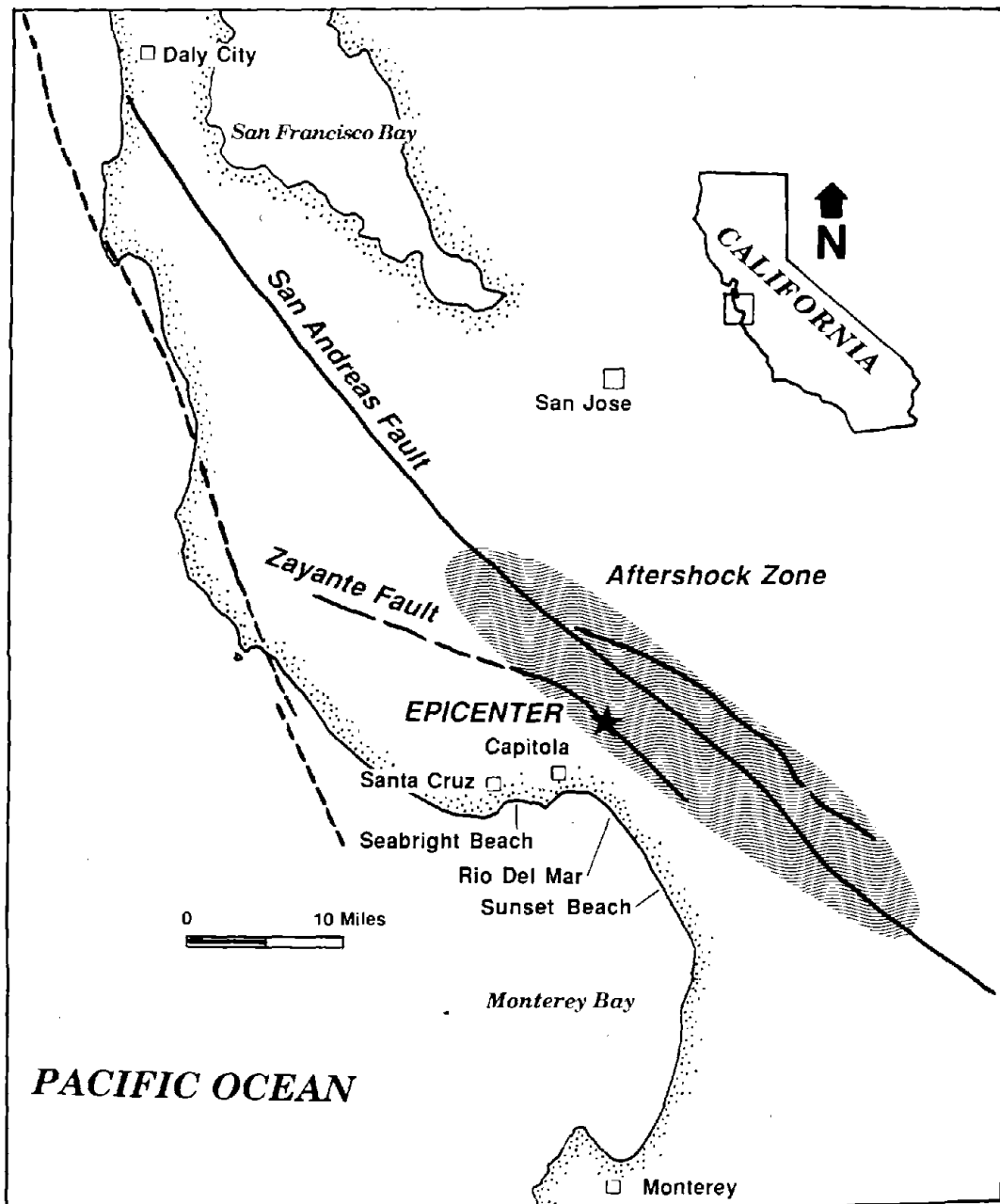


Figure 4.—San Francisco Bay-Monterey Bay region, Calif., showing locations of epicenter of 1989 Loma Prieta earthquake, aftershock zone, major faults (heavy lines, dashed where approximate, dotted where concealed), and coastal cities.

Damage to private property and public infrastructure was minimal along the cliffs in this area, except for those immediately east of Capitola (fig. 4). An apartment complex that was already overhanging the seacliff was additionally undermined as both bedrock and terrace deposits toppled to the beach below (fig. 11). Earthquake-induced failure led to partial loss of concrete caisson support and cracking of the foundation slab and perimeter wall of six apartments. Tension cracks were visible as far as 10 m inland of the cliff edge.

The apartment shown in figure 11 was originally built within a few meters of the bluff edge in 1967. Long-term (60 year) cliff-erosion rates at this site average 30 cm/yr (Griggs and Johnson, 1979). A cantilevered foundation was initially used to provide additional support in the event of the presumably anticipated foundation undermining due to the ongoing seacliff erosion. Continued bluff failure led to emplacement of a concrete caisson support system during the early 1980's. Plans to resupport the foundation and protect the base of the eroding bluff were in the design-review process at the time of the earthquake but were subsequently reconsidered by the project engineers and geologist. Owing to the extensive blufftop cracking, the loss of foundation support, and the cracking of walls and foundation, as well as the threat to beach users at the base of the bluff, the protection and foundation plans were no longer deemed adequate, and six threatened apartment units were demolished by the Federal Emergency Management Agency at a public cost of \$85,000.

The longest continuous area of coastal landsliding was from east of Capitola to Rio Del Mar (figs. 4, 12, 13), where sandstone of the Purisima Formation supports 30-m-high cliffs. About 5 m of terrace deposits consisting of poorly consolidated sand and gravel and a soil horizon caps the Purisima in this area. Most of the base of the cliff has been isolated from wave erosion by seawalls, which protect the beachfront development. The steep upper parts of the cliffs fail periodically during periods of sustained and (or) intense rainfall, for example, during the severe winter of 1982 (fig. 1; Griggs, 1982).

Translational failure along joints or weathering surfaces produced many large (30–60 m wide) concave upward scarps in the upper 12 to 15 m of the cliff in this area (figs. 8, 12). These scarps tended to cut vertically through the terrace deposits and then flatten to parallel the slope as they approached the Purisima Formation. Deep tension cracks cut through the upper terrace deposits and soils as far as 6 m landward of many of the scarps; this distance tended to increase with the size of the scarp and the height of the cliff. Coherent blocks overlying loose soil disintegrated as they cascaded down the cliff face. Talus piles, as much as 12 m high, blocked access to homes (fig. 14) and partly buried automobiles. Two blufftop homes ultimately were demolished because of such failures, which produced deep tension cracks through the building sites

(fig. 15). Both homesites were on narrow, steep-sided peninsulas along the crest of the coastal bluff, locations where seismic shaking appears to have been particularly severe.

In the lower 10 m of the cliff, fracturing along intersecting joints undercut the sandstone. Blocks 1 m thick and as much as 3 m high broke up easily as they moved downslope and formed talus cones at the base of the bluffs. Though fractured and partly detached from the cliff, other blocks did not fall; these blocks remain as unstable areas.

From Rio Del Mar southward (figs. 4, 16), semiconsolidated eolian and fluvial sand of the Pleistocene Aromas Sand forms 25- to 40-m-high steep cliffs. The top 2 to 5 m is more cohesive than the underlying, partly consolidated, weakly cemented sand. Seawalls protect much of the base of the bluff and the backbeach development from wave erosion. Interpretation of aerial photographs, however, indicates periodic shallow failure or sloughing of the upper parts of the bluffs in response to periods of intense or prolonged rainfall. These failures commonly initiated in the blufftop terrace deposits but typically extended to the base of the bluff.

Several types of earthquake-induced failures were typical along this stretch of coastal bluffs. The first type consisted of shallow (1–3 m deep), large (max 100 m wide) translational slides (figs. 8, 16, 17). At one site, such a failure undermined 5 to 10 m of the clifftop, leading to collapse and toppling of large cohesive blocks of soil. These detached masses rolled downslope and blocked access to condominiums built on the talus slope at the base of the bluff (fig. 18). This same failure also undermined a blufftop home that was subsequently demolished.

Another type of failure occurred in weakly consolidated Pleistocene dune sand near Sunset Beach (fig. 4) that has been partially stabilized by vegetation. Homes have been built on the edge of this ancient, partially vegetated dune complex. Slope failure took the form of shallow (max 1 m thick), dry sandflows that initiated well below the blufftop (figs. 9, 19). A vertical scarp cut through a thin, cohesive soil layer to a failure surface that paralleled the bluff face. Loose sand or small blocks of more cohesive material, commonly held together by roots, slid downslope along this surface and then ramped over the less steep talus deposits at the base of the bluff. The foundations of several homes were threatened, and one home was relocated.

Despite these recent failures, building permits are still being sought for new homes that would be sited on the talus slopes at the base of bluffs in the Rio Del Mar area (figs. 4, 20). The geologic hazards consistently identified at these sites in consulting reports are slope failure induced by excess water and by seismic shaking. The 1989 Loma Prieta earthquake provided an opportunity to check the distribution and characteristics of seismically induced failures. Eyewitness accounts of the bluffs during the earthquake by one of us (N.P.) noted virtually instantaneous, shallow slope failures along the bluffs in this area during

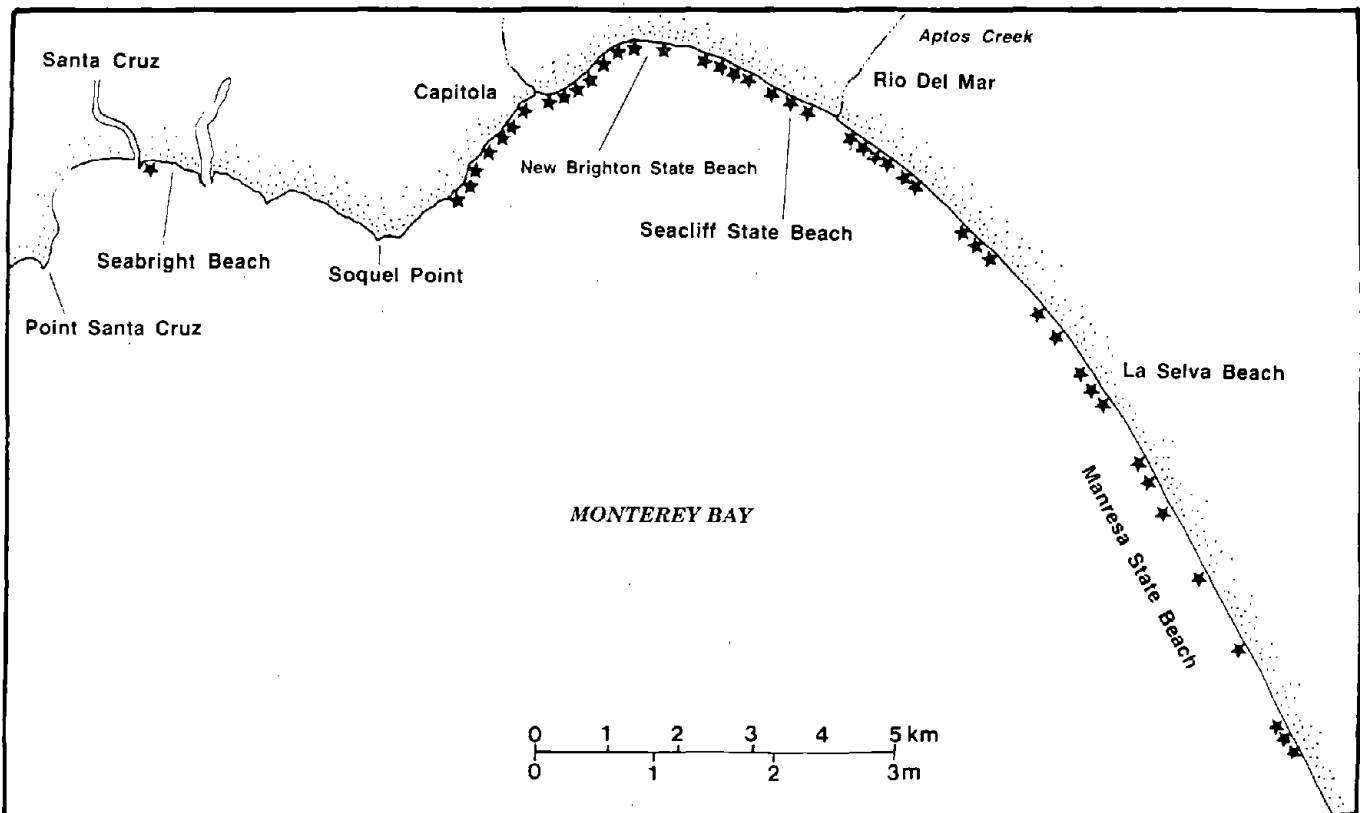


Figure 5.—North shoreline of Monterey Bay, Calif., showing locations of coastal-bluff failures (dots) induced by 1989 Loma Prieta earthquake.

the main shock. The mitigation measures proposed for downslope homes to reduce the risk of collapse involve upgrading standards for rear walls and roofs so as to absorb or deflect the loading associated with failure.

It is somewhat puzzling that the cliffs fronting northern Monterey Bay in the Rio Del Mar area (fig. 4), though consisting of only weakly cemented sand, are able to stand at such steep slopes. Past bluff failures, whether from intense rainfall or seismic shaking, have consistently produced relatively shallow slides. Large, deep-seated or rotational slides do not appear to have taken place in this geologic setting, despite its rainfall and seismic history.

Recent laboratory study and fieldwork indicate that cemented sand and gravel derive their strength from a combination of their interlocking grain structure and varying amount of cementation (Sitar, 1990). Seismic failures of steep slopes in natural sand and gravel deposits apparently initiate by tensile splitting in the upper parts of the slopes (Sitar, 1990), followed by toppling of the upper blocks or by shear failure of the lower slopes. Both types of failure lead to relatively shallow slides, rarely involving more than 2 to 5 m of material. Both natural and manmade slopes in cemented sand and gravel generally are quite steep and tend to perform surprisingly well when subjected to seismic loading. A problem does exist in



Figure 6.—Large coastal landslide near Daly City (fig. 4) resulting from 1989 Loma Prieta earthquake. Note proximity of cliff-top houses to headscarp.

evaluating the in-place strength of these deposits because conventional sampling techniques tend to break down the structure of cemented sand and are generally unsuitable for gravel. Sitar (1990) suggested alternative approaches, such as in-place freezing, block sampling, or onsite testing.

Although the lithology of the seaciff materials controlled the mode of seismic failure in most places, steep-sided promontories and narrow peninsulas or ridges along the coast consistently failed most extensively throughout the study area. Scientists also noted this effect in the Santa Cruz Mountains as a result of the 1989 Loma Prieta earthquake (Plafker and Galloway, 1989) and in other areas where large earthquakes have occurred in the past (Harp and others, 1981). In these other, noncoastal areas, the topography reflected seismic waves; constructive interference amplified the earthquake motion and caused rock or soil failures due to the intensified dynamic stresses. How-

ever, the size of a structure that can reflect incident waves must be approximately one wavelength (Harp and others, 1981). The abundance of failures along the coastal promontories and narrow peninsulas is probably attributable to the absence of lateral support at these bluff faces during the intense shaking.

## SUMMARY AND IMPLICATIONS FOR LAND-USE PLANNING

Seismically induced coastal-bluff failures were common as far as 80 km from the epicenter of the 1989 Loma Prieta earthquake. The failures in developed areas of the coast posed risks to development on the blufftop, as well as to private and public development on the beach below. One death occurred on a beach north of Santa Cruz when a section of weak bedrock collapsed onto a sunbather.

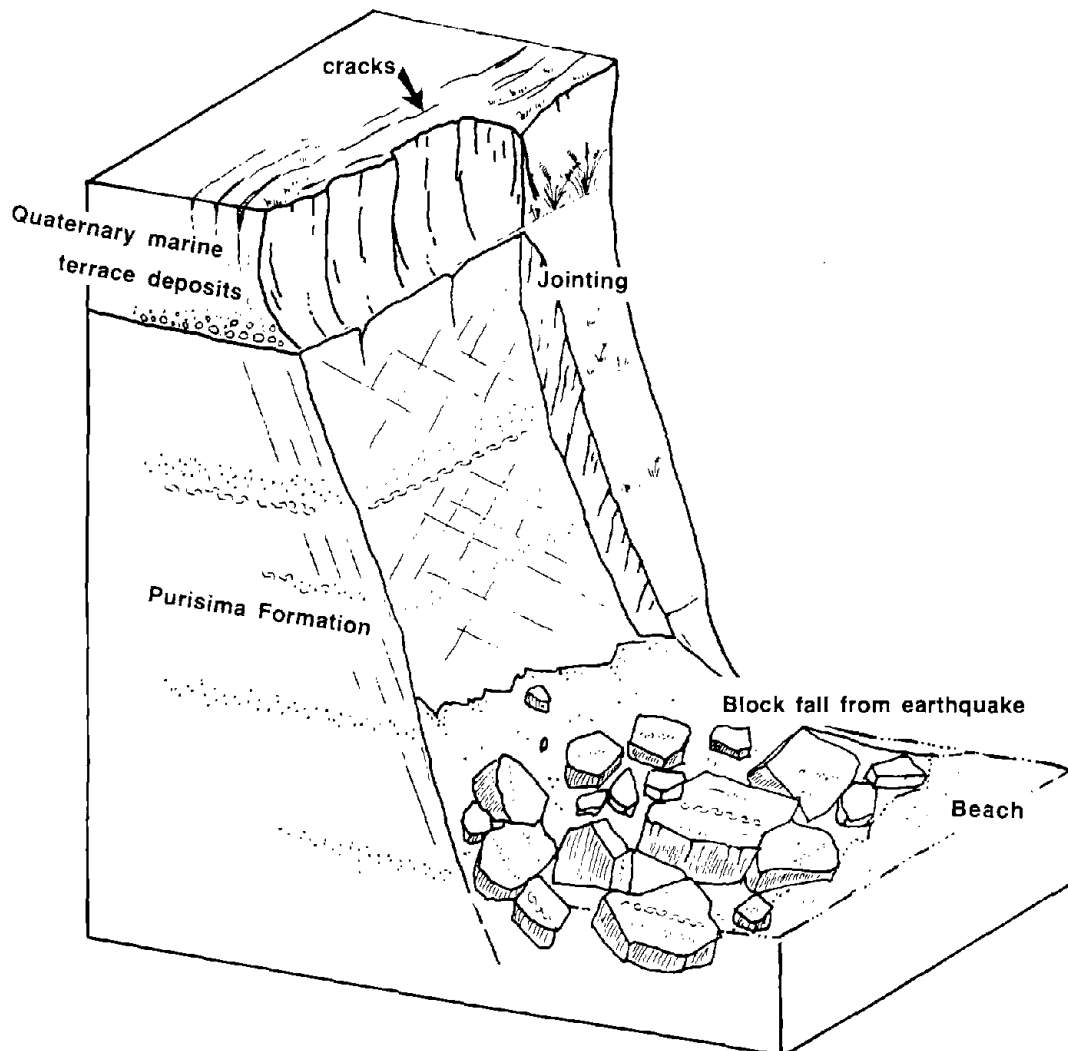


Figure 7.—Geologic structure and style of typical rockfall in seacliffs underlain by well-jointed siltstone of the Purisima Formation. Note undercut cliff and tension cracks in Pleistocene terrace deposits.

The top, slope, and base of seacliffs along northern Monterey Bay all proved to be unstable during the earthquake. At the cliff tops, several structures were immediately damaged when cliff failure undermined their foundations. At several sites, cracks formed 3 to 10 m inland from the cliff edge and, in some places, cut through foundations. Cracking and bluff failure were sufficiently damaging at four blufftop sites that three homes and six apartment units had to be demolished. The blufftop cracks exposed at these sites appear to represent incipient slides or detachment surfaces that may fail under renewed seismic shaking or elevated pore pressures during prolonged rainfall. We believe that the extent of this cracking can be used as a reasonable indicator of expected failures during seismic shaking in other California coastal bluffs consisting of similar materials.

Hazards to houses at beach level resulted from failure of the cliffs above them. Several houses in the Rio Del

Mar area (fig. 4) were either damaged or posted as unsafe and evacuated when the cliffs behind them failed. The houses most susceptible to damage were those built closest to the base of the bluffs. In addition, the bluff areas where the most extensive failures occurred during the earthquake, and where homes were most heavily damaged, were those that had failed most frequently during past episodes of intense rainfall, as evidenced in aerial photographs. Along the north shoreline of Monterey Bay, the areas of most frequent failure were the steep bluffs of Purisima Formation from Capitola to Rio Del Mar and the bluffs consisting of weakly cemented Aromas Sand that extend down the coast to Sunset Beach. Owing to the high value of ocean-front or ocean-view property, new homes are still being proposed for construction on the talus slopes at the base of the in the Rio Del Mar area (fig. 20), with rear walls and roofs engineered to absorb the impact of expected future slope failures.

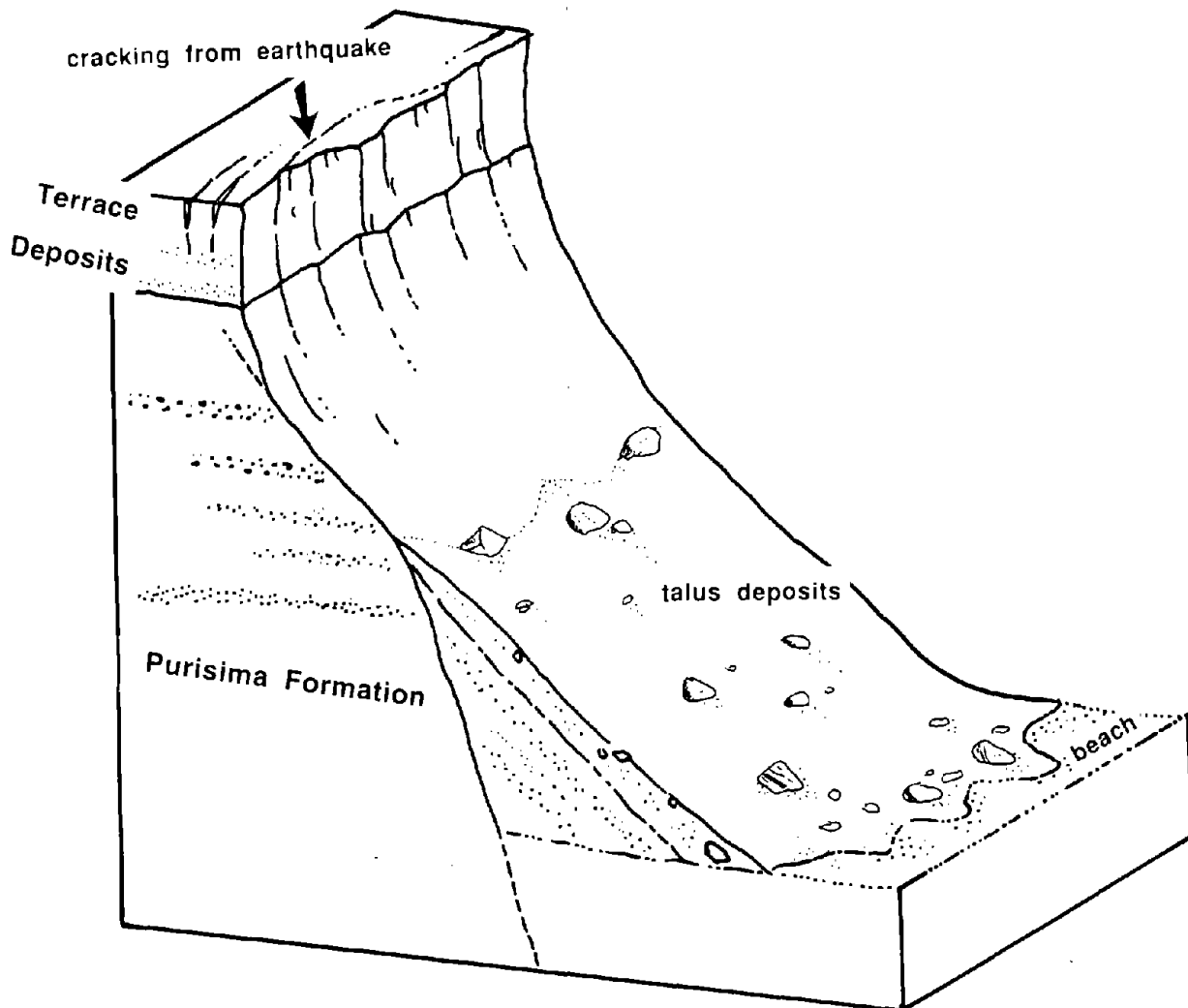


Figure 8.—Geologic structure and typical debris slide in seacliffs underlain by sandstone of the Purisima Formation.

The 1989 Loma Prieta earthquake, which was the largest earthquake to strike northern California in 83 years, initiated slope failure along approximately 240 km of coastline. The slope failures induced by seismic shaking provided the geological, geotechnical, and land-use-regulatory community with a unique opportunity to observe the effects of a large earthquake on coastal-bluff stability. The potential hazards of seismic shaking to ocean-front and seacliff construction have been well documented. The close proximity of virtually the entire 1,750 km of the California coastline to active faults ensures that seismic shaking can reasonably be expected at any ocean-front site during the lifetime of any structure built today.

## RECOMMENDATIONS

We need to both anticipate and plan for the inevitable earthquake-induced landslides that will take place along the State's coastal bluffs during future large earthquakes. Failure during the 1989 Loma Prieta earthquake occurred

not only along bluffs that were actively eroding but also along bluffs that were protected from marine erosion.

- Encroachment of public or private structures and utilities in the coastal zone should be permitted only after a complete assessment of geologic hazards and risks.
- We need a regional understanding of long-term bluff or shoreline erosional rates and their relation to both coastal processes and regional seismicity.
- Although the main shock of the earthquake caused widespread instantaneous failure, erosional and failure rates in earthquake-weakened bedrock and soils may increase as future winter storms and rain batter the coastline.
- Current and future development proposals along the coast should consider the evidence and experience gained from this earthquake to evaluate both building setbacks and the feasibility of hazard-mitigation measures. Reconstruction on earthquake-damaged sites should proceed only after extensive geologic and geotechnical investigations conclude that appropriate mitigation measures have been taken to reduce the future risks of damage to an acceptable level.

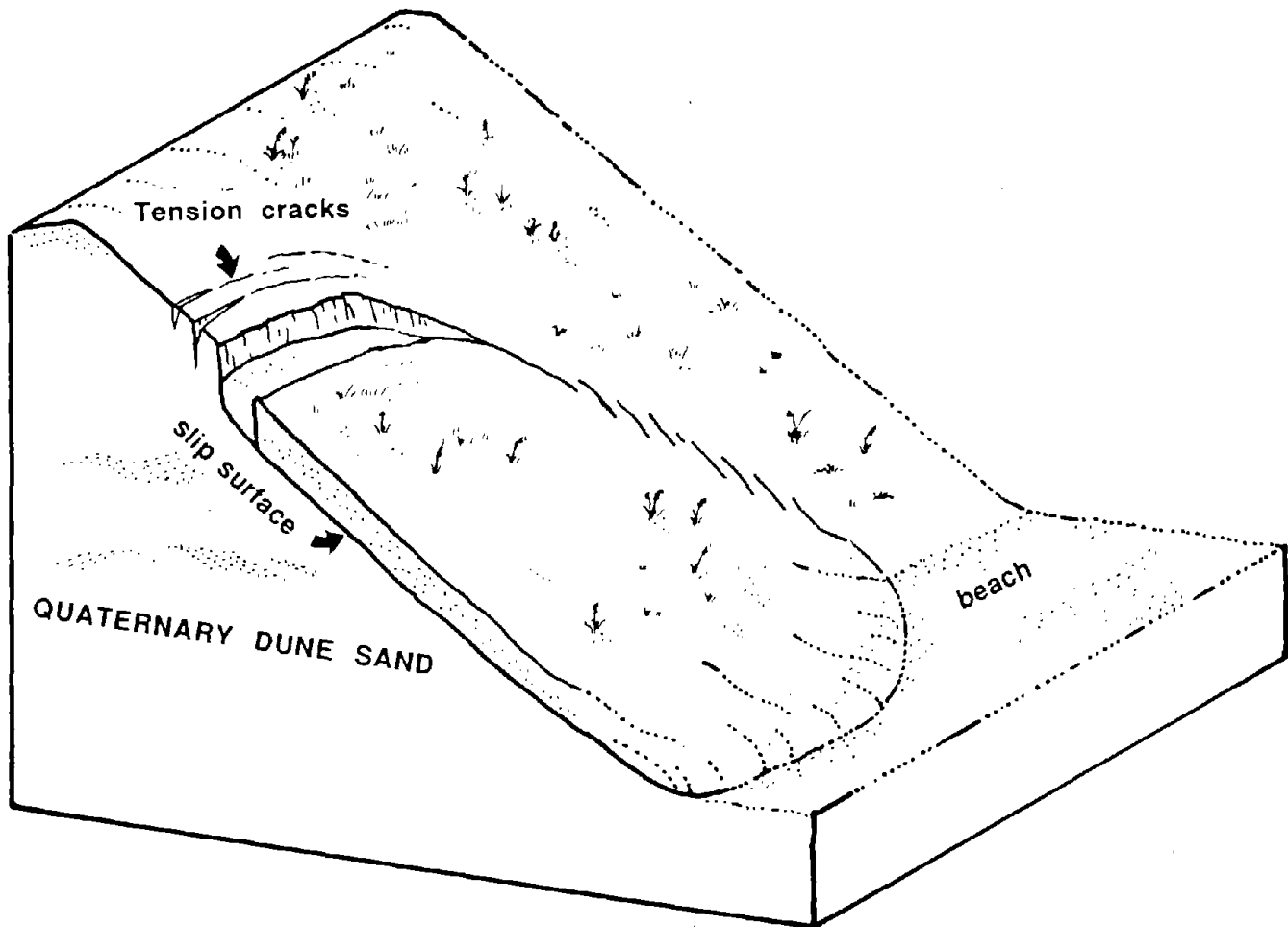


Figure 9.—Dry sandflow in uncemented eolian deposits. Note tension cracks in overlying, more cohesive surficial soils.

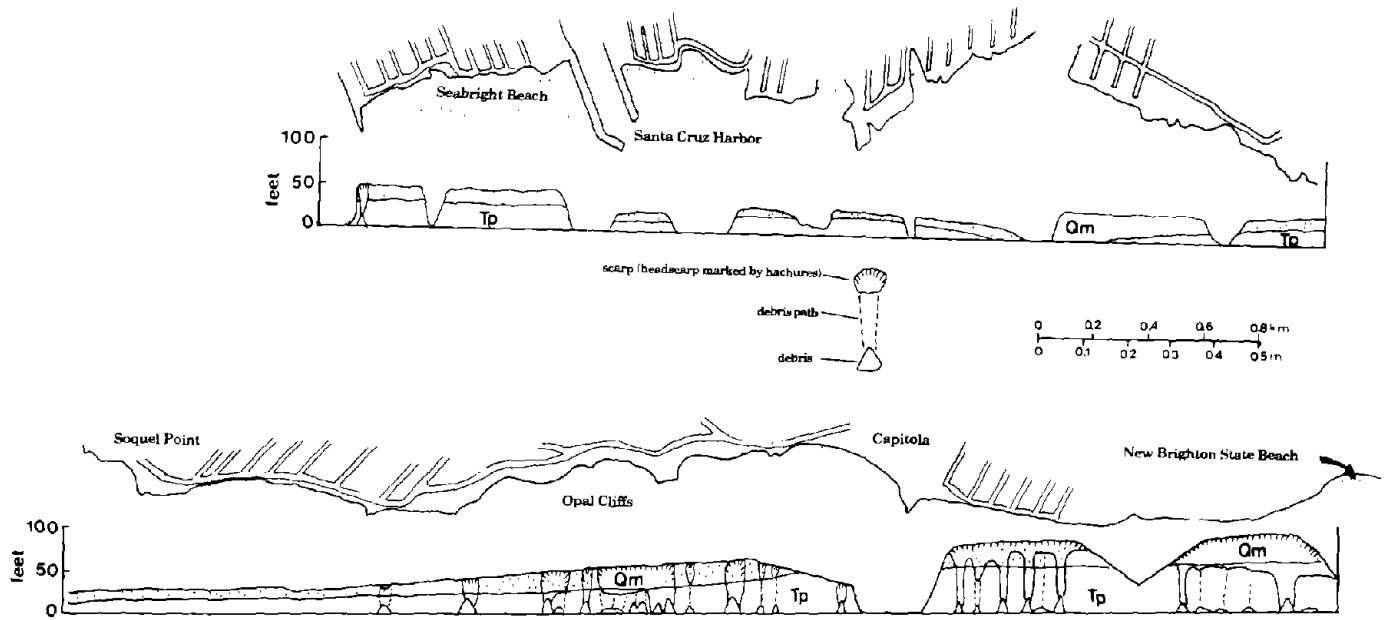


Figure 10.—Plan view and longitudinal section showing locations and sizes of earthquake-induced seaciff failures and geology between Seabright Beach and Soquel Point (A) and between Soquel Point and New Brighton State Beach (B) (see fig. 5 for locations). Units: Qm, marine-terrace deposits (Quaternary); Tp, Purisima Formation (late Miocene and Pliocene).

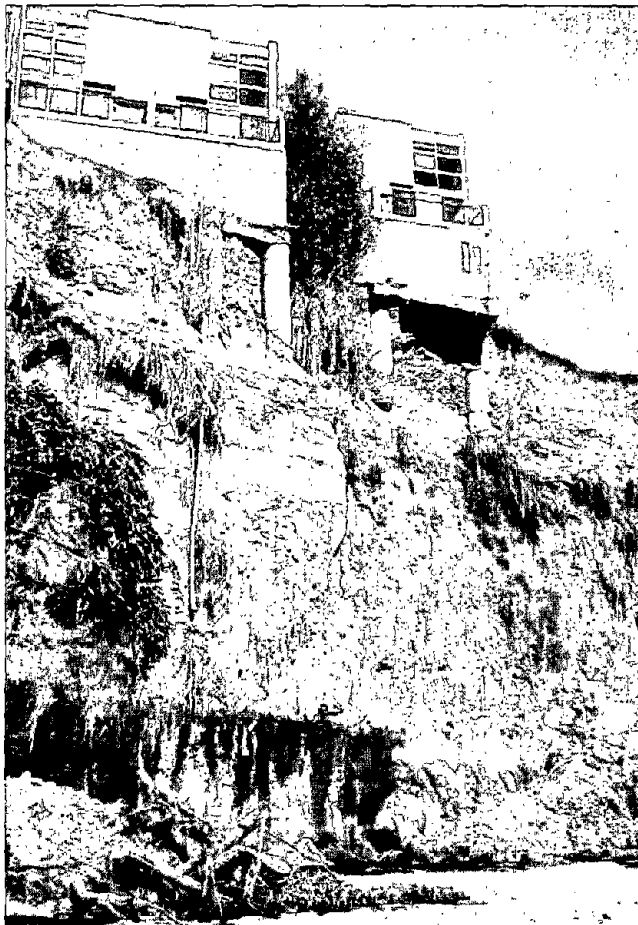


Figure 11.—Collapse of terrace deposits and underlying jointed bedrock of the Purisima Formation at Capitola (fig. 5) as a result of the 1989 Loma Prieta earthquake. These six apartment units were subsequently demolished, owing to blufftop cracking and loss of foundation support.





Figure 12 —Earthquake-induced failure of terrace deposits and sandstone of the Purisima Formation between Capitola and Rio Del Mar (see fig. 5 for location).

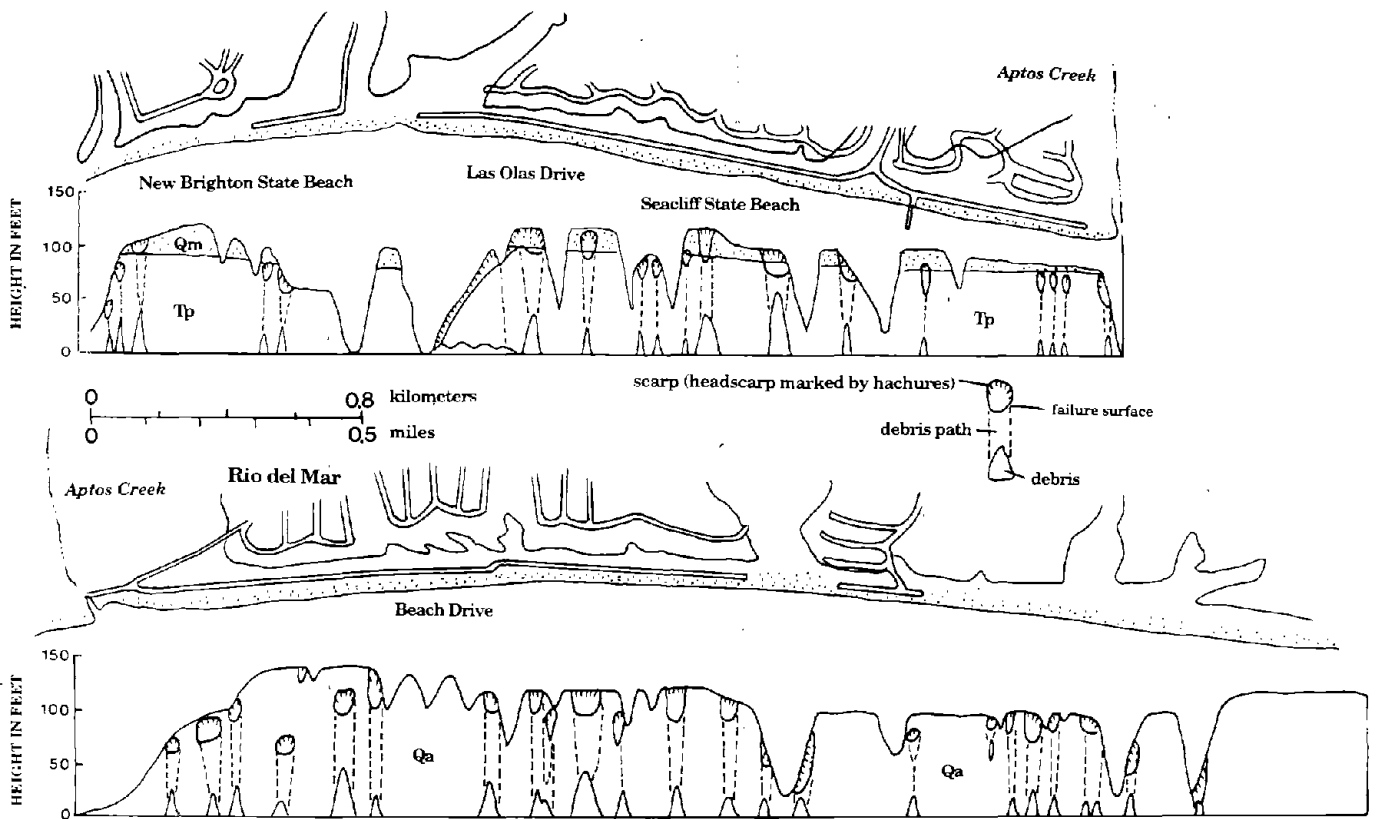


Figure 13.—Plan view and longitudinal section showing locations and sizes of seaciff failures and geology between New Brighton State Beach and Aptos Creek (A), and between Aptos Creek and Rio Del Mar (B) (see fig. 5 for locations). Units: Qa, Aromas Sand (Pleistocene); Qd, dune sand (Quaternary); Qm, marine terrace deposits (Quaternary); Tp, Purisima Formation (late Miocene and Pliocene).



Figure 14.—Base of seaciff in area of figure 12 where material from bluff failure has blocked access to beach-front homes.



Figure 15.—Deep tension cracks (arrows) in terrace deposits in Rio Del Mar (fig. 5). Cracks cut through house foundation and indicate potential extent of future failure. At this site, house was demolished, and unstable material was removed to stabilize site.

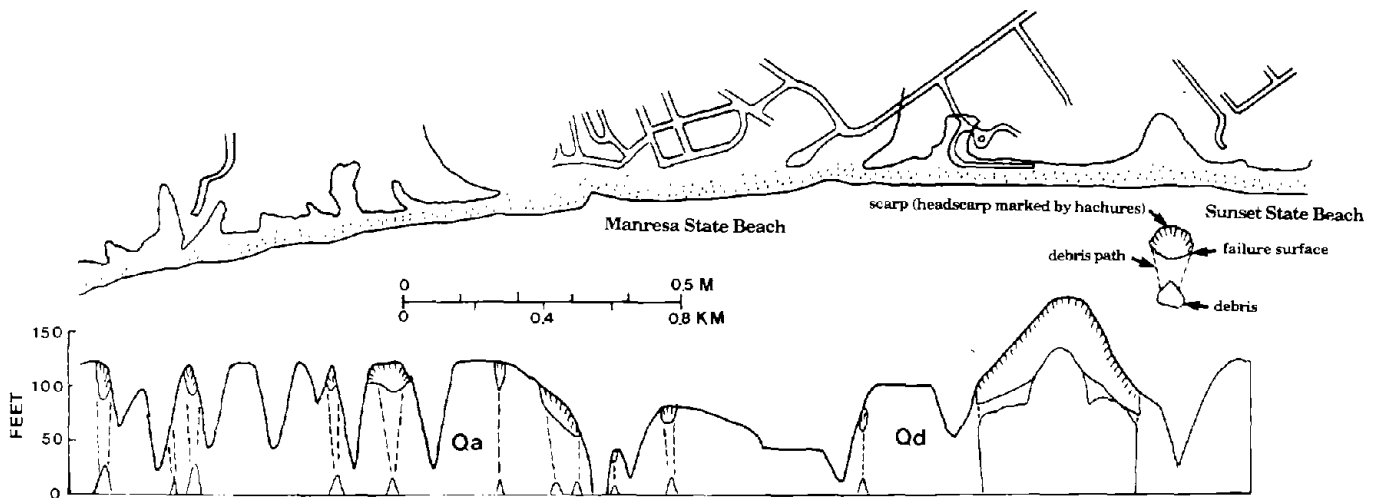


Figure 16.—Plan view and longitudinal section showing locations and sizes of seacliff failures and geology between Rio Del Mar and Sunset State Beach (see fig. 5 for locations). Units: Qa, Aromas Sand (Pleistocene); Qd, dune sand (Quaternary).

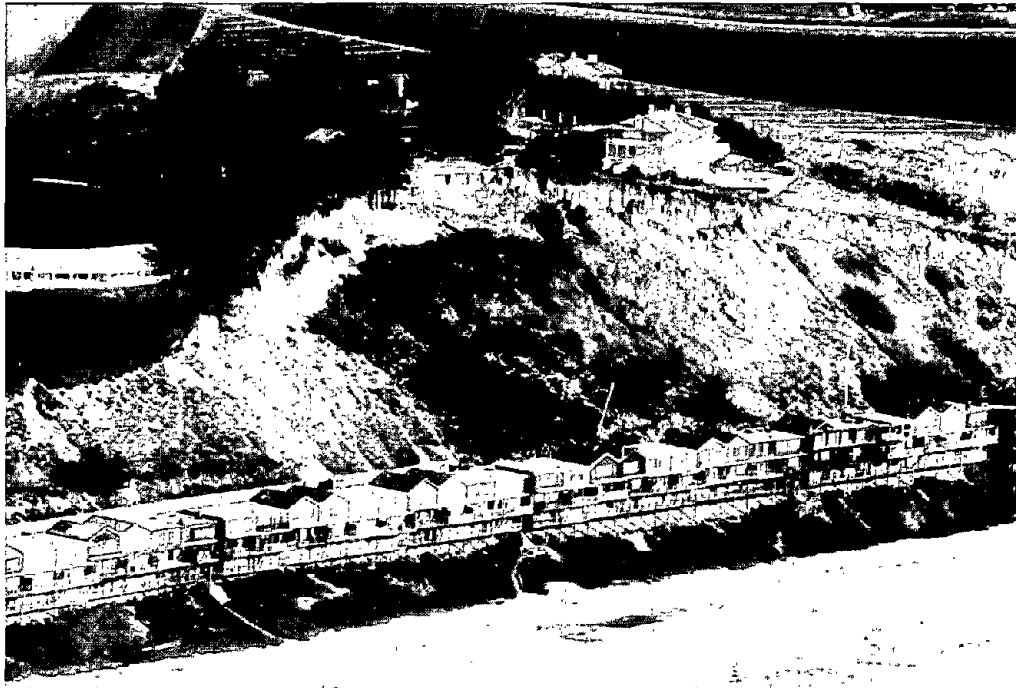


Figure 17.—Large translational slide above condominium development south of Rio Del Mar (fig. 5). One house at top of bluff had to be demolished; homes at base of bluff were threatened, and access partly blocked (see fig. 18).



Figure 18.—Weakly consolidated sand of the Aromas Sand disintegrated and flowed downhill to block access and threaten condominiums at base of bluff (see fig. 16). Tires had been placed on slope in an attempt to control erosion.

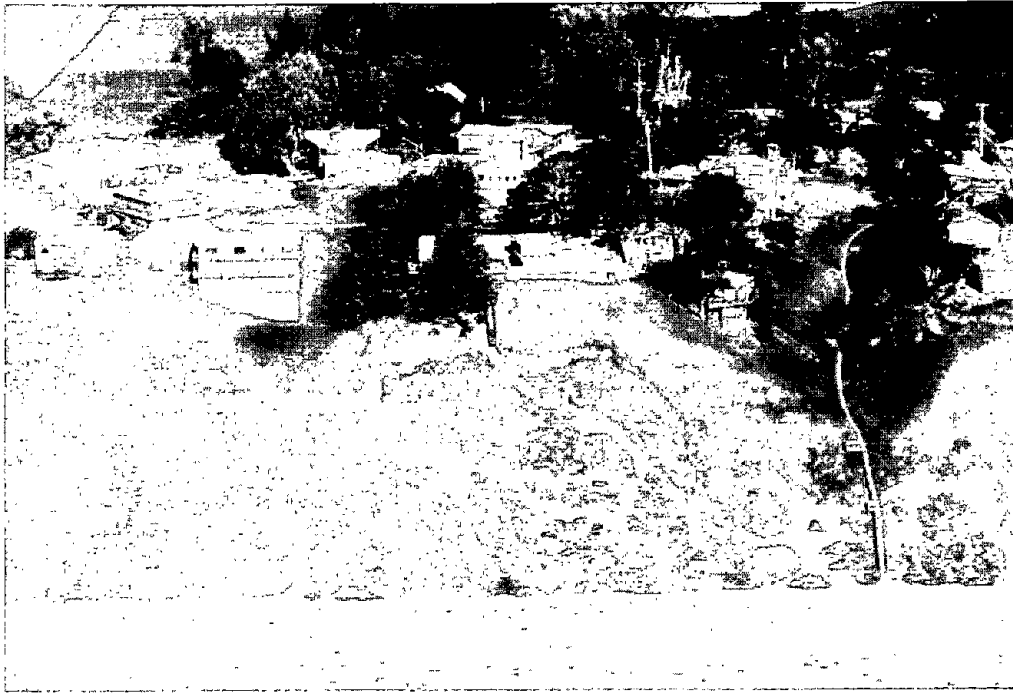


Figure 19.—Large sandflows above Sunset State Beach (fig. 5). One blufftop house was to be relocated.



Figure 20.—Earthquake-induced bluff failures in Beach Drive area of Rio Del Mar (fig. 5). New homes are being proposed at base of this bluff behind existing beach-front homes.

## REFERENCES CITED

- Griggs, G.B., 1982. Flooding and slope failure during the January 1982 storm, Santa Cruz County, California: *California Geology*, v. 35, no. 7, p. 158-163.
- Griggs, G.B., and Johnson, R.E., 1979. Coastline erosion, Santa Cruz County: *California Geology*, v. 32, no. 4, p. 67-76.
- Griggs, G.B., Pepper, J.E., and Jordan, M.E., 1991. California's coastal hazards policies: a critique, in Domurat, G.W. and Wakeman, T.H., eds., *The California coastal zone experience*: New York, American Society of Civil Engineers, p. 89-107.
- Harp, E.L., Wilson, R.C., and Wieczorek, G.F., 1981. Landslides from the February 4, 1976, Guatemala earthquake: U.S. Geological Survey Professional Paper 1204-A, 35p.
- Jennings, C.W., 1975, compiler. Fault map of California with locations of volcanoes, thermal springs, and thermal wells: California Division of Mines and Geology Geologic Data Map 1, scale 1:750,000.
- Lawson, A.C., chairman, 1908, *The California earthquake of April 18, 1906*; report of the State Earthquake Investigation Commission: Carnegie Institution of Washington Publication 87, 2 v.
- Plafker, George, and Galloway, J.P., 1989, *Lessons learned from the Loma Prieta, California, earthquake of October 17, 1989*: U.S. Geological Survey Circular 1045, 48 p.
- Plant, Nathaniel, and Griggs, G.B., 1989, *Coastal landslides caused by the October 17, 1989 earthquake, Santa Cruz County, California*: *California Geology*, v. 43, no. 4, p. 75-84.
- Sitar, Nicholas, 1990, *Seismic response of steep slopes in weakly cemented sands and gravels*: H.B. Seed Memorial Symposium, Berkeley, Calif., 1990, Proceedings, p. 67-82.
- Sydnor, R.H., Griggs, G.B., Weber, G.E., McCarthy, R.J., and Plant, Nathaniel, 1990, *Coastal bluff landslides in Santa Cruz County resulting from the Loma Prieta earthquake of 17 October 1989*, in McNutt, S.R., and Sydnor, R.H., eds., *The Loma Prieta (Santa Cruz Mountains) California earthquake of October 17, 1989*: California Division of Mines and Geology Special Publication 104, p. 67-82.
- U.S. Geological Survey, 1989. *The Loma Prieta earthquake of October 17, 1989*: Menlo Park, Calif., 16 p.
- 1990, *The next big earthquake in the Bay Area may come sooner than you think*: Menlo Park, Calif., 23 p.
- Working Group on California Earthquake Probabilities, 1990, *Probabilities of large earthquakes in the San Francisco Bay region, California*: U.S. Geological Survey Circular 1053, 51 p.

THE LOMA PRIETA, CALIFORNIA, EARTHQUAKE OF OCTOBER 17, 1989:  
STRONG GROUND MOTION AND GROUND FAILURE

LANDSLIDES

LANDSLIDE DAMS IN SANTA CRUZ COUNTY, CALIFORNIA,  
RESULTING FROM THE EARTHQUAKE

By Robert L. Schuster and Gerald F. Wieczorek,  
U.S. Geological Survey;  
and  
David G. Hope II,  
Santa Cruz County Planning Department

CONTENTS

	Page
Abstract .....	C51
Introduction .....	51
Historical landslide dams in California .....	52
Landslide dams caused by the 1906 San Francisco earthquake .....	52
Landslide dams caused by the 1989 Loma Prieta earthquake --	55
Locations and characteristics .....	55
West Branch Soquel Creek .....	55
Hinckley Creek .....	59
Corralitos Creek, upper dam .....	59
Corralitos Creek, lower dam .....	60
Browns Creek .....	60
Effects .....	60
Upstream flooding .....	60
Downstream flooding .....	60
Deterioration of water quality .....	62
Deterioration of fish habitats .....	62
Factors affecting the distribution of landslide dams .....	63
Seismic intensity .....	63
Slope steepness/topography .....	63
Lithology/weathering properties .....	63
Soil moisture/ground water .....	64
Influence of climate and hydrology .....	65
Mitigation of stream damming .....	68
Conclusions .....	68
References cited .....	69

ABSTRACT

In mountainous areas, landslide blockages of streams are an occasional, but hazardous, result of landslides triggered by seismic activity. These natural dams may have the following negative effects: (1) upstream (backwater) flooding, (2) downstream flooding as a result of dam failure, (3) deterioration of water quality, and (4) deterioration of fish habitats. Eight reported landslide dams occurred over a widespread area in northern and central California as a result of the 1906 San Francisco earthquake, and five dams were formed in Santa Cruz County by landslides triggered by the 1989 Loma Prieta earthquake. Because of

the smaller size of the 1989 earthquake and because of drought conditions, the 1989 landslides and their resulting dams also were smaller (max 7 m high), had smaller impoundments (max 6,000 m<sup>3</sup> volume), and were distributed over a smaller area than those that formed under the wetter soil conditions in 1906.

Two landslide dams on Corralitos Creek were removed by "stage" (that is, incremental) excavation to eliminate the possibility of minor downstream flooding as a result of breaching. One dam on West Branch Soquel Creek and another on Hinckley Creek failed during subsequent heavy rainfall, but downstream channel capacity was not exceeded by the resulting small floods; thus, no flood damage occurred to homes or property. However, sediment deposited immediately downstream from these two breached dams locally damaged spawning beds for anadromous (that is, sea-run) steelhead trout.

INTRODUCTION

Landslide dams form most frequently where narrow, steep valleys are bordered by high, rugged mountains (Costa and Schuster, 1988). This setting is common in geologically active areas where earthquakes, volcanoes, or glacially oversteepened slopes occur. The most common types of landslides that form landslide dams are rock/debris avalanches, earth slumps and slides, and debris flows. The most common initiation mechanisms for dam-forming landslides are excessive precipitation (rainfall and snowmelt) and earthquakes.

A landslide dam differs from a constructed embankment dam because it consists of a heterogeneous mass of unconsolidated or poorly consolidated material and because it includes no engineered water barrier (impervious core), no filter zone to prevent piping (that is, internal erosion), and no drain zones to control pore pressures within the mass. It also has no spillway or other protected outlet; thus, landslide dams commonly fail. Failure mostly

occurs by overtopping, followed by erosion by the overflowing water, although a few landslide dams have breached as a result of piping. Some dams fail soon after they form, some last for months or years, and some never fail. Evidence of long-term landslide dams can be noted in mountain ranges worldwide, where landslide-dammed lakes are common features.

In addition to catastrophic downstream flooding caused by failure of a landslide dam, upstream (that is, backwater) flooding behind dams can inundate communities and valuable agricultural land. Some of the most catastrophic failures have been of large landslide dams formed by earthquake-induced landslides. The most disastrous recorded case of downstream flooding occurred in central China in 1786, when an estimated  $M=7.5$  earthquake caused a major landslide that dammed the Dadu River for 10 days (Li Tianchi, 1989). When the landslide dam overtopped and breached, a flood that extended 1,400 km downstream drowned as many as 100,000 people, whereas the earthquake had killed only 400 to 500 people directly. A graphic account of the 1841 failure of an earthquake-induced landslide dam on the Indus River, India, was provided by Mason (1929). When this natural dam, which was more than 200 m high and impounded a lake 65 km long, breached, the entire lake drained within 24 hours, causing a tremendous flood. Hundreds of towns and villages were swept away, with great numbers of casualties. In 1933, at least 2,400 people died in the flood caused by failure of the 240-m-high earthquake-induced ( $M=7.5$ ) Deixi landslide dam on the Min River in central China (Li Tianchi and others, 1986). In 1986, the sudden failure of an earthquake-induced ( $M=7.1$ ) debris-avalanche dam on the Bairaman River on the island of New Britain, Papua New Guinea, resulted in a 100-m-deep flood in the canyon downstream (King and others, 1989).

#### HISTORICAL LANDSLIDE DAMS IN CALIFORNIA

The locations of 29 historical landslide dams in California are shown in figure 1. All of these natural dams occurred in the north half of the State. Of the blockages, 16 were formed by landslides triggered by precipitation (rainfall or snowmelt), and 13 were earthquake triggered (8 by the 1906 San Francisco earthquake and 5 by the 1989 Loma Prieta earthquake). A literature search for possible leads to the historical occurrence of landslide dams in southern California found only the following two examples, both of which are either too controversial or lack enough detail to be included in figure 1.

1. As reported by Townley and Allen (1939, p. 153), the San Francisco *Chronicle* of April 25, 1909, stated that an earthquake had caused a great slide in Santa Paula Canyon, in the Coast Ranges of Ventura County, blocking the

drainage and creating a lake. Townley and Allen noted, however, that no seismic activity had been reported in the vicinity; instead, the slide seemed to have been caused by extremely heavy spring rains.

2. As a result of the 1952 Arvin-Tehachapi earthquake ( $M=7.6$ ) in Kern County, Buwalda and St. Amand (1955) noted, "Canyons were dammed with rock debris, and some small lakes were formed."

Most of the recorded landslide dams in California failed without serious downstream flooding or were intentionally removed to prevent flooding; however, two large dams failed catastrophically, resulting in serious flooding. The earliest recorded landslide dam in California formed on December 20, 1867, on the South Fork of the Kaweah River (fig. 1) in what is now Sequoia National Park (Fry, 1933). A period of 41 days of rain had triggered a large debris avalanche/debris flow that dammed the river at its confluence with Garfield Creek. The 20-m-high blockage soon failed; the flood swept down the Kaweah River, carrying with it trees and debris and inundating part of the San Joaquin Valley. The town of Visalia (fig. 1), 60 km downstream from the dam, was flooded to a depth of nearly 2 m on December 23. Several other rainfall-induced landslides have blocked streams in northern California since then, but none has produced a comparable flood.

The 1906 San Francisco earthquake ( $M=8.2$ ) resulted in eight recorded landslide dams (Costa and Schuster, 1991), and the 1989 Loma Prieta earthquake ( $M=7.1$ ) triggered landslides that formed five stream blockages, all of which were small. This paper describes the landslide dams caused by the 1989 earthquake, in comparison with those caused by the 1906 earthquake.

#### LANDSLIDE DAMS CAUSED BY THE 1906 SAN FRANCISCO EARTHQUAKE

The 1906 San Francisco earthquake triggered thousands of landslides throughout a 600-km-long stretch of the California Coast Ranges from southern Monterey County in the south to Eureka in the north (Lawson, 1908; Youd and Hoose, 1978; Keefer, 1984). As shown in figure 1, streams were dammed in eight places by landslides triggered by the earthquake. In addition, there were sketchy reports of other small landslide dams in Santa Cruz County, but available information on these dams is so vague that we have not included them in this paper. The locations of the recorded dams ranged from the Eel River near Island Mountain in Trinity County (approx 260 km north of San Francisco) to Hinckley Creek in Santa Cruz County (approx 90 km southeast of San Francisco). Most of these natural dams were small (max 10 m high, table 1). A typical example was the dam that formed on Los Gatos Creek in Santa Clara County (fig.2). However, the Olive



Springs landslide (also called the Sawmill slide because it destroyed the Loma Prieta Mill, fig. 3) in Santa Cruz County dammed Hinckley Creek to a depth of 20 m (Santa Cruz Morning Sentinel, 1906), and a large debris slide in

Lake County formed a 30-m-high blockage of Cache Creek (Scott, 1970; Manson, 1990).

Within 13 days after the earthquake, the  $2.4 \times 10^6 \text{ m}^3$ -volume Cache Creek debris slide in Lake County (approx

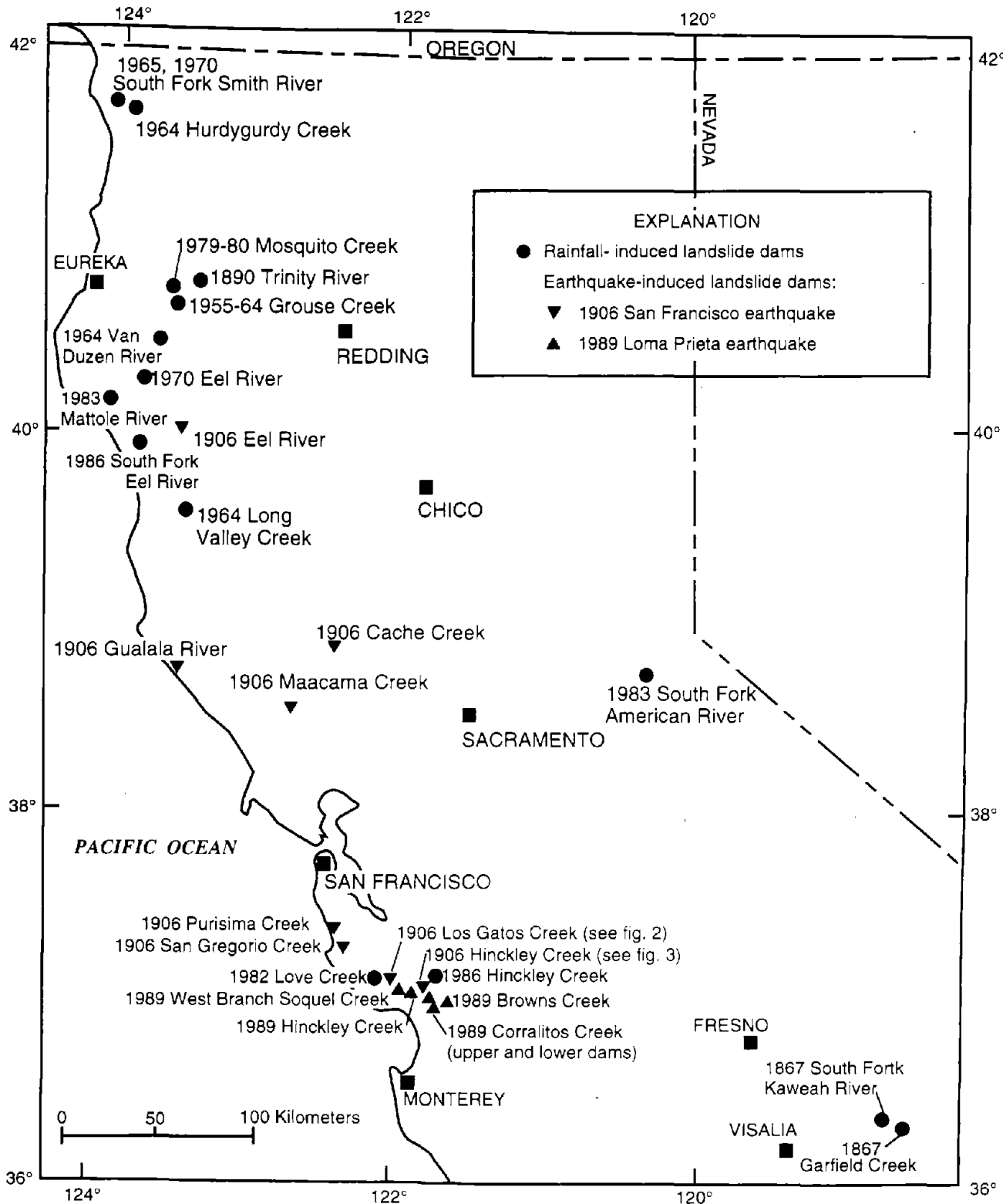


Figure 1.—Northern California, showing distribution of 29 historical landslide dams. Data primarily from Costa and Schuster (1991).

Table 1.—Landslide dams caused by the 1906 San Francisco earthquake

River/stream	Dam height (m)	Comments	References
Eel River -----	?	Reported by Northwestern Pacific Railroad.	Dwyer and others (1971).
Cache Creek -----	30	Dam failure caused downstream flooding.	Scott (1970), Manson (1990).
Gualala River -----	?	"*****river was temporarily dammed up by slides from both slopes."	Lawson (1908).
Maacama Creek -----	?	"*****avalanche cut its way through a fir forest and dammed Maacama Creek."	Do.
Purisima Creek -----	8-10	"*****slide*****dammed the creek to a depth of 25 or 30 feet."	Do.
San Gregorio Creek -----	2	"*****creek was dammed up to a depth of 6 feet."	Do.
Los Gatos Creek ----- (fig. 2).	?	"Large pond" formed.	Do.
Hinckley Creek ----- (fig. 3).	20	Nine killed by "Sawmill slide."	Santa Cruz Morning Sentinel (1906).



Figure 2.—Landslide that dammed Los Gatos Creek, Santa Clara County, Calif. (fig. 1), as a result of 1906 San Francisco earthquake. Photograph courtesy of J.C. Branner Papers, Stanford University Archives.

120 km north of San Francisco) formed; the slide dammed Cache Creek (fig. 1; Scott, 1970). In including this slide with others triggered by the earthquake, Lawson (1908, p. 390) stated, "This earth-avalanche cannot be so directly referred to the earthquake of April 18 [1906] as the others heretofore described, but it was probably indirectly caused by the shock." In the absence of proof, this slide most probably was caused by a change in the ground-water regimen as a result of the earthquake. In this regard, Scott (1970) noted:

According to the Carnegie report [Lawson, 1908], Cache Canyon was in a seismic intensity zone of about V to VI. This ground motion could have opened incipient failure planes in the slide mass along which ground-water percolation and increased hydrostatic pressures developed until, 12 [sic] days later, the slope failed.

Then, 5 days later, the natural dam failed by overtopping and (or) piping, releasing approximately  $15 \times 10^6 \text{ m}^3$  of impounded water as a flood that entered Capay Valley to the southeast and devastated the small town of Rumsey on Cache Creek, 30 km downstream from the landslide. The flood destroyed several buildings, carried away the Rumsey post office and store, and damaged Southern Pacific Railroad facilities and the county bridge over Cache Creek (Manson, 1990). No one was killed or injured.

## LANDSLIDE DAMS CAUSED BY THE 1989 LOMA PRIETA EARTHQUAKE

### LOCATIONS AND CHARACTERISTICS

Five landslides triggered by the 1989 Loma Prieta earthquake formed small dams on streams in Santa Cruz County (figs. 4, 5; table 2). All five of these landslides occurred in rocks of the upper Miocene and Pliocene Purisima Formation (McLaughlin and others, 1988; Brabb, 1989; Clark and others, 1989; Weber and Nolan, 1992). The general characteristics of these landslides and the resulting dams and impoundments are described below.

### WEST BRANCH SOQUEL CREEK

The rockslide on West Branch Soquel Creek (fig. 6), which occurred on a rather remote stretch of the creek (fig. 4), is the largest of the five 1989 landslides discussed in this paper. This slide was approximately 250 m long, averaged 50 m in width, and had an estimated maximum thickness of 6 m and a volume of  $50,000 \text{ m}^3$ . The slide began in Purisima Formation sandstone, siltstone,



Figure 3.—Workers removing toe of earthquake-induced landslide that dammed Hinckley Creek at Olive Springs sawmill in 1906 (see fig. 4 for location). Landslide killed nine workers at Olive Springs and formed a 20-m-deep impoundment where it dammed the creek. Photograph courtesy of California Department of Parks and Recreation.

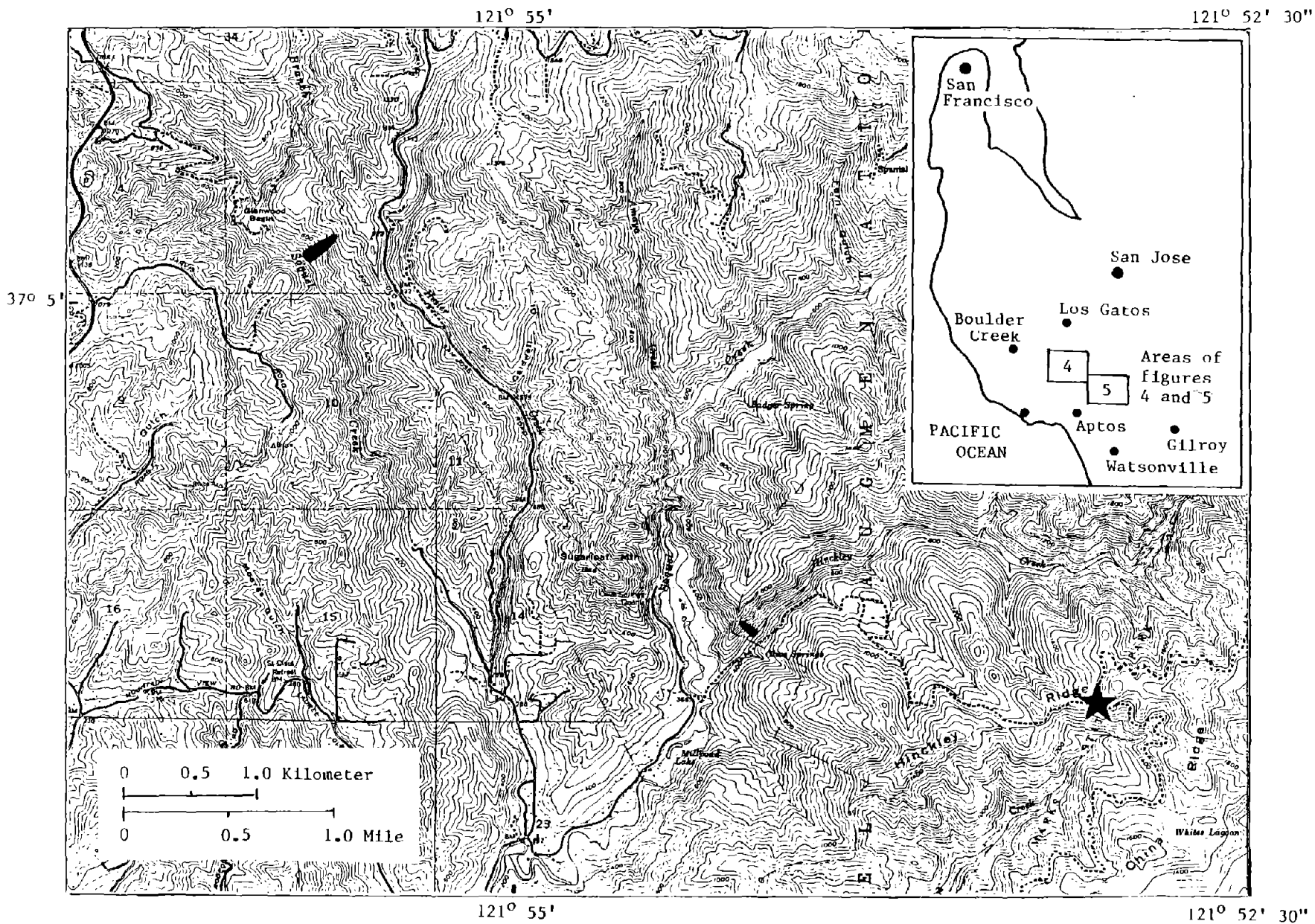


Figure 4.—Area of Santa Cruz Mountains, Calif., showing locations of 1989 landslide dams on West Branch Soquel Creek and Hinckley Creek and of epicenter of 1989 Loma Prieta earthquake (star). Base from U.S. Geological Survey 7 1/2-minute Laurel quadrangle, Calif.; contour interval, 40 ft.

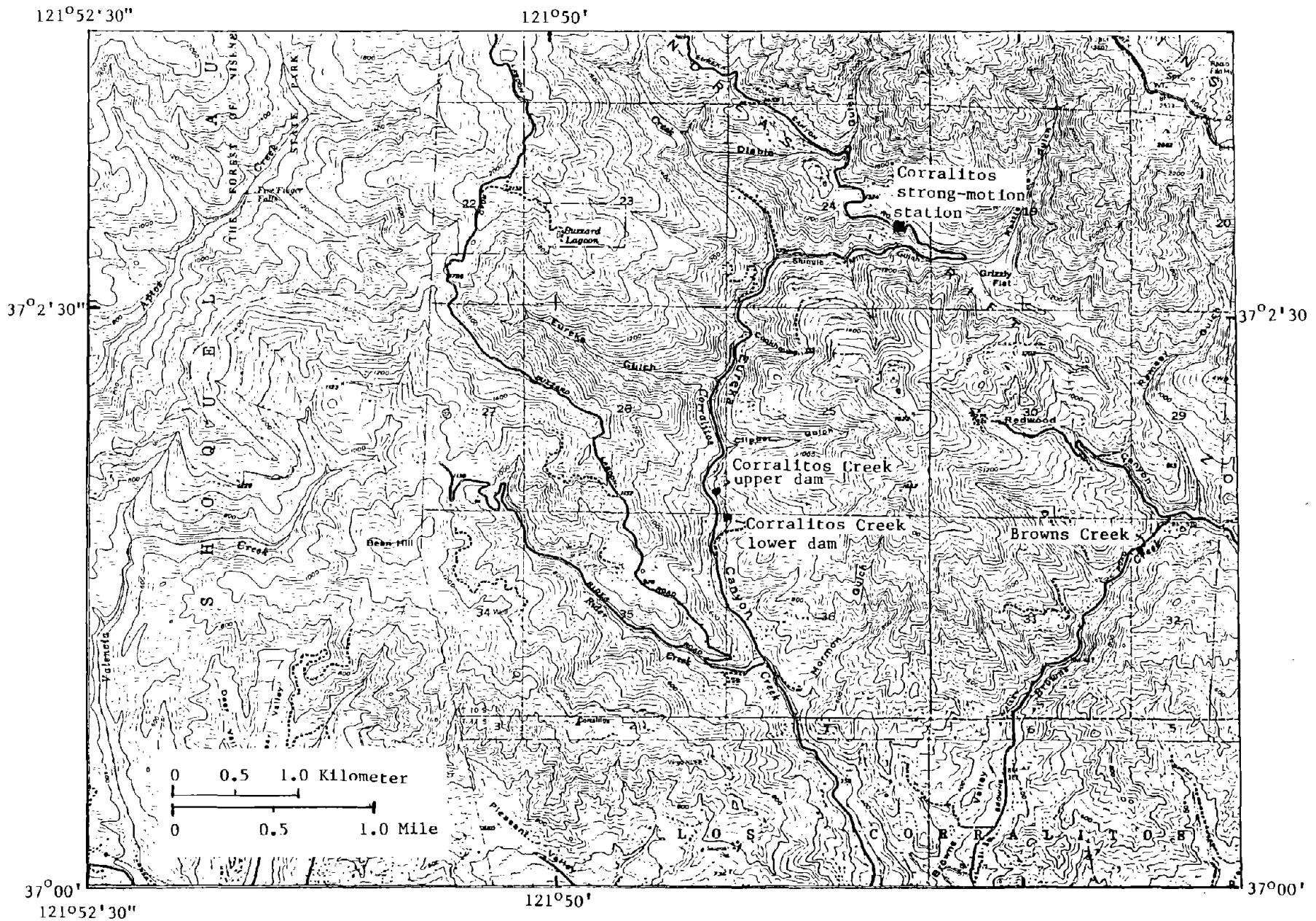


Figure 5.—Area of Santa Cruz Mountains, Calif., showing locations of 1989 landslide dams on Corralitos Creek and Browns Creek and of Corralitos strong-motion station. Base from 7 1/2-minute Loma Prieta quadrangle, Calif.; contour interval, 40 ft.

Table 2.—Summary of characteristics of landslides and landslide dams in Santa Cruz County resulting from the 1989 Loma Prieta earthquake

Location/ stream	Site geology	Failed slope	Landslide type	Landslide volume (m <sup>3</sup> )	Dam height (m)	Lake volume (m <sup>3</sup> )	Comments
West Branch Soquel Creek	Purisima Formation (sandstone, siltstone, mudstone).	26°	Rock slide	50,000	4	1,800	Dam failed 61 days after earthquake; minor stream flooding and sedimentation.
Hinckley Creek (Olive Springs)	Purisima Formation (sand- stone).	60°	Rock fall	1,600	4	3,500	Soil matrix of dam failed in February 1992.
Corralitos Creek, upper dam.	---do---	75°	---do---	3,500	7	6,000	Spillway excav- ated; then dam removed.
Corralitos Creek, lower dam.	Purisima Formation (sandstone, siltstone, mudstone).	30°	Rock slide	3,500	3	1,200	Do.
Browns Creek	Purisima Formation (sandstone).	70°	Rock fall	200	2	150	Dam failed by overtopping.



Figure 6.—Toe of this 50,000-m<sup>3</sup>-volume earthquake-induced slide dammed West Branch Soquel Creek (see fig. 4 for location). Dam failed in December 1989, 61 days after 1989 Loma Prieta earthquake. Photograph taken in May 1992.

and mudstone at the site of a spring on the valley wall. Initial failure probably occurred in a weak layer of silt or clay in the Purisima Formation. The slide crosses the Zayante fault (Clark and others, 1989) on a slope averaging  $26^\circ$ , and its toe lies on rocks of the Eocene Butano sandstone in the valley bottom. The existing, nearly vertical headscarp in Purisima Formation rocks is 12 m high and 30 m long and has a spring issuing from its base. As indicated by Clark and others, the strike of the Purisima Formation beds at this site approximately parallels West Branch Soquel Creek, and the dip is back into the valley wall. Thus, this slide was not a dip-slope failure; instead, failure probably was related to the low shear strength of mudstone and siltstone that had been saturated locally by ground water from the spring.

Although this slide is much larger than the others discussed here, it barely crossed the creek, forming only a low dam and a resulting small impoundment. The minimum crest height of the blockage formed by the toe of the slide was 4 m. The original landslide dam was 10 m long (perpendicular to the stream) by 55 m wide (parallel to the stream); it impounded an  $1,800\text{-m}^3$ -volume lake. The dam was composed of a heterogeneous, fairly impervious mass of clay, silt, sand, and small blocks of sandstone. On December 17, 1989, 61 days after the earthquake, the landslide dam failed, causing minor downstream flooding and deposition of  $5,000\text{ m}^3$  of sediment in the streambed.

### HINCKLEY CREEK

The 1989 Hinckley Creek rock fall occurred near Olive Springs (fig. 4) on a  $60^\circ$  slope in weathered sandstone of the Purisima Formation, 60 m high, about 800 m downstream from the 1906 Hinckley Creek "Sawmill slide" (table 1). As shown by Clark and others (1989), the Purisima Formation strikes nearly normal to Hinckley Creek at this site and dips about  $20^\circ$  upstream; thus, the attitude of the formation had little influence on the 1989 slope failure. Weathering and joints at the surface of the sandstone probably were the important elements in failure of the slope. The 1989 rock fall had an estimated volume of  $1,600\text{ m}^3$ , consisting mainly of broken blocks of soft sandstone that disintegrated to silt and fine sand in the valley bottom. This broken-up sandstone, combined with timber debris, dammed Hinckley Creek to a depth of 4 m, impounding a lake 160 m long with an estimated volume of  $3,500\text{ m}^3$ . The blockage, which was 20 m long (normal to the creek) by 15 m wide (parallel to the creek), breached in February 1992 after heavy rain.

### CORRALITOS CREEK, UPPER DAM

The upper dam on Corralitos Creek in Eureka Canyon (fig. 5) was formed by a rock fall (fig. 7) from the weath-

ered surface of a 35-m-high,  $75^\circ$  face of Purisima Formation sandstone. In the vicinity of the rock fall, the Purisima Formation strikes nearly normal to the creek and dips  $35^\circ$  upstream (McLaughlin and others, 1988); thus, the failure was related to surficial weathering and jointing, not to the attitude of the sandstone forming the face. The volume of the rock fall was only  $3,500\text{ m}^3$ , but because it fell into a very narrow (10 m wide) canyon bottom, it formed a blockage that was 7 m high at the low point of the crest. This



Figure 7.—Rock fall on upper Corralitos Creek (see fig. 5 for location) triggered by 1989 Loma Prieta earthquake. Note logs and brush intermingled with earth material to form landslide dam at base of slope. Impoundment is outside photograph to immediate left. Photograph taken October 25, 1989, 1 week after 1989 Loma Prieta earthquake.

mass of silt and fine sand from disintegrated rock-fall blocks impounded an estimated 6,000 m<sup>3</sup> of water. Just 1 day after the earthquake, a spillway was excavated across the 25-m-wide landslide dam by a Santa Cruz County Flood and Water Conservation District crew, and within 2 weeks the dam was removed. No downstream flooding occurred.

### CORRALITOS CREEK, LOWER DAM

The lower dam on Corralitos Creek in Eureka Canyon (100 m downstream from the upper dam, fig. 5) was formed by a shallow rockslide from a 30° valley wall consisting of weathered sandstone, siltstone, and mudstone of the Purisima Formation. A spring at the site of the slide was a prime factor in the failure. As shown by McLaughlin and others (1988), the Purisima Formation in the vicinity of the site strikes nearly normal to the creek, and the rocks dip 37° upstream; thus, the attitude of the formation probably was not a factor in the failure. The slide formed a dam of clay, silt, and fine sand that was 3 m high, 20 m long (normal to the creek), and 20 m wide (parallel to the creek), and it impounded a pond with an estimated volume of 1,300 m<sup>3</sup>. Just 1 day after the earthquake, a spillway was constructed across the landslide dam by a Santa Cruz County Flood and Water Conservation District crew, and within 2 weeks the dam was removed. No downstream flooding occurred.

### BROWNS CREEK

The small landslide dam on Browns Creek (fig. 5) was formed by a 200-m<sup>3</sup> rock fall on a 70° canyon wall of weathered and jointed Purisima Formation sandstone. In the vicinity of the dam, the Purisima Formation strikes nearly normal to the creek and dips about 20° downstream (McLaughlin and others, 1988); thus, the attitude of the bedding had little influence on the stability of the steep face. As in the rock falls described above, the failure was related primarily to jointing in the soft, weathered sandstone composing the steep face above the creek. The dam was only 2 m high at the low point in the crest, 8 m long (normal to the stream), and 8 m wide (parallel to the stream) at its narrowest part. The impoundment was only 40 m long. The blockage failed by overtopping, but the volume of the pond (about 150 m<sup>3</sup>) was so small that no downstream flooding occurred.

In summary, all five of the landslides that formed dams occurred in Purisima Formation weathered sandstone, siltstone, or mudstone on slopes ranging from 26° for the slide on West Branch Soquel Creek to 75° for the rock fall that formed the upper dam on Corralitos Creek. Landslide volumes ranged from only 200 m<sup>3</sup> for the rock fall

on Browns Creek to about 50,000 m<sup>3</sup> for the slide on West Branch Soquel Creek. The effective heights of the landslide dams were all small, ranging from 2 m for the dam on Browns Creek to 7 m for the upper dam on Corralitos Creek. In addition, these small landslide dams occurred in narrow canyons with steep gradients; thus, the impoundments were also small, ranging from 150 m<sup>3</sup> behind the lower dam on Corralitos Creek to 6,000 m<sup>3</sup> behind the upper Corralitos Creek dam. None of the impounded lakes was large enough to cause damage from upstream flooding or to pose a serious downstream flooding hazard if its dam had failed.

### EFFECTS

Damming of streams in Santa Cruz County by landslides triggered by the 1989 Loma Prieta earthquake caused no permanent change in the gradients of the streams because the dams were small and either were soon removed by the Santa Cruz County Flood and Water Conservation District or breached owing to natural causes. However, they did affect the streams in regard to (1) upstream flooding due to impoundment, (2) downstream flooding resulting from dam failure, (3) deterioration of water quality downstream, and (4) deterioration of fish habitats.

### UPSTREAM FLOODING

As noted earlier, upstream or backwater flooding was minimal from all five landslide dams because of low dam heights, narrow canyons, and steep stream gradients, all of which resulted in small impoundments. The longest lake, behind the Hinckley Creek landslide dam, was only 160 m long. In addition, no buildings or other structures were located immediately upstream of the dams. Thus, the impoundments caused no significant upstream damage or economic loss.

### DOWNSTREAM FLOODING

Although the impoundments were small, there still was some danger of downstream flooding if the dams were to breach rapidly. For this reason, the Santa Cruz County Flood and Water Conservation District and its contractors excavated spillways across both of the Corralitos Creek landslide dams within 72 hours after the earthquake. Excavation was difficult because large amounts of tree and brush remnants (logs, limbs, and so on) were incorporated into the dams (fig. 8). This same wood material, however, protected the constructed spillways against erosion. Within 2 weeks after the earthquake, both Corralitos Creek landslide dams were completely removed by Santa Cruz County



Flood and Water Conservation District crews because of the potential danger of dam failure and flooding during future heavy rains. Nothing was done to the Browns Creek landslide dam because its impoundment was too small to be considered a threat downstream; it was allowed to fail naturally.

On the day after the earthquake, the landslide dam on West Branch Soquel Creek (fig. 6) was noted from the air (Capt. Dennis Smith, Santa Cruz County Sheriff's Office, oral commun., 1989). However, because this landslide dam was in an unpopulated, untraveled area and its impoundment was small, no mitigative measures were undertaken.



Figure 8.—Rock-fall and timber debris forming dam on Hinckley Creek (see fig. 4 for location). Arrows denote downstream end of impoundment. Photograph taken on October 25, 1989, 1 week after 1989 Loma Prieta earthquake.



Figure 9.—Downstream view of remnants of 1989 Hinckley Creek landslide dam after it had failed in February 1992. Arrows denote previous shoreline of now-drained 4-m-deep impoundment. Photograph taken May 1992.

Then, 61 days after the earthquake, the dam failed, causing minor downstream flooding in the channels of West Branch Soquel Creek and Soquel Creek. Channel capacity was not exceeded; thus, no damage occurred as a result of flooding.

The 4-m-high Hinckley Creek landslide dam was naturally reinforced by timber debris (logs and limbs) within the landslide, and so, because it was thought to be stable, it was not removed, as both the Corralitos Creek landslide dams were. During heavy rain in February 1992, however, the soil matrix of the dam was removed by erosion, resulting in rapid drainage of the impoundment (fig. 9) and minor downstream flooding that did not exceed channel capacity. Most of the interwoven logs, branches, and brush that had held the dam together remained in place (fig. 10).

#### DETERIORATION OF WATER QUALITY

No formal studies were conducted on the effects of the five 1989 landslide dams on the water quality of Soquel, Hinckley, Corralitos, and Brown Creeks, although it was noted that Corralitos Creek received only small amounts of sediment over a short period of time because its two landslide dams were effectively removed by Santa Cruz County Flood and Water Conservation District crews. Although the Browns Creek landslide dam failed, it was so small that only about 200 m<sup>3</sup> of earth material washed down the stream.



Figure 10.—Closeup of log/brush remnant of 1989 Hinckley Creek landslide dam after soil matrix of dam had eroded away in February 1992. Photograph taken May 1992.

The effects of the West Branch Soquel Creek and Hinckley Creek landslide dams on downstream water quality were more serious because both of these dams failed and both were made up of moderate amounts of earth material that was flushed downstream. As noted above, the landslide dam on West Branch Soquel Creek failed in December 1989, 61 days after the earthquake. During this 61-day period, approximately 2,500 m<sup>3</sup> of soil eroded from the upstream part of the landslide and was deposited in the impoundment. When the dam failed, this material, plus an equal amount from the dam itself, was carried downstream by the floodwaters. Gravel and coarse sand were deposited within the first few hundred meters, but silt was carried as far as 2 km downstream on West Branch Soquel Creek. Clay-size particles were carried in suspension even farther.

When the soil matrix of the rest of the Hinckley Creek landslide dam eroded away in February 1992, the effect on downstream water quality was similar to that from the failure of the landslide dam on West Branch Soquel Creek, except that only about 1,000 m<sup>3</sup> of sediment was washed downstream. The coarse materials were deposited within 200 m of the dam, but a significant amount of silt and fine sand was carried as far as the confluence of Hinckley and Soquel Creeks, 1 km downstream (fig. 4).

The clay in sediment from the failures of the landslide dams on both West Branch Soquel Creek and Hinckley Creek evidently was carried farther downstream in suspension, as were small amounts of suspended sediment from both Corralitos Creek landslide dams, but these small amounts of suspended material had no evident long-term effect on water quality in the streams.

#### DETERIORATION OF FISH HABITATS

Soquel, Hinckley, Corralitos, and Browns Creeks serve as spawning grounds for steelhead trout and as permanent habitats for a few other species of nonsport fish. The anadromous steelhead require stable gravelly stream bottoms as spawning beds. Spawning is unsuccessful when these gravel beds are buried by silt and fine sand, as occurred immediately downstream of the failed landslide dams on West Branch Soquel Creek and Hinckley Creek. However, because the stretches of these streams that were subjected to fine-grained sedimentation constituted only a small percentage of the total spawning areas on the headwaters of these streams, and because very little sedimentation occurred in Corralitos and Browns Creeks, the overall effects of the 1989 landslide dams on steelhead reproduction were insignificant. Because spawning occurs in the fall and winter, the sediment was deposited at a critical time; however, other factors, such as below-normal streamflow due to the prolonged drought, may have had a greater effect on spawning in 1989–90 than did sediment from the failed landslide dams.

## FACTORS AFFECTING THE DISTRIBUTION OF LANDSLIDE DAMS

### SEISMIC INTENSITY

The distribution of landslide dams caused by the 1989 Loma Prieta earthquake was geographically restricted close to the epicentral area (figs. 4, 5). All five landslide dams occurred within about 10 km or less northwest, west-northwest, or southeast of the epicenter (table 3). Bilateral fault rupture to the northwest and southeast of the epicenter (Beroza, 1991; Wald and others, 1991) may have influenced the distribution of strong ground shaking and of landslide-dam sites to the northwest and southeast in this vicinity.

The Corralitos strong-motion station on Eureka Canyon Road was located only 7 km west of the earthquake epicenter (figs. 4, 5); two other stations at Capitola and Santa Cruz were also near ( $\leq 16$  km from) the epicenter. All three stations recorded comparable peak accelerations of 0.4 to 0.6 *g* (table 4) for both horizontal and vertical components. The fact that these three stations are at distances comparable to or slightly greater than the distances of all five landslide dams from the epicenter suggests that the peak accelerations recorded there were at least as great at these landslide-dam sites.

The Corralitos strong-motion station is located on a landslide deposit derived from the same bedrock geologic unit, the Purisima Formation (Brabb, 1989), as that of all five 1989 landslide dams. The Santa Cruz station, however, is founded on limestone, and the Capitola station on alluvium (Shakal and others, 1989). Therefore, the site response at the Corralitos station most nearly represents the strong ground motion at the landslide-dam sites because of a similarity of geologic materials and a distance from the epicenter that is comparable to those of all the landslide dams.

In addition to peak accelerations, the duration of strong shaking is important for evaluating seismic intensity and the ability to trigger landslides. Strong shaking from the earthquake lasted at least 15 to 20 s, as recorded at these three stations closest to the epicenter (Shakal and others, 1989). The Arias intensity,  $I_a$ , is defined as:

$$I_a = (\pi/2g) \int_0^{\infty} [a(t)]^2 dt,$$

where  $a$  is the acceleration,  $t$  is the time, and  $g$  is the acceleration due to gravity (Arias, 1970). The Arias intensity is expressed in units of velocity, usually meters per second. Because calculation of the Arias intensity involves the entire record, its value is proportional to the duration as well as the amplitude of the shaking record.

The high  $I_a$  values, ranging from 0.9 to 4.3 m/s (table 4), for Corralitos and Capitola, the two stations closest to the epicenter, are significant because they greatly exceed  $I_a=0.11$  m/s as a shaking threshold for falls, disrupted slides, and avalanches (category I landslides; Keefer and Wilson, 1989) and  $I_a=0.32$  m/sec as a shaking threshold for slumps, block slides, and slow earth flows (category II landslides; Keefer and Wilson, 1989). The large (50,000- $m^3$  volume) rock slide on West Branch Soquel Creek is a category II landslide, whereas the other smaller ( $\leq 3,500$   $m^3$  volume) rock falls and rock slides at the other sites were category I landslides—generally shallow and highly to very highly disrupted internally.

With the combination of strong horizontal and vertical components and long duration of strong shaking, the high  $I_a$  values from these three strong-motion records nearest the epicenter are among the highest ever measured. This intensity of seismic shaking in the area of the landslide dams generally corresponds to the heavy structural damage and firsthand observations of extreme shaking in the near-epicentral area.

### SLOPE STEEPNESS/TOPOGRAPHY

Slope steepness strongly affected the distribution of landslide dams caused by the earthquake. Steep slopes are common throughout the near-epicentral area. Regional tectonism has uplifted the southern Santa Cruz Mountains to maximum elevations of about 1,150 m at Loma Prieta. In this earthquake, the maximum surface uplift on the west side of the San Andreas fault was 592 mm (Marshall and others, 1991). Active tectonics, in combination with downcutting by streams in this area of moderately high average annual rainfall (860–1,120 mm; Rantz, 1971), has produced steeply sloped canyons that are prone to landsliding due to both seismic shaking and precipitation.

The sites of the landslide dams caused by the earthquake were all on steep slopes. The steepest slopes ( $\geq 60^\circ$ ) sustained rock falls (Hinckley Creek; Corralitos Creek, upper dam; and Browns Creek). The other two sites (West Branch Soquel Creek and Corralitos Creek, lower dam) had lesser slopes (approx  $30^\circ$ ) but also had springs near their crowns, suggesting that ground water played a significant part in slide initiation. No common or predominant slope aspect was observed.

### LITHOLOGY/WEATHERING PROPERTIES

The Purisima Formation forms most of the surface area of the southern Santa Cruz Mountains in the vicinity of the five landslide-dam sites (figs. 4, 5; McLaughlin and others, 1988; Brabb, 1989, Clark and others, 1989). The

Table 3.—Distance and direction of landslide-dam sites from the epicenter of the 1989 Loma Prieta earthquake

Location/ stream	Slope aspect	Distance from epicenter (km)	Direction from epicenter
West Branch Soquel Creek.	SW	7.0	NW
Hinckley Creek (Olive Springs).	SE	2.8	W-NW
Corralitos Creek, upper dam.	W-SW	6.8	SE
Corralitos Creek, lower dam.	W-SW	7.0	SE
Browns Creek.	NW	10.2	SE

Table 4.—Seismic intensity of the 1989 Loma Prieta earthquake near landslide dams

[From Shakal and others (1989); Arias intensities from E.L. Harp (written commun., 1992)]

Strong- motion station name	Epicentral distance (km)	Comp- onent	Peak accel- eration, g	Arias Intensity, $I_a$ (m/s)	Site Geology
Corralitos --- 7		90	.50	2.572	Landslide deposits.
		Up	.47	0.917	
		360	.64	3.258	
Capitola ----- 9		90	.47	2.373	Alluvium.
		Up	.60	4.279	
		360	.54	4.382	
Santa Cruz --- 16		90	.44	2.043	Lime- stone.
		Up	.40	1.072	
		360	.47	2.666	

Purisima Formation consists of upper Miocene and Pliocene, very thick bedded, tuffaceous, diatomaceous siltstone with thick interbeds of semifriable, fine-grained andesitic sandstone. As mapped in some areas, the Purisima Formation includes Santa Cruz Mudstone, a medium- to thick-bedded, blocky-weathering, siliceous organic mudstone. The area is thickly vegetated by redwood and other evergreen forest. The relatively few outcrops expose deeply weathered bedrock. A generally deep weathering profile in the Purisima Formation bedrock resulted in mainly shallow (<3 m deep) landslides representative of most of those that dammed streams in this earthquake.

#### SOIL MOISTURE/GROUND WATER

Soil-moisture contents and ground-water levels at the time of the earthquake were probably at or near record historical lows. The third consecutive season (1986-87, 1987-88, 1988-89) of abnormally low rainfall or drought conditions, combined with the end of the summer dry season before the onset of fall rains, set the hydrogeologic stage for the region at the time of the earthquake. In the Santa Cruz Mountains, hillside ground-water levels typically fluctuate about 5 m during years of near-average rainfall (Rojstaczer and Wolf, 1991). This semiannual cycle

ranges from high hillside ground-water levels at or slightly after the height of the January–March rainy season to low ground-water levels at the end of the summer dry season before the onset of fall rains in October or November (fig. 11). The seasonal ground-water trends from 1976 to 1990 and the low ground-water levels at the time of the earthquake in the Santa Cruz Mountains were well documented in one well that was monitored weekly (fig. 12), and confirmed by numerous other well and stream-gage records in basins in the area affected by the earthquake (Rojstaczer and Wolf, 1991).

The exceptionally low ground-water levels at the time of the earthquake probably minimized the number and volumes of landslides triggered by the earthquake, particularly limiting deeper-seated coherent landslides (category II landslides; Keefer and Wilson, 1989). Some deep hillside soils and rocks that normally would have been below ground-water levels and thus would have been saturated were probably dry and thus more resistant to sliding at the time of the earthquake. However, springs at the head of the West Branch Soquel Creek and lower Corralitos Creek sites indicated that in isolated places ground water remained moderately high and may have assisted in triggering landslides.

Ground-water flow in fracture networks immediately after the earthquake was suggested to be important. The earthquake apparently caused discharge of water from fractures and resulting short-term increases in streamflow. Water-well levels on ridgecrests generally fell within several weeks after the earthquake (Rojstaczer and Wolf, 1991), and streamflows in the basins increased by a factor of 2 to 5 within hours of the main shock (Briggs, 1991; Curry and others, 1994). This sudden increase in fracture flow and streamflow probably had a minimal effect on the triggering of landslides at the time of the earthquake because of the delay times needed for water to flow through the fractures. However, the increased flows probably significantly affected landslide dams because their impoundments were able to fill at faster rates than would have been expected for preearthquake streamflow.

### INFLUENCE OF CLIMATE AND HYDROGEOLOGY

Landslide dams are a potential hazard in areas that are subject to large earthquakes and vulnerable to landslides

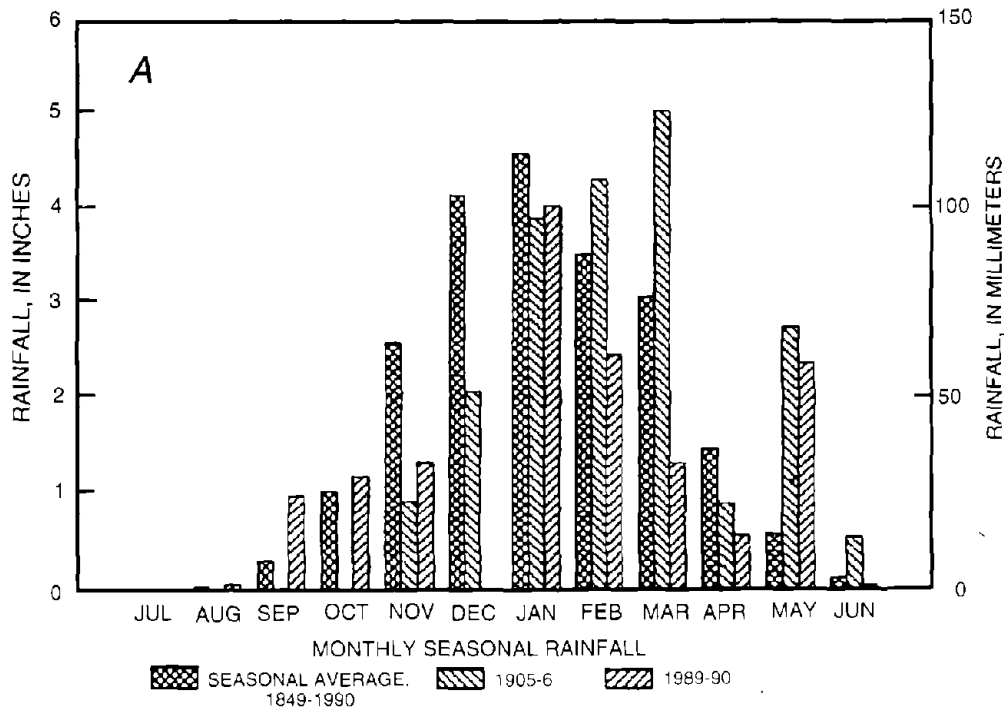


Figure 11.—Monthly seasonal rainfall for San Francisco (A), Santa Cruz (B), and Watsonville (C) for 1905–6 and 1989–90, in comparison with long-term monthly averages. In 1905–6, before 1906 San Francisco earthquake, rainfall during months of January, February, and March, normally wettest part of year, was about equal to or above long-term monthly averages for these months. During 1989–90, before 1989 Loma Prieta earthquake, monthly rainfall in July, August, and September was above average, but total was extremely low during this normally dry part of season. Data from U.S. Department of Agriculture (1907) and U.S. National Oceanic and Atmospheric Administration (1988, 1989, 1990).

on steep slopes. The seasonal climatic and hydrologic characteristics of a region, however, are extremely important in establishing the severity of hazard. Of the

historical landslide dams in California, very few have occurred in seismically active southern California, where seasonal rainfall, hillside ground-water levels, and

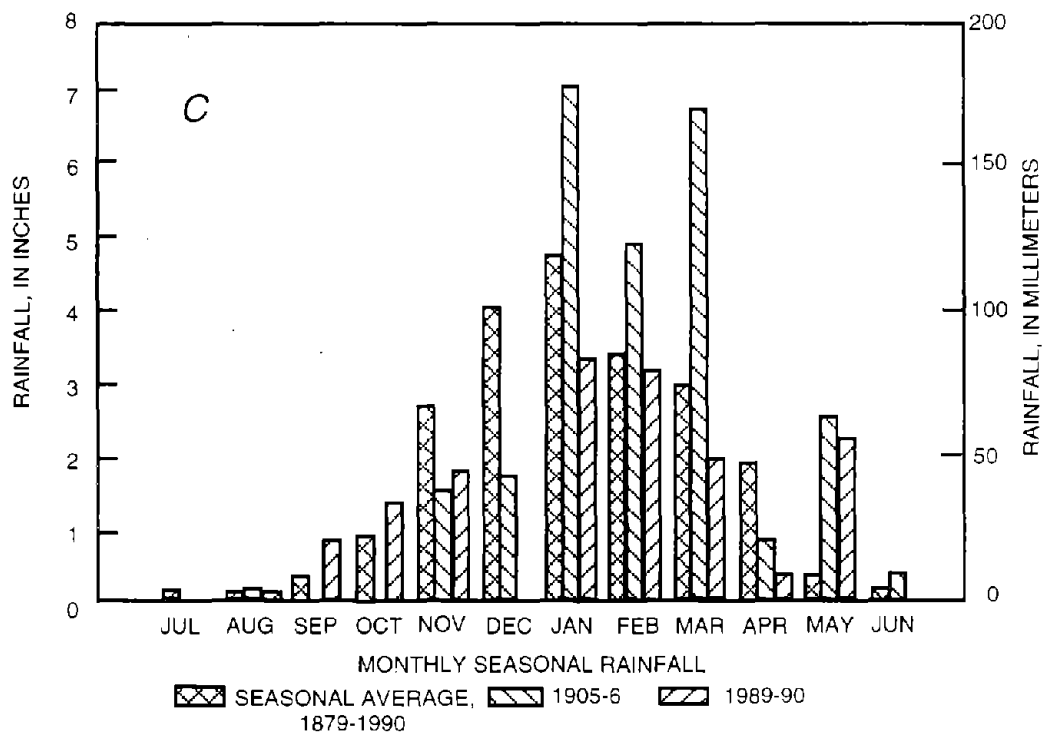
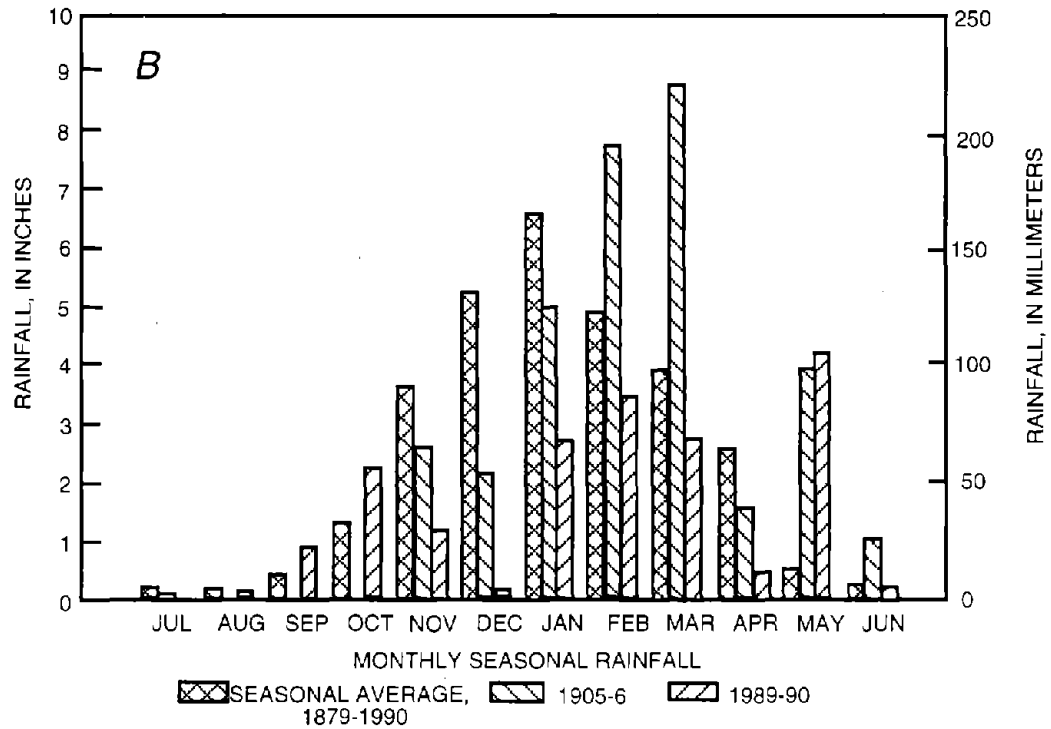


Figure 11.—Continued.

streamflow are generally lower than in central and northern California.

On the basis of a comparison of the ground-failure effects of the 1906 and 1989 earthquakes, apparently more numerous deep-seated landslides (category II) and landslide dams occur during wet periods, although differences in earthquake magnitude and duration, topography, and geologic site conditions could account for some of the observed variations. The difference in size between the 1906 San Francisco earthquake ( $M=8.2$ ) and the 1989 Loma Prieta earthquake ( $M=7.1$ ) can certainly account for the major difference in the number of landslides and landslide dams caused by these two earthquakes, but hydrogeologic conditions, as influenced by antecedent rainfall, probably also were a significant factor. The influence of antecedent rainfall on the seismic triggering of landslides that form dams can be examined by comparing the 1906 San Francisco earthquake with the 1989 Loma Prieta earthquake. The 1906 earthquake triggered many large, deep-seated landslides throughout the coastal area of central and northern California (Youd and Hoose, 1978), and created at least eight landslide dams, some of which were large (fig. 1; table 1). In contrast, the 1989 earthquake triggered mostly shallow landslides, commonly less than about  $100 \text{ m}^3$  in volume. Of the five landslides that dammed streams in Santa Cruz County in 1989, four were small ( $\leq 3,500 \text{ m}^3$  volume). The resulting small landslide dams might have gone unnoticed in remote areas or been underreported during postearthquake investigations, and so the number of landslide dams resulting from the 1906 earthquake may have been even higher than reported. Thus, the largest (category II) landslide dam (on West Branch Soquel Creek) that occurred in the 1989 earthquake can be compared to each of six that occurred in the 1906

earthquake. Because category II landslides are commonly larger and more deep seated than category I landslides, they are more likely to fill or constrict narrow canyons and to form large landslide dams.

Although it had not rained for 17 days before the April 18, 1906, earthquake (Youd and Hoose, 1978), the month of March 1906 was exceptionally wet (fig. 11). Cumulative rainfall for San Francisco, Santa Cruz, and Watsonville for 1-, 3-, and 6-month periods before the earthquake was about  $1\frac{1}{2}$  to 2 times normal (table 5). Thus, at the time of the 1906 earthquake, although surface soils may have dried, hillside ground-water levels probably were relatively high throughout central and northern California as a result of the high antecedent rainfall in the preceding several months (Youd and Hoose, 1978). The exact period of antecedent rainfall that is most effective in recharging and raising ground-water levels at a particular site depends on site-specific characteristics of the soil and rock—thickness, permeability, and stratigraphy. The fact that much higher than normal rainfall occurred consistently during the 1- to 6-month period before the 1906 earthquake suggests that ground-water levels were significantly above normal, if recent ground-water measurements after heavy seasonal rainfall in northern California are any indication (Wieczorek, 1981; Wilson and Dietrich, 1987; Wilson, 1989; Rojstaczer and Wolf, 1991).

In comparison, rainfall recorded at San Francisco, Santa Cruz, and Watsonville before the 1989 earthquake was significantly below normal for the preceding 1-, 3-, 6-, and 12-month periods or for seasonal totals (table 5). In addition, significant gradual decreases in ground-water levels for the 1989–90 season before the earthquake were measured in the Santa Cruz Mountains (Rojstaczer and Wolf, 1991). These generally low ground-water levels were probably at least partly responsible for the relatively few large, deep-seated landslides that occurred or that moved only short distances in the earthquake (Plafker and Galloway, 1989; Keefer, 1991; Keefer and Manson, this volume; Keefer and others, this volume).

The time required for a landslide-dam impoundment to fill depends (1) on the rate of stream discharge, which in California is controlled by seasonal patterns of rainfall, infiltration, and runoff; and (2) on the basic characteristics of the dam, including height, potential storage capacity, and permeability. The 61-day period after the 1989 Loma Prieta earthquake before the failure of the landslide dam on West Branch Soquel Creek attests at least in part to the relatively low runoff during the fall rains after a 3-year drought.

There appears to be inadequate accurate historical information available for a statistically significant characterization of the expected size of landslide dams in California. Given the specific size and location of a postulated earthquake, then the areal limits of category I and II landslides can be estimated by the methods of Keefer

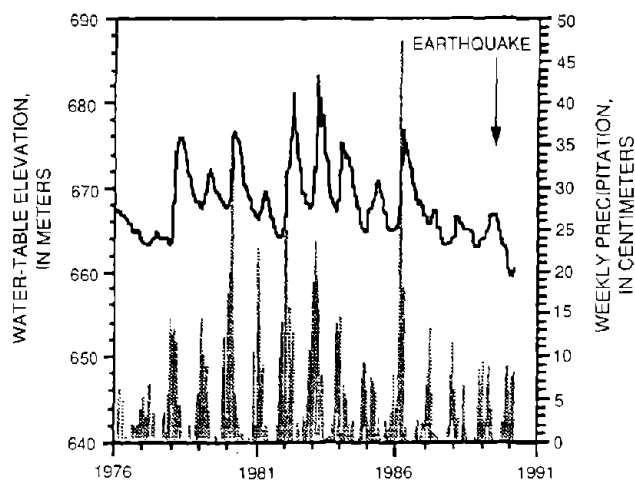


Figure 12.—Water-table elevation (from well on east edge of Pescadero Basin, 25–35 km northwest of landslide dams in this paper) as a function of precipitation for period 1976–90 (Rojstaczer and Wolf, 1991).

Table 5.—Antecedent, seasonal, and average rainfall for 1-, 3-, 6, and 12-month periods before the 1906 San Francisco and 1989 Loma Prieta earthquakes measured in San Francisco (1849–1990), Santa Cruz (1879–1990), and Watsonville (1879–1990)

[Data from U.S. Department of Agriculture (1907) and U.S. National Oceanic and Atmospheric Administration (1988, 1989, 1990)]

Antecedent time period	San Francisco rainfall (mm)	Santa Cruz rainfall (mm)	Watsonville rainfall (mm)
<b>1 month:</b>			
Mar. 1906	127.5	220.1	167.9
(avg)	(65.5)	(96.3)	(74.2)
Sept. 1989	24.9	22.1	21.8
(avg)	(6.1)	(9.9)	(8.9)
<b>3 months:</b>			
Jan.-Mar. 1906	260.35	541.5	468.1
(avg)	(251.2)	(383.8)	(278.6)
July-Sept. 1989	26.2	23.9	22.9
(avg)	(9.1)	(17.3)	(13.5)
<b>6 months:</b>			
Oct. 1905-Mar. 1906	411.2	658.1	549.9
(avg)	(431.5)	(638.8)	(471.4)
April-Sept. 1989	47.2	45.2	41.9
(avg.)	(59.4)	(97.3)	(72.4)
<b>12 months:</b>			
Apr. 1905-Mar. 1906	497.1	806.5	698.5
(avg)	(544.3)	(736.1)	(543.8)
Oct. 1988-Sept. 1989	413.3	614.7	444.0
(avg.)	(544.3)	(736.1)	(543.8)
<b>Seasonal totals:</b>			
1905-6 (July 1905-June 1906)	518.7	819.4	645.4
1988-9 (July 1988-June 1989)	387.9	590.8	421.1
1989-90 (July 1989-June 1990)	363.7	444.2	377.2
Yearly average -----	544.3	736.1	543.8

and Wilson (1989) and used to predict the extent of landslide-dam occurrence.

## MITIGATION OF STREAM DAMMING

The 1989 Loma Prieta earthquake occurred at 5:04 p.m. P.d.t. October 17. By 10:00 a.m. the next morning, reconnaissance by helicopter and fixed-wing aircraft, coupled with coordinated ground reconnaissance, had located all of the landslide dams caused by the earthquake. This rapid reconnaissance was a critical factor in the success of the dam-failure-control program.

After the reconnaissance, a priority assessment was conducted to review dam size, impoundment volume, potential for failure, and potential flood discharge. Dams close to homes and public infrastructure were given the highest

priority for mitigative efforts, although water quality and fish habitats were also considered. Access by earth-moving equipment to the two landslide dams on Corralitos Creek was facilitated by use of Santa Cruz County roads.

The two landslide dams on Corralitos Creek were given the highest priority, and Santa Cruz County Flood and Water Conservation District crews immediately began to excavate spillways across both dams. The spillway inverts were positioned significantly below the crests of the dams, thus reducing the volume of impounded water and preventing erosion failures by overtopping of the unprotected crests of the original dams. Each spillway was constructed across the low side of the dam crest opposite the landslide source. In general, this part of the landslide dam contained the most woody debris. Wherever possible, this debris was left in place along the bottom and sides of the spillway for stabilization.



There was concern that impending winter storms would greatly increase streamflows, possibly mobilizing upstream logs and debris that could block the newly excavated spillways and cause dam failure. In addition, there also was concern that the dams would block upstream migration of anadromous steelhead trout. Thus, Santa Cruz County Flood Control and Water Conservation District crews used earth-moving equipment to remove the dams. The operation was completed by "stage" (that is, incremental) excavation. Soils and debris either were trucked to offsite locations or were spread in thin layers across existing flood plains.

Removal of landslide-dam materials was followed by seeding and mulching of the newly exposed surfaces and of spoil areas to which the materials had been hauled. The complete removal of the dams and seeding/mulching of fresh soil surfaces left the sites with the same stream gradients and crossprofiles that they had before the earthquake. The long-term effect on fish habitats was minimal. Water quality was temporarily affected by increased turbidity during operations, but monitoring of water conditions and aquatic-life responses indicated little or no loss of stream life or long-term damage to fish habitats.

## CONCLUSIONS

Precipitation totals in Santa Cruz County in the months before the 1989 Loma Prieta earthquake were considerably lower than those before the 1906 San Francisco earthquake. As a result of a smaller earthquake and less antecedent rainfall, fewer landslides and landslide dams occurred in 1989 than in 1906; furthermore, the 1989 blockages were smaller and impounded only small lakes. Because of their small size, the effects of these dams and their impoundments were minor. However, if future earthquakes in California are larger and (or) occur during or soon after periods of heavy and prolonged rainfall that result in saturated soil conditions, landslide dams can be expected to be more numerous and larger than those caused by the 1989 earthquake. Thus, the hazards due to potential landslide dams and their impoundments should be considered in planning for future earthquake hazard mitigation in California.

Downstream and upstream flooding are probably the most serious hazards to be expected from future landslide dams. Downstream flooding from breaching of a dam commonly is more serious, especially if the flood is unexpected; the severity of downstream flooding depends on the volume of the impoundment, the quickness of failure of the dam, and the velocity of flow. Upstream flooding is generally more gradual and leaves adequate time for evacuation. Other potential hazards from landslide dams include sedimentation, deterioration of water quality, and erosion of the channel or flood plain. Disruption or block-

age of streamflow below the dam, as well as sedimentation, may pose a hazard to fish habitats.

## REFERENCES CITED

- Arias, Arturo, 1970, A measure of earthquake intensity, in Hansen, R.J., ed., *Seismic design for nuclear power plants*: Cambridge, Mass., MIT Press, p. 438-483.
- Beroza, G.C., 1991, Near-source modeling of the Loma Prieta earthquake; evidence for heterogeneous slip and implications for earthquake hazard: *Seismological Society of America Bulletin*, v. 81, no. 5, p. 1603-1621.
- Brabb, E.E., 1989, *Geologic map of Santa Cruz County, California*: U.S. Geological Survey Miscellaneous Investigations Series Map I-1905, scale 1:62,500.
- Briggs, R.O., 1991, Effects of Loma Prieta earthquake on surface waters in Waddell Valley: *Water Resources Bulletin*, v. 27, no. 6, p. 991-999.
- Buwalda, J.P., and St. Amand, Pierre, 1955, Geological effects of the Arvin-Tehachapi earthquake, in Oakeshott, G.B., ed., *Earthquakes in Kern County, California, during 1952*: California Division of Mines Bulletin 171, p. 41-56.
- Clark, J.C., Brabb, E.E., and McLaughlin, R.J., 1989, *Geologic map and structure sections of the Laurel 7 1/2' Quadrangle, Santa Clara and Santa Cruz Counties, California*: U.S. Geological Survey Open-File Map 89-676, 30 p., 2 sheets.
- Costa, J.E., and Schuster, R.L., 1988, The formation and failure of natural dams: *Geological Society of America Bulletin*, v. 100, no. 7, p. 1054-1068.
- , 1991, Documented historical landslide dams from around the world: U.S. Geological Survey Open-File Report 91-239, 486 p.
- Curry, R.R., Emery, B.A., and Kidwell, T.G., 1994, Sources and magnitudes of increased streamflow in the Santa Cruz Mountains for the 1990 water year after the earthquake, in Rojstaczer, Stuart, ed., *The Loma Prieta, California, earthquake of October 17, 1989—hydrologic disturbances*: U.S. Geological Survey Professional Paper 1551-E, p. E31-E50.
- Dwyer, M.J., Scott, R.G., and Lorens, P.J., 1971, Reconnaissance study of landslide conditions and related sediment production on a portion of the Eel River and selected tributaries: California Department of Water Resources Memorandum Report, 69 p.
- Fry, Walter, 1933, The great Sequoia avalanche: *Sierra Club Bulletin*, v. 18, no. 1, p. 118-120.
- Keefer, D.K., 1984, Landslides caused by earthquakes: *Geological Society of America Bulletin*, v. 95, no. 4, p. 406-421.
- , ed., 1991, *Geologic hazards in the Summit Ridge area of the Santa Cruz Mountains, Santa Cruz County, California, evaluated in response to the October 17, 1989 Loma Prieta earthquake*; report of the Technical Advisory Group: U.S. Geological Survey Open-File Report 91-618, 427 p.
- Keefer, D.K., and Wilson, R.C., 1989, Predicting earthquake-induced landslides, with emphasis on arid and semi-arid environments, in Sadler, P.M., and Morton, D.M., eds., *Landslides in a semi-arid environment*: Riverside, Calif., Inland Geological Society, v. 2, p. 118-149.
- King, Jonathan, Loveday, Ian, and Schuster, R.L., 1989, The 1985 Bairaman landslide dam and resulting debris flow, Papua New Guinea: *Quarterly Journal of Engineering Geology*, v. 22, no. 4, p. 257-270.
- Lawson, A.C., chairman, 1908, *The California earthquakes of March 27, 1906*: report of the State Earthquake Investigation Commission:

- Carnegie Institution of Washington Publication 87, 2 v.
- Li Tianchi, 1989, Landslides—extent and economic significance in China, in Brabb, E.E., and Harrod, B.L., eds., International Geological Congress, 28th, Symposium on Landslides—Extent and Economic Significance, Washington, D.C., 1989, Proceedings, p. 271–287.
- Li Tianchi, Schuster, R.L., and Wu Jishan, 1986, Landslide dams in south-central China, in Schuster, R.L., ed., Landslide dams—processes, risk, and mitigation: American Society of Civil Engineers Geotechnical Special Publication 3, p. 146–162.
- Manson, M.W., 1990, Landslide and flood potential along Cache Creek, Lake, Colusa, and Yolo Counties, California: California Geology, V. 43, no. 5, p. 99–106.
- Marshall, G.A., Stein, R.S., and Thatcher, Wayne, 1991, Faulting geometry and slip from co-seismic elevation changes: the October 1989, Loma Prieta, California, earthquake: Seismological Society of America Bulletin, v. 81, no. 5, p. 1660–1693.
- Mason, Kenneth, 1929, Indus floods and Shyok glaciers: Himalayan Journal, v. 1, p. 10–29.
- McLaughlin, R.J., Clark, J.C., and Brabb, E.E., 1988, Geologic map and structure sections of the Loma Prieta 7 1/2' quadrangle, Santa Clara and Santa Cruz Counties, California: U.S. Geological Survey Open-File Report 88–0752, 32 p., scale 1:24,000, 2 sheets.
- Plafker, George, and Galloway, J.P., eds., 1989, Lessons learned from the Loma Prieta, California, earthquake of October 17, 1989: U.S. Geological Survey Circular 1045, 48 p.
- Rantz, S.E., 1971, Mean annual precipitation and precipitation depth-duration-frequency relations for the San Francisco Bay region, California: U.S. Geological Survey Open-File Report, 23 p.
- Rojstaczer, S.A., and Wolf, S.C., 1991, Hydrologic changes associated with the Loma Prieta earthquake in the San Lorenzo and Pescadero drainage basins: U.S. Geological Survey Open-File Report 91–567, 21 p.
- Santa Cruz Morning Sentinel, 1906, Santa Cruz, Calif., April 26, p. 1.
- Scott, R.G., 1970, Landslides in Cache Canyon downstream from the Wilson Valley damsites: California Department of Water Resources Memorandum Report, 28 p.
- Shakal, A.F., Huang, M.J., Reichle, M.S., Ventura, C., Cao, T., Sherburne, R.W., Savage, M., Darragh, R.B., and Petersen, C., 1989, CSMIP strong-motion records from the Santa Cruz Mountains (Loma Prieta), California earthquake of 17 October 1989: California Division of Mines and Geology, Office of Strong Motion Studies Report OSMS 89–06, 196 p.
- Townley, S.D., and Allen, M.W., 1939, Descriptive catalogue of earthquakes of the Pacific Coast of the United States, 1769 to 1928: Seismological Society of America Bulletin, v. 29, no. 1, 572 p.
- U.S. Department of Agriculture, 1907, Report of the Chief of the Weather Bureau, 1905–1906: Washington, D.C., U.S. Government Printing Office, 405 p.
- U.S. National Oceanic and Atmospheric Administration, 1988, Climatological data annual survey—California: Washington, D.C., v. 92, no. 13, 47 p.
- 1989, Climatological data annual survey—California: Washington, D.C., v. 93, no. 13, 47 p.
- 1990, Climatological data annual survey—California: Washington, D.C., v. 94, no. 13, 47 p.
- Wald, D.J., Helmberger, D.V., and Heaton, T.H., 1991, Rupture model of the 1989 Loma Prieta earthquake from the inversion of strong-motion and broadband teleseismic data: Seismological Society of America Bulletin, v. 81, no. 5, p. 1540–1572.
- Weber, G.E., and Nolan, J.M., 1992, Landslides and associated ground failures in the epicentral region of the October 17, 1989, Loma Prieta earthquake—factors affecting the distribution and nature of seismically induced landslides: Symposium on Engineering Geology and Geotechnical Engineering, 28th, Boise, Idaho, 1992, Proceedings, p. 361–377.
- Wieczorek, G.F., 1981, Ground-water level and precipitation data for slopes near La Honda, California: U.S. Geological Survey Open-File Report 81–376, 25 p.
- Wilson, C.J., and Dietrich, W.E., 1987, The contribution of bedrock groundwater flow to storm runoff and high pore pressure development in hollows, in Beschta, R.L., Blinn, T., Grant, G.E., Swanson, F.J., and Ice, G.G., eds., Erosion and sedimentation in the Pacific rim: International Association of Hydrological Sciences Publication 165, p. 49–59.
- Wilson, R.C., 1989, Rainstorms, pore pressures, and debris flows—a theoretical framework, in Sadler, P.M., and Morton, D.M., eds., Landslides in a semi-arid environment: Riverside, Calif., Inland Geological Society, v. 2, p. 101–117.
- Youd, T.L., and Hoose, S.N., 1978, Historic ground failures in northern California triggered by earthquakes: U.S. Geological Survey Professional Paper 993, 177 p.

**THE LOMA PRIETA, CALIFORNIA, EARTHQUAKE OF OCTOBER 17, 1989:  
STRONG GROUND MOTION AND GROUND FAILURE**

LANDSLIDES

**LARGE LANDSLIDES NEAR THE SAN ANDREAS FAULT  
IN THE SUMMIT RIDGE AREA,  
SANTA CRUZ MOUNTAINS, CALIFORNIA**

By David K. Keefer,  
U.S. Geological Survey;  
Gary B. Griggs,  
University of California, Santa Cruz;  
and  
Edwin L. Harp,  
U.S. Geological Survey

**CONTENTS**

	Page	
Abstract .....	C71	
Introduction .....	72	
Physical, cultural, and seismic setting .....	72	
Location, topography, vegetation, and population .....	72	
Climate and rainfall .....	74	
Geologic setting .....	74	
Seismicity and characteristics of the 1989 Loma Prieta earthquake .....	75	
Previous landslides and landslide-hazard mapping in the Summit Ridge area .....	75	
Landslides caused by previous earthquakes .....	75	
Landslides caused by precipitation .....	75	
Landslide damage to roads .....	81	
Previous landslide-hazard mapping .....	81	
Identification and characteristics of earthquake-induced landslides .....	81	
Data and criteria for identifying landslides .....	81	
Summary of landslide characteristics .....	83	
Old Santa Cruz Highway landslide complex .....	85	
Upper Schultheis Road landslide .....	89	
Ralls Drive landslide .....	92	
Villa Del Monte landslide .....	94	
Sunset Drive area .....	95	
Upper Skyview Terrace-Bel Air Court area .....	95	
Deerfield Road area .....	96	
Lower Skyview Terrace area .....	99	
Overall landslide dimensions, movement, and setting Subsurface conditions and materials .....	99 100	
Upper Morrell Road landslide .....	103	
Burrell landslide .....	104	
Upper Redwood Lodge Road landslide .....	104	
Amaya Ridge landslide .....	108	
Lower Schultheis Road West landslide .....	108	
Other large landslides .....	110	
Postearthquake monitoring .....	110	
Surface monitoring .....	110	
Methods .....	110	
Results .....	111	
Renewed movement on the Upper Schultheis Road landslide .....	112	
Renewed movement on the Villa Del Monte landslide .....	114	
Renewed movement on the Hester Creek North landslide .....	115	
Subsurface monitoring .....	116	
Inclinometers .....	116	
Piezometers .....	117	
Discussion and conclusions .....	118	
Acknowledgments .....	127	
References cited .....	127	

**ABSTRACT**

In the Summit Ridge area, the 1989 Loma Prieta earthquake generated many anomalously large, complex landslides that differed from other landslides triggered by this or other, comparable historical earthquakes. The area in which these large landslides occurred was immediately southwest of the San Andreas fault and contained abundant other coseismic ground-deformation features. The landslides were recognized and differentiated from other coseismic effects by detailed mapping and analysis of the geomorphology of the study area. In addition to mapping and analysis, investigations included postearthquake monitoring of movement and ground-water levels; determination of subsurface conditions through drilling, trenching, and a survey of earthquake-related damage to water wells; and analytical slope-stability modeling.

Distinctive characteristics of the landslides in the Summit Ridge area included their large sizes: The landslides were as much as 980 m long and as much as 1,220 m wide, and had surface areas as great as 85 ha. Maximum landslide depths ranged from 27 to possibly more than 100 m, and estimated landslide volumes were as great as 27 million m<sup>3</sup>.

Other distinctive features of the landslides included irregular shapes and boundaries, defined by discontinuous sets of surface cracks, scarps, and compressional features. Commonly, main scarps and heads were well developed and marked by conspicuous, relatively continuous scarps and cracks; flanks were moderately developed and delineated by discontinuous, locally echelon cracks; and toes were poorly developed, with local compressional features present on some landslides but absent on others. Measured landslide displacements, which ranged from 25 to 244 cm, were small relative to landslide lengths, and the incomplete development of landslide boundaries probably resulted from these comparatively small displacements.

Material in the landslides was heterogeneous colluvium and bedrock consisting of poorly to moderately cemented sandstone, mudstone, siltstone, and shale, which were locally sheared, faulted, and folded. The largest landslides occurred where folding was most intense and faults were most numerous. Virtually all the earthquake-induced landslides exhibited geomorphic indications of previous landslide movement.

Postearthquake movement and ground-water levels were monitored through spring 1991. Rainfall during that 2-year period was below normal, except for a short time in February and March 1991, when renewed displacement and associated ground cracking occurred along and adjacent to the main scarps of three landslides. This activity, which was the only significant landslide movement recorded during the 2 years of monitoring, was probably due to local upslope migration (retrogressive failure) of the landslide heads. Measured ground-water levels during the 1991 period of high rainfall rose as much as 6.1 m.

These large, complex landslides occurred only where ground cracks produced by other coseismic processes were also abundant. This correlation indicates that the two types of features are mechanistically related. Many of the coseismic ground cracks were almost certainly produced either directly by tectonic deformation or by the effects of seismic shaking on preexisting planes of weakness. Once these ground cracks formed, they provided loci for downslope movement and landslide formation as shaking continued. This mechanism implies that landslides of this type are specifically generated by seismic shaking, a conclusion supported both by slope-stability modeling and by the historical record of landslides in the study area.

## INTRODUCTION

The 1989 Loma Prieta earthquake ( $M_S=7.1$ ,  $M=7.0$ ) generated thousands of landslides throughout an area of approximately 15,000 km<sup>2</sup> (see Keefer and Manson, this chapter). Most of these landslides were similar to those triggered by other worldwide historical earthquakes of approximately the same size (Keefer, 1984; Keefer and Manson, this chapter). In the Summit Ridge area, how-

ever, immediately southwest of the rupture zone (fig. 1), the earthquake produced many particularly large and complex landslides with uncommon characteristics. These landslides were restricted to a small area of approximately 40 km<sup>2</sup> that also contained the highest known concentration of coseismic ground cracks (see pl. 3; Spittler and Harp, 1990; additional data from Ponti and Wells, 1991 and in press, and Harp, this chapter). Outside this area, landslides were predominantly shallow, small to moderate-size rock falls, rock slides, and soil slides and small to moderate-size slumps and block slides that typically had relatively simple morphologies (Manson and others, 1991; Keefer and Manson, this chapter). Inside this area, landslides were exceptionally large and deep, complex, irregular in shape, and bounded by intricate networks of discontinuous ground cracks and other features.

The landslides in the Summit Ridge area were first recognized and differentiated from other coseismic ground-deformation effects as a result of detailed mapping initiated immediately after the earthquake (Spittler and Harp, 1990). The landslides had caused considerable damage to residences, roads, and other structures, mostly in Santa Cruz County; and because of the potential continuing hazard, a comprehensive investigation was carried out as part of the U.S. Government disaster-relief effort to Santa Cruz County (Keefer, 1991). Components of this investigation included (1) mapping ground cracks; (2) surveying selected topographic profiles; (3) reviewing historical and scientific literature on pre-1989 landslides in the area; (4) compiling data on earthquake-induced damage to water wells in the area; (5) trenching across selected scarps; (6) drilling, sampling, and testing landslide materials; (7) installing and monitoring arrays of survey stakes and strain gages to measure any surficial, postearthquake landslide movements; (8) installing and monitoring borehole inclinometers and piezometers to measure subsurface movements and ground-water levels; and (9) performing analytical slope-stability modeling.

This paper describes the unusual features of these landslides, summarizes the results of investigations, and suggests a mechanism for landslide generation. Some aspects of the investigations are also discussed in other publications (Griggs and others, 1990; Spittler and Harp, 1990; William Cotton and Associates, 1990; Keefer, 1991; Marshall and Griggs, 1991; Harp, this chapter; Nolan and Weber, this chapter).

## PHYSICAL, CULTURAL, AND SEISMIC SETTING

### LOCATION, TOPOGRAPHY, VEGETATION, AND POPULATION

The Summit Ridge area is adjacent to the northeast edge of Santa Cruz County, Calif., approximately 80 km

southeast of San Francisco, 16 km south of San Jose, and 16 km north of Santa Cruz (fig. 1). The boundaries of the area studied in most detail (see pl. 3), which contained most of the large, complex landslides, were chosen on the basis of criteria established for U.S. Government disaster assistance (Keefer, 1991).

Much of the north and northeast boundary of the study area coincides with the crest of the Santa Cruz Mountains, which separate the San Francisco Bay region to the north and east from the Monterey Bay region to the south and west. The highest point in the Santa Cruz Mountains is the summit of Loma Prieta, approximately 6 km east of the study area, which has an elevation of 1,155 m above mean sea level. Within the study area itself, elevation

ranges from approximately 160 to 661 m. The study area includes parts of Skyland Ridge, the features locally known as Summit Ridge and Amaya Ridge, and several adjacent ridges and valleys (see pl. 3). Surveyed profiles show that average slopes in the area typically range from 10° to 25°. Many slopes also exhibit irregular, benched topographic profiles, with alternating steep and gentle stretches. Much of the study area is covered with dense forest, dominated in some zones by coast redwood (*Sequoia sempervirens*) and in others by oak (*Quercus sp.*). Nonforested areas are typically covered by chaparral or grassland vegetation.

Despite the proximity of the study area to an urban metropolis of 5.9 million people in the San Francisco Bay region, the study area is primarily rural to locally subur-

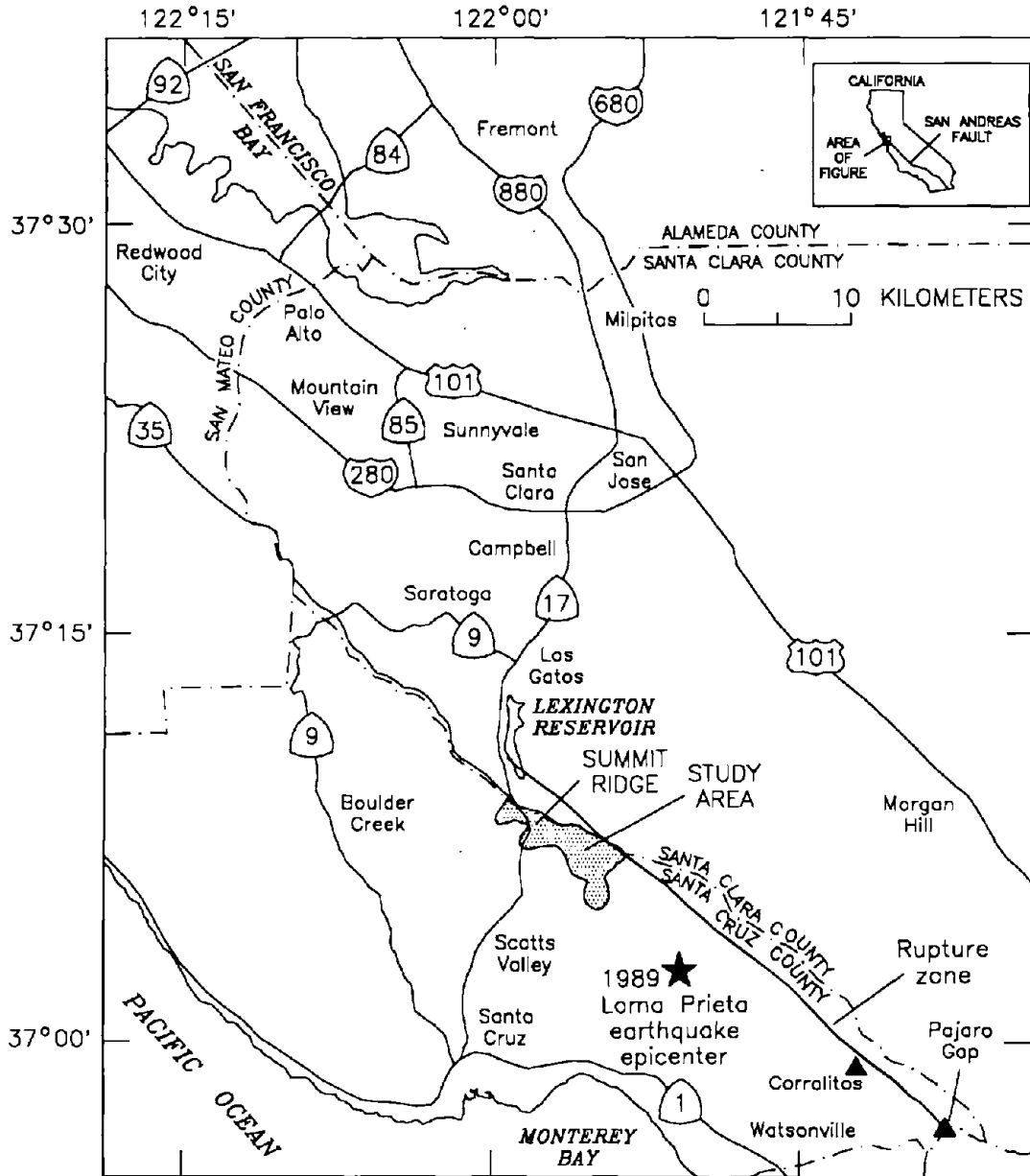


Figure 1.—Loma Prieta region, Calif., showing locations of study area, epicenter of 1989 earthquake, and rupture zone.

ban, with a total population of approximately 4,000. The largest communities are the Villa Del Monte neighborhood, which contains 195 residential lots and approximately 165 single-family homes, and the Redwood Lodge-Summit Woods neighborhood, where approximately 100 lots are located. In addition to the several hundred private residences, one public school and several churches are located in the study area. More than 100 residences in the study area were heavily damaged by earthquake-induced landslides and ground cracks (Spittler and Harp, 1990).

### CLIMATE AND RAINFALL

The area has a Mediterranean climate, characterized by warm, dry summers and cool, rainy winters. Temperatures rarely exceed 40°C or fall below 0°C. Virtually all precipitation occurs as rain, about 90 percent of which falls during the winter months of November through April, inclusive; precipitation varies substantially from year to year (fig. 2).

Mean annual precipitation in the Summit Ridge area ranges from 1,140 to 1,270 mm (Rantz, 1971). However, the 1989 Loma Prieta earthquake occurred in the midst of a 5-year drought: Annual precipitation during the 3 years before and the 2 years after the earthquake was, respectively, 71, 56, 64, 67, and 78 percent of normal (fig. 2). The earthquake also occurred near the end of the dry summer season: The only precipitation in the area between June 1 and October 17, 1989, was 30 mm of rain that fell between September 16 and 29. Thus, the area was unusually dry at the time of the earthquake.

### GEOLOGIC SETTING

Bedrock in and around the Summit Ridge area consists primarily of Tertiary marine sedimentary rocks—mostly sandstone, mudstone, siltstone, and shale (see pl. 3). The rocks, which generally strike northwest, have been intensely folded and locally faulted, so that they typically dip steeply, are vertical, or are overturned.

The rocks in the area are assigned to the Butano Sandstone, San Lorenzo Formation, Vaqueros Sandstone, Lambert Shale, and Purisima Formation (see pl. 3: Clark and others, 1989, with landslide boundaries revised by R.J. McLaughlin and J.C. Clark, unpub. data, 1990; McLaughlin and others, 1991). These rocks are generally poorly to moderately cemented, contain numerous shear surfaces, and locally are deeply weathered, intensely fractured, or both. Exposures of bedrock within the area are few because the rocks are typically mantled by several meters or more of colluvium.

The geologic structure of the Summit Ridge area is dominated by northwest-striking faults and folds (see pl.

3). The San Andreas fault passes along the northeast boundary of the area. The Butano and Zayante faults, as well as many minor, unnamed faults, also pass through the area (see pl. 3). Major folds include the Laurel anticline, the Summit syncline, and the Glenwood syncline (see pl. 3).

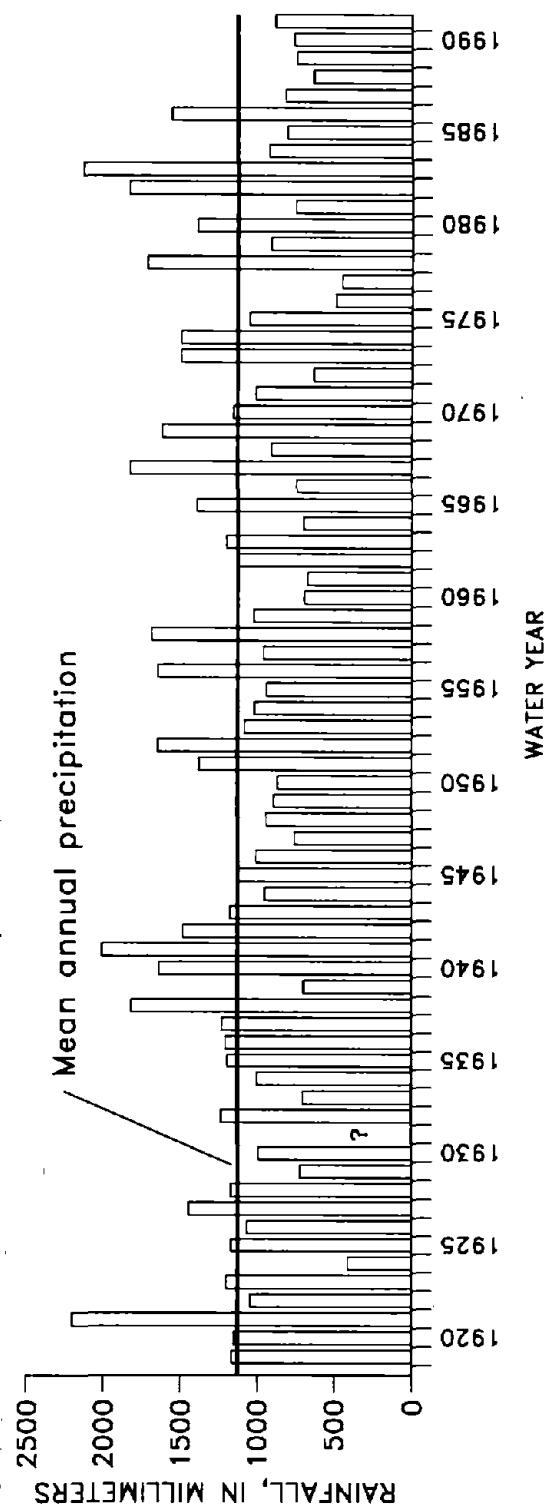


Figure 2.—Annual precipitation in Summit Ridge area for water years 1919–91 (modified from Griggs and others, 1990). Data for 1919–86 from Wrights rain gage (no data available for 1931 or 1987–91), for 1988–91 from Burrell rain gage (see pl. 3 for locations).

### SEISMICITY AND CHARACTERISTICS OF THE 1989 LOMA PRIETA EARTHQUAKE

Previous historical earthquakes in the San Francisco Bay-Monterey Bay region have included 23 events of  $M \geq 6.0$ , of which 2 were approximately as large as the 1989 Loma Prieta earthquake ( $M=7.0$  in 1838 and  $M=7.0$  in 1868) and 1 was substantially larger ( $M=8.2-8.3$  in 1906; Wesnousky, 1986; U.S. Geological Survey, 1990).

The hypocenter of the 1989 Loma Prieta earthquake ( $M_S=7.1$ ;  $M=7.0$ ) was at a depth of approximately 18 km, located at lat  $37^{\circ}02'$  N., long  $121^{\circ}53'$  W., 4.1 km south-east of the study area (fig. 1). The earthquake is inferred to have ruptured a 40-km-long fault segment extending from near Pajaro Gap, east of Watsonville, northwestward through the Summit Ridge area, to just north of California Highway 17 (Plafker and Galloway, 1989; Working Group on California Earthquake Probabilities, 1990).

The aftershock distribution indicates that the fault plane dips approximately  $70^{\circ}$  SW. under the Summit Ridge area (Plafker and Galloway, 1989). The coseismic fault slip at depth had both right-lateral strike-slip and vertical, compressional components. The inferred fault slip at depth was approximately 1.9 m right lateral, 1.3 m reverse, and 2.3 m total (Plafker and Galloway, 1989). No throughgoing surface fault rupture was found.

Preearthquake and postearthquake leveling surveys showed that the fault slip produced a zone of ground-surface subsidence northeast of the San Andreas fault and a zone of uplift southwest of the fault, in and around the Summit Ridge area. Maximum measured uplift was 592 mm, and maximum measured subsidence was 173 mm (Marshall and others, 1991).

During the earthquake, ground shaking in the Summit Ridge area was violent, as indicated by eyewitness accounts and such effects as the snapping of large redwood trees, movement of heavy vehicles, and destruction of homes and other structures. The free-field strong-motion station closest to the study area was in Corralitos (fig. 1), maintained by the California Division of Mines and Geology. That station, located on landslide deposits 200 m from the San Andreas fault and 12 km southeast of the study area, recorded a peak horizontal ground acceleration of  $0.64 g$  and peak vertical acceleration of  $0.47 g$  (Shakal and others, 1989).

### PREVIOUS LANDSLIDES AND LANDSLIDE- HAZARD MAPPING IN THE SUMMIT RIDGE AREA

Preexisting landslide deposits are widespread in the Summit Ridge area, as well as throughout much of the rest of the Santa Cruz Mountains, and abundant historical

landslides have occurred in the Santa Cruz Mountains in association with earthquakes (Lawson, 1908; Youd and Hoose, 1978; Marshall, 1990), storms (Keefer and others, 1987; Ellen and Wieczorek, 1988), and other events.

### LANDSLIDES CAUSED BY PREVIOUS EARTHQUAKES

Landslides are known to have occurred in the Santa Cruz Mountains during both the October 8, 1865, earthquake ( $M=6.5$ ) on the San Andreas fault and the October 21, 1868, earthquake ( $M=7.0$ ) on the Hayward fault. The landslides in those events, however, were poorly documented, and the available historical information is fragmentary (Youd and Hoose, 1978; Marshall, 1990).

Documentation of landslides caused by the much larger April 18, 1906, San Francisco earthquake ( $M=8.2-8.3$ ), though incomplete, was substantially more extensive, owing to the report by Lawson (1908) and many other reports, books, and newspaper articles. The 1906 earthquake triggered or reactivated thousands of landslides throughout an area of approximately  $32,000 \text{ km}^2$  (Keefer, 1984), including all of the Santa Cruz Mountains.

The severity of landsliding in the Summit Ridge vicinity during the 1906 earthquake was described in general terms by an article in the *Santa Cruz Morning Sentinel* of May 1, 1906 (in Griggs and others, 1990), as follows:

From all reports, the higher altitudes of the Santa Cruz Mountains all the way from beyond Saratoga to Loma Prieta, on both slopes, appear to have been more seriously disturbed than many localities in the valleys and foothills. In places the roads are or were impassable, not only on account of great avalanches of stones and earth, but of wide deep cracks in the earth where the ground was rent asunder.

More specific, detailed descriptions of the ground cracks and landslides caused by the 1906 earthquake in and around the Summit Ridge area are listed in table 1. Even though the reports from the 1906 earthquake are incomplete and locations are, for the most part, imprecise, the available information indicates that landslides occurred in many parts of the Summit Ridge area, including Summit Ridge, Skyland Ridge, the Morrell, Burrell School, and Laurel areas, and along Old San Jose and Redwood Lodge Roads (see pl. 3). These reports indicate that several of the landslides were large and that, at several localities, many landslides occurred.

### LANDSLIDES CAUSED BY PRECIPITATION

As with the historical record of landslides caused by earthquakes, the record concerning landslides caused by

Table 1.—Landslides and ground cracks in and around the Summit Ridge area produced by the San Francisco earthquake of April 18, 1906 [Modified from Youd and Hoose (1978, table 6) and Marshall (1990)]

Location (pl. 4)	Description	Original Reference
Eva	A 10-acre slide dammed the creek at Eva station until the water crossed the railroad tracks following a new raised channel.	Santa Cruz <u>Morning Sentinel</u> , April 26, 1906, p. 8.
	A "huge earth slide dammed the creek at Eva station, creating a natural lake that blocked all [railroad] travel...for months." It took until December to remove the slide and lake.	Young (1979, p. 39)
Alma to Wrights	The railroad between Alma [6.4 km northwest of Wrights] and Wrights was impassable, owing to several landslides and boulders on the tracks.	Santa Cruz <u>Morning Sentinel</u> , April 26, 1906, p. 8.
	A landslide dammed Los Gatos Creek at the News Letter Ranch, forming a lake ranging in depth from 50 to 100 ft.	Santa Cruz <u>Morning Sentinel</u> , May 1, 1906, p. 2.
Patchin to Wrights	"On the ridge road, about 5 miles northwest of Wright Station, the fault again shows slightly in a few 2-inch cracks.... Going down the slope from here to Wright, the cracks rapidly become larger. ...At Patchin, 3 miles west of Wright Station, there are fissures over a foot wide trending mainly in the direct line of the fault (S. 33° E.). Several stretches of numerous small cracks alternating with a few long continuous fissures, mark the course from Patchin to Wright Station."	Lawson (1908, p. 109-110).
	"Just north of Wright's Station, on the west bank of Los Gatos Creek, there was a landslide 0.5 mile wide which had slid into the creek and dammed it. The top of this slide was near the Summit school-house and was close to the main fault-line."	Lawson (1908, p. 276).
	"The main fault fracture is about 500 feet northeast of the [Summit] hotel, and a secondary crack close to it had a downthrow of from 5 to 7 feet on the north or downhill side. The crack was about 4 feet wide here, and the line of fracture was parallel with the direction of the ridge. The Summit school-house was dropt [sic] 4 feet downhill from its original position toward the northeast." Just below the Summit schoolhouse was the headscarp of the landslide that dammed Los Gatos Creek near Wright Station.	Lawson (1908, p. 275-276).
	"At Freely's place, 4 or 5 miles north of Morrell's, some 15 acres of woodland have slid into Los Gatos Creek, making a large pond. There are many other slides in the neighborhood and many broken trees."	Lawson (1908, p. 278).
	"Into this [Los Gatos] creek, from the Freely ranch, some ten acres of land was thrown in a great landslide. At the head of the creek is the long tunnel which cuts under the saddle, from Wright's to Laurel."	Jordan (1907, p. 27).
	"Landslides were abundant, especially in the Santa Cruz Mountains, where the topography is more rugged. One slide, a few miles from Wright's Station, involved eight to ten acres of ground."	Carey (1906, p. 297).
Wrights	"Large fissures and ridges" formed in the ground at Wrights.	Santa Cruz <u>Evening Sentinel</u> , April 21, 1906, p. 2.



Table 1.—Continued.

Location (pl. 4)	Description	Original Reference
Wrights to Laurel	The Wrights-to-Laurel railroad tunnel collapsed in the earthquake just hours before the planned inaugural run of the first standard-gage train along this previously narrow-gage line. Where the tunnel crosses the summit, it was offset laterally 5 ft. Almost all other railroad tunnels in the Santa Cruz Mountains partly collapsed or were blocked by slides at their entrances.	Payne (1978, p. 49).
	The Wrights-to-Laurel railroad tunnel cracked in the middle and settled several inches out of line.	Young (1979, p. 38-39).
	"The tunnel floors have raised as much as three to four feet in places...."	Santa Cruz <u>Morning Sentinel</u> , April 26, 1906, p. 8.
Laurel to Glenwood	Minor slides blocked the Laurel-to-Glenwood tunnel.	Young (1979, p. 39).
	About 400 ft of tunnel No. 3 between Laurel and Glenwood caved in.	Santa Cruz <u>Evening Sentinel</u> , April 19, 1906, p. 5.
Morrell Ranch	"The Morrell ranch is located 1 mile south of Wright's Station.... the house itself was built exactly upon a fissure, which opened up under the house at the time of the earthquake. The house was completely wrecked, being torn in two pieces and thrown from its foundation....There was an apparent downthrow upon the northeast side of the fault, as seen in the orchard; but under the house the vertical movement was not so apparent. ...The fence and road near the house were crost [sic] by the fault and showed an offset which indicated a relative movement of the southwest side toward the southeast. ...The "splintering" of the main fracture raised a long, low ridge across which a creek had been forced to cut its way thru a vertical distance of 1.5 feet to get down to its original level."	Lawson (1908, p. 276-277).
	"The earthquake crack past thru [sic] [the Morrell] ranch, a branch of it going under the house. The main body of the house was thrown to the east, away from the crack, the ground there slumping several feet and the house being almost totally wrecked. All thru [sic] the orchard the rows of trees are shifted about 6 feet, those on the east side being farther north, and the east side, which is downhill, seems to have fallen. The crack is largely open and in one place is filled with water. This should be attributed to slumping. A little farther on, the crack passes thru [sic] a grassy hill on which there is no slumping. The Morrells say that this hill has been raised. What appears to be the fact is that the east side of the hill overrides the other. The whole top of the hill is more or less cracked for a width of about 10 feet. The east side is a little higher than the west side, and it looks as though the hill had been shoved together and raised, the east overriding. About 1 mile beyond Morrell's house, at the end of the ranch, there is a blacksmith shop, and the road is crost [sic] by the crack. Here there is a break of 3 or 4 feet like a waterfall, the east side being the lower; but this is part, I take it, of the general slumping of the east side of the crack where it stands near the ravine above Wright. Morrell's place is right over the Wright tunnel, the tunnel and the rocks near by being finely broken rock and very much subject to slides and other breaks."	Lawson (1908, p. 277-278).

Table 1.—Continued.

Location (pl. 4)	Description	Original Reference
Burrell	"In the Burrell district there is one fissure in the hillside fully 3 feet wide. This crossed the road and tumbled Ingraham's store building into the gulch."	Santa Cruz <u>Morning Sentinel</u> , April 24, 1906, p. 7).
Burrell [Laurel] Creek	"Near the Burrell school-house, 1.5 miles southeast of Wright Station, a crack extends across the road by a blacksmith shop and shows a downthrow of four feet on the northeast." "Gulches appear to have been contracted as the bridges crossing them show that they were squeezed. The banks of Burrell Creek appear to have approached each other, so that the creek has become very much narrowed. Water pipes were broken and twisted, and filled with dirt."	Lawson (1908, p. 276). Lawson (1908, p. 276).
Highland	"Half a mile to the northwest of the [Beecher] house [on Loma Prieta Avenue], a fissure 2 feet wide appeared.... The fissure runs from north to south, and the earth was piled up on the west side from 2 to 4 feet high across the road. On Highland, a mile to the west, a fissure 5 feet was opened at an elevation of 2,500 feet."	Lawson (1908, p. 276).
Skyland	"Large landslides occurred in the neighborhood." "The road between the King and Crane places has slid into the orchard below." "There seems to have been a narrow strip, about two miles wide, east of Skyland, with Skyland as the center, where hardly a building remains standing or unbroken. ..."One section of road of about 3 miles long is hardly without a crack.... At one place in the road it has been lifted fully 5 feet." The road was still impassable after 3 days of heavy work by a crew of 6 men. "...the cracks run up over the ridge just west of Skyland. Large fissures show in the orchards and fields on the eastern side of the ridge, but are not so evident on the western slope. Here instead, great landslides occurred, and redwoods were snapt [sic] off or uprooted." "The slides which obliterated Fern Gulch at Skyland...lie to the west of the crack [fault]."	Lawson (1908, p. 278). Santa Cruz <u>Evening Sentinel</u> , April 21, 1906, p. 4. Santa Cruz <u>Morning Sentinel</u> , April 24, 1906, p. 7.
	On the western slopes of the ridge just west of Skyland, several earth-avalanches were caused by the shock; and great slides of a similar character occurred on both sides of Aptos Creek for 0.75 mile. Besides these, there were many smaller earth-avalanches in many parts of the Santa Cruz Mountains which can not be enumerated."	Lawson (1908, p. 110). Lawson (1908, p. 278). Lawson (1908, p. 389-390).

Table 1.—Continued.

Location (pl. 4)	Description	Original Reference
"About Four Miles South of Wright Station" [probably near Laurel township]	"The ridge...was full of cracks, ranging up to 2 and 3 feet in width, and in length from a few rods to 0.25 mile, all trending west of north to northwest. ...The canyon south of us was filled with landslides. In this canyon the stratification of the rocks is plainly shown. The strike is northwest-southeast and the dip is almost vertical. The cracks coincide in direction with the strike of the strata. Cold water was flowing from some of the cracks."	Lawson (1908, p. 278).
San Jose-Soquel Road	San Jose-Soquel Road was extensively damaged in the earthquake but was reopened by July 4, 1906.	Payne (1978, p. 17).
Redwood Lodge Road	The earthquake "severely damaged Redwood Lodge Road, and workmen took until June 1906 to complete repairs."	Payne (1978, p. 17).
Upper Soquel Creek	A newspaper article of May 7, 1906, reported an eyewitness story that the headwaters of Soquel Creek were dammed by two landslides, forming a pond 100 ft deep. The upper Soquel Creek basin was reportedly ravaged by fallen trees and boulders, as well as "great fissures and landslides. ...The roads were gone, and in their stead were chaotic masses of debris from the hillsides." An article of May 9 corrected the account after the site was visited by another eyewitness. This second account claimed that the damming of the creek resulted not from landslides but from an upward vertical displacement of the creekbed of from 5 to 30 ft in places. The pond averaged 15 ft in depth but was no more than 20 ft deep. Many fissures in the ground near Soquel Creek were "now largely filled in."	Santa Cruz <u>Evening Sentinel</u> , May 7, 1906, p. 1, and May 9, 1906, p. 1)
Hinckley Creek (Olive Springs) [2.6 km SSE of study area]	"The mountains are said to have come together and 17 lives...lost." [Nine people were actually killed.]	Santa Cruz <u>Evening Sentinel</u> , April 18, 1906, p. 1, and April 19, 1906, p. 7.
	With the first severe shock of the earthquake, a landslide 500 ft wide, extending up to the ridgetop, descended with "extraordinary speed," burying the Loma Prieta lumber mill under a mass of rock and trees of "about 100 feet in depth at the worst places and gradually diminishing at the edges to 25 feet." Nine men were buried instantly, while others, only several hundred feet away, were spared. "The mountainside where the land fell was swept bare of vegetation. Massive redwoods and pines were jammed on top of the mill in the gulch below. ...The landslide filled the water course. The stream was dammed, and the water rose to a depth of sixty feet in the gulch. A pump was set to working, and the water is now being used to wash away the earth from the machinery." Hundreds of people were involved in a massive digging effort in the following week, but only three bodies had been discovered by 5 days later. [More than a year passed before the last body was finally removed from the debris.]	Santa Cruz <u>Morning Sentinel</u> , April 26, 1906, p. 1)

Table 1.—Continued.

Location (pl. 4)	Description	Original Reference
	The mill was buried under 60 ft of earth and trees, whereas the nearby bunkhouse, where nine men were sleeping, was buried under 10 to 15 ft of debris.	Patten (1969, p. 79).
	A second slide occurred during an aftershock at 11 p.m. April 19, interfering with rescue efforts.	Santa Cruz <u>Evening Sentinel</u> , April 21, 1906, p. 2.
	"Near Olive Springs, 12 miles north of Santa Cruz, an earth-avalanche demolished Loma Prieta Mill and killed several men."	Lawson (1908, p. 389).
	"At Santa Cruz the inhabitants reported that near Olive Springs, 12 miles north of Santa Cruz, a landslide demolished Loma Prieta Mill and killed 9 men."	Lawson (1908, p. 271).
	"...the [fault] crack goes into Hinckley's Gulch, in which the Loma Prieta Mills are situated, and which are buried under the slides."	Lawson (1908, p. 278).
	"On the northern side of Bridge Creek Canyon there are typical cracks from 1 to 8 inches wide, and here also occurred a great landslide which buried the Loma Prieta Mill."	Lawson (1908, p. 110).
	"Wreck of Loma Prieta Sawmill, Hinckley's Gulch, Santa Cruz County." [Picture caption]	Jordan (1907, p. 30).
	"Site of Loma Prieta Sawmill, covered to a depth of 125 feet." [Picture caption]	Jordan (1907, p. 31).
	"Loma Prieta Lumber Company's Mill. The mill, boarding house and other buildings of the plant were situated in a gulch, and were overwhelmed by a portion of the mountain, 1500 feet long, 400 feet wide, and 100 feet deep, which slid down upon them. The mill and everything in the gulch were forced up the opposite slope of the mountain and there buried to a depth of one hundred feet. Pine and redwood trees 100 feet high came down with the slide and are now standing over the mill site as though they had grown there. Nine men were killed."	Salinas <u>Daily Index</u> , April 25, 1906, p. 3.
	"LOMA PRIETA CO'S LOSS. When the earthquake occurred yesterday morning it caused a large mountain of earth to slide into the canyon and completely covering the new mill. Continuing its course up the mountain on the other side it covered what is known as the bunk house and buried ten men, who were asleep at the time."	Salinas <u>Daily Index</u> , April 19, 1906, p. 3.

rainfall in and around the Summit Ridge area is incomplete. Sources of available data include the following.

1. Marshall (1990), who compiled information on landslides in the central Santa Cruz Mountains before and after the 1865 and 1906 earthquakes, reported that landslides were abundant there in rainstorms that occurred during the winters of 1866–67 and 1906–7. For example, on December 29, 1866, the Santa Cruz *Evening Sentinel* reported that the road between Santa Cruz and Santa Clara was impassable after heavy rains caused landslides and flooding (Marshall, 1990). Landslides along roads and railroads in the central Santa Cruz Mountains were reported from at least five storms in the winter of 1906–7, although the accounts do not mention the Summit Ridge area specifically (Marshall, 1990).
2. Wieczorek and others (1988) mapped landslides in Santa Cruz County caused by the storm of January 3–5, 1982. This storm, which produced as much as 610 mm of rain within 34 hours, caused more than 18,000 landslides and more than \$66 million in landslide-related damage throughout the San Francisco Bay-Monterey Bay region (Ellen and others, 1988). This is the only storm for which detailed and comprehensive data on landslide distribution are available. Within the Summit Ridge area, approximately 20 shallow, fast-moving debris flows were mapped (Wieczorek and others, 1988); this number was probably a minimum because the dense vegetation cover in many areas made detection of debris flows difficult. In addition to mapped debris flows, Santa Cruz County road-repair records show that lower Schultheis and Redwood Lodge Roads required repairs as a result of landslide damage in 1982 (fig. 3; table 2).
3. Keefer and others (1987) included the Summit Ridge area in a zone of high landslide concentration associated with the storm sequence of February 12–21, 1986, but did not report the locations of individual landslides within that zone.
4. In addition to the landslide activity discussed above, Brown (1988) reported that rainstorms caused significant landslide activity in parts or all of the San Francisco Bay-Monterey Bay region during the winters of 1949–50, 1955–56, 1961–62, 1962–63, 1964–65, 1966–67, 1968–69, 1969–70, 1972–73, 1974–75, and 1977–78. Documentation of landslides from these seasons, however, is fragmentary, and the number of landslides that may have occurred in the Summit Ridge area, if any, is unknown.

#### LANDSLIDE DAMAGE TO ROADS

Griggs and others (1990) described landslide damage to roads in the Summit Ridge area, obtained from a review of Santa Cruz County Public Works Department files

and a field trip through the area with Ray Geyon, one of the department's senior staff members. Landslide damage reportedly occurred at seven localities in 1975, 1976, 1980, 1982, 1983, and 1986 (circled numbers, fig. 3; table 2). Although all seven of these localities were also sites of landslides and (or) ground cracks generated by the 1989 Loma Prieta earthquake, the pre-1989 landslides were all smaller than those triggered by the earthquake.

#### PREVIOUS LANDSLIDE-HAZARDS MAPPING

Preexisting landslide deposits in the Summit Ridge area are shown on the map of landslide deposits in Santa Cruz County by Cooper-Clark and Associates (1975), which was prepared from interpretation of vertical, black-and-white aerial photographs (fig. 4). Limitations of that map include a minimum size of landslide deposits that could be mapped (length or width of 15 m), possible incomplete identification of landslide deposits in areas of dense vegetation, and difficulties in differentiating landslide deposits from such similar-appearing features as alluvial terraces (Cooper-Clark and Associates, 1975). To reflect the various degrees of certainty in identification, landslide deposits were classified as "definite" (D), "probable" (P), or "questionable" (?) (fig. 4). Many landslide deposits are also shown on U.S. Geological Survey geologic-quadrangle maps of the study area (see pl. 3; Clark and others, 1989, with landslide boundaries revised by R.J. McLaughlin and J.C. Clark, unpub. data, 1990; McLaughlin and others, 1991).

### IDENTIFICATION AND CHARACTERISTICS OF EARTHQUAKE-INDUCED LANDSLIDES

#### DATA AND CRITERIA FOR IDENTIFYING LANDSLIDES

Coseismic ground cracks in the Summit Ridge area were probably the result of several different processes, including landsliding. Other crack-forming processes are inferred to include discontinuous surface fault rupture (Aydin and others, in press), slip along bedding planes (Cotton, 1990; Ponti and Wells, 1991), adjustments to the local tectonic uplift that accompanied the earthquake (Ponti and others, 1990; Ponti and Wells, 1991), and extension over active bedrock folds (Ponti and Wells, 1991). Many of the ground cracks produced by the various coseismic processes, including landsliding, showed evidence of control by structures in the underlying bedrock, such as bedding planes and faults (Ponti and others, 1990; Keefer, 1991; Ponti and Wells, 1991 and in press; Harp, this chapter).

Table 2.—Landslide-related damage to roads before the 1989 Loma Prieta earthquake, as reported by the Santa Cruz County Public Works Department

[Modified from Griggs and others (1990)]

Locality (fig. 3)	Description and date of damage
1	<b>Lower Schultheis Road--1982:</b> The slope below Lower Schultheis Road failed in 1982 approximately 0.5 km east of the intersection with Laurel Road, destroying the roadway and requiring evacuation of local residents. A private company was retained to engineer the slope stabilization. Since repair work was completed in 1983(?), the road has settled at least an additional 60 cm. In 1989, earthquake-induced ground cracks were found across the road, around the margins of the previous failure. This failure was on the northeast flank of the larger Lower Schultheis Road East landslide.
2	<b>Redwood Lodge Road--repeated failures:</b> Over the years, Redwood Lodge Road has had many maintenance problems due to slope failure associated with heavy rainfall, in particular during 1983 and 1986. Numerous landslides, both large and small, have plagued the road along its entire length. The only landslide with significant movement as a result of the 1989 Loma Prieta earthquake was the Upper Redwood Lodge Road landslide, which displaced the road west of its intersection with Old San Jose Road. This section of road, in particular, has a long history of repeated landslide damage and repair.
3	<b>Redwood Lodge Road--1981-82 and 1983:</b> During the winter of 1981-82, a large landslide covered the road near the confluence of Laurel Creek and Burns Creek. Residents living below the damaged road were trapped and had to be evacuated. The road was reconstructed, sustained additional failure during 1983, and was again reconstructed. Individual slide blocks still remain on the steep slope above the road. Slope instability in this area is typically associated with heavy rainfall and has been a concern for at least 30 to 40 years. The 1989 Loma Prieta earthquake reactivated the landslide; ground cracks were opened along approximately 240 m of steep hillside above the road and extended headward from the preexisting main scarp.
4	<b>Morrell Road--1982-83:</b> A landslide, approximately 60 m long by 60 m wide, buried Morrell Road immediately south of its crossing of Laurel Creek. The main scarp of the landslide was approximately 10 m upslope from the road. The County of Santa Cruz had to evacuate local residents and rebuild the road, which was covered with more than 6 m of debris. The slope was stabilized in 1984. Ground cracks from the Lower Morrell landslide complex, which moved during the 1989 Loma Prieta earthquake, crossed the road on both the right and left flanks of the 1982-83 landslide.
5	<b>Morrell Road--1980:</b> Northwest of where Morrell Road crosses Laurel Creek, a stretch of the road moved downhill approximately 2 to 3 m during a 2-year period. A house was moved to protect it from landslide damage. The slope movement was relatively rapid, forming large cracks and a 1.2-m-high scarp across the road; however, the landslide did not bulge below the road to compensate for the extensional movement associated with this scarp. County of Santa Cruz road crews graded and filled the roadway until the movement stopped. This area was on the eastern margin of the Upper Morrell Road landslide, which moved during the 1989 Loma Prieta earthquake.
6	<b>Morrell Road--repeated damage:</b> Although the area downslope from the 1989 Upper Morrell Road landslide was never reported as a problem area, several stretches of the road have been patched repeatedly. Road-repair records did not identify this patching as landslide related, but the repeated, slow offset of the road may be related to a landslide. Ground cracks caused by the 1989 Loma Prieta earthquake crossed the road in several places. Cuthanks both upslope and downslope from the road have required cribbing and maintenance in the past, evidently because of local roadcut failures. Several of these roadcuts failed during the 1989 Loma Prieta earthquake.
7	<b>Villa Del Monte--1975-76 and repeated damage:</b> Within the Villa Del Monte landslide are several areas that have required road maintenance, most of which is evidently related to local cribbing or fill failures. In 1975-76, the hillside upslope from Skyview Terrace moved slowly downslope during a period of 2 years. County of Santa Cruz maintenance crews cleared the road approximately once a week during that time.

Because of the complexity of the coseismic ground cracking, the extent of large landslides was recognized only by interpreting detailed postearthquake maps of the area (Spittler and Harp, 1990, with landslide boundaries defined by Keefer, 1991). These maps were initially compiled on a planimetric base at a scale of 1:4,800 (Spittler and Harp, 1990), and later on a topographic base at a scale of 1:6,000 (Keefer, 1991).

Supplemental data for delineating some landslide features were obtained from a postearthquake survey of water wells (Brumbaugh, 1990). However, these water-well data were used only on a limited basis because (1) most reports of damage (or absence of damage) were second-hand, (2) many well locations were determined only approximately, (3) the causes of well damage were typically

unknown, (4) the extent to which reportedly undamaged wells were actually surveyed is unknown, and (5) the ground displacements that the wells could tolerate without damage are also unknown.

**SUMMARY OF LANDSLIDE CHARACTERISTICS**

Within the Summit Ridge area, 20 large landslides and landslide complexes, with surface areas larger than 1 ha, were identified as having moved during the earthquake (see pl. 3; table 3). (The term "landslide complex" here denotes a feature made up of several to many coalescing, juxtaposed, and (or) superimposed landslides.) The largest landslide complex had an area of about 85 ha. Of

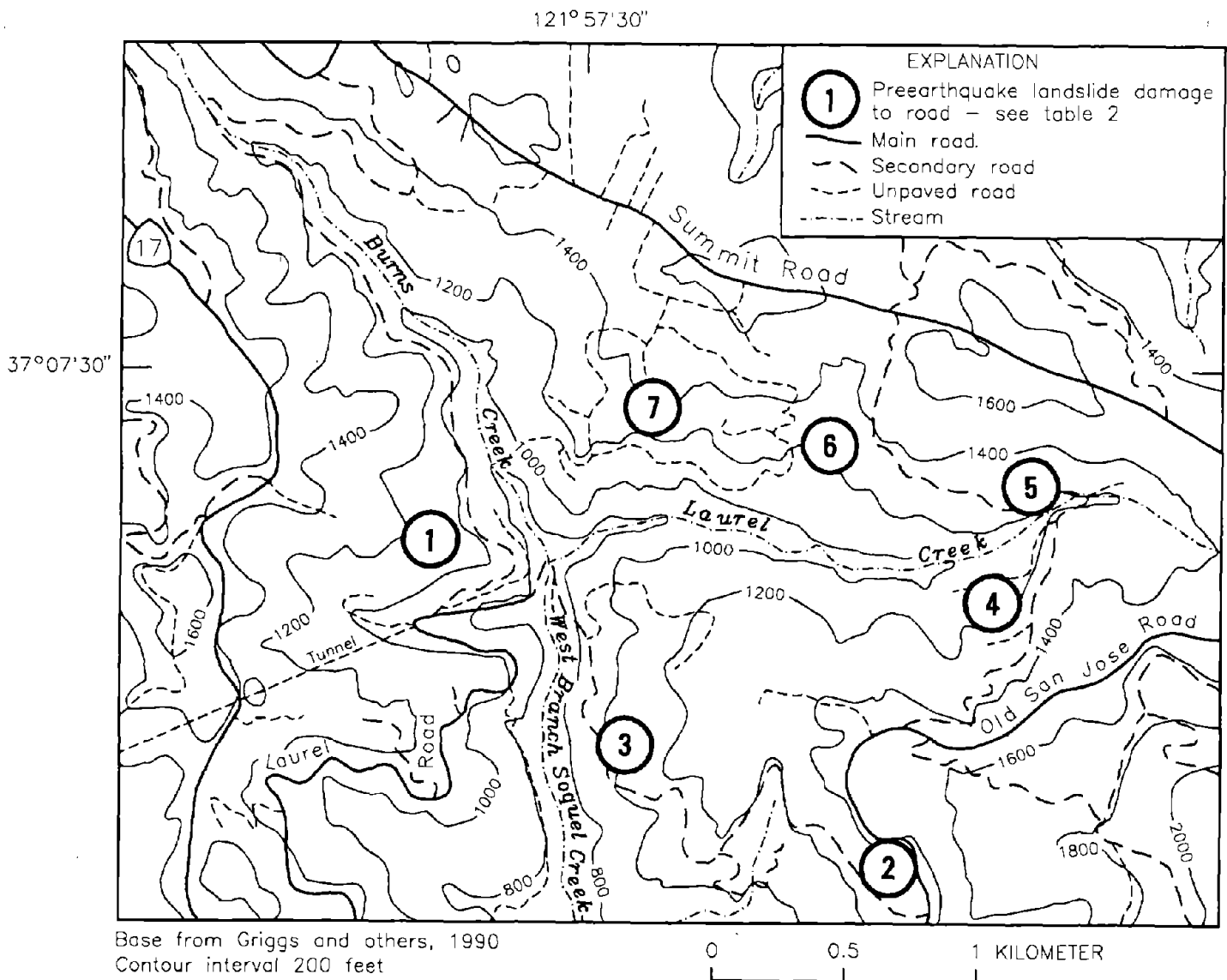


Figure 3.—Summit Road area, showing localities of preearthquake landslide damage to roads (circled numbers) as reported by Santa Cruz County Public Works Department (modified from Griggs and others, 1990). See table 2 for detailed descriptions of localities.

these landslides and landslide complexes, 18 were within the area delineated for detailed study (see pl. 3). Most of the largest landslides and landslide complexes were on the southwest flank of Summit Ridge, in an area extending eastward from California Highway 17 to near Morrell Road. In that area, about 60 percent of the ridge flank was involved in large earthquake-induced landslides (see pl. 3). The characteristics of the landslides are summarized in table 3, and the terms used to describe various landslide features are defined in figure 5.

In general, such surficial features as scarps, ground cracks, or pressure ridges were not continuous around the

boundaries of the landslides in the Summit Ridge area (fig. 6). The best developed, most continuous sets of cracks and scarps typically occurred in and around the landslide crowns and heads (figs. 5, 6). Those cracks and scarps commonly (1) had trends approximately across the slope (perpendicular to the gradient); (2) were linear or, more commonly, arcuate and concave downslope in plan view; and (3) exhibited extensional components of displacement and (or) downslope-facing scarp segments, features consistent with generation by downslope movement. Such cracks and scarps formed the main scarps of the landslides, as defined in figure 5.

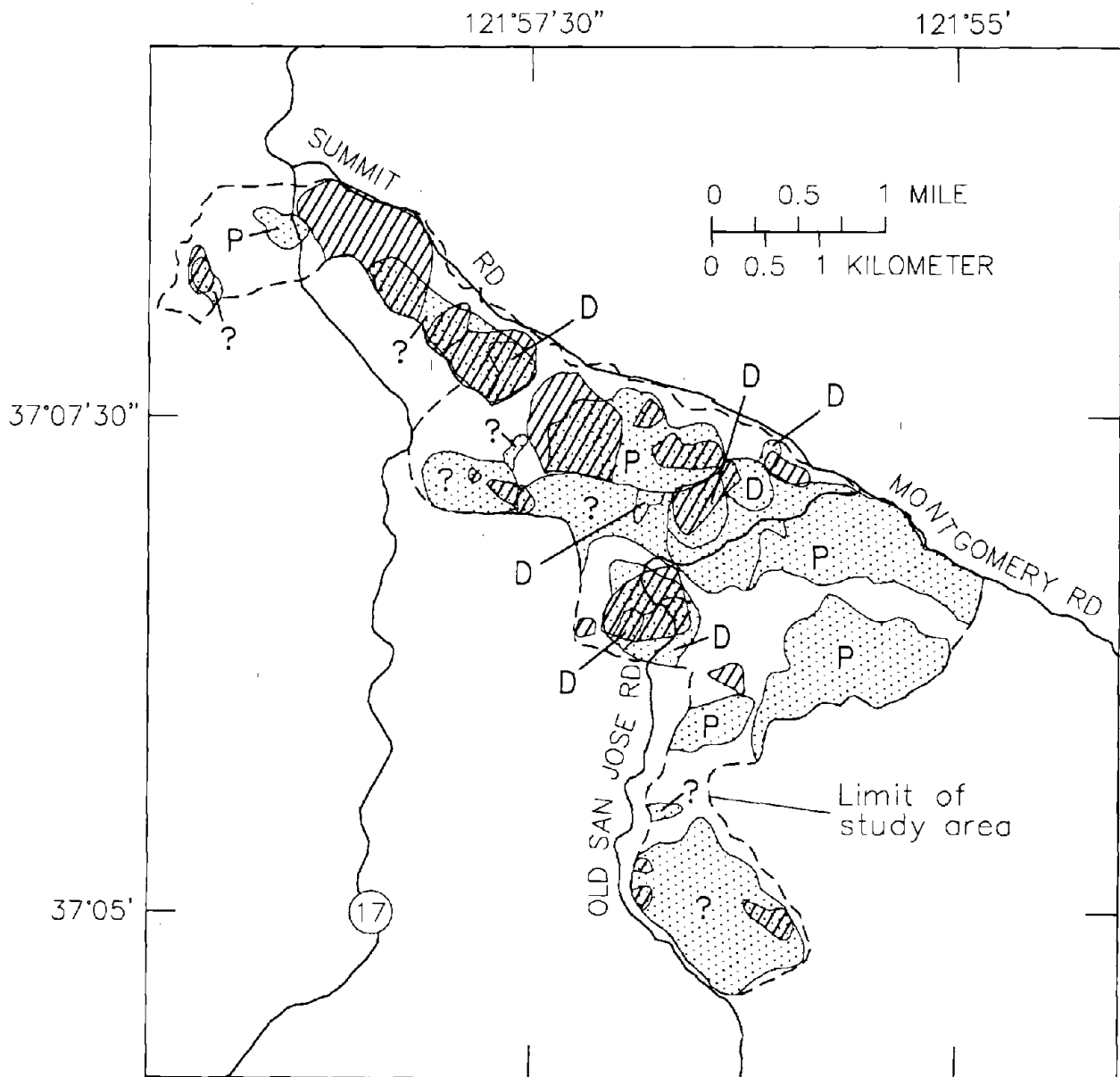


Figure 4.—Summit Ridge study area, showing generalized boundaries of large earthquake-generated landslides (diagonal-lined areas) in relation to generalized landslide deposits and landslide scarps (dotted areas) identified on preearthquake landslide-hazard map of Cooper-Clark and Associates (1975); D, definite; P, probable; ?, questionable.



Table 3.—Characteristics of landslides generated by the 1989 Loma Prieta earthquake

[Longitudinal strain is ratio of displacement to length; Percentage of compressional features across toe is based on ratio of total length of compressional features to width of toe. Presence of previous landslides according to Cooper-Clark and Associates (1975). Predominant dip/slope is direction of bedrock dip relative to direction of surface slope. n.d., not determined]

No. (pl. 4)	Landslide name	Area (ha)	Length (m)	Width (m)	Slope (°)	Displacement (m)	Longitudinal strain (percent)	Compressional features across toe (percent)	Distance from San Andreas fault (km)	Distance from epicenter (km)	Distance from Zayante fault (km)	Geologic unit at crown	Predominant geologic unit(s) (pl. 5)	Previous landslides	Predominant dip/slope
1	Majestic Drive	5.3	420	170	20	n.d.	n.d.	0	2.56	15.3	4.2	Tb	Tb	Yes	Opposite
2	Old Santa Cruz Highway	85.0	670	1300	15-20	n.d.	n.d.	n.d.	1.09	14.5	4.9	Tv	Tv	Yes	Do.
3	Upper Schultheis Road	13.0	460	390	15	2.44	.53	22	1.21	13.3	4.2	Tv	Tb, Tv	Yes	Do.
4	Raille Drive	50.0	910	730	15	1.02	.11	13	1.01	12.8	4.1	Tv	Tb, Tv	Yes	Do.
5	Villa Del Monte	68.0	980	870	12-15	.53	.05	9	0.91	12.4	4.2	Tsr	Tsr, Tst, Tb	Yes	Do.
6	Taylor Gulch	5.7	210	16	16	.53	.25	0	.5	11.8	4.2	Tsr	Tsr	Yes	Do.
7	Upper Morrell Road	14.0	270	550	15	2.01	.74	100	.5	11.4	4.1	Tsr	Tsr	Yes	Do.
8	Lower Morrell Road	22.0	460	670	15	n.d.	n.d.	n.d.	.68	10.6	3.9	Tb	Tb, Tbm	Yes	Oblique
9	Burrell	9.0	230	460	15-20	.71	.31	8	.1	10.5	4.4	Tbm	Tbm	Yes	Do.
10	Upper Redwood Lodge Road	37.0	820	640	15-20	.25	.03	0	1.73	10.0	2.9	Tsr	Tsr, Tv	Yes	Oblique/vertical.
11	Long Branch	2.0	120	180	22	.46	.38	0	2.34	10.3	2.2	Tv	Tv	No	Same.
12	Station Road	4.5	200	460	20	.61	.31	0	1.9	9.2	2.6	Tsr	Tsr	No	Opposite.
13	Amaya Ridge	1.6	120	240	22	1.00	.83	65	3.6	7.2	9.6	Tp	Tp	Yes	Same.
14	Hester Creek North	1.2	150	90	23	.79	.53	0	3.9	8.2	.67	Tp	Tp	Yes	Same?
15	Hester Creek South	1.80	180	25-30	25	.25	.14	0	4.06	8.1	.38	Tp	Tp	Yes	Do.
16	Lower Redwood Lodge Road	2.4	180	280	20-25	n.d.	n.d.	0	1.97	11.5	3	Tsr	Tsr	Yes	Oblique/vertical.
17	Lower Schultheis Road East	4.5	300	120	20	.69	.23	0	2.2	11.9	2.8	Tsr	Tsr	Yes	Do.
18	Lower Schultheis Road West <sup>2</sup>	1.2	110	110	15-20	.65	.59	38	2.3	12.0	2.7	Tsr	Tsr	Yes	Same/vertical.
Outside study area															
A	Soquel-San Jose Road	2.3	170	170	n.d.	.46	.27	24	3.74	8.7	0.74	Tp	Tp	Yes	Oblique.
B	Comstock Mill Road	10.0	820	150	n.d.	.65	.08	0	2.9	8.5	1.5	Tv	Tsr	Yes	Do.

<sup>1</sup> Northwestern landslides only.  
<sup>2</sup> Confirmed landslide only.

Downslope from the main scarps, landslide flanks were delineated either by cracks trending nearly parallel to gradient or by complex sets of echelon cracks (fig. 6). In some places, flank cracks were continuous with the main scarps farther upslope. These flank cracks exhibited relative displacements consistent with downslope movement, with components of right-lateral shear along right flanks and left-lateral shear along left flanks.

Downslope from some landslide flanks were local to relatively continuous pressure ridges or areas of bulging ground, convex upward in profile, that were interpreted as marking landslide toes (fig. 5). In several places where such features were absent, the positions of other ground cracks suggested that the landslides extended all the way to the stream channels at the bases of the slopes. In addition to main scarps, flank cracks, and toe features, the landslides also contained abundant internal scarps and cracks, as well as a few internal ridges (fig. 5).

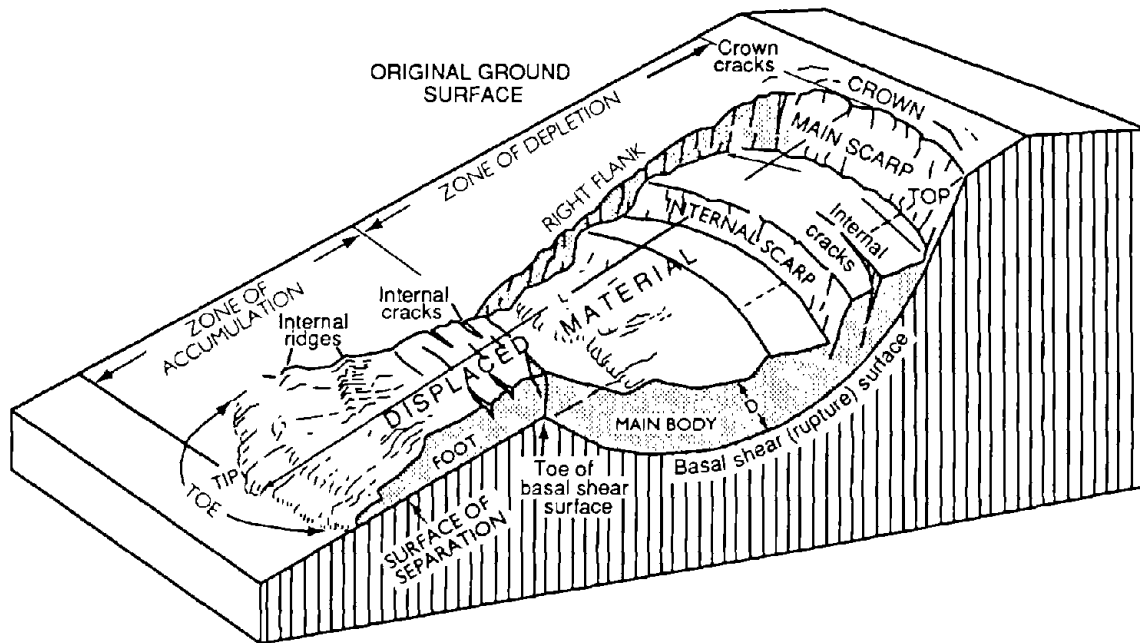
In the following sections, we describe several of these landslides and landslide complexes individually to illustrate their characteristics and to provide the evidence used to delineate them and to differentiate them from other coseismic features. The landslides and landslide complexes described here include all of the largest, those where the most detailed investigations were performed, and those with features judged to be particularly significant. Following the individual descriptions is a summary of the characteristics of the other landslides.

### OLD SANTA CRUZ HIGHWAY LANDSLIDE COMPLEX

The Old Santa Cruz Highway area (area 2, pl. 3), on the southwest flank of Summit Ridge, encompasses a complex of earthquake-induced landslides, about 670 m long, 1,300 m wide, and 85 ha in area (fig. 7).

The longest ground-cracking feature within this area is a nearly continuous, southeast-trending line of cracks and scarps (fig. 8), approximately 1,200 m long (leg A-A', fig. 7A). Displacements across this feature vary along its length; maximum displacement components are about 60 cm vertical (down to the southwest), 75 cm left lateral, and 15 cm extensional.

A second, virtually continuous, 420-m-long scarp strikes parallel to this line of cracks and scarps and crosses Summit Road 500 m farther



**MAIN SCARP** - A steep surface on the undisturbed ground around the periphery of the slide, caused by the movement of slide material away from undisturbed ground. The projection of the scarp surface under the displaced material becomes the basal shear surface.

**INTERNAL SCARP** - A steep surface on the displaced material produced by differential movements within the sliding mass.

**HEAD** - The upper parts of the slide material along the contact between the displaced material and the main scarp.

**TOP** - The highest point of contact between the displaced material and the main scarp.

**TOE OF BASAL SHEAR SURFACE** - The intersection (sometimes buried) between the lower part of the basal shear surface and the original ground surface.

**TOE** - The margin of displaced material most distant from the main scarp.

**TIP** - The point on the toe most distant from the top of the slide.

**FOOT** - That part of the displaced material that lies downslope from the toe of the basal shear surface.

**MAIN BODY** - That part of the displaced material that overlies the basal shear surface between the main scarp and the toe of the basal shear surface.

**CROWN CRACKS** - Cracks in the ground surface upslope from the crown.

**CROWN** - The material that is still in place, practically undisplaced, and adjacent to the highest parts of the main scarp.

**FLANK** - The side of the landslide.

**ORIGINAL GROUND SURFACE** - The slope that existed before the movement that is being considered took place.

**LEFT AND RIGHT** - Compass directions are preferable in describing a slide, but if these terms are used, they refer to the slide as viewed downslope from the crown.

**SURFACE OF SEPARATION** - The surface separating displaced material from stable material but not known to have been a surface on which failure occurred.

**DISPLACED MATERIAL** - The material that has moved away from its original position on the slope. It may be in a deformed or undeformed state.

**ZONE OF DEPLETION** - The area within which the displaced material lies below the original ground surface.

**ZONE OF ACCUMULATION** - The area within which the displaced material lies above the original ground surface.

**LENGTH (L)** - The distance from top to tip.

**WIDTH (W)** - The maximum distance from the left flank to the right flank, measured perpendicular to length.

**DEPTH (D)** - The maximum depth to the basal shear surface, measured perpendicular to the ground surface.

**BASAL SHEAR (or RUPTURE) SURFACE** - The surface at the base of the main body on which landslide movement took place.

Figure 5.—Idealized deep-seated, complex landslide, illustrating nomenclature for constituent parts (modified from Varnes, 1978).

east (leg B-B', fig. 7A). Measurements across this scarp showed 20 to 30 cm of movement downslope (to the southwest). Stratigraphic and structural relations exposed in a trench excavated across the scarp revealed at least three and, possibly, many more, pre-1989 movements, including one that probably took place during the 1906 San Francisco earthquake (Keefer, 1991; Nolan, in press; Nolan and Weber, this chapter).

These two long ground-crack features have characteristics that are consistent with formation by landslide movement and significant control by bedrock structure. Characteristics consistent with a landslide origin are strikes approximately perpendicular to the slope inclination and measured displacements that in nearly all places are downslope (to the south and southwest; U.S. Geological Survey staff, 1989; Spittler and Harp, 1990). Characteristics that indicate structural control and, possibly, a tectonic rather than landslide origin are (1) strikes parallel to

other structurally controlled cracks, (2) linear trends and great lengths, (3) a few uphill-facing scarp segments, and (4) location of the 420-m-long scarp approximately over a fault mapped by McLaughlin and others (1991), as shown in plate 5.

If these two features are of landslide origin, the landslide movement was relatively deep and involved part of the crest of Summit Ridge, north of Summit Road near California Highway 17. Even if the cracks and scarps were produced originally by coseismic tectonic processes, these features could also have served as surfaces of weakness along which landslide movement took place later in the earthquake. The seven reportedly undamaged water wells between these two features (wells 173-175, 177-180, fig. 7B) and the linearity of the line of cracks and scarps (leg A-A', fig. 7A) where it crosses a deep valley north of Summit Road (loc. C, fig. 7) are consistent either with landslide movement on a basal shear surface more than

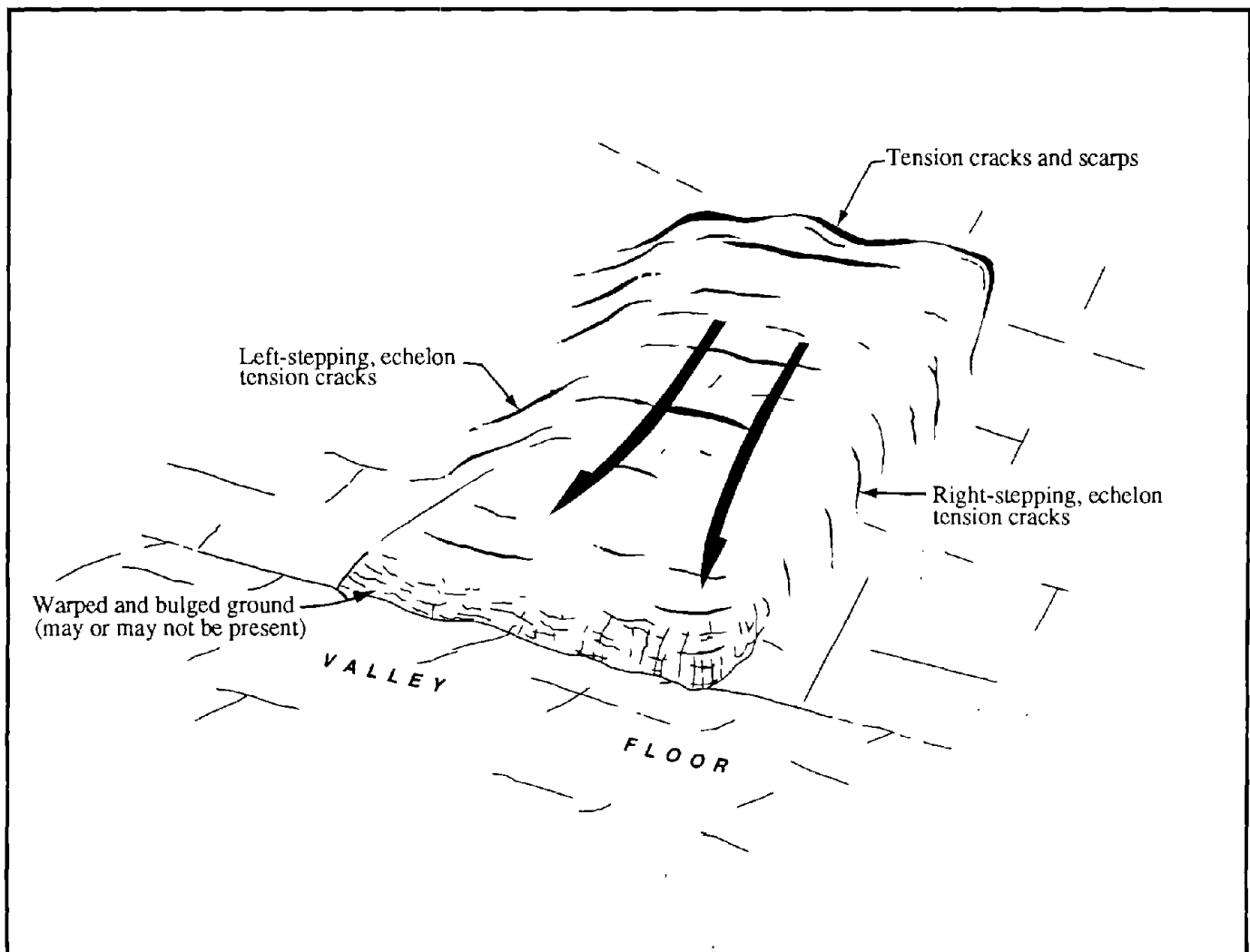
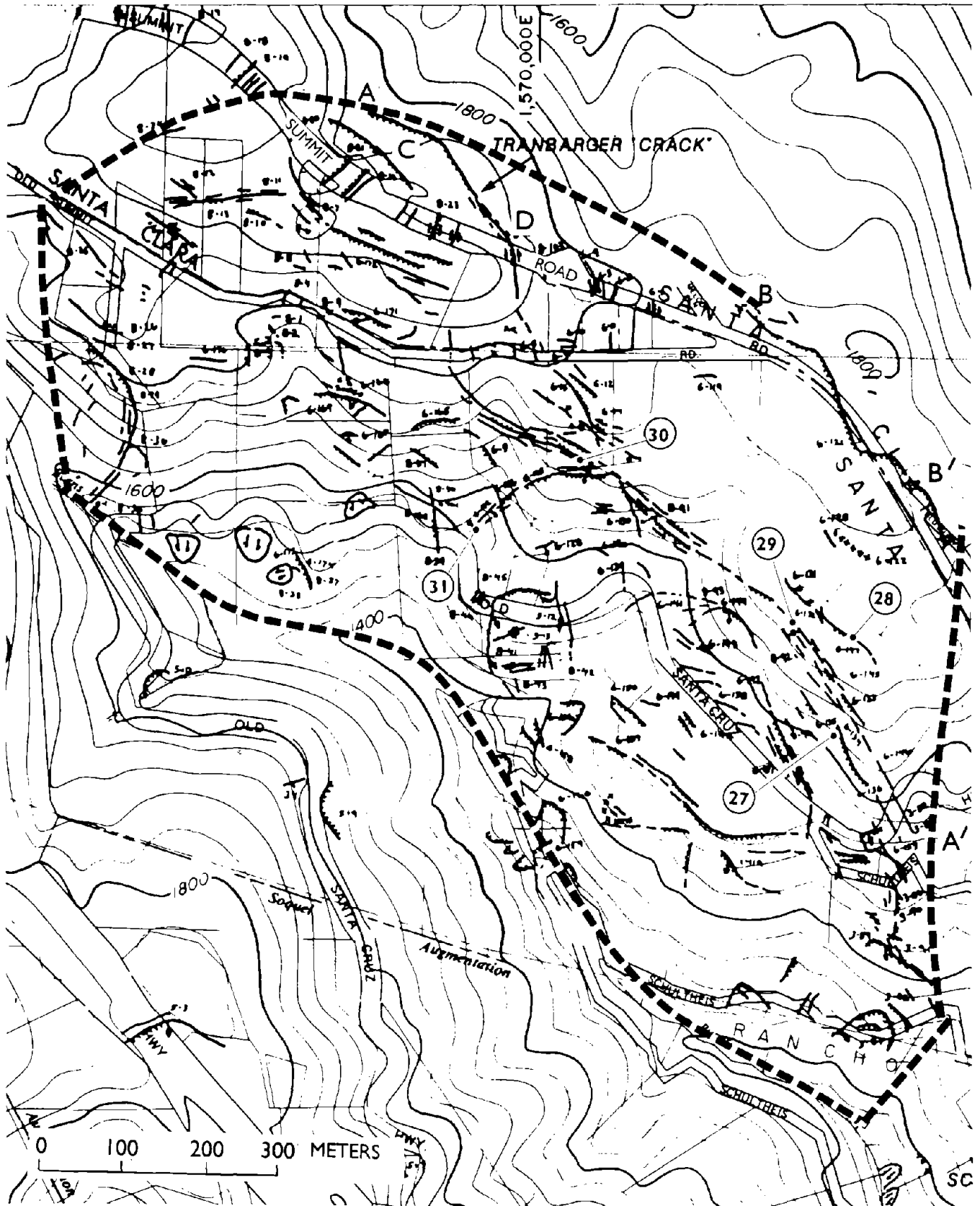


Figure 6.—Idealized landslide bounded by discontinuous surface features, as was typical for large landslides in Summit Ridge area (modified from William Cotton and Associates, Inc., 1990).

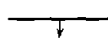
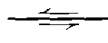
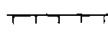
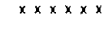


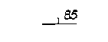

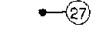




100 m deep or with movement produced by some other deep-seated process. Damage to wells immediately east of California Highway 17 and south of Old Summit Road (wells 171, 220, 222, fig. 7B), all reportedly disturbed at depths of 21 to 23 m (Brumbaugh, 1990), indicates that a 21- to 23-m-deep landslide shear surface underlies that area.

Downslope and southwest of the line of cracks and scarps (leg A-A', fig. 7A) are shorter, arcuate scarps and

### EXPLANATION

[Composite explanation for part A of figures 7, 9, 12, 17, and 20 and figures 19, 21, 22, and 24-28. Surface features modified from Spittler and Harp (1990). Symbols may be combined]

-  Fissure, fracture, or shear generated by the 1989 Loma Prieta earthquake—Dashed where approximately located; dotted where concealed; queried where uncertain. Arrow indicates direction of separation where present
-  Fracture generated by the 1989 Loma Prieta earthquake along which there has been horizontal displacement—Half arrows indicate direction of relative horizontal movement
-  Scarp generated by the 1989 Loma Prieta earthquake—Formed by relative vertical displacement along fissure. Dashed where approximately located; hachures on downthrown side
-  Compressional feature generated by the 1989 Loma Prieta earthquake—Queried where uncertain
-  Small (<1 ha) landslide generated by the 1989 Loma Prieta earthquake—Dashed where approximately located; queried where uncertain; opened where only scarp was mapped. Half arrows indicate direction of downslope movement
-  Approximate boundary of large (>1 ha) landslide or landslide complex—From Keefer (1991)
- 8-37 Geologic notes locality—See Spittler and Harp (1990)
-  Strike and dip of bedding
-  Locality mentioned in text—May include shaded area
-  Quadrilateral array—Numbers are array identifiers, as discussed in text and by Griggs and others (1990) and Marshall and Griggs (1991)
-  Quadrilateral array removed before December 1990—Numbers are array identifiers, as discussed in text and by Griggs and others (1990)
-  Strain gage

Base note:

Planimetric base from Santa Cruz County, 1989

cracks and other features that indicate the presence of several smaller, shallower landslides. These scarps, cracks, and other features, which include localized areas of compression or bulging ground, indicating landslide toes, are so numerous as to form a virtually continuous landslide complex between the longest ground-cracking feature and Burns Creek (fig. 7).

Slope inclinations in the Old Santa Cruz Highway area average 15°–20°, and much of the area also displays the uneven, hummocky topography and benched topographic profiles characteristic of landslide terrain. The southeastern part of this area was mapped as a landslide deposit by Cooper-Clark and Associates (1975) (fig. 4) and by McLaughlin and others (1991) (see pl. 3).

The Butano fault is projected under the southeastern part of this area (see pl. 3), but the local strike of this fault is oblique to the main zones of ground cracking. Northeast of the projected fault trace, the landslide complex is underlain by the Vaqueros Sandstone; southwest of the trace, bedrock is the Butano Sandstone. The axis of the Summit syncline passes through the northeastern margin of the area, and the axis of the Laurel anticline passes through the southern part of the area and is truncated against the Butano fault (see pl. 3). Because of these complex structural relations, the dip of the bedrock beneath the landslide complex varies but under most of the complex is probably northeastward (into the slope).

Two 61-cm-diameter boreholes were drilled into the southeastern part of this landslide complex (Cole and others, 1991). The boreholes, logged to depths of 11 and 17 m, evidently did not penetrate through landslide material into undisturbed bedrock. They revealed fractured, deeply weathered siltstone and sandstone overlain by as much as 0.3 m of topsoil (silty sand and silty clay) and 5 m of colluvium (clayey sand, clayey silt, sandy silt, and silty sand). Free water was penetrated at depths of 10 and 12.5 m (Cole and others, 1991).

### UPPER SCHULTHEIS ROAD LANDSLIDE

The Upper Schultheis Road landslide is immediately east of the Old Santa Cruz Highway landslide complex, separated from it by less than 100 m of ground with no observed cracks (area 3, pl. 3). The crown, head, and upper west flank of the landslide are delineated by a continuous main scarp that is arcuate and concave downslope in plan view (figs. 9, 10). The east flank of the landslide is marked by a set of discontinuous pressure ridges and cracks that extend about 275 m downslope from the main scarp. Together, these features encompass a landslide about 300 m wide. A few small pressure ridges are present low on the slope above Burns Creek; these features are interpreted to be internal ridges on the basis of their small size and discontinuity. The landslide probably extends

◀ Figure 7.—Old Santa Cruz Highway landslide complex, showing boundary of landslide and locations of (A) surficial features, surface-monitoring stations, and localities discussed in text and of (B) boreholes (from Cole and others, 1991) and water wells (from Brumbaugh, 1990). Ground cracks and compressional features from Spittler and Harp (1990); landslide boundaries from Keefer (1991). Base from Towill, Inc., using topography from U.S. Geological Survey Los Gatos, Calif., 7.5-minute quadrangle and culture from County of Santa Cruz planimetric base and interpretation of aerial photographs taken July 24, 1990. Contour interval, 40 ft.

B

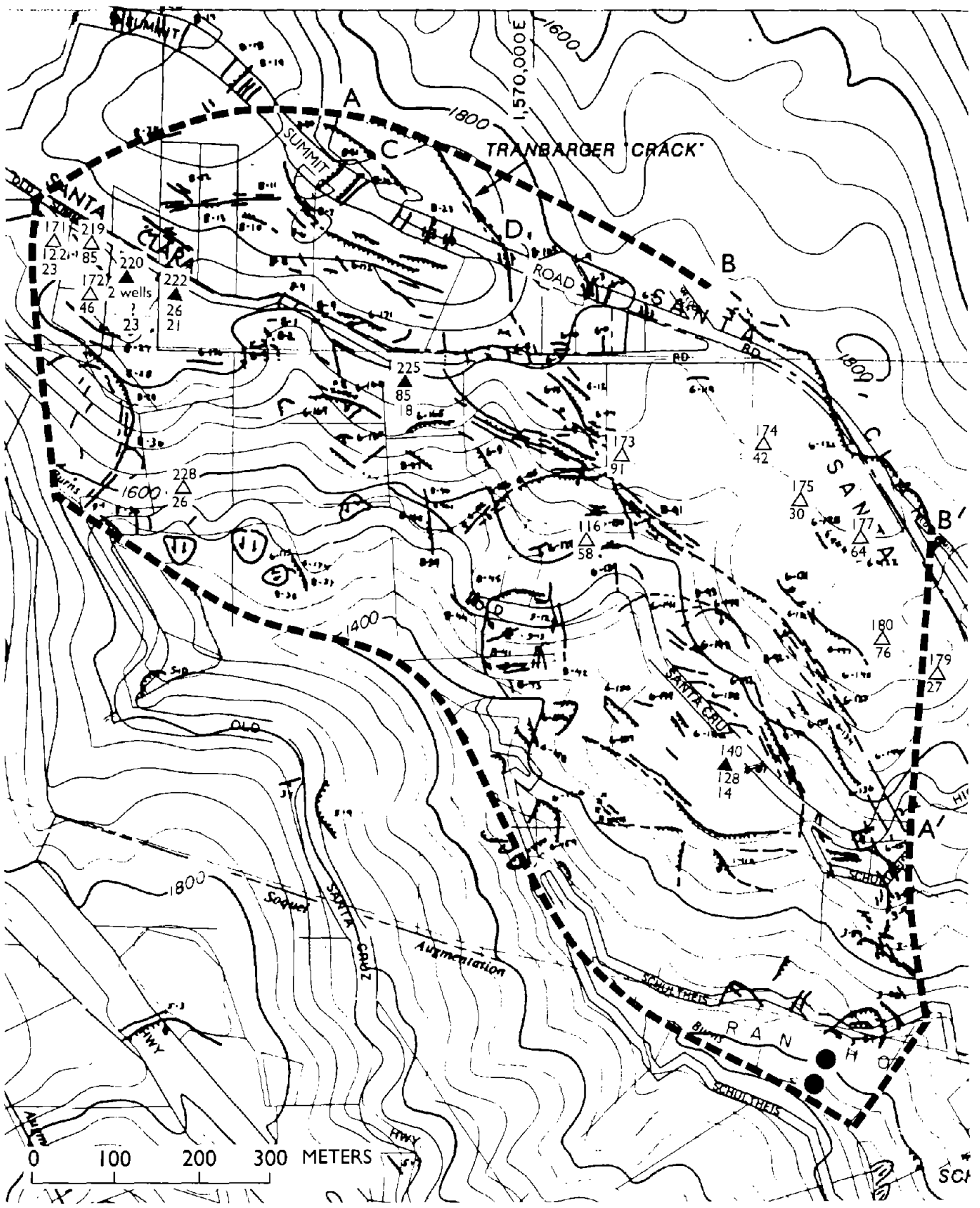


Figure 7.—Continued.

downslope through the steep, heavily vegetated terrain below Schultheis Road to Burns Creek itself (fig. 9). The landslide thus delineated is approximately 460 m long and 13 ha in area.

The Upper Schultheis Road landslide exhibits a benched topographic profile (fig. 11), indicative of previous landslide movement. The slope inclination along this profile averages 15°. The arcuate main scarp of the landslide also partly coincides with the base of a steep slope, inferred to be the scarp of a preexisting landslide. Both Cooper-Clark and Associates (1975) and McLaughlin and others (1991) mapped almost all of the area of the 1989 landslide as landslide material (see pl. 3; fig. 4).

Displacements measured along a transect across the main scarp indicate that the head of the landslide moved 1.16 m downslope. An additional 1.28 m of downslope displacement was measured across a series of internal fissures and scarps that extended for 62 m downslope from the main scarp. The total measured displacement of the landslide along that transect was thus 2.44 m.

Bedrock beneath the landslide is sandstone, siltstone, and shale of the Butano Sandstone and Vaqueros Sandstone, which are separated by the Butano fault (see pl. 3). Upslope from this fault, dips are steeply northeastward (into the slope). Downslope from the fault, bedding is folded around the axis of the Laurel anticline, but except for local southwestward dips under the inferred toe of the landslide, dips downslope from the fault also are predominantly steeply northeastward (see pl. 3; fig. 11).

Subsurface exploration of the landslide included five small-diameter (12.4–16.5 cm) boreholes drilled to depths

of 25 to 92 m (William Cotton and Associates, Inc., 1990), and three 61-cm-diameter boreholes drilled to depths of 16 to 22 m (Cole and others, 1991). Materials consisted of (1) a layer of colluvium (locally mantled by topsoil and manmade fill), ranging in thickness from less than 0.6 to about 11 m, consisting mainly of silty clay, clayey silt, silt, sandy silt, and silty sand; (2) a layer, 3 to 18 m thick, made up of varying weathered shale, siltstone, sandstone, clay, sandy silt, and sand; and (3) bedrock consisting of approximately 58 percent sandstone, 9 percent siltstone, and 33 percent shale and claystone. (The percentages were virtually the same for both bedrock units represented.) The rock was locally weathered and (or) intensely fractured and contained localized zones of crushed, very soft, or sheared materials and zones where drilling circulation was lost, indicating open fractures at depths as great as 55 m.

Particularly conspicuous shear zones were penetrated in borehole SR-2 at a depth of 27.1 to 27.4 m, and in the larger-diameter boreholes SR-5, SR-6, and SR-7 at depths of 6.7, 5.3 to 6.7, and 10.4 m, respectively (figs. 9B, 11). The deeper shear zone contained a sheared mixture of highly plastic clay, silty clay, sandstone, and fractured shale overlying 0.5 to 1.3 cm of sheared, mixed silty clay and clayey silt of varying plasticity (William Cotton and Associates, Inc., 1990); the shallower shear zone separated intensely weathered and oxidized materials from unoxidized rocks (Cole and others, 1991). In borehole SR-5, this shallower shear zone consisted of 3 to 13 cm of sheared siltstone and clay with polished surfaces; in borehole SR-6, the zone contained three separate faulted and sheared contacts; and in borehole SR-7, the zone was a 5- to 10-cm-thick layer of swelling clayey siltstone, which separated an overlying brecciated and fractured siltstone from an underlying sandstone (Cole and others, 1991).

Two of three known water wells within the landslide were reportedly damaged during the earthquake. In well 141 (fig. 9B), located less than 30 m from borehole SR-2, the well-pump motor was reportedly broken off, and the motor shaft bent to a 45° angle at 30-m depth, corresponding closely to the 27-m depth of the shear zone in borehole SR-2. In well 218, about 3 m from borehole SR-6 (fig. 9B), an offset of 20 to 30 cm was reported to have occurred at about 4.5-m depth in a 76-cm-diameter casing. This offset corresponds closely in depth to the shallower shear zone. These correspondences indicate that landslide displacements during the earthquake probably occurred in both the shallower and deeper shear zones. A cross section showing the inferred landslide basal shear surfaces is shown in figure 11. If the average landslide thickness is assumed to be half of the maximum thickness shown on this cross section, the total volume of the landslide is  $4.3 \times 10^6 \text{ m}^3$ .

## EXPLANATION

[Composite explanation for part B of figures 7, 9, 12, and 20. See figure 7A for explanation of surface features and localities discussed in text. Water-well data from Brumbaugh (1990); borehole data from William Cotton and Associates (1990) and (or) Cole and others (1991)]

- |                       |  |
|-----------------------|--|
| 179<br>△<br>90        | <b>Water well reported undamaged by 1989 Loma Prieta earthquake</b> —Upper number, well number; lower number, total depth (in meters)  |
| 140<br>▲<br>420<br>27 | <b>Water well reported damaged by 1989 Loma Prieta earthquake</b> —Upper number, well number; upper lower number, total depth (in meters); lower lower number, depth of damage (in meters); queried where no depth of damage given |
| SR-4<br>●             | <b>Borehole</b> —Number identifies borehole, as discussed in text and by William Cotton and Associates (1990) and Cole and others (1991)   |

Figure 7.—Continued.

### RALLS DRIVE LANDSLIDE

The Ralls Drive landslide is immediately east of the Upper Schultheis Road landslide, on the southwest flank of Summit Ridge (area 4, pl. 3). The main scarp is a set of ground cracks and scarps, some arcuate and concave downslope and others linear, intersecting to form an angular or zigzag pattern in plan view (leg B-B', fig. 9A). Two faults with northwestward strikes, parallel to segments of the main scarp, also pass through the head of the landslide (see pl. 3). This association, as well as the angular pattern of the main scarp between localities B and B' (fig. 9A), indicates that bedrock structure controlled scarp formation there.

Part of the east flank of the Ralls Drive landslide is delineated by a set of northwest-trending echelon scarps and cracks (fig. 9); the west flank abuts the Upper Schultheis Road landslide. A major internal ground crack, striking approximately downslope, divides the Ralls Drive landslide into two main blocks (leg B-C, fig. 9A). The smaller, western block formed on the spur ridge adjacent to the Upper Schultheis Road landslide, and the larger, eastern block formed around and under a short valley, tributary to Burns Creek. Both landslide blocks were moderately disrupted by other internal scarps and cracks; the area of greatest disruption was adjacent to the east flank (fig. 9). Local indications of compression were present near the downslope termination of the crack separating the two blocks, particularly where this crack curved to the east (leg C-C', fig. 9A).

The Ralls Drive landslide is about 730 m wide and at least 480 m long. No visible surface feature marks the toe, but small internal scarps low on the slope suggest that the landslide extends an additional 150 to 430 m downslope from the flank cracks to Burns Creek. The area of the landslide thus is approximately 50 ha.

Displacements measured across the main scarp and internal scarps are downslope, to the south, southeast, or southwest. These measurements indicate that the head of the western block moved downslope 0.55 to 1.02 m, that the head of the eastern block moved downslope 0.28 to 0.97 m, and that the most disrupted parts of the eastern block moved downslope as much as 1.80 m.

Within the Ralls Drive landslide, one well (125, fig. 9B) was reportedly damaged at 17-m depth, whereas five wells (19, 20, 119, 122, 126, fig. 9B), 46 to 61 m deep, were reportedly undamaged by the earthquake. Three of the reportedly undisturbed wells are near the main scarp, and the other three are within the eastern block. The reported absence of damage to these wells could indicate either that local displacements were not large enough to damage the wells or that the basal shear surface is deeper than 46 to 61 m. The damage to well 125 may thus indicate a shallower, subsidiary shear surface, or it may be unrelated to landslide movement.

The slope through the Ralls Drive landslide averages 15°, but it is also irregular and contains benches and steeper segments, indicating previous landslide activity. Most of the landslide was mapped as landslide material by Cooper-Clark and Associates (1975) and McLaughlin and



Figure 8.—Segment of Tranbarger fracture (leg A-A', fig. 7A), a 1,200-m-long zone of scarps and cracks in Old Santa Cruz Highway landslide complex. View northwestward from north edge of Summit Road (loc. D, fig. 7A).



others (1991) (see pl. 3; fig 4), and part of the main scarp was at the base of an older scarp.

The trace of the Butano fault passes through the Ralls Drive landslide about 140 m downslope from the crown (see pl. 3). Upslope from the fault, bedrock is the north-east-dipping Vaqueros Sandstone; downslope from the

fault, bedrock is mostly the Butano Sandstone, with a small area underlain by the San Lorenzo Formation (see pl. 3). The axis of the Laurel anticline is projected to pass near the base of the slope; thus, most rocks downslope from the Butano fault dip northeast (into the slope), whereas rocks under the landslide toe dip southwest.

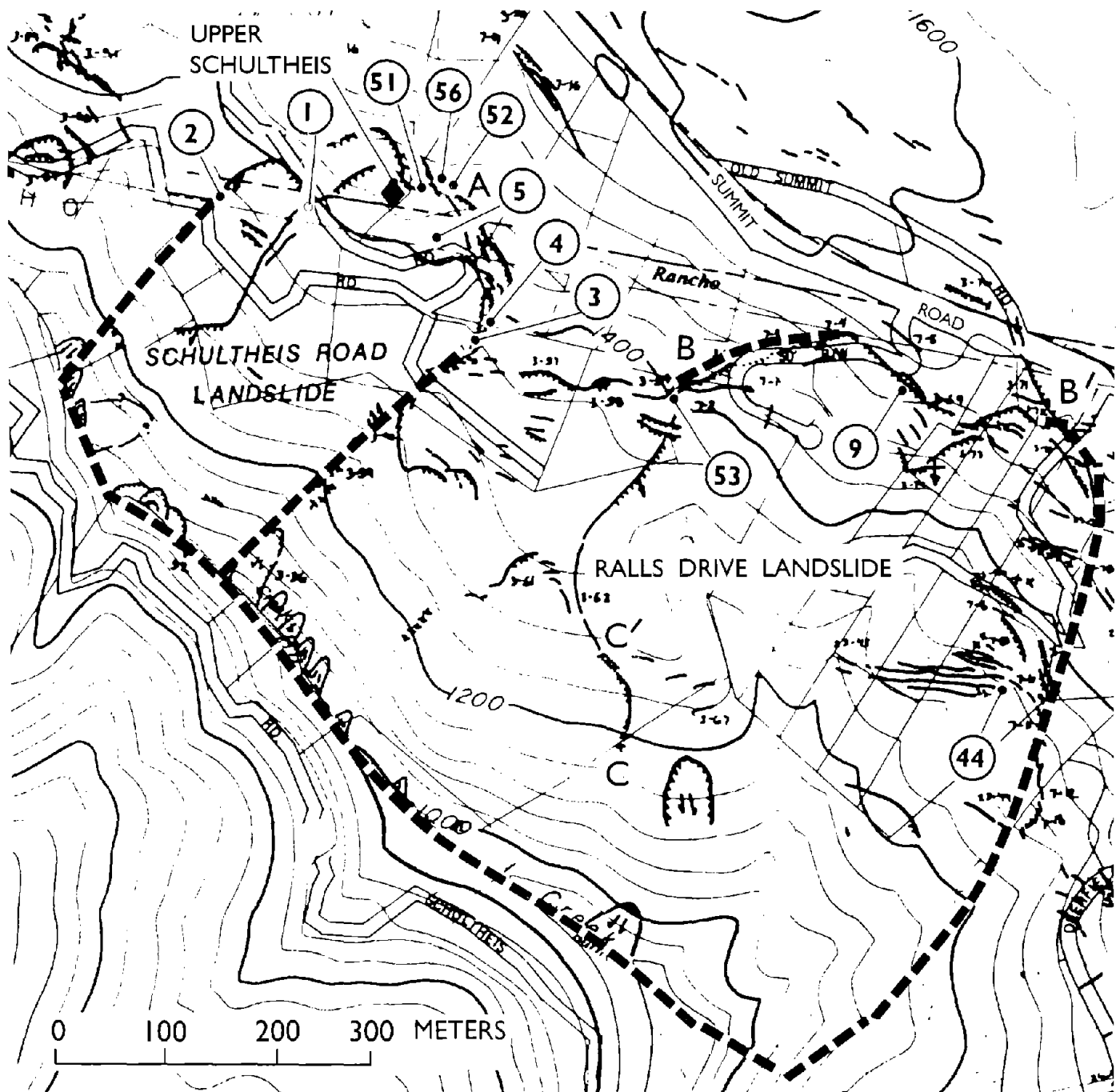


Figure 9.—Upper Schultheis Road and Ralls Drive landslides, showing boundary of landslides and locations of (A) surficial features, surface-monitoring stations, and localities discussed in text and of (B) boreholes (from William Cotton and Associates, 1990, and Cole and others, 1991).

cross section in figure 11, and water wells (from Brumbaugh, 1990). Ground cracks and compressional features from Spittler and Harp (1990); landslide boundaries from Keefer (1991). See figure 7 for explanation and base-map information.

### VILLA DEL MONTE LANDSLIDE

The Villa Del Monte landslide is also on the southwest flank of Summit Ridge, on the broad spur ridge between the Ralls Drive landslide and Taylor Gulch (area 5, pl. 3; fig. 12). Surveyed topographic profiles show average slope inclinations of 12°–15°. Many gently sloping benches alternate with steeper stretches of slope, especially in the

central and eastern parts of the area; slopes near the base of the ridge, in particular, are relatively steep. Numerous roads and building sites have been located in this area to take advantage of these gently sloping benches, and the Villa Del Monte neighborhood, which contains approximately 165 homes, is the most densely populated part of the Summit Ridge area. Earthquake-induced ground movement caused substantial damage in this neighborhood.

B

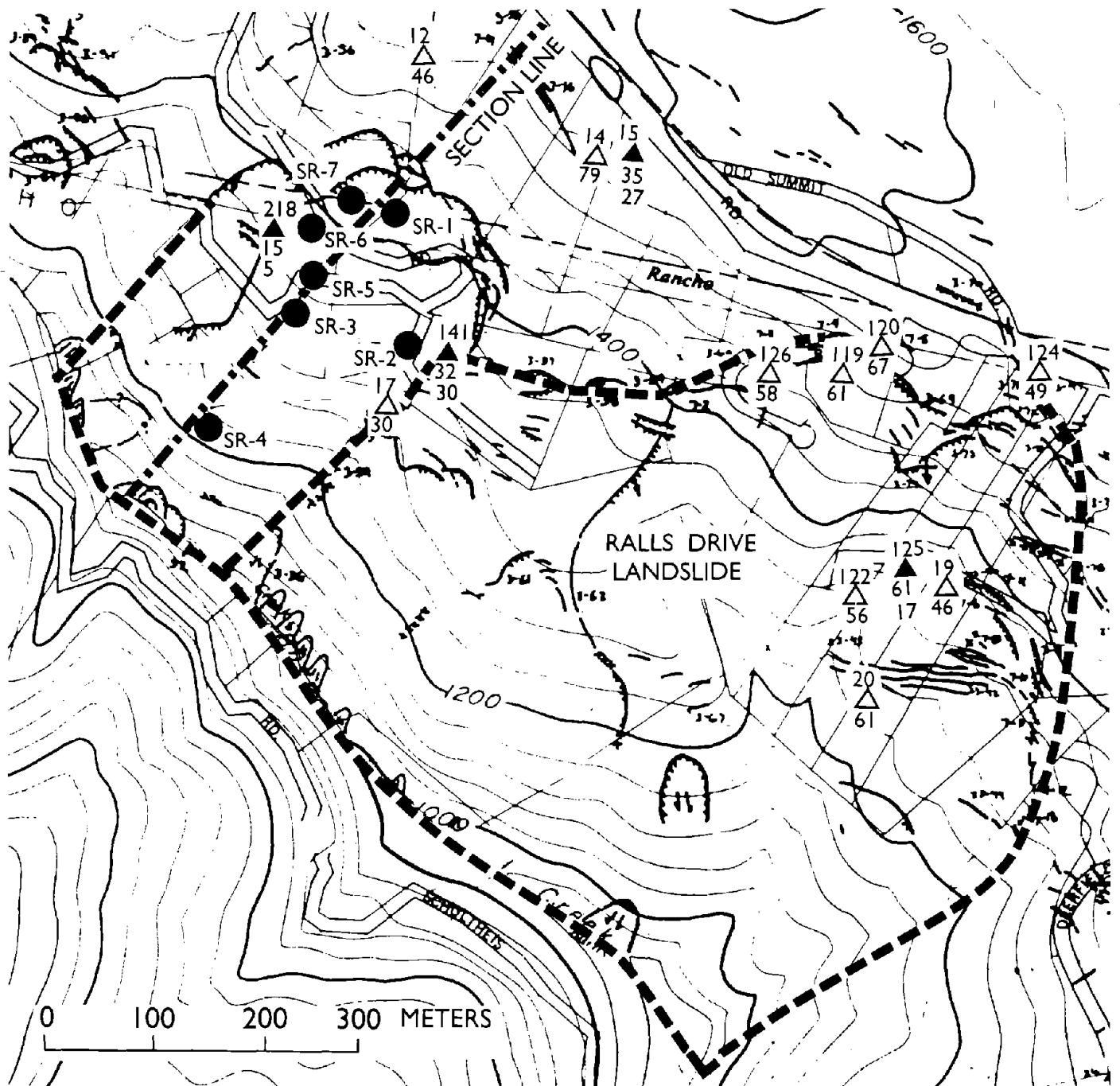


Figure 9.—Continued.

Several distinct zones of ground cracks are present within the Villa Del Monte landslide. The major zones of ground cracks are along Sunset Drive, in the area of upper Skyview (or "Sky View") Terrace and Bel Air (or "Belair," "Bel-Air," or "Bel Aire") Court, along and east of Deerfield Road, and along lower Skyview Terrace (fig. 12). Additional, smaller zones of ground cracks along the westernmost extension of Deerfield Road and around the Troy Road-Skyview Terrace intersection (fig. 12) are probably associated with separate, smaller landslides.

#### SUNSET DRIVE AREA

The ground cracks and scarps in the Sunset Drive area (figs. 12, 13) extend approximately 420 m across the slope (leg A-A', fig. 12A) and 210 m down the slope (leg B-B', fig. 12A). For parts of their lengths, these cracks and scarps cross a gentle slope downslope from a 3- to 5-m-high bedrock scarp composed of intensely fractured sandstone. A few northwest-striking ground cracks in this area are subparallel to local faults (see pl. 3), indicating that their

formation was controlled by bedrock structures. Displacements measured across individual cracks and scarps were from 8 to 53 cm, downslope toward the southwest and southeast.

Six wells in this area (wells 71, 74, 75, 82, 83, 88, fig. 12B) were reportedly damaged. The damage to wells 74 and 75, which involved collapsed casings at 5- and 23-m depth (Brumbaugh, 1990), suggests that the ground crack immediately upslope from them marks the upslope boundary of the landslide.

#### UPPER SKYVIEW TERRACE-BEL AIR COURT AREA

The upper Skyview Terrace-Bel Air Court area, in the eastern part of the Villa Del Monte neighborhood, is the second zone of concentrated and pervasive ground cracking (figs. 12, 14). The cracks and scarps in this area extend approximately 300 m across the slope and 670 m downslope, from immediately above upper Skyview Terrace (leg C-C', fig. 12A) to Laurel Creek (leg D-D', fig.



Figure 10.—Part of main scarp of Upper Schultheis Road landslide. Measurements near this locality showed 1.07 m of extensional displacement and 46 cm of vertical displacement across main scarp. View eastward from near landslide crown (loc. A, fig. 9A).

12A). At the upslope margin of this zone is a scarp (leg C-C', fig. 12A), 240 m long, that is arcuate and concave downslope, toward the south. The ground cracks between upper Skyview Terrace and Bel Air Court (leg E-E', fig. 12A), along Bel Air Court and middle Skyview Terrace (leg F-F', fig. 12A), and along Tree View Trail and lower Skyview Terrace (leg D-D', fig. 12A) also form arcuate-downslope patterns subparallel to the upper scarp zone. In addition, the area contains several small pressure ridges.

With one exception, displacement measurements in the upper Skyview Terrace-Bel Air Court area showed movement to the southeast, south, and southwest, toward Laurel Creek. The sole exception, which showed 15 cm of extension and 33 cm of vertical displacement on an upslope-facing scarp, could be due to graben formation or differential movement within the landslide. Measured local downslope displacements elsewhere in the area were 10 to 107 cm.

Several wells along the eastern margin of the area of ground cracks (wells 26, 91-94, fig. 12B) were reportedly undamaged by the earthquake, indicating that the land-

slide did not extend eastward of that margin to Taylor Gulch. This margin defines the east flank of the landslide.

DEERFIELD ROAD AREA

In the western part of the Villa Del Monte area, another major zone of ground cracks, scarps, and pressure ridges occurs along Deerfield Road and between Deerfield Road and Evergreen Lane (area G-G'-H-H', fig. 12A). This zone extends approximately 240 m from west to east and 370 m downslope (fig. 12). The cracks and scarps (fig. 15) in the zone strike predominantly northeast, oblique to the main structural elements in the bedrock (see pl. 3). Displacement measurements show predominantly southeastward to locally southwestward movement of 5 to 41 cm. Both the strike of the main ground cracks and the predominantly southeastward direction of displacements indicate that this zone forms the west (or right) flank of the landslide.

All five wells in this zone, along Deerfield Road (wells 85, 88, 89, 233, 234, fig. 12B), were reportedly damaged

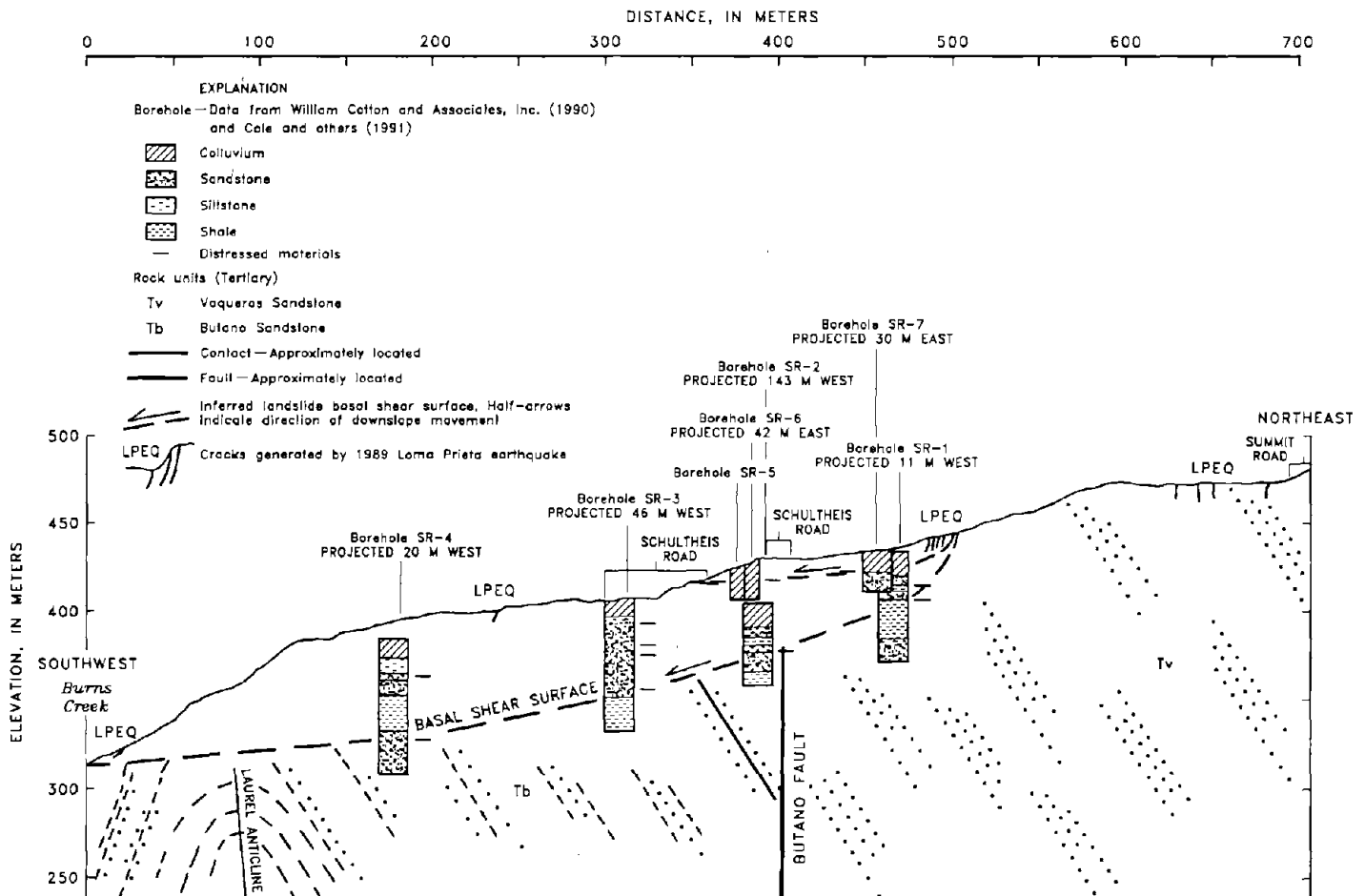


Figure 11.—Geologic cross section through Upper Schultheis Road landslide (fig. 9B). Locations of landslide basal shear surfaces inferred from borehole data of William Cotton and Associates, Inc. (1990), and Cole and others (1991).

A

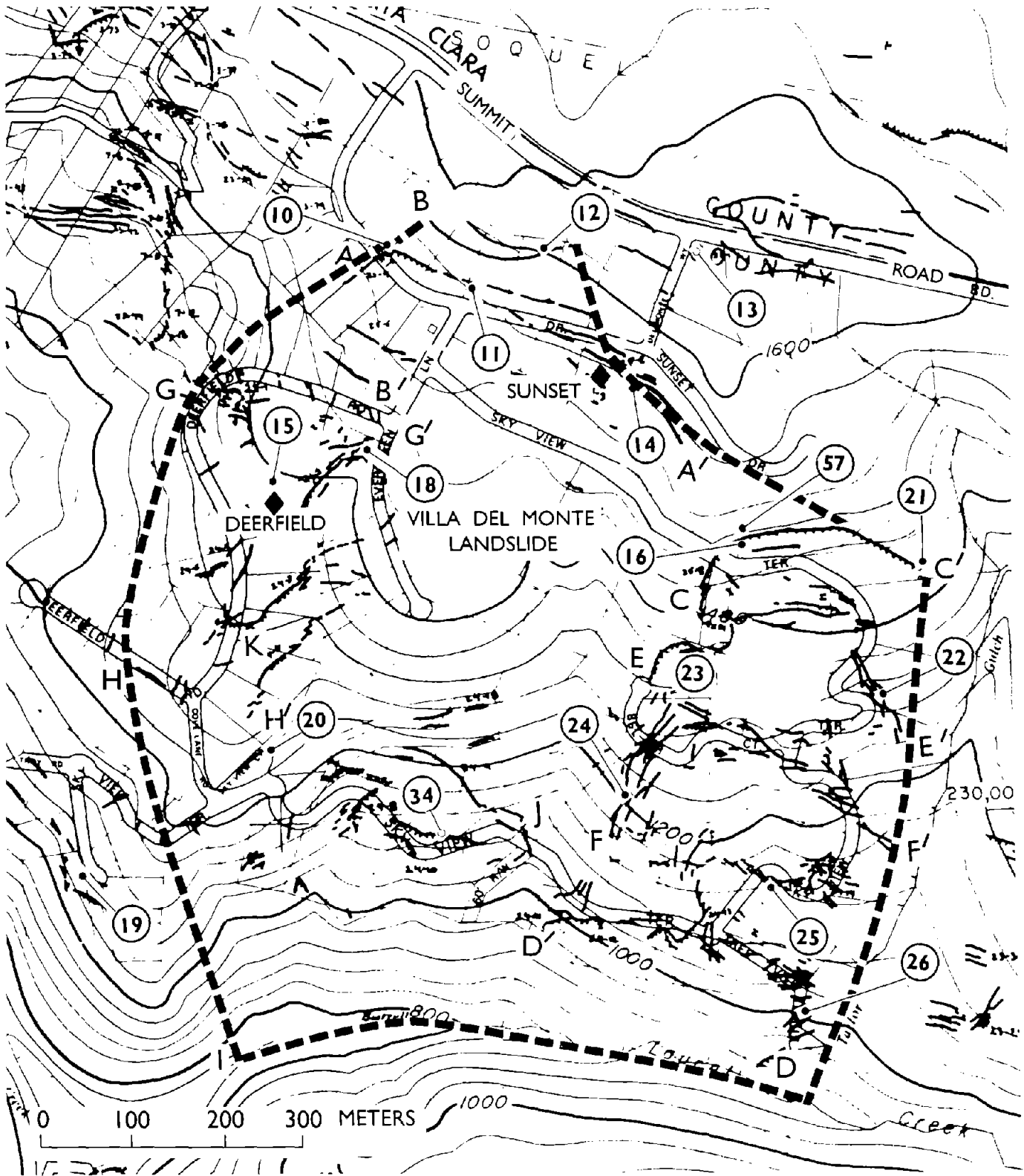


Figure 12.—Villa Del Monte landslide, showing boundary of landslide and locations of (A) surficial features, surface-monitoring stations, and localities discussed in text and of (B) boreholes (from William Cotton and Associates, 1990, and Cole and others, 1991), cross section in figure 16, and water wells (from Brumbaugh, 1990). Ground cracks and compressional features from Spittler and Harp (1990); landslide boundaries modi-

fied from Keefer (1991). Base from Towill, Inc., using topography from U.S. Geological Survey Los Gatos and Laurel, Calif., 7.5-minute quadrangles and culture from County of Santa Cruz planimetric base and interpretation of aerial photographs taken July 24, 1990. See figure 7 for explanation. Contour interval, 40 ft.

by the earthquake. However, seven of the eight wells along westernmost Deerfield Road and westernmost Skyview Terrace (wells 105-108, 235a, 235b, 237, fig. 12B) were

reportedly undamaged. This zone of undamaged wells suggests that the smaller zones of ground cracks farther west (fig. 12) were not part of the larger landslide. These

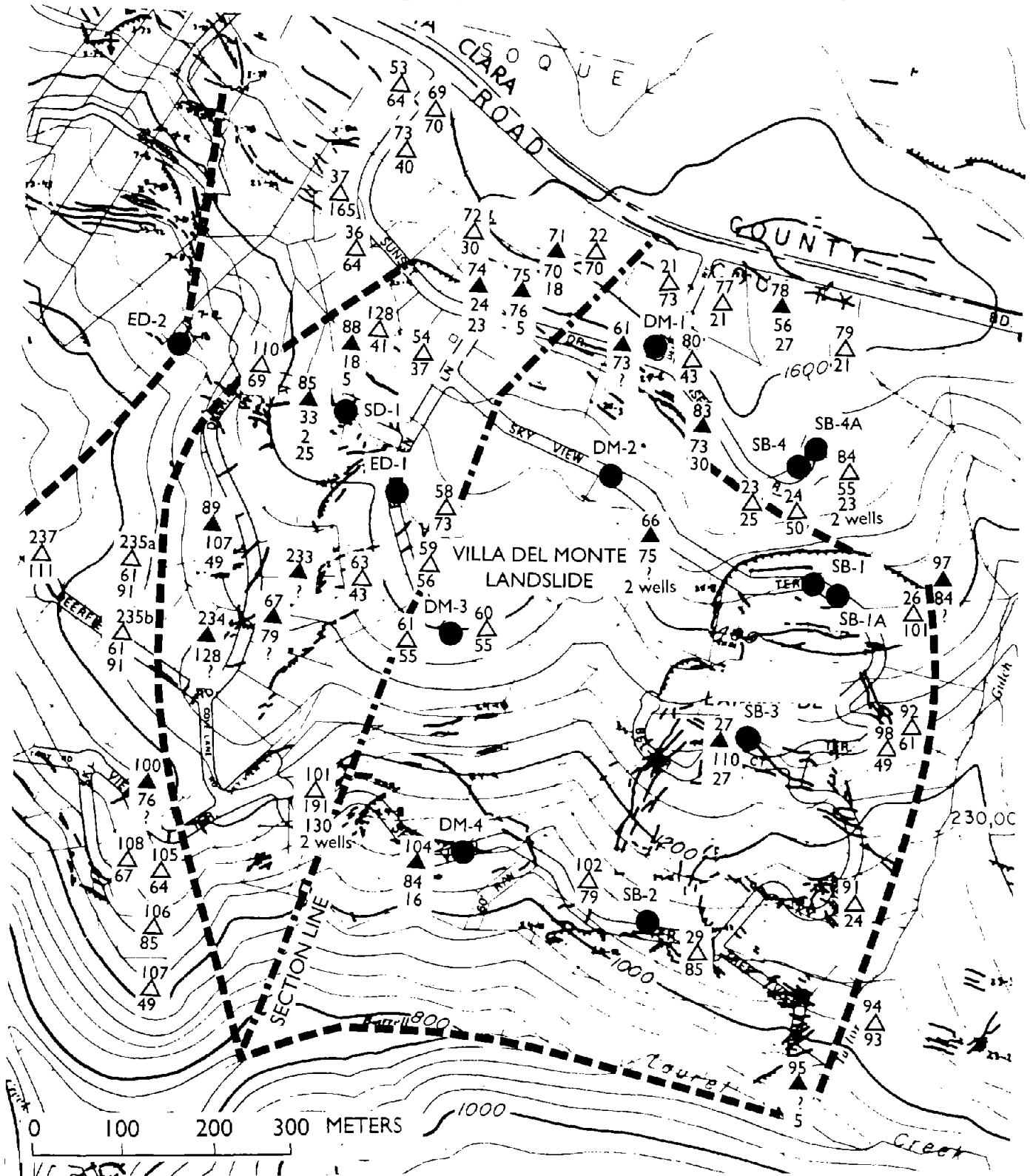


Figure 12.—Continued.

westernmost ground cracks were almost certainly associated with smaller landslides. Although the boundary of the large landslide is inferred to lie generally in the area between the damaged and undamaged wells (approx between locs. H and I, fig. 12A), the landslide limits in this area were poorly defined by the available data.

#### LOWER SKYVIEW TERRACE AREA

Along lower Skyview Terrace, for a distance of approximately 400 m east of Cove Lane Road, is a zone of mostly arcuate, concave-southward scarps and cracks (leg H'-J, fig. 12A). The zone extends approximately 200 m from north to south, on both sides of lower Skyview Terrace. The water well within the area of most concentrated

cracking (well 104, fig. 12B) was reportedly damaged, whereas three nearby wells (wells 101-103, fig. 12B), in less disturbed areas, were reportedly undamaged. One measurement across a ground crack in this area showed 33 cm of displacement downslope, toward the southeast.

#### OVERALL LANDSLIDE DIMENSIONS, MOVEMENT, AND SETTING

The Villa Del Monte landslide extends downslope from the Sunset Drive area to Laurel Creek and thus is 980 m in overall length. The right flank of the landslide is inferred to be the western margin of the Deerfield Road area, and the better defined left flank is the eastern margin of ground cracking in the upper Skyview Terrace-Bel



Figure 13.—Segment of main scarp of Villa Del Monte landslide in Sunset Drive area. View northwestward from near quadrilateral-array station 14 (fig. 12A). Photograph by Kevin M. Schmidt, U.S. Geological Survey.

Air Court area (leg C'-D, fig. 12A). Thus, the overall width of the landslide is 870 m, and its surface area is about 68 ha. Displacements measured across individual ground cracks and scarps throughout the Villa Del Monte landslide ranged from 5 to 107 cm; most local displacements ranged from 33 to 53 cm.

Cooper-Clark and Associates (1975) mapped the east two-thirds of the Villa Del Monte landslide as a "probable" landslide (fig. 4). Clark and others (1989, with landslide boundaries revised by R. J. McLaughlin and J.C. Clark, unpub. data, 1990) and McLaughlin and others (1991) show all but the westernmost part of the landslide as underlain by a particularly large preexisting landslide deposit that stretches along Summit Ridge for about 1.6 km; most of the northern, eastern, and southern margins of the Villa Del Monte landslide correspond closely in

location to the mapped boundaries of that deposit (see pl. 3). In addition, the benched topography in the Villa Del Monte area indicates previous landslide activity, and Santa Cruz County road-repair records show that previous landslide movement occurred in the Skyview Terrace area in 1975-76 (fig. 3; table 2).

#### SUBSURFACE CONDITIONS AND MATERIALS

Bedrock beneath the Villa Del Monte landslide is the Butano Sandstone and the Twobar Shale and Rices Mudstone Members of the San Lorenzo Formation (see pl. 3). The axis of the Laurel anticline is projected to pass through the southwestern part of the landslide. Rocks northeast of this axis dip obliquely into the slope, to the north and



Figure 14.—Internal scarp of Villa Del Monte landslide in Upper Skyview Terrace-Bel Air Court area. View northwestward from near quadrilateral-array station 23 (fig. 12A). Photograph from Griggs and others (1990).





A



B

Figure 15.—Internal scarps and compressional features of Villa Del Monte landslide in Deerfield Road area. *A*, Internal scarps, which are part of a zone about 200 m long. View northeastward from just east of Deerfield Road (loc. K, fig. 12A). *B*, Internal ridge, consisting of compressed ground, marked by broken and buckled pavement. View northwestward from near east end of Deerfield Road (loc. *B'* on fig. 12A).

northeast. Southwest of the axis, dip may be steeply southwestward, locally overturned to the northeast, or both (see pl. 3). Several northwest-striking faults are mapped through the crest and upper flanks of Summit Ridge, into and just north of the landslide (see pl. 3).

A total of 13 small-diameter (14.9–16.5 cm) boreholes (fig. 12B), drilled to depths as great as 92 m, showed materials consisting of as much as 4 m of fill and colluvium and 3 to 17 m of weathered rock overlying bedrock (William Cotton and Associates, Inc., 1990). The fill and colluvium were composed of clayey silt, silty clay, silty sand, sandy clay, and clayey sand. The weathered rock contained similar materials, as well as weathered sandstone, siltstone, and shale that were locally brecciated, crushed, or intensely fractured. Bedrock to the depths penetrated by the boreholes consisted of sandstone, siltstone, and shale. Among the three geologic units, the Twobar Shale Member contained the most sandstone (85 percent of drilled interval) and the least siltstone (12 percent) and shale (3 percent). The drilled interval of the Butano Sandstone consisted of 32 percent sandstone, 44 percent siltstone, and 25 percent shale, and that of the Rices Mudstone

Member consisted of 39 percent sandstone, 41 percent siltstone, and 20 percent shale.

The soil, weathered rock, and bedrock contained approximately 45 intervals in the boreholes with indications of distressed materials—sheared, intensely fractured, or faulted rocks; very soft zones; crushed materials; intervals of collapsing or caving of the boreholes; or zones of lost circulation (fig. 16; William Cotton and Associates, Inc., 1990). These zones occurred in all rock types at depths from near the surface to near the maximum depth of drilling. However, the small diameters, discontinuous sampling, and absence of geophysical logging of the boreholes made identification of landslide shear surfaces within the boreholes uncertain. The numerous zones with indications of disturbance and reports of water well damage at various depths (fig. 12B) indicate that localized internal shearing occurred at several depths during landslide movement. An inferred deep basal shear surface, which is compatible with the drilling and surface data, is shown in figure 16. If the average landslide thickness is assumed to be half of the maximum thickness shown on this cross section, the landslide volume is  $27 \times 10^6 \text{ m}^3$ .

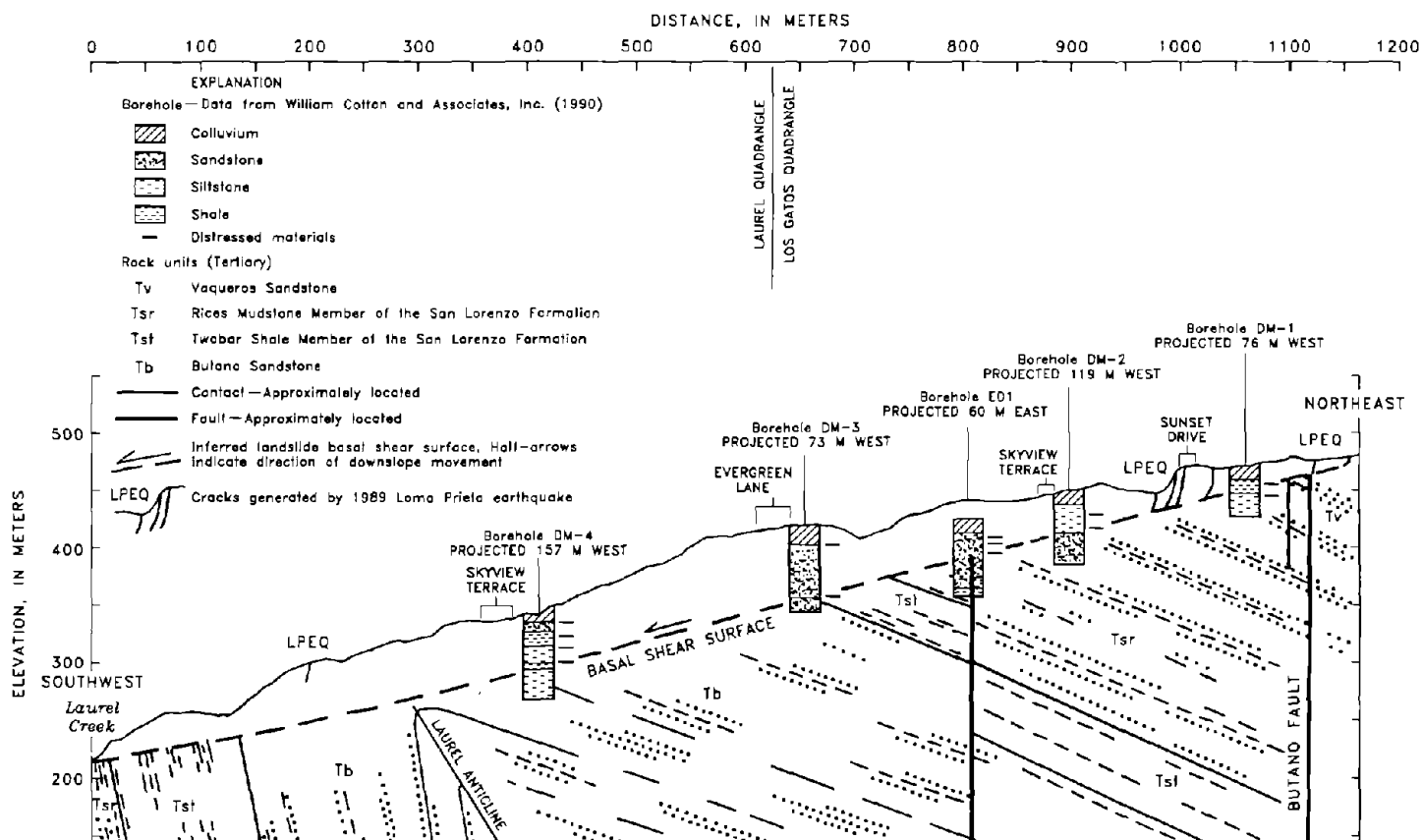


Figure 16.—Geologic cross section through Villa Del Monte landslide (see fig. 12B for location). Basal shear surface inferred from borehole data of William Cotton and Associates, Inc. (1990). See figure 11 for explanation.

## UPPER MORRELL ROAD LANDSLIDE

The Upper Morrell Road landslide is on the south flank of Summit Ridge east of Taylor Gulch (area 7, pl. 3). The main scarp of the landslide is made up of two adjoining zones of ground cracks and scarps, each of which is arcuate, concave downslope in plan view (leg A-A', fig. 17). Together, these zones extend approximately 550 m across the slope. The orientation of ground cracks in these zones

and the relation of these cracks to other northwest-striking cracks nearby (leg B-B', fig. 17) suggest significant control by bedrock structures. Displacement measurements across the main zones of cracks (fig. 18) indicate downslope movement of as much as 2.01 m. Southeast of the main scarp, a shorter scarp is inferred to mark part of the east flank of the landslide (loc. C, fig. 17).

The toe of the landslide is a gentle, east-west-striking bulge in the ground surface, 430 m long and 180 to 270 m

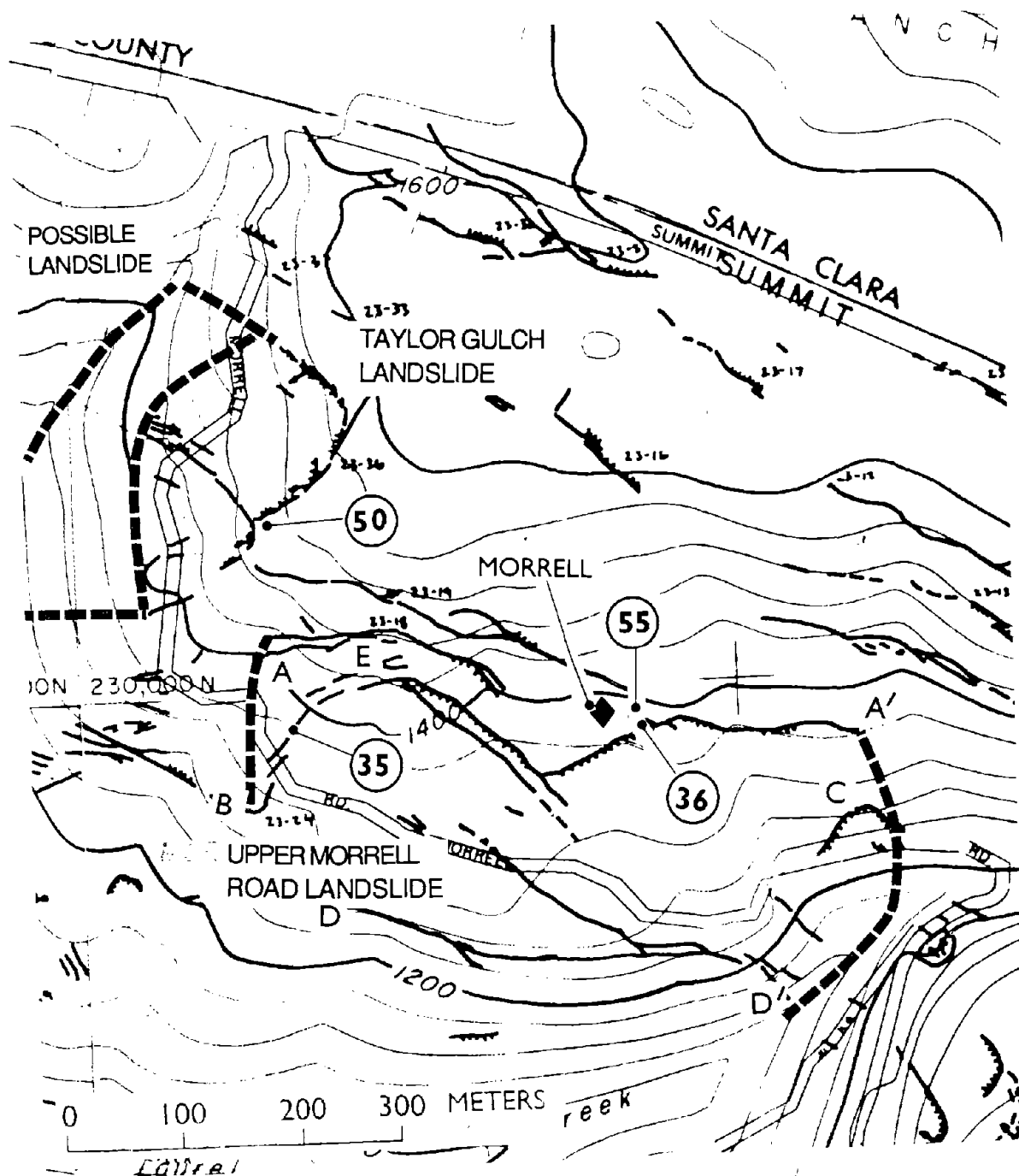


Figure 17.—Taylor Gulch and Upper Morrell Road landslides. Ground cracks and compressional features from Spittler and Harp (1990); landslide boundaries from Keefer (1991). See figure 7 for explanation and figure 12 for base-map information.

downslope from the main scarp. A zone of fractures and grabens along the crest of this bulge is evidence of local extension of the ground that accompanied upward bulging of the landslide toe. Between the crown cracks and the toe, the landslide encompasses an area of approximately 14 ha.

Two topographic profiles surveyed through the landslide exhibit the benched form characteristic of landslide terrain and show that the average slope is about 15°. In agreement with the topographic indications of previous landslide activity, Cooper-Clark and Associates (1975) and Clark and others (1989, with landslide boundaries revised by R.J. McLaughlin and J.C. Clark, 1990) mapped most or all of the Upper Morrell Road landslide as landslide material (see pl. 3; fig. 4). Santa Cruz County road-repair records additionally indicate several episodes of previous landslide damage to Morrell Road in this area (fig. 3; table 2). Bedrock underlying the landslide is mostly mudstone and sandstone of the Rices Mudstone Member of the San Lorenzo Formation, and small areas are underlain by igneous diabase and gabbro, the Vaqueros Sandstone, and the Butano Sandstone (see pl. 3). The beds dip generally northeast, into the slope.

#### BURRELL LANDSLIDE

The Burrell landslide is on the south flank of Summit Ridge, less than 100 m from the trace of the San Andreas fault (area 9, pl. 3). Features interpreted as the main scarps

of two landslide blocks (legs A-A', B-B', fig. 19) were differentiated from other ground cracks in the area on the basis of their arcuate forms, their location at the upslope margin of a gently sloping topographic bench, and the occurrence of a pressure ridge downslope from one of them, which partly delineates the landslide toe (loc. C, fig. 19). These two main scarps were separated by a zone of discontinuous cracks. The landslide is approximately 230 m long by 460 m wide and encompasses an area of about 9 ha. Downslope displacements measured across the main scarps were from 28 to 71 cm. The slope averages 15°–20°, and bedrock is the Butano Sandstone (see pl. 3), which dips east to northeast, oblique to the slope direction.

Trenching studies in the main scarp area show that the Burrell landslide is a reactivated preexisting landslide that first moved about 3 ka ago and later moved at least twice before the 1989 Loma Prieta earthquake (Keefer, 1991; Nolan and Weber, this chapter). The western part of the landslide was mapped as landslide material by Cooper-Clark and Associates (1975) (fig. 4).

#### UPPER REDWOOD LODGE ROAD LANDSLIDE

The Upper Redwood Lodge Road landslide is in the Redwood Lodge area, about 2 km south of Summit Road (area 10, pl. 3). The landslide was delineated primarily by three sets of discontinuous ground cracks and scarps, which indicate the presence of three large landslide blocks. The



Figure 18.—Part of main scarp of Upper Morrell Road landslide where scarp crosses gravel road. View northeastward from just east of Morrell Road (loc. E, fig. 17).

main scarp of the landslide is a series of discontinuous, straight to slightly arcuate cracks and scarps approximately 580 m long, that strikes about N. 30° W. (leg A–A', fig. 20A). The linearity and strike direction suggest that crack formation was controlled by bedrock structures (Keefer, 1991; Harp, this chapter). The most conspicuous ground cracks and scarps are in a nearly flat meadow, at the base of a steep stretch of slope; for part of their length, they are associated with a preexisting graben, about 30 m long, a few meters wide, and about 1 m deep. These relations indicate that the area is the head both of a large landslide that moved during the 1989 Loma Prieta earthquake and of a large preexisting landslide. Earthquake-induced displacements across the ground cracks and scarps were as great as 25 cm.

A second conspicuous zone of ground cracks and scarps crosses Soquel-San Jose Road ("Old San Jose Road") north of its intersection with Redwood Lodge Road (leg B–B', fig. 20A). This zone is arcuate and concave downslope in

plan view. The southern part of the zone is at the base of an older bedrock scarp, and the slope between this zone and the creek channel to the west has a benched topographic profile. Both the older scarp and the benched profile are additional indicators of previous landslide movement. Santa Cruz County road-repair records also describe repeated landslide damage to Redwood Lodge Road there (fig. 3; table 2). Earthquake-related displacements of 3 to 30 cm were measured across individual ground cracks in this zone but were inconsistent in direction.

A third conspicuous zone of cracks and scarps, farther downslope, trends west-northwest along and downslope from Redwood Lodge Road, between Old San Jose Road and Long Branch Gulch (leg C–C', fig. 22A). This zone, which is 580 m long, is the most continuous of the three.

The location of the northeast boundary of the landslide is poorly determined but is inferred to be at least as far northeast as the limits of the three conspicuous zones of

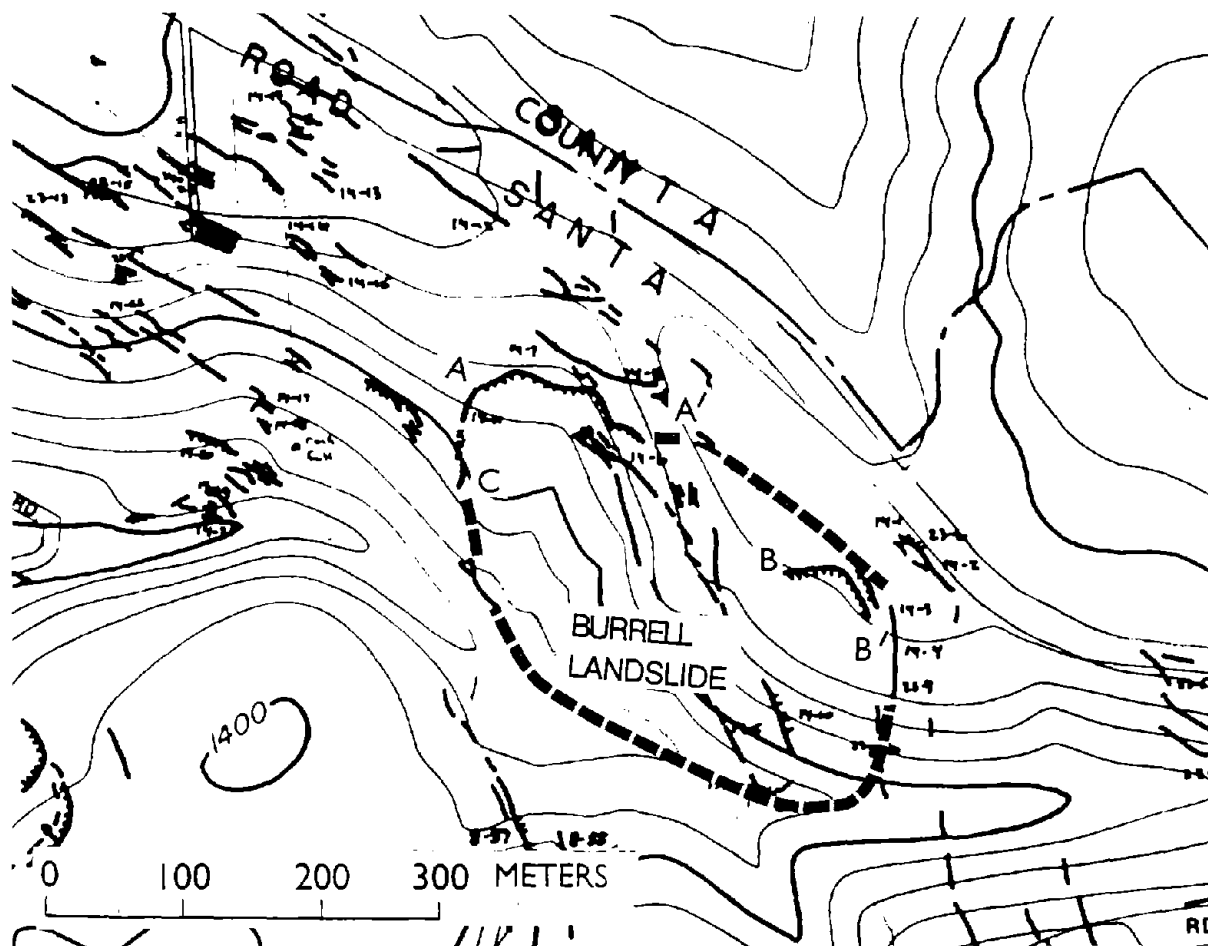


Figure 19.—Burrell landslide. Ground cracks and compressional features from Spittler and Harp (1990); landslide boundaries from Keefer (1991). Base from Towill, Inc., prepared using topography from U.S. Geological Survey Laurel, Calif., 7.5-minute quadrangle and culture from County of Santa Cruz planimetric base and interpretation of aerial photographs flown July 24, 1990. See figure 7 for explanation. Contour interval, 40 ft.

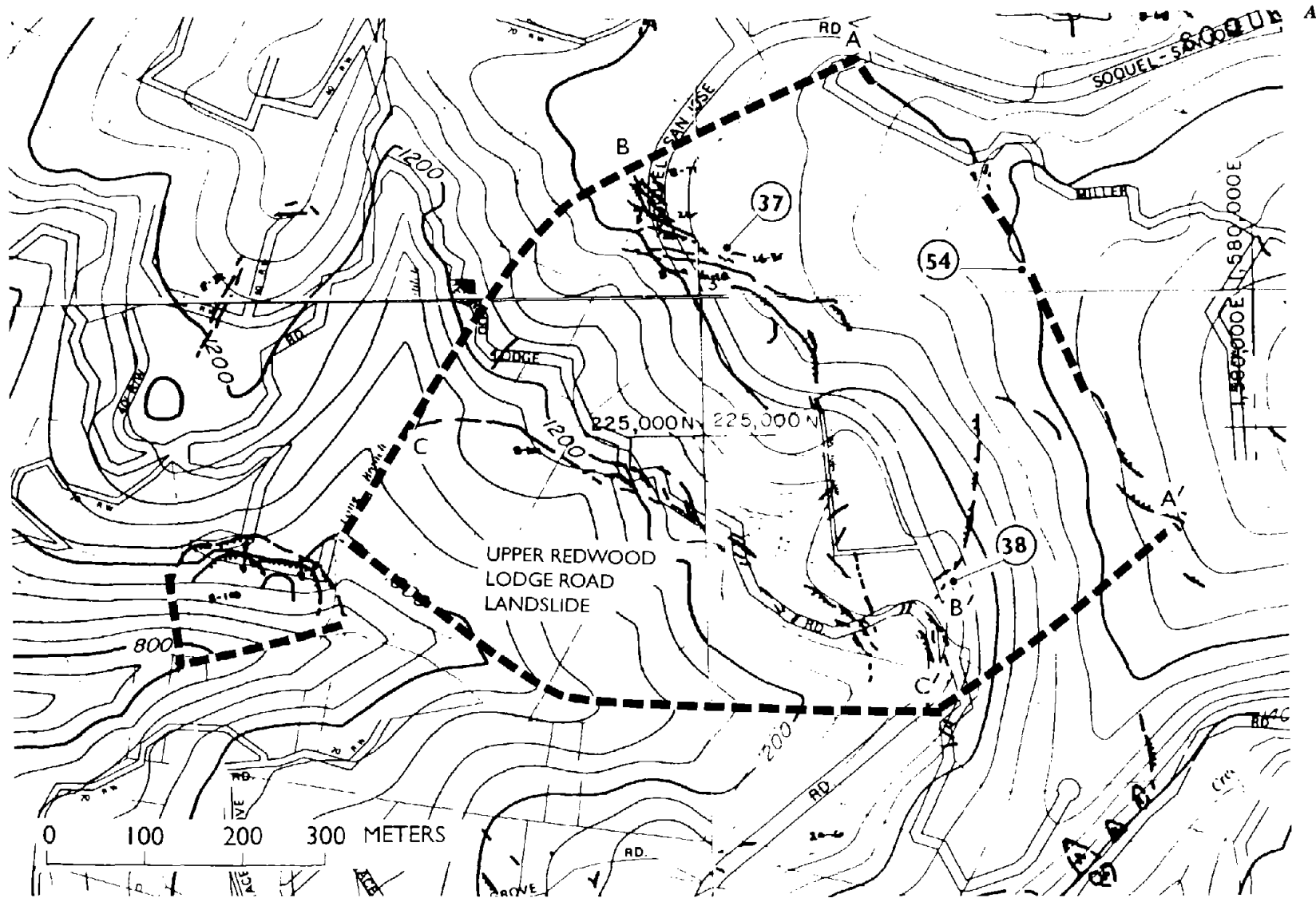


Figure 20.—Upper Redwood Lodge Road and Long Branch landslides, showing locations of (A) surficial features, surface-monitoring stations, and localities discussed in text and of (B) water wells (from Brumbaugh, 1990). Ground cracks and compressional features from Spittler and Harp (1990); landslide boundaries from Keefer (1991). See figure 7 for explanation and figure 19 for base-map information.

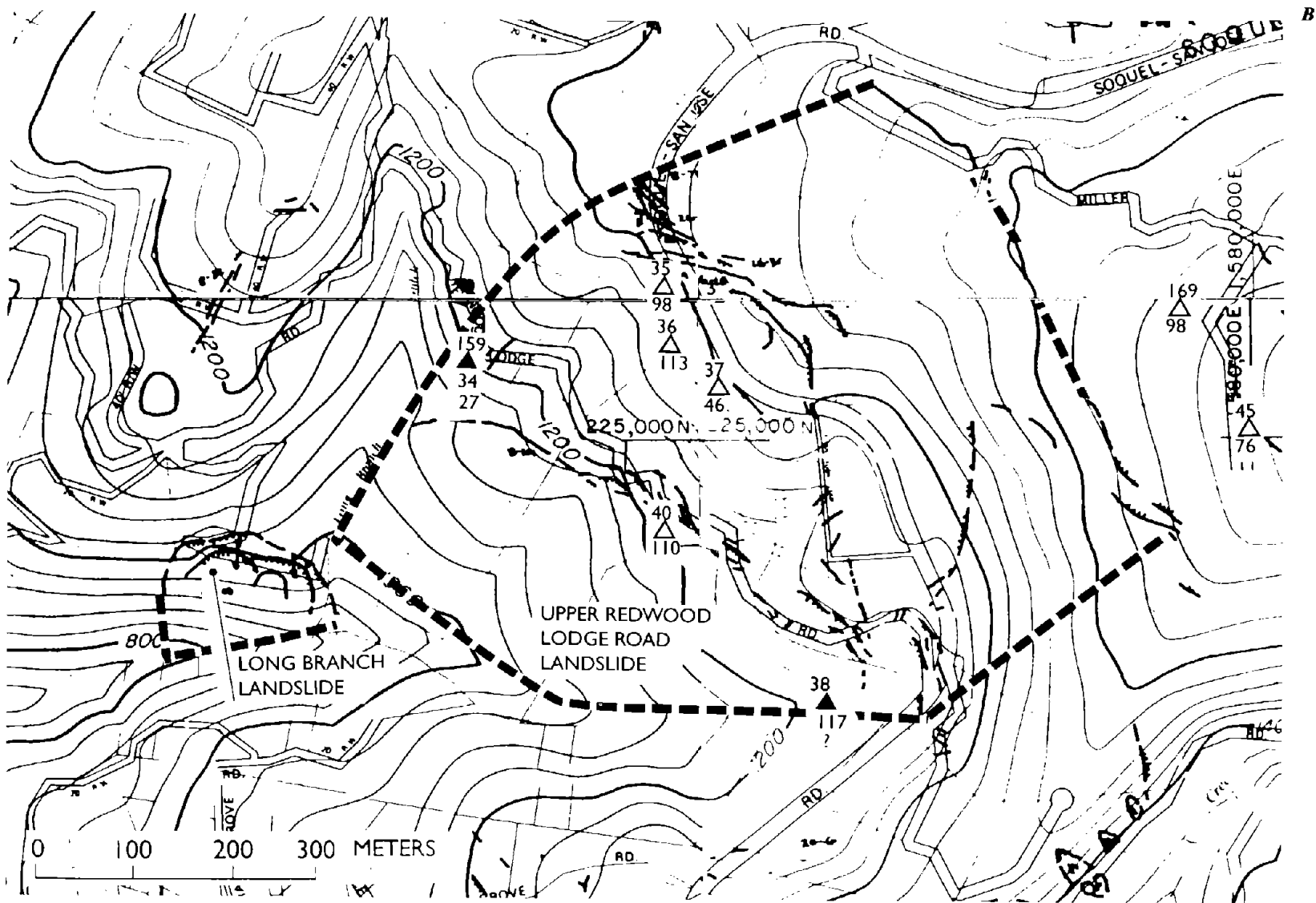


Figure 20.—Continued.

cracks and scarps (fig. 20); the landslide is thus at least 640 m wide. The southwest (downslope) boundary is likewise not marked by any surface features, but the position and pattern of the westernmost cracks and scarps suggest that the landslide extends to the creek at the base of the slope (fig. 20). The landslide is thus about 820 m long and at least 37 ha in area. The slope through the landslide averages 15°–20°.

Two wells within the landslide were reportedly damaged by the earthquake—well 159, at a depth of 27 m and well 38, at undetermined depth—and four wells (35–37, 40, fig. 20B), with depths of 45 to 113 m, were reportedly undamaged (Brumbaugh, 1990). The two damaged wells are both located near the margins of the landslide. The four reportedly undamaged wells are farther from these margins, and the absence of reported damage could indicate either a basal shear surface locally deeper than the wells or local displacements too small to cause damage.

Cooper-Clark and Associates (1975) mapped the area of the Upper Redwood Lodge landslide as containing three preexisting landslide deposits (fig. 4), and two landslides were mapped in this area by Clark and others (1989, with landslide boundaries revised by R.J. McLaughlin and J.C. Clark, 1990; see pl. 3). Bedrock consists of mudstone and sandstone of the Rices Mudstone Member of the San Lorenzo Formation and the Vaqueros Sandstone (see pl. 3). Dips range from steeply southwestward (oblique to slope direction) to vertical.

#### AMAYA RIDGE LANDSLIDE

The Amaya Ridge landslide is on the southwest flank of Amaya Ridge, in the southern part of the study area (area 13, pl. 3). Two sets of ground cracks and associated features are present (fig. 21). The northwestern set consists of a relatively continuous, arcuate zone of ground cracks that are concave downslope in plan view (leg A–A', fig. 21), and a nearly straight compression feature farther downslope (leg B–B', fig. 21). These features are interpreted to be, respectively, the main scarp and toe of a landslide, approximately 120 m long, 240 m wide, and 1.6 ha in area. Measurements across the main scarp indicated local downslope displacements of 8 to 100 cm or more.

Southeast of the landslide is a 300-m-long zone of ground cracks and scarps (line C–C', fig. 21) that is linear to slightly arcuate, parallel, and echelon to the main scarp to the northwest. This southeastern set of ground cracks and scarps may represent the main scarp of a separate landslide, an easterly and upslope extension of the other landslide, or cracks produced by some other process: One displacement measurement across a ground crack in this set indicated movement of 15 to 20 cm downslope, to the

southwest. The area between this set of ground cracks and scarps and the base of the slope is 4.5 ha.

Both sets of ground cracks and scarps (legs A–A', C–C', fig. 21) are near breaks in slope; the slope above them is relatively steep, and the slope below them is a broad, gently sloping bench, 90 m wide. A topographic profile surveyed through the northwestern set of ground cracks and scarps shows an average slope inclination of 22° and an inclination of the steep segment above the scarps of 24°. Marshy areas just below the base of the steep stretch of slope indicate a local water table near the surface.

The northwestern landslide (fig. 4) is in preexisting landslide material, as mapped by Cooper-Clark and Associates (1975), and the southeastern set of ground cracks and scarps closely follows the trace of a landslide scarp shown on their map. Bedrock consists of sandstone and siltstone of the Purisima Formation that dip southwest, generally parallel to the slope direction (see pl. 3).

#### LOWER SCHULTHEIS ROAD WEST LANDSLIDE

The Lower Schultheis Road West landslide is near Laurel, on a short ridge immediately south of Summit Ridge (area 18, pl. 3). The main scarp of the landslide is a 90-m-long series of slightly arcuate cracks and a graben (leg A–A', fig. 22). For part of its length, this main scarp is south of the ridge crest (fig. 23), and so part of the ridge crest is involved in the landslide, having been displaced to the north. Measurements along the scarp showed 30 to 65 cm of northward displacement.

A set of discontinuous ground cracks (leg A'–B, fig. 22) west of the scarp indicates that the landslide may extend an additional 90 m in that direction. These ground cracks also nearly parallel the bedrock strike (see pl. 3), suggesting that they and, by extension, the better developed main scarp to the east probably are structurally controlled. An elongate bulge in the ground about 110 m downslope from the main scarp marks part of the landslide toe (loc. C, fig. 22). The landslide defined by this bulge and the main scarp is at least 110 m long, 110 m wide, and 1.2 ha in area; if the landslide also encompasses the zone of ground cracking to the north and also extends there as far downslope as the bulge, its area may be as large as 2 ha. The slope through the landslide averages 15°–20°.

The area within and adjacent to the Lower Schultheis Road West landslide contains several surface features almost certainly associated with shallow preexisting landslides, and the topography of the ridge and the meadow immediately to the north suggests that deep-seated landslide movements have also occurred in the past. Cooper-Clark and Associates (1975) mapped this area as being within a landslide deposit (fig. 4). Bedrock consists of mudstone and sandstone of the Rices Mudstone Member



of the San Lorenzo Formation, which are overturned steeply northeast or, locally, vertical (see pl. 3).

Subsurface exploration, consisting of direct observations in two 61-cm-diameter boreholes, 4 and 11 m downslope from the main scarp, revealed two shear surfaces (Cole and others, 1991 and this chapter). The shallower shear surface, at 4.9-m depth, consisted of a layer of soft, slickensided clay, 1.2 to 5 cm thick, which sepa-

rated overlying, oxidized material from underlying, unoxidized but intensely fractured rock. The oxidized material consisted of clayey silt containing sandstone and siltstone clasts; the underlying rocks consisted of moderately hard sandstone and siltstone. The deeper shear surface, which was exposed only in the upslope borehole, at 7.3-m depth, consisted of a sheared siltstone interbed within a massive sandstone unit. This shear surface

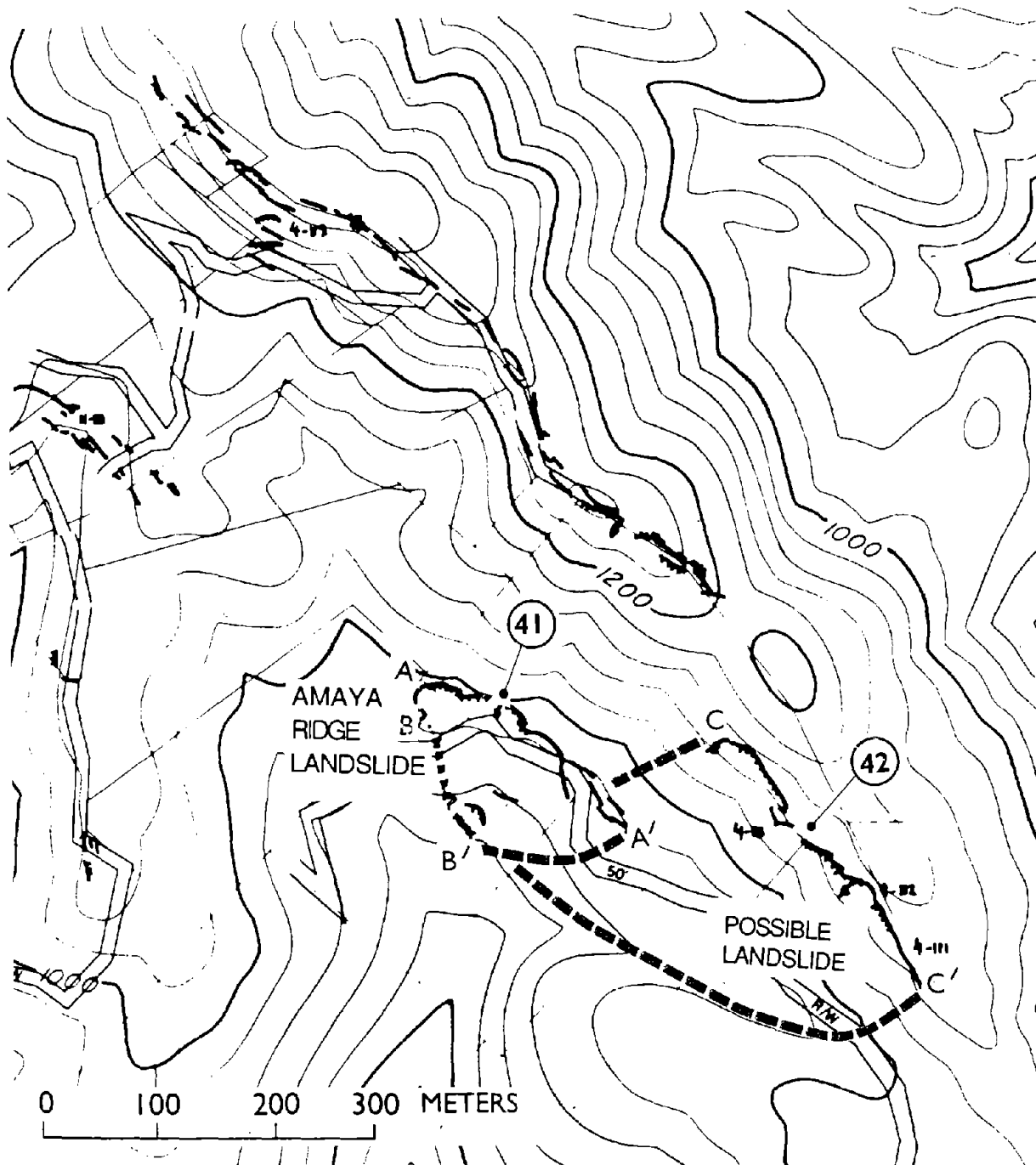


Figure 21.—Amaya Ridge landslide. Ground cracks and compressional features from Spittler and Harp (1990); landslide boundaries from Keefer (1991). See figure 7 for explanation and figure 19 for base-map information.

separated overlying, fractured rock from underlying, unfractured material (Cole and others, 1991 and this chapter).

maximum depth of 29 m, was also reported in the Redwood Estates area in Santa Clara County, about 1.6 km north of the study area (Seed and others, 1990).

### OTHER LARGE LANDSLIDES

The earthquake also caused displacements on nine other large landslides and landslide complexes within the study area (areas 1, 6, 8, 11, 12, 14–17, pl. 3) and on two additional landslides in the Summit Ridge area but outside the study area (areas A, B, pl. 3). Though typically smaller than the landslides described individually above, these 11 landslides had characteristics generally similar to those of the landslides discussed in detail, including (1) boundaries marked by discontinuous cracks and scarps, (2) well developed main scarps and head areas, (3) moderately well-developed flanks, (4) poorly developed toes, (5) involvement of preexisting landslide material, (6) occurrence on slopes of  $15^{\circ}$ – $30^{\circ}$ , (7) displacements of 25 to 79 cm, and (8) association with ground cracks that show evidence of control by bedrock structures. The characteristics of these landslides are summarized in table 3, and detailed maps are shown in figs. 17, 20, 22, and 24 through 28. One additional landslide with similar characteristics, which encompassed an area of about 10 ha and had a

### POSTEARTHQUAKE MONITORING

#### SURFACE MONITORING

A total of 11 landslides and landslide complexes (areas 1–5, 7, 10, 13–15, 17, pl. 3) were monitored for postearthquake displacements from December 1989 through June 1990 and again from December 1990 through July 1991, using surveys of arrays of stakes; three of these landslides (areas 3, 5, 7) were also monitored continuously, using recording strain gages, as described in detail by Griggs and others (1990) and Marshall and Griggs (1991).

#### METHODS

Survey stakes were initially placed in 51 quadrilateral arrays of four stakes each, according to the method of Baum and others (1988). These arrays were placed to span selected cracks and scarps along the heads and flanks of

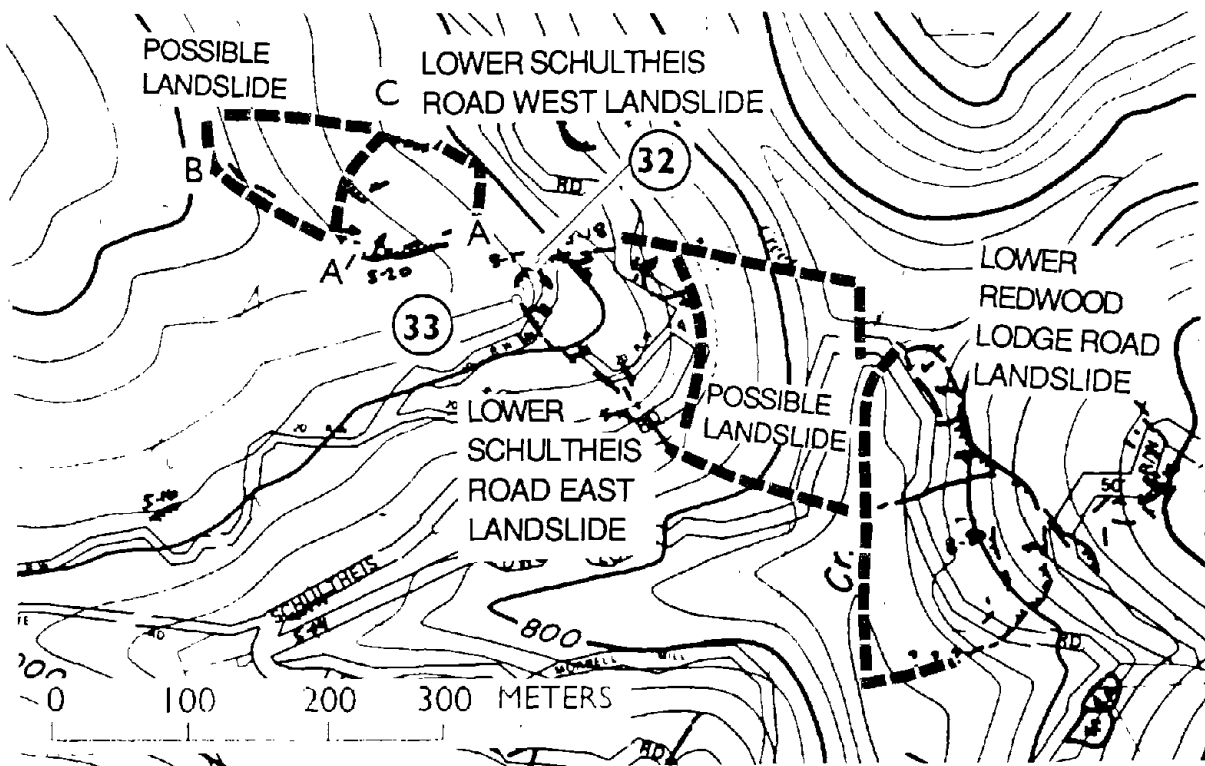


Figure 22.—Lower Redwood Lodge Road, Lower Schultheis Road East, and Lower Schultheis Road West landslides. Ground cracks and compressional features from Spittler and Harp (1990); landslide boundaries from Keefer and others (1991). See figure 7 for explanation and figure 19 for base-map information.

the landslides. The locations of these arrays are shown in figures 7A, 9A, 12A, 17, 20A, 21, 22, 24, and 27. Stakes were set at least 0.5 m away from crack edges; depending on crack size and geometry, distances between stakes were typically from 1 to 3 m, and in some places as much as 7 m. A fiberglass tape was used to measure the distances between stakes, and repeated measurements at control arrays showed a precision of  $\pm 1.0$  cm.

During the first winter after the 1989 Loma Prieta earthquake, arrays were surveyed every 15 to 20 days and after significant rainfall. Of the 51 original quadrilateral arrays, 13 were either damaged, removed, or abandoned before the second winter of monitoring. During this second winter, most of the remaining 38 arrays were checked at least once a month, and as often as once a week during a period of heavy rainfall in March 1991. Two new quadrilateral arrays were installed during the March 1991 storms at sites of renewed cracking on the Upper Schultheis Road and Villa Del Monte landslides.

Four pairs of potentiometer-based strain gages, linked to continuously recording data loggers, were installed across scarps in the Upper Schultheis Road, Villa Del Monte, and Upper Morrell Road landslides (figs. 9A, 12A, 17). Details of strain-gage operation and installation were given by Griggs and others (1990) and Keefer (1991). The data loggers were programmed to record at 30-minute intervals, and displacements were measured with a resolution of  $\pm 0.5$  mm. All four strain-gage systems operated during the first monitoring period, and three (all but the Deerfield Road instrument, fig. 12A) were reinstalled for the second period.

## RESULTS

During the first 7-month monitoring period, from December 1989 through June 1990, no significant displacements that could be related to renewed landslide movement



Figure 23.—Part of main scarp of Lower Schultheis Road West landslide. View eastward from just west of Schultheis Road (loc. A', fig. 22). Ridgecrest to left (north) is involved in landslide.

were recorded at any of the quadrilateral arrays or strain-gage sites. During this period, rainfall was exceptionally low—total rainfall in the Summit Ridge area during the winter of 1989–90 was only about 737 mm, or 67 percent of normal (fig. 2). Thus, the absence of recorded displacements provided no indication about the potential for renewed landslide movement during wetter periods. Quadrilateral arrays and strain gages did record contraction across some cracks and scarps during rainy periods in February and March 1990; this contraction was evidently due to swelling of the near-surface soil as it absorbed moisture.

Rainfall in the area during most of the second winter after the earthquake also was substantially below normal; total rainfall from July 1, 1990, through February 25, 1991, was only 171 mm (table 4). However, the period between

February 26 and March 26, 1991, was exceptionally wet: Approximately 668 mm of rain fell during this 29-day period (table 4). Monitoring of quadrilateral arrays was intensified during this period of heavy rainfall, and displacements were measured on March 5, 15, 19, 25, and 27, after major storms. During this period, the quadrilateral-array data showed cross-crack contractions of 2 to 4 cm across cracks at 12 monitored sites on the Majestic Drive, Upper Schultheis Road, Ralls, Villa Del Monte, and Upper Redwood Lodge landslides and the Old Santa Cruz Highway landslide complex (arrays 3, 5, 10, 11, 14, 21, 30, 37, 46, 52–54, figs. 7A, 9A, 12A, 20A, 24A). Field observations indicated that these contractions were probably caused by swelling of surficial soil as water contents increased (Marshall and Griggs, 1991).

During this period, greater cross-crack contractions of 9 to 14 cm were recorded at array 55 on the Upper Morrell Road landslide (fig. 17) and 15 to 36 cm at array 16 on the Villa Del Monte landslide (fig. 12A). Also during this period, cross-crack extensions of 3 to 7 cm were recorded at array 36 on the Upper Morrell Road landslide (fig. 17), and 3 to 4 cm at array 49 on the Hester Creek North landslide (fig. 27). The cross-crack extension at array 36 and the contraction at array 55 were caused by local slumping of material bordering the cracks (Marshall and Griggs, 1991). The displacements at arrays 16 and 49, as well as other observed displacements that did not disturb survey stakes, were associated with deeper-seated, renewed cracking along and near major scarps formed during the earthquake (Marshall and Griggs, 1991). This renewed cracking along major scarps occurred on the Upper Schultheis Road, Villa Del Monte, and Hester Creek North landslides (areas 3, 5, 14, pl. 3) as discussed below.

#### RENEWED MOVEMENT ON THE UPPER SCHULTHEIS ROAD LANDSLIDE

The first evidence of postearthquake ground cracking related to landslide movement was discovered on March 5, 1991, when new echelon cracks were observed on repaired pavement where Schultheis Road crosses the main scarp of the Upper Schultheis Road landslide (loc. A, fig. 29). The cracks were 1.5 to 3 m long and 1 to 2 cm wide, and showed as much as 2 cm of downslope vertical displacement. Observations on March 15 and 19, after additional rain, revealed increases of 1 to 2 cm in crack widths and vertical displacements, and increases of 0.5 to 1 m in crack lengths (Marshall and Griggs, 1991).

On March 25, a new set of cracks was observed upslope from the main scarp that formed during the earthquake (leg B–B', fig. 29). Because these new cracks did not occur along the traces of the preexisting, earthquake-induced cracks, associated displacements were not detected at nearby quadrilateral arrays 51 or 52 or by the adjacent

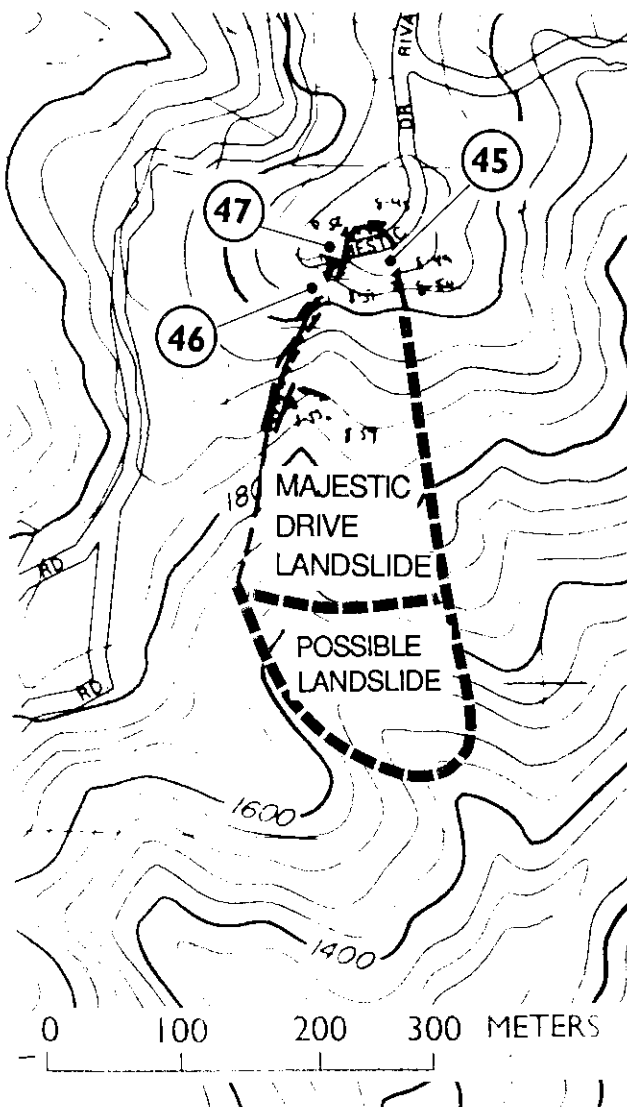


Figure 24.—Majestic Drive landslide. Ground cracks and compressional features from Spittler and Harp (1990); landslide boundaries from Keefer (1991). See figure 7 for explanation and base-map information.

Schultheis strain gage (fig. 29). The new set of cracks extended eastward and southeastward from a point (B, fig. 29) on the earthquake-generated main scarp. From there eastward, a new crack was virtually continuous for about 50 m. This crack was arcuate and concave downslope in plan view, and along part of the crack was a graben, 15 m long, 2 to 3 m wide, and 0.5 m deep, that showed 20 to 30 cm of net vertical displacement between its upslope and downslope margins. Elsewhere, the crack was 5 to 10 cm wide and showed 5 to 10 cm of vertical displacement. Southeast of the continuous crack, shorter echelon cracks continued for an additional 50 m (to loc. B', fig. 29). These shorter cracks were 10 to 20 cm wide and showed

as much as 10 cm of vertical displacement. At several localities upslope from the main scarp, storm runoff was observed flowing into the newly formed cracks on March 25 (Marshall and Griggs, 1991).

A new quadrilateral array (56, figs. 9A, 29) was installed on March 27, 1991, across the newly formed graben. Measurement of this array 2 weeks later, on April 11, showed 3 cm of additional downslope displacement. Subsequent measurements on April 18, 23, and 30, May 8, and July 17 indicated no additional displacements, but field observations during those surveys showed that minor ground cracking had occurred in several places along the main scarp (between locs. A and B, fig. 29).

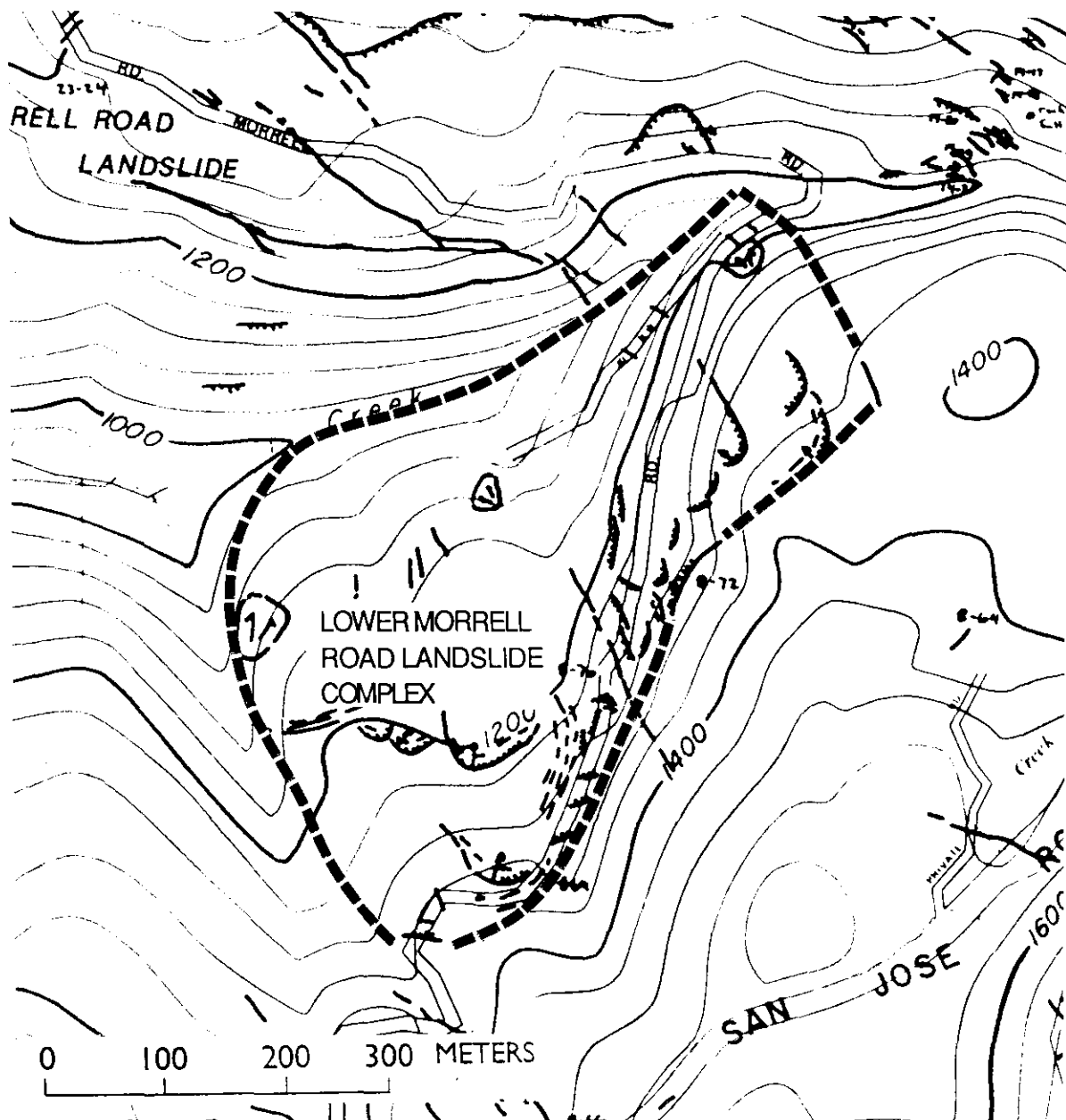


Figure 25.—Lower Morrell Road landslide complex. Ground cracks and compressional features from Spittler and Harp (1990); landslide boundaries from Keefer (1991). See figure 7 for explanation and figure 19 for base-map information.

### RENEWED MOVEMENT ON THE VILLA DEL MONTE LANDSLIDE

Renewed ground cracking and displacement along the major scarp near upper Skyview Terrace was detected on March 19, 1991, when a survey of quadrilateral array 16 (figs. 12, 30), showed 1 to 2 cm of contraction. Field inspection revealed that the contraction was associated with extension across a new crack, less than 1 m upslope from the site (inset, fig. 30). This crack, which formed sometime between March 15 and 19, was 2 to 5 cm wide and showed no vertical displacement. The crack was traceable 10 m eastward from the array, until lost beneath thick vegetation. Small cracks, less than 1 cm wide, also broke the pavement of upper Skyview Terrace near quadrilateral array 16 (point A, fig. 30).

Measurements at quadrilateral array 16 on March 25 revealed additional contractions of 11 to 19 cm. The new crack noted on March 19 appeared to be unchanged, but a larger crack, about 1 m farther upslope, had formed between March 19 and 25. This new crack, 5 to 15 cm wide and showing 5 to 15 cm of downslope vertical displacement, was subparallel to the preexisting scarp

and traceable continuously approximately 40 m eastward. From that point east, a series of shorter cracks were traceable an additional 70 to 80 m. These shorter cracks were 5 to 15 cm wide and showed vertical displacements of as much as 15 cm. The cracks in Skyview Terrace (loc. A, fig. 30) had also become larger by March 25.

On March 27, another new crack was observed, trending obliquely upslope, northeast from the earthquake-generated scarp (inset, fig. 30). This crack, which averaged 5 cm in width and showed as much as 5 cm of vertical displacement, was traceable for 4 m and passed between two of the stakes in quadrilateral array 16 (stakes A, B, inset, fig. 30). The March 27 survey showed 11 cm of cross-crack contraction on the two legs involving stake B (that is, legs B-C, B-D) and no significant change on the two legs involving stake A (that is, legs A-C, A-D). On March 27, a new quadrilateral array (57, figs. 12A, 30) was installed across the new crack observed on March 25 (fig. 30). Subsequent measurements made at both quadrilateral arrays 16 and 57 on April 11, 18, and 23 and May 8, 1991, showed that no additional displacements had occurred.

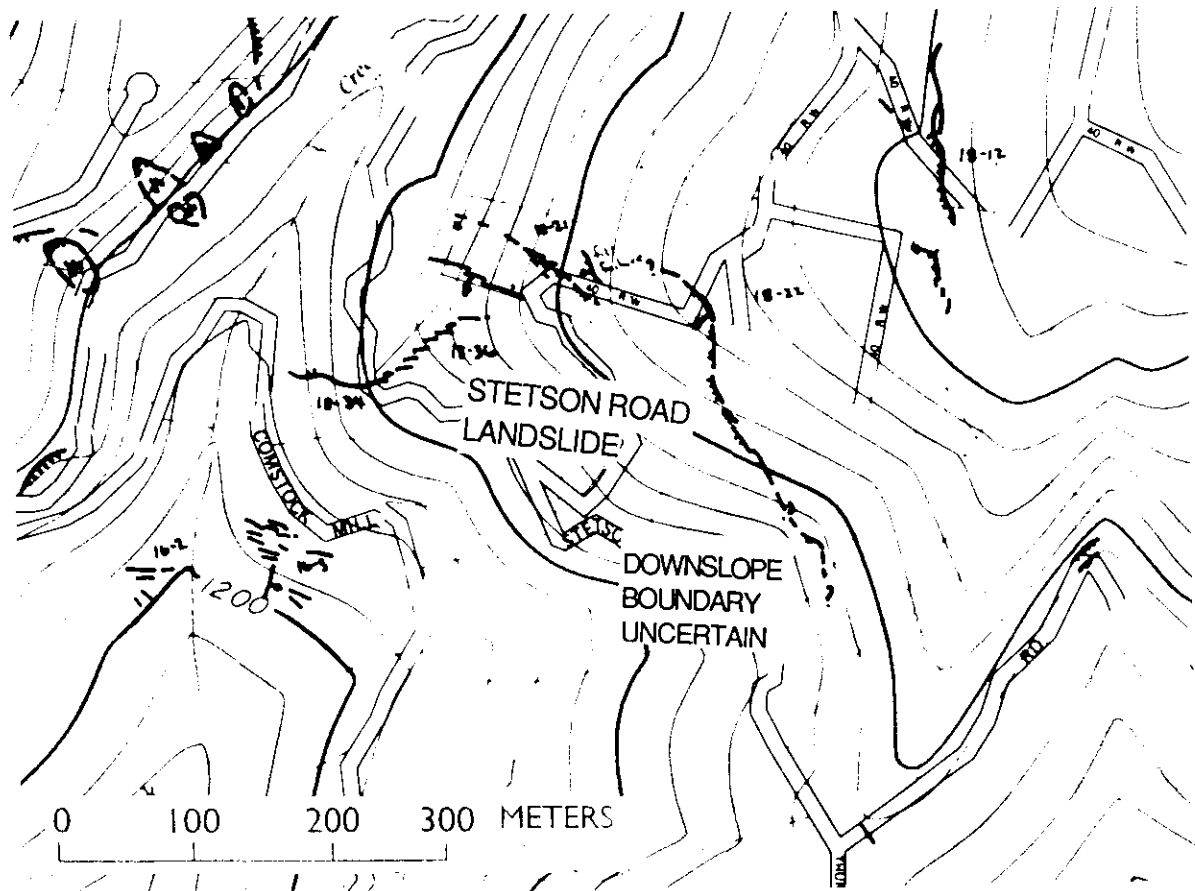


Figure 26.—Stetson Road landslide. Ground cracks and compressional features from Spittler and Harp (1990); landslide boundaries from Keefer (1991). See figure 7 for explanation and figure 19 for base-map information.

### RENEWED MOVEMENT ON THE HESTER CREEK NORTH LANDSLIDE

Renewed displacement was first detected along the main scarp of the Hester Creek North landslide on March 19, 1991. Measurements at quadrilateral array 49 (fig. 27) indicated 2 cm of extension between March 15 and 19,

and on March 25, measurements at the site revealed an additional 2 cm of extension. During the March 25 survey, renewed minor cracking was also observed across the unpaved access road, downslope from quadrilateral array 49 (fig. 27), at both localities where the road crossed the main scarp. Those cracks were 1 to 2 cm wide and showed slight vertical displacements.

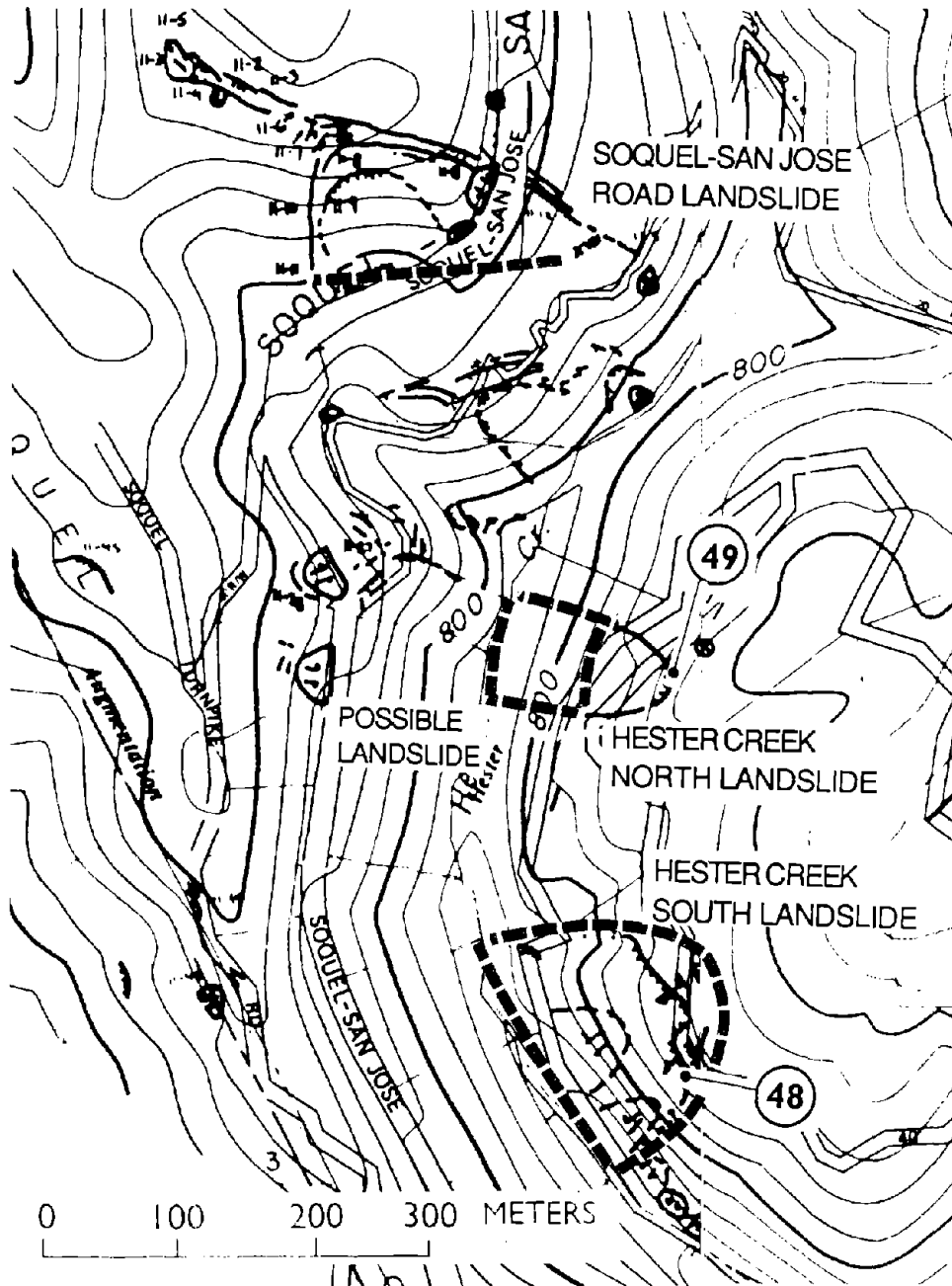


Figure 27.—Hester Creek North, Hester Creek South, and Soquel-San Jose Road landslides. Ground cracks and compressional features from Spittler and Harp (1990); boundaries of Hester Creek North and South landslides from Keefer (1991). See figure 7 for explanation and figure 19 for base-map information.

## SUBSURFACE MONITORING

Subsurface monitoring of postearthquake conditions in the Upper Schultheis Road and Villa Del Monte landslides was carried out by using borehole inclinometers, for measuring subsurface movement, and borehole piezometers, for measuring ground-water levels and pore-water pressures. Piezometers and inclinometers were installed by William Cotton and Associates, Inc.; the instruments and their installation were described in detail by William Cotton and Associates, Inc. (1990), and Keefe (1991).

## INCLINOMETERS

Inclinometer casings were installed in all the small-diameter boreholes in the Upper Schultheis Road and Villa Del Monte landslides except SR-1A, SB-1A, and SB-4A (figs. 9B, 12B; table 5). The inclinometer probe used to monitor vertical deflections in the casings was a SINCO Digitilt Sensor, with a sensitivity of 1 part in 10,000 and a rated system error of less than 6.4 mm of deflection per 30 m of casing.

Initial readings on the inclinometers were taken during the period January–March 1990 as installation was com-

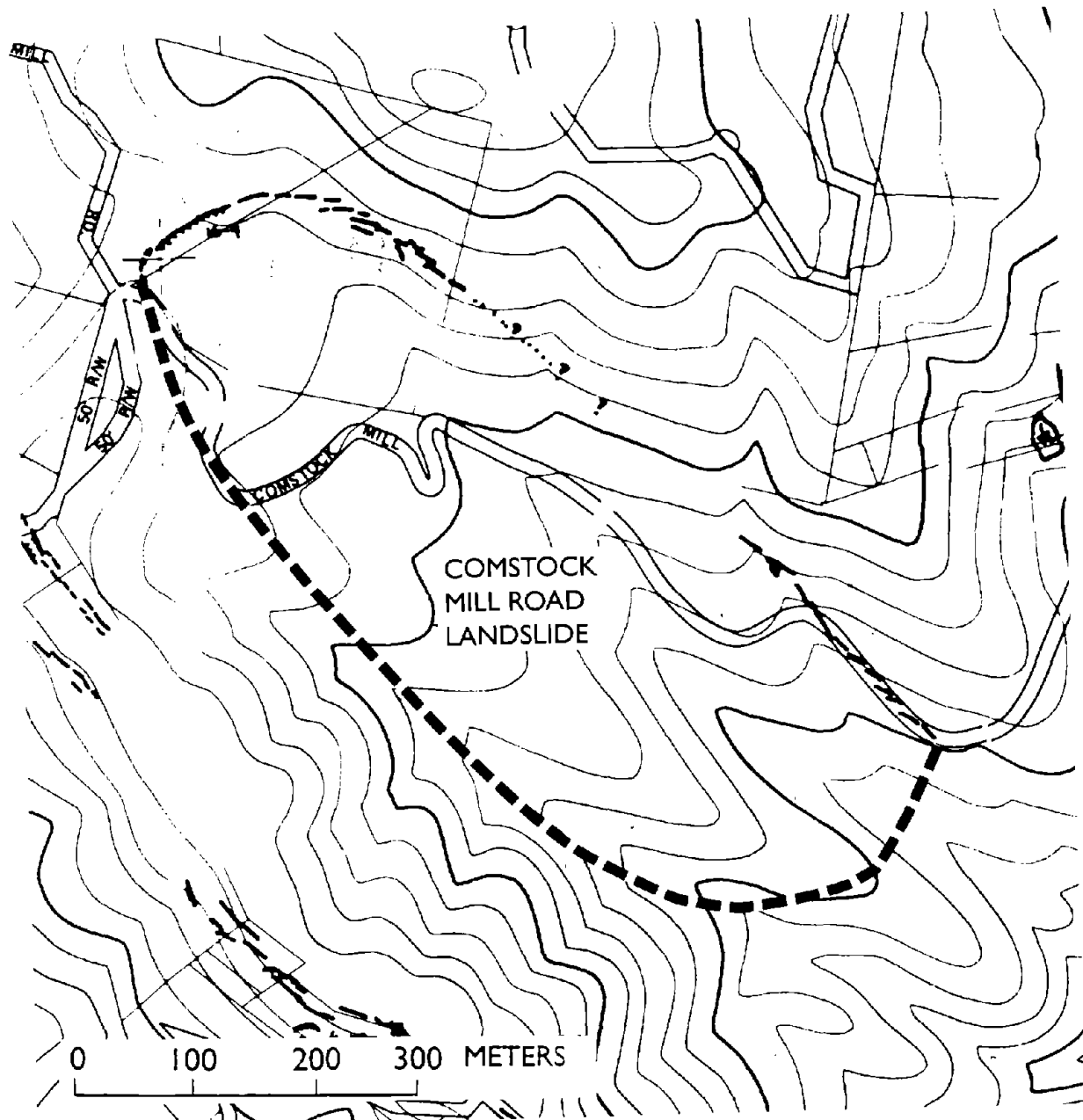


Figure 28.—Comstock Mill Road landslide. Ground cracks and compressional features from Spittler and Harp (1990). See figure 7 for explanation and figure 19 for base-map information.



Table 4.—Rainfall in the area of the Burrell landslide, July 1, 1990–June 30, 1991

Date (1990-91)	Daily rainfall (mm)	Cumulative rainfall (mm)
July 1-Nov. 18		23.6
Nov. 19	.3	23.9
Nov. 20	.5	24.4
Nov. 25	10.2	34.5
Dec. 10	14.5	49.0
Dec. 14	14.0	63.0
Dec. 15	9.7	72.6
Dec. 18	4.8	77.5
Dec. 19	3.8	81.3
Jan. 6	5.3	86.6
Jan. 7	2.3	88.9
Jan. 8	8.1	97.0
Jan. 9	.3	97.3
Feb. 1	25.1	122.4
Feb. 2	25.9	148.3
Feb. 4	22.4	170.7
Feb. 26	1.3	172.0
Feb. 27	54.6	226.6
Feb. 28	42.7	269.2
Mar. 1	16.8	286.0
Mar. 2	55.1	341.1
Mar. 3	134.6	475.7
Mar. 4	28.7	504.4
Mar. 10	22.9	527.3
Mar. 12	27.4	554.7
Mar. 13	1.5	556.3
Mar. 14	2.8	559.1
Mar. 16	25.4	584.5
Mar. 17	46.2	630.7
Mar. 19	25.4	656.1
Mar. 20	10.4	666.5
Mar. 21	3.8	670.3
Mar. 23	27.2	697.5
Mar. 24	96.5	794.0
Mar. 25	34.3	828.3
Mar. 26	9.9	838.2
Apr. 1	4.3	842.5
Apr. 19	11.4	853.9
Apr. 20	2.5	856.5
Apr. 24	.5	857.0
Apr. 30	.8	857.8
May 13	1.3	859.0
June 26	.3	859.3
June 27	5.1	864.4
June 28	16.3	881.4

pleted; subsequent readings were taken in May 1990, November 1990, and March 1991. Between early 1990 and March 1991, these inclinometer measurements recorded only one displacement that exceeded the rated instrument system error; this displacement of 1.3 to 1.9 cm occurred about 15 to 30 m below the surface in borehole DM-4 (figs. 12B, 31). Although this displacement indicated localized postearthquake movement, probably due to small-scale slumping toward the steep creekbank downslope from the instrument, the absence of any other significant displacements indicated that large-scale reactivation of the monitored landslides did not occur. Full records of the inclinometer measurements were presented by Keefer (1991).

### PIEZOMETERS

The piezometers installed in most boreholes were continuously recording electronic-strain-gage Thor model DPXE instruments with a pressure range of 690 kPa and an overrange capacity of 1.5×. The piezometers were installed in canvas bags, which were filled with sand, secured onto the outside of the inclinometer casings, and sealed with the relatively impermeable grout used to emplace the inclinometer casings. Three such piezometers were installed in all boreholes except SR-1A, SB-1A, and SB-4A at depths ranging from 10.7 to 88.1 m (tables 5, 6).

To monitor the performance of the strain-gage piezometers, Casagrande open-standpipe piezometers were installed at two depths each in boreholes SR-1A and SB-1A and at depths near the intermediate strain-gage piezometer tips in boreholes DM-1, DM-3, SB-2, SB-3, SR-3, and SR-4 (table 5). Data from these Casagrande piezometers generally agreed well with those from the adjacent strain-gage piezometers (Keefer, 1991).

In all the boreholes, ground-water levels were progressively deeper, as measured by the deeper piezometer tips (table 6); differences in ground-water levels among the various boreholes also indicated a complex hydraulic regime. Within the Upper Schultheis Road landslide, the highest ground-water levels as measured by shallow piezometers were at 8.5- to 20-m depth; comparable measurements were 3.4- to 30-m depth as measured by intermediate-depth piezometers and 5.1- to 49-m depth as measured by deep piezometers. In the Villa Del Monte landslide, the highest ground-water levels were at 0.3- to 20-m depth as measured by shallow piezometers, 4.5- to 30-m depth as measured by intermediate-depth piezometers, and 13- to 42-m depth as measured by deep piezometers (table 6).

Ground-water levels were relatively constant throughout most of the monitoring period but rose significantly in response to the period of heavy rainfall in spring

1991 (figs. 32, 33; table 6). The dates and times of rise in ground-water levels due to the spring 1991 rains are listed in table 7. These times reflect a relatively rapid ground-water response to the rainfall, particularly to that in February and early March. Complete plots of the piezometric records were presented by Keefer (1991).

### DISCUSSION AND CONCLUSIONS

The landslides in the Summit Ridge area were larger and more complex than virtually all other landslides triggered by the 1989 Loma Prieta earthquake (Keefer and Manson, this chapter) or by other historical earthquakes of comparable magnitude (Keefer, 1984). The occurrence

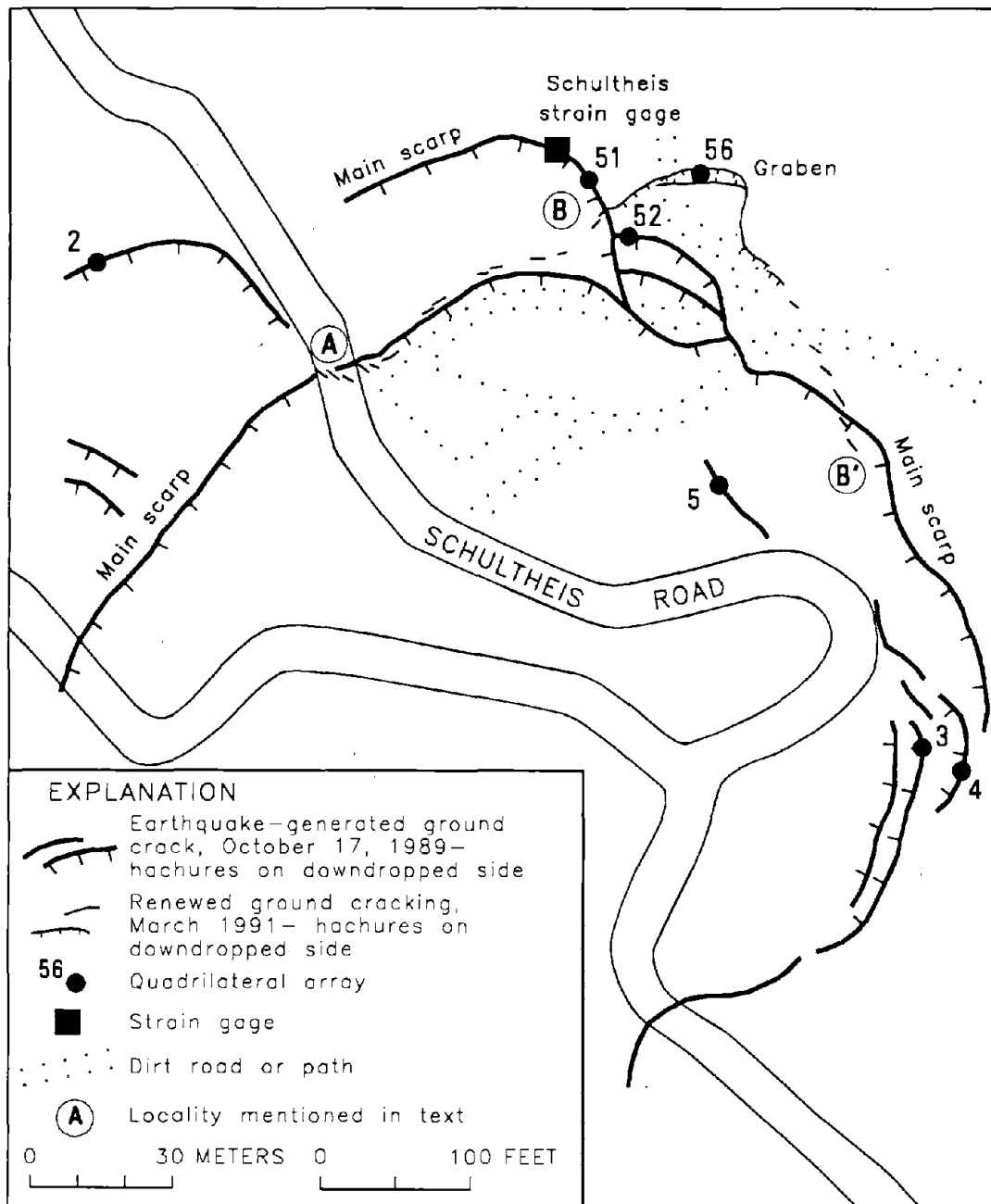


Figure 29.—Area around main scarp of Upper Schultheis Road landslide, showing ground cracks and scarps that resulted from earthquake; ground cracks, scarps, and grabens formed during period of heavy rainfall in March 1991; and locations of quadrilateral arrays and strain gage.

of these landslides only in the Summit Ridge area indicates that their formation was related to specific seismic and (or) geologic conditions there. Among those conditions is the proximity of the landslides to the trace of the San Andreas fault. All of these landslides are within 4.1 km of the fault trace, and all of those larger than 10 ha in area are within 1.8 km of the fault trace (fig. 34). In addition, although the data plotted in figure 34 show considerable scatter, a generally inverse relation between landslide area and distance from the fault trace is evident.

The occurrence of these large landslides only near the San Andreas fault could correlate with exceptionally strong near-field shaking that attenuated rapidly with distance away from the fault. Eyewitness accounts and other evidence of such effects as the snapping of redwood trees, movement of vehicles and other heavy objects, and major shaking damage to residences imply locally severe ground shaking. The Corralitos strong-motion station, 12 km

southeast of the study area and 200 m from the fault (fig. 1), recorded a moderately high peak acceleration of 0.64 g (Shakal and others, 1989) and a moderately high Arias intensity of 4.0. Shaking could have been even more severe in the Summit Ridge area. The absence of strong-motion recordings in that area preclude direct verification of this hypothesis; however, from a study of 20 strong-motion records, Beroza (1991) concluded that an area of concentrated fault slip was centered 7 km northwest of the hypocenter, nearly under the Summit Ridge area. Such concentrated slip could presumably cause anomalously strong shaking.

The Summit Ridge area was also in the region of maximum tectonic ground deformation, as determined by geodetic analysis of surface uplift and mapping of off-fault ground cracking. The maximum measured coseismic uplift of 592 mm was near the south boundary of the study area, and uplift within the study area itself ranged from

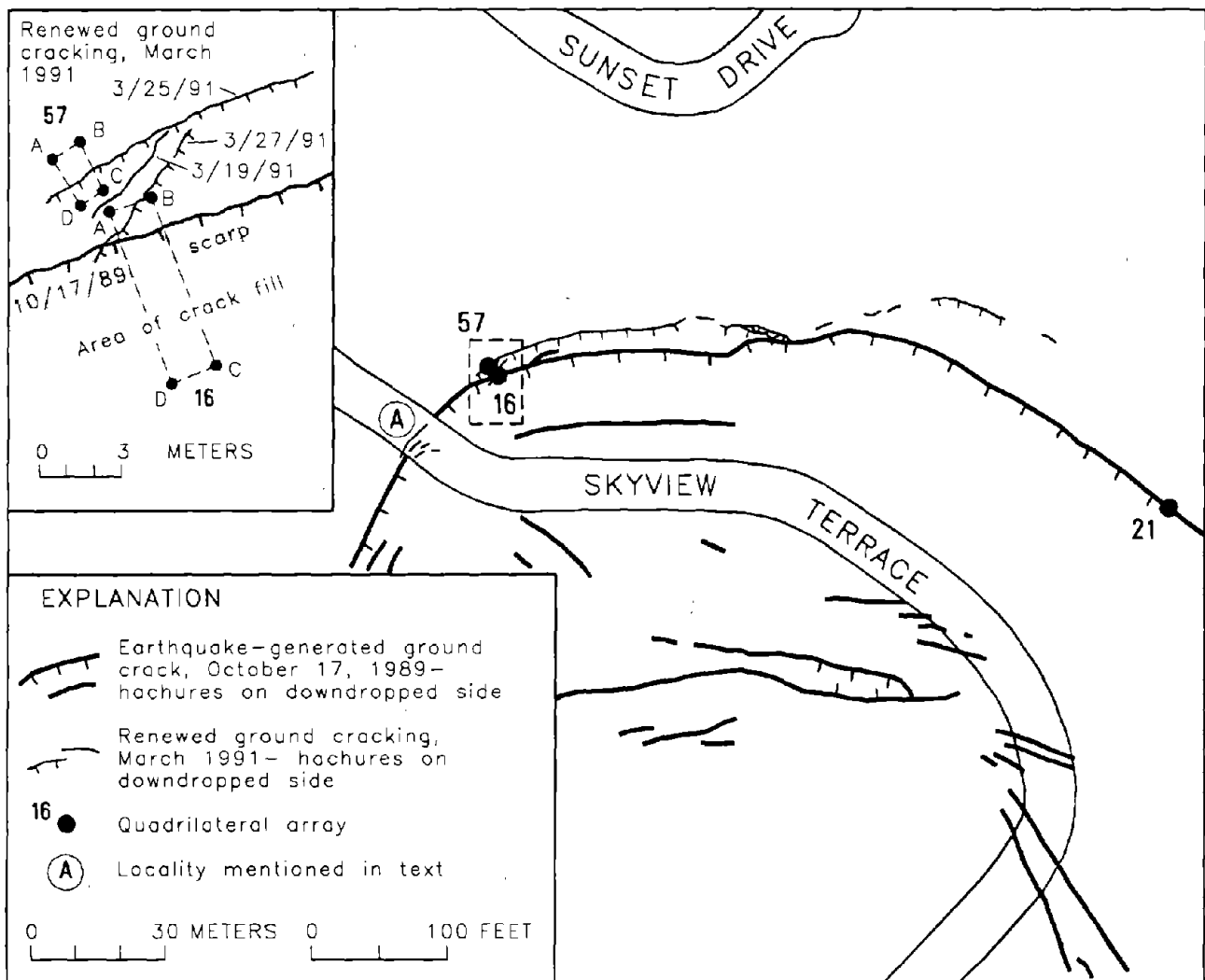


Figure 30.—Area around part of upper Skyview Terrace on Villa Del Monte landslide, showing ground cracks and scarps that resulted from earthquake; ground cracks and scarps formed during period of heavy rainfall in March 1991; and locations of quadrilateral arrays.

Table 5.—General information on boreholes drilled in the Upper Schultheis Road and Villa Del Monte landslides

[Do., ditto]

Borehole	Total depth (m)	Date (1989-90)		Drilled by	Depth of inclinometer casing (m)	Date of initial inclinometer reading	Piezometer depths (m)			Casagrande
		Start	Finish				Shallow	Inter-mediate	Deep	
SR-1	62.0	12/18	12/22	Pitcher-----	61	1/8/90	12	24.2	60.4	
SR-1A	25.0	12/29	01/02	---do-----	--	--	--	--	--	11.6, 23.5
SR-2	46.8	01/03	01/05	---do-----	46	1/9/90	21.2	30.3	45.6	--
SR-3	75.6	01/08	01/02	---do-----	76	3/19/90	18.2	51.7	73.2	55.3
SR-4	76.2	01/29	03/13	---do-----	74	2/1/90	20.1	35.4	53.6	35.4
ED-1	63.4	01/17	01/23	---do-----	61	3/8/90	15.1	28.8	60.7	--
ED-2	61.6	01/23	01/30	---do-----	61	1/12/90	16.8	33.4	60.8	--
SD-1	61.9	01/04	01/10	---do-----	61	1/12/90	11.8	29	57.5	--
DM-1	43.0	01/29	01/31	All Terrain-----	43	3/14/90	12	18.6	42.5	18.6
DM-2	62.5	01/15	01/23	Pitcher-----	61	2/27/90	21.2	36.4	60.8	--
DM-3	76.2	01/30	03/09	---do-----	76	3/14/90	18.3	36.6	76.2	36.6
DM-4	77.1	01/18	01/25	All Terrain-----	76	2/14/90	21.3	39.6	76.2	--
SB-1	62.2	12/21	12/30	Pitcher-----	61	1/9/90	11.6	27.4	39.6	--
SB-1A	30.5	01/02	01/03	---do-----	--	--	--	--	--	11.2, 27.3
SB-2	89.0	01/02	01/10	All Terrain-----	88	3/13/90	21.2	45.6	88.1	45.7
SB-3	92.4	01/10	01/18	---do-----	91	3/13/90	21.2	42.5	66.9	42.1
SB-4	47.2	01/11	01/12	Pitcher-----	46	3/1/90	10.6	21.2	45.6	--
SB-4A	6.1	01/15	01/15	---do-----	--	--	--	--	--	--

about 100 to slightly less than 592 mm (fig. 35; Marshall and others, 1991). The Summit Ridge area also had the highest concentration of ground cracks produced by the earthquake (see pl. 3; Spittler and Harp, 1990; Ponti and Wells, 1991). Within the area, ground cracks were most abundant along the south flank of Summit Ridge, where most of the largest landslides occurred.

The coseismic ground cracks evidently formed parallel to elements of the bedrock structure, such as bedding planes, joint surfaces, and faults; their orientations are generally consistent with tectonic extension across the crest of the uplifted hanging-wall block, but most of them also exhibit displacements indicating extension due to gravitational, downslope movement (Ponti and Wells, 1991). The relation of ground cracks to the large landslides is demonstrated in detail by the many specific examples of structurally controlled ground cracks forming landslide boundaries and other landslide elements described above, by Keefer (1991), and by Harp (this chapter). This evidence indicates that although many ground cracks were produced directly by tectonic deformation, by the initial effects of seismic shaking on preexisting planes of weakness, or both, once these cracks formed, they then served as loci around which continued shaking caused downslope movement and landsliding. This mechanism of landslide formation is consistent with the highly irregular shapes and typically discontinuous boundaries of the landslides and with the restriction of these landslides to the Summit Ridge area; other areas that had no significant numbers of ground cracks also produced no large landslides.

Within the Summit Ridge area, all but one of the largest landslides occurred along the southwest flank of Summit Ridge itself (see pl. 3). That part of the area, which is generally nearest the San Andreas fault, also has the most complex geologic structure, as evidenced by overturned, tightly folded bedding and numerous subsidiary faults. Because of this complex structure, subsurface shear zones and other planes of weakness probably are most common under that part of the area, which, as noted above, also had the highest concentration of ground cracks.

Among the bedrock units in the study area, the Vaqueros Sandstone was most involved in landsliding: earthquake-induced landslides covered about 51 percent of the area underlain by this unit (table 8), in comparison with 26 percent for the Rices Mudstone Member of the San Lorenzo Formation, 18 percent for the Butano Sandstone, 10 percent for the Twobar Shale Member of the San Lorenzo Formation, 6 percent for the Purisima Formation, and 0 percent for the Lambert Shale. The Vaqueros Sandstone, Rices Mudstone Member, Butano Sandstone, and Twobar Shale Member were sampled during drilling in the upper Schultheis Road and Villa Del Monte areas. For those units, some correlation exists between the abundance of shale and the percentage of area involved in landsliding (table 8): The Vaqueros Sandstone contained the most shale (33 percent), the Twobar Shale Member the least (3 percent), and the Rices Mudstone Member and Butano Sandstone intermediate amounts (20 and 29 percent, respectively). Neither the Purisima Formation nor the Lambert Shale was sampled. The Lambert Shale un-

derlies only a small part of the study area; however, the Purisima Formation is more extensive and is described as being relatively poorly consolidated (Clark and others, 1989). The relatively small percentage of area involved in landsliding on this unit is probably due to its occurrence in the study area farther away from the San Andreas fault than the other units, to its lesser structural complexity, and to the relatively low concentration of coseismic ground cracks in that part of the study area.

A high correlation exists between the locations of large landslides triggered by the 1989 Loma Prieta earthquake and mapped, preexisting landslide deposits (fig. 4; table 3). Of the 20 large landslides in and near the study area, 18 were partly or completely within areas mapped as preexisting landslide deposits (Cooper-Clark and Associates, 1975), and virtually all of the earthquake-generated landslides examined in the field also exhibited clear geomorphic evidence of previous movement. Additional evidence of recurrent movement of the landslides comes from trenching studies, discussed by Keefer (1991) and Nolan and Weber (this chapter). Thus, the earthquake largely reactivated preexisting landslide material in the Summit Ridge area.

Landslide occurrence and direction of movement did not generally correlate with the dip of bedding. Of the 20 large landslides, 8 moved in directions opposite to the dip, 7 moved in directions oblique to the dip, and only 5 possibly moved generally in the same direction as the dip (table 3). Along the southwest flank of Summit Ridge, in particular, in the area of the largest landslides, bedding most commonly dips northeast or is overturned to the northeast, into the slope (see pl. 3). Thus, the other conditions discussed above evidently were more significant than the dip of bedding in determining where large landslides formed.

The distinctive surface morphology of the large landslides in the Summit Ridge area is probably due in part to earthquake-induced displacements that were small relative to the landslide lengths. Typically, landslide heads and main scarps were relatively well developed, flanks were moderately well developed, and toes were poorly defined by surface features. Such morphology is consistent with small displacements and longitudinal strains (defined as the ratio of displacement to landslide length), whereby extensional displacements in the head of a landslide may be accommodated by distributed internal compression downslope, so that little or no actual displacement of the landslide toe may occur. This process is illustrated for a longitudinal strain of 0.2 percent in figure 36. Longitudinal strains calculated for the landslides in the Summit Ridge area ranged from 0.05 to 0.83 percent (table 3).

With increasing longitudinal strain, landslide features, particularly those in the landslide toes, should be more fully formed. The relation between longitudinal strain and the formation of surface features across toes for the landslides in the Summit Ridge area is plotted in figure 37. Half of the landslides exhibited no mapped pressure ridges or other features marking the toes; however, the toe features observed on other landslides were typically small, and so many toe features could have been hidden in heavily vegetated terrain. For those landslides where toe features were mapped, the data show a trend of increasing development of toe features with increasing longitudinal strain.

The landslide materials themselves were heterogeneous and composed of generally thick layers of colluvium and varyingly sheared and weathered sandstone, siltstone, and shale bedrock. Basal shear surfaces were identified in boreholes at depths ranging from about 5 to 27 m, and other data from boreholes and from undamaged water wells suggests that some basal shears may be more than 100 m deep. The identified basal shears consisted of (1) a zone of sheared material, 30 cm thick, containing highly plastic clay, silty clay, sandstone, and fractured shale and a basal layer, 0.5 to 1.3 cm thick, of sheared silty clay and clayey silt; (2) a 5- to 10-cm-thick layer of swelling, clayey siltstone separating oxidized from unoxidized materials; (3) a 2.5- to 5-cm-thick layer of soft, slickensided clay separating oxidized from unoxidized rock; and (4) a sheared

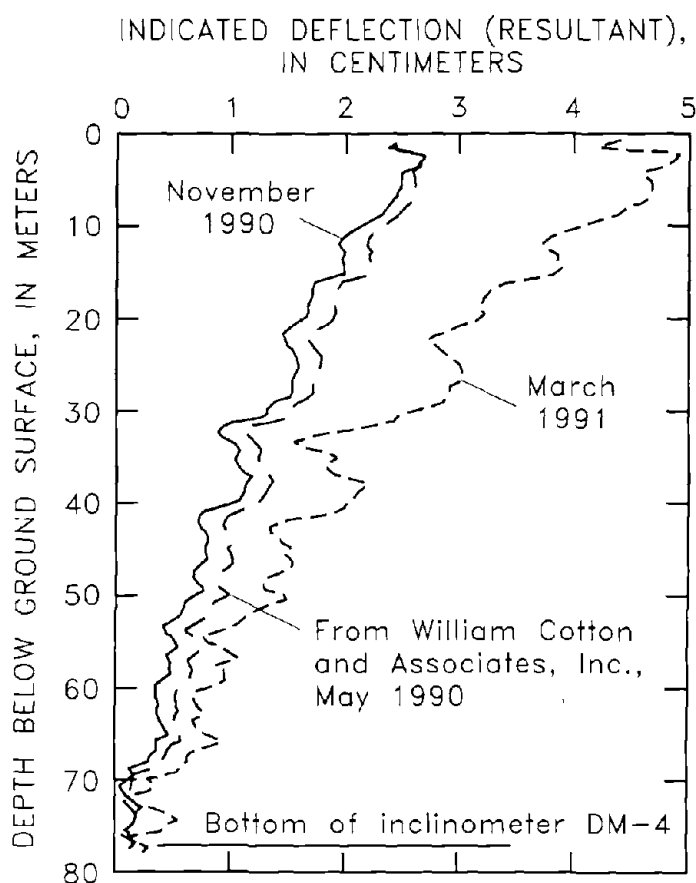


Figure 31.—Deflections measured by inclinometer in borehole DM-4 on Villa Del Monte landslide (see fig. 12B for location).

Table 6.—Piezometric data on the Upper Schultheis Road and Villa Del Monte landslides

[n.d., no data; do., ditto]

Borehole	Piezometer depth	Surface elevation (m)	Elevation of highest ground-water level (m)	Depth of piezometer tip (m)	Depth of highest ground-water level (m)	Fluctuation in ground-water level during Spring 1991 (m)
DM-1	Shallow-----	486.7	482.5	12.0	4.2	1.7
DM-2	---do-----	460.9	447.1	21.2	13.8	2.7
DM-3	---do-----	425.2	410.3	18.3	14.9	4.3
DM-4	---do-----	332.4	312.4	21.3	20.0	.0
ED-1	---do-----	439.5	424.0	15.1	15.5	.0
ED-2	---do-----	420.3	406.9	16.8	13.4	1.5
SB-1	---do-----	435.3	434.9	11.6	.3	2.1
SB-2	---do-----	321.4	309.7	21.2	11.8	.9
SB-3	---do-----	385.2	n.d.	21.2	n.d.	n.d.
SB-4	---do-----	470.3	469.1	10.7	1.2	1.5
SD-1	---do-----	470.6	470.3	11.8	.3	4.0
DM-1	Intermediate-----	486.7	476.7	18.6	10.0	1.6
DM-2	---do-----	460.9	431.3	36.4	29.7	.3
DM-3	---do-----	425.2	406.3	36.6	18.9	2.7
DM-4	---do-----	332.4	303.7	39.6	28.7	-1.2
ED-1	---do-----	439.5	415.1	28.8	24.3	2.4
ED-2	---do-----	420.3	406.9	33.4	13.4	.0
SB-1	---do-----	435.3	420.9	27.4	14.4	.6
SB-2	---do-----	321.4	293.2	45.6	28.2	.6
SB-3	---do-----	385.2	375.8	42.5	9.4	2.1
SB-4	---do-----	470.3	465.7	21.2	4.5	2.4
SD-1	---do-----	470.6	465.6	29.0	5.0	3.5
DM-1	Deep-----	486.7	468.5	42.5	18.2	.3
DM-2	---do-----	460.9	419.1	60.8	41.8	-3.0
DM-3	---do-----	425.2	385.6	76.2	39.6	.0
DM-4	---do-----	332.4	n.d.	76.2	n.d.	n.d.
ED-1	---do-----	439.5	414.5	60.7	24.9	n.d.
ED-2	---do-----	420.3	405.4	60.8	14.9	2.1
SB-1	---do-----	435.3	395.3	39.6	40.0	.9
SB-2	---do-----	321.4	283.5	88.1	38.0	.3
SB-3	---do-----	385.2	372.5	66.9	12.7	1.5
SB-4	---do-----	470.3	452.0	45.6	18.3	2.7
SD-1	---do-----	470.6	445.6	57.5	25.0	3.7
SR-1	Shallow-----	441.4	430.7	12.0	10.8	.9
SR-2	---do-----	412.0	n.d.	21.2	n.d.	n.d.
SR-3	---do-----	413.8	405.4	18.1	8.4	6.1
SR-4	---do-----	390.3	370.3	20.1	20.0	.0
SR-1	Intermediate-----	441.4	429.8	24.2	11.7	3.0
SR-2	---do-----	412.0	408.7	30.3	3.3	1.8
SR-3	---do-----	413.8	396.2	51.7	17.6	1.5
SR-4	---do-----	390.3	360.3	35.4	30.1	.0
SR-1	Deep-----	441.4	425.5	60.4	15.9	2.4
SR-2	---do-----	412.0	406.9	45.6	5.1	.6
SR-3	---do-----	413.8	390.8	73.2	23.1	.6
SR-4	---do-----	390.3	341.4	53.6	49.0	.6

siltstone interbedded with a massive sandstone (Cole and others, 1991 and this chapter). No simple relation between geologic materials, stratigraphy, or local structure and the formation of basal shear surfaces was evident. Two of the

basal shears evidently separated weathered material from bedrock, and two were within the bedrock itself.

Two shear surfaces each were documented under the Upper Schultheis Road and Lower Schultheis Road West

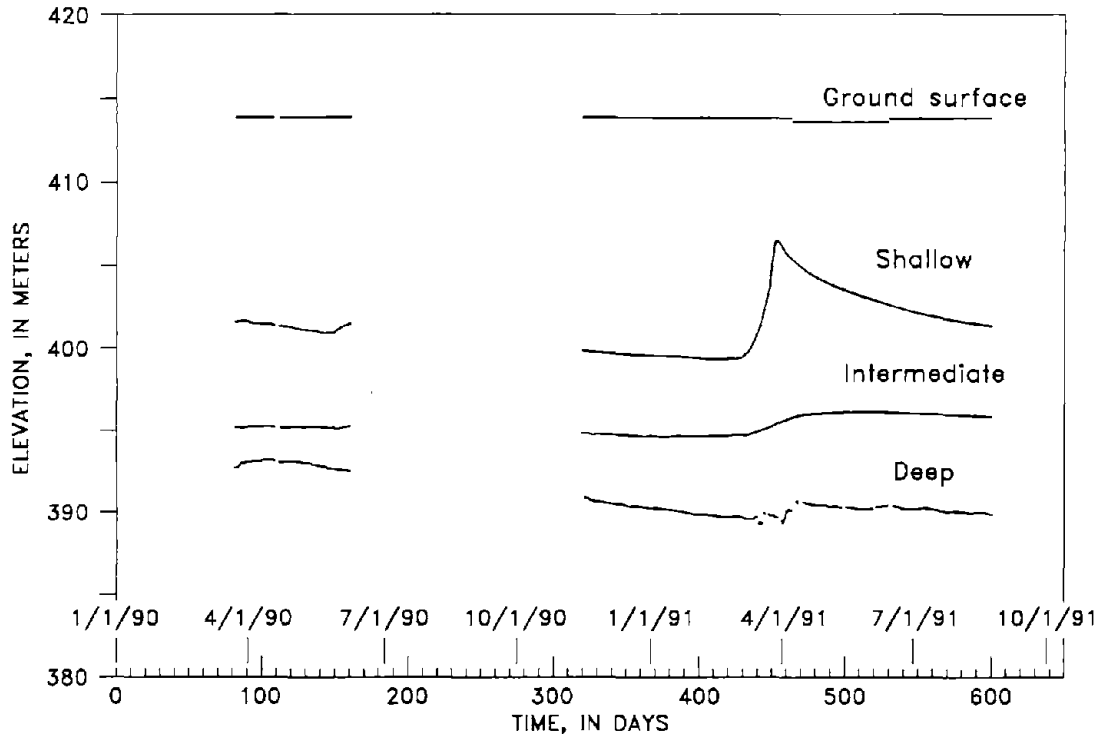


Figure 32.—Elevation of piezometric surface versus time for piezometers in borehole SR-3 on Upper Schultheis Road landslide (see fig. 9B for location).

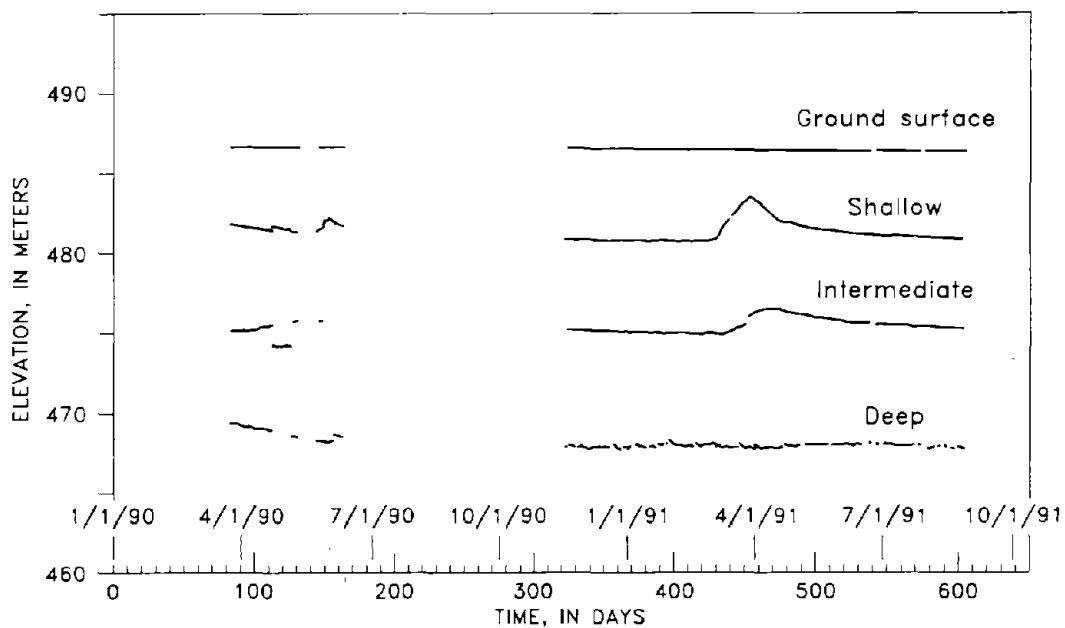


Figure 33.—Elevation of piezometric surface versus time for piezometers in borehole DM-1 on Villa Del Monte landslide (see fig. 12B for location).

Table 7.—Rises in ground-water level in response to rainfall, February–March 1991

Piezometer Depth	Date of Initial Rise (1991)		Amount of Rise (m)	
	Range	Average	Range	Average
Shallow-----	Feb. 24 to Mar. 4	Mar. 1	0-6.1	1.7
Intermediate-----	Feb. 26 to Apr. 10	Mar. 7-8	-1.2 to 3.5	1.3
Deep-----	Feb. 4 to Apr. 20	Mar. 6	-3.0 to 3.7	.9

landslides (William Cotton and Associates, Inc., 1990; Cole and others, 1991 and this chapter). Additionally, bore-hole data from the Villa Del Monte landslide and the distribution of well damage there and elsewhere suggests (1) that multiple shear surfaces could exist under other landslides as well and (2) that the degree of development of shear surfaces varied locally. In particular, the absence of reported well damage within some landslide areas suggests that local basal shear displacements were small, distributed over a broad range of depths, or both.

Direct comparisons between the large landslides generated by the 1989 Loma Prieta earthquake and the landslides triggered or reactivated by the 1906 San Francisco earthquake are difficult because of the incomplete descrip-

tions and imprecise locations in reports on the 1906 earthquake. However, those reports do suggest that landslide activity in and around the Summit Ridge area was more widespread and severe in 1906 than in 1989 (table 1). The greater landslide activity in 1906 is consistent with at least two major differences in conditions: (1) the 1906 earthquake ( $M=8.2-8.3$ ) was much larger than the 1989 earthquake ( $M_S=7.1$ ); and (2) rainfall was heavier before the 1906 earthquake, and so ground-water levels were presumably higher than in 1989 (Youd and Hoose, 1978; Schuster and others, this chapter).

Surface and subsurface monitoring of selected landslides in the Summit Ridge area showed no significant postearthquake displacements during the unusually dry period from December 1989 through late February 1991. Precipitation of 668 mm during late February and March 1991 did trigger localized ground cracking and displacements near the main scarps of the Upper Schultheis Road, Hester Creek North, and Villa Del Monte landslides. The maximum movement recorded across ground cracks and (or) surface-monitoring arrays was 13 to 20 cm. The ground cracking and displacement were probably due to local upslope migration, or retrogressive failure, of the landslide heads, a process that could continue through subsequent periods of heavy rainfall.

The period of heavy rainfall and observed landslide cracking in February and March 1991 coincided with a period of rising ground-water levels, as monitored by piezometers in the upper Schultheis Road and Villa Del Monte areas. Ground-water levels measured by individual piezometers during this period rose as much as 6.1 m from February through April. The average rise in ground-water level was 1.7 m as measured by shallow piezometers, 1.3 m as measured by intermediate-depth piezometers, and 0.9 m as measured by deep piezometers. These rises in ground-water level were associated with a month-long period of heavy rainfall, which occurred after a much longer (5 year) period of exceptionally light rainfall. Although these data show that significant changes in ground-water levels are possible within these slopes as a

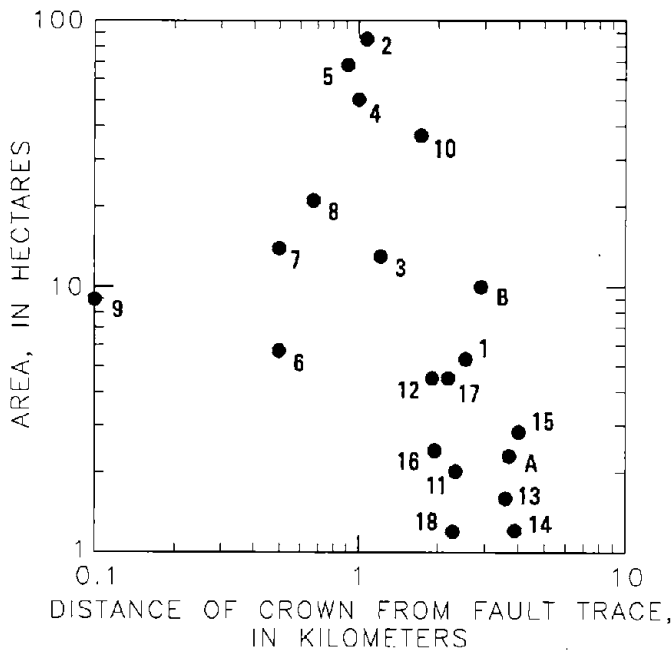


Figure 34.—Area of landslide versus distance from landslide crowns to surface trace of San Andreas fault. Letters and numbers refer to landslides mapped on plate 3 and listed in table 3.



result of rainfall, extrapolation to other short- or long-term rainfall cycles requires additional data and analysis.

The dry ground conditions before and during the 1989 Loma Prieta earthquake almost certainly limited the extent and severity of landsliding. If the earthquake had occurred under wetter conditions, when ground-water levels in slopes were higher, many additional areas of coseismic ground cracks that exhibited small downslope displacements would probably have developed additional landslides. A larger earthquake under wetter conditions would probably produce much more severe and extensive landsliding in the Summit Ridge area, as evidently occurred during the 1906 earthquake.

The inferred mechanism for landslide formation in the Summit Ridge area, with initiation associated with coseismic ground cracks, implies that such landslides are specifically generated by earthquakes. This inference is

supported both by the historical record and by slope-stability analyses of the Upper Schultheis Road and Villa Del Monte landslides. The historical record indicates that although landslides are commonly triggered by intense or long-duration rainfall in the area, such landslides are much smaller, shallower features, primarily debris flows and less complex slumps and block slides. Slope-stability analyses, as described in detail by Keefer (1991), indicate that (1) deep-seated basal shear surfaces of large areal extent are the most unstable under seismic conditions and (2) shallower shear surfaces of more limited areal extent are the most unstable under conditions of rising ground-water levels in the absence of seismic shaking. Thus, the large landslides in the Summit Ridge area probably are uniquely earthquake related, and, in this area, such earthquake-generated landslides are probably major recurring hazards and significant agents of landscape evolution.

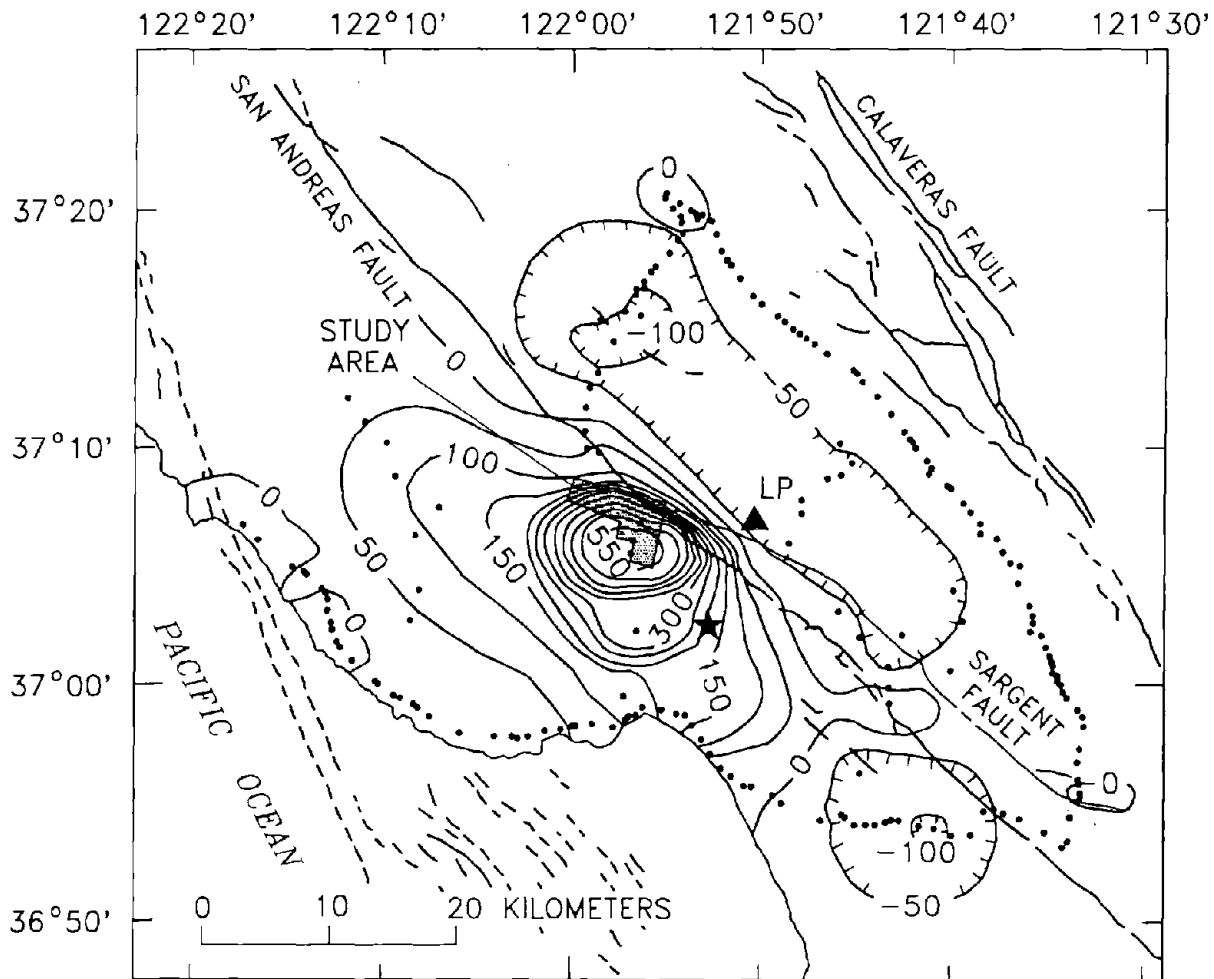


Figure 35.—Loma Prieta area, showing contours of coseismic uplift and subsidence caused by 1989 earthquake (from Marshall and others, 1991). Star, earthquake epicenter; triangle LP, geodetic station on Loma Prieta; dots, bench-mark locations; irregular thin lines, faults (dashed where approximately located, dotted where concealed). Contour interval, 50 mm; subsidence contours hachured.

Table 8.—Percentage of areas and shale in geologic units involved in landslides

[Percentage of area is based on ratio of area of landslides within unit to total mapped area of unit in study area. Percentage of shale is based on ratio of total length of shale to total length of unit in boreholes drilled in the Upper Schulteis Road and Villa Del Monte areas; drilling logs from William Cotton and Associates, Inc. (1990). n.d., not determined]

Geologic unit	Percentage of area involved in landsliding	Percent shale (percent)
Vaqueros Sandstone-----	51	33
Rices Mudstone Member of the San Lorenzo Formation-----	26	20
Butano Sandstone-----	18	29
Twobar Shale Member of the San Lorenzo Formation-----	10	3
Purisima Formation-----	6	n.d.
Lambert Shale-----	0	n.d.

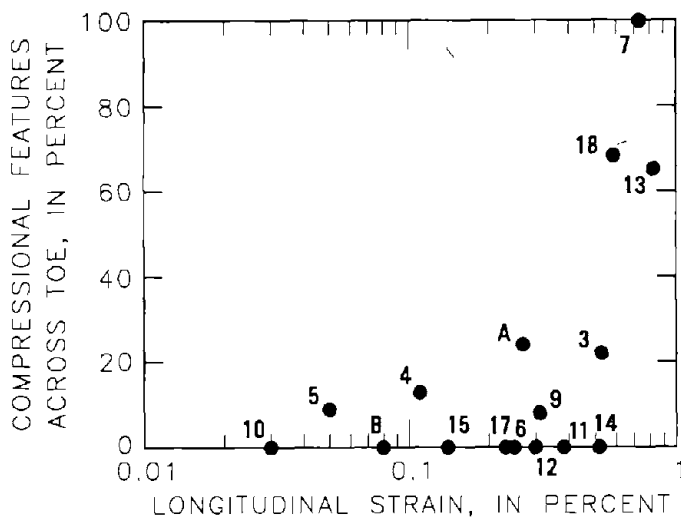
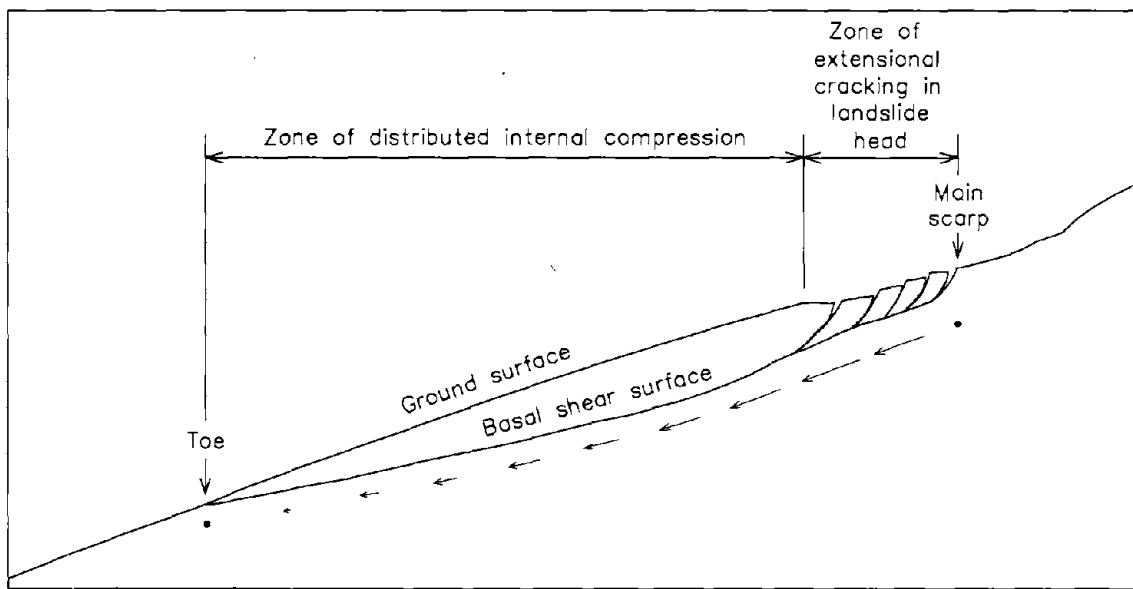


Figure 36.—Idealized landslide cross section, illustrating accommodation of extensional displacement in head by distributed internal compression of rest of landslide, with no bulging of ground surface at landslide toe. Lengths of arrows along basal shear surface represent relative downslope displacement of points along basal shear surface; dots, no displacement. For example, within a landslide 1,000 m long, 2 m of extensional displacement across main scarp could be accommodated by 0.2 percent of distributed longitudinal compressive strain within landslide material, with no movement at toe and no bulging of ground surface (assuming a constant thickness of landslide material).

Figure 37.—Percentage of landslide toes marked by compressional features (calculated from ratio of total length of compressional features in landslide toe to width of toe) versus longitudinal strain (calculated from ratio of displacement to landslide length) for landslides in Summit Ridge area. Letters and numbers refer to landslides mapped on plate 3 and listed in table 3.

## ACKNOWLEDGMENTS

This research was supported by the Federal Emergency Management Agency as part of the U.S. Government's disaster-relief program, provided at the request of the County of Santa Cruz. We are grateful for the assistance of the following people, who aided in various aspects of our investigation: Thomas E. Spittler (California Division of Mines and Geology), Paia Levine and Robert Brumbaugh (County of Santa Cruz); John M. Andersen, Sonia Diaz, Kenneth Harrington, Mary E. Hynes, Colin C. McAneny, Arijis A. Rakstins, H.M. Taylor, Brian Walls, and Tak Yamashita (U.S. Army Corps of Engineers); William M. Brown III, Ethel P. Lopez-Cavender, Alan F. Chleborad, Raymond R. Eis, Randall W. Jibson, Mark E. Reid, Kevin M. Schmidt, and Robert L. Schuster (U.S. Geological Survey); Nicholas Sitar (University of California, Berkeley); I.M. Idriss and Martin Hudson (University of California, Davis); Jeffrey S. Marshall and Nan A. Rosenbloom (University of California, Santa Cruz and Gary B. Griggs and Associates); Gerald E. Weber (University of California, Santa Cruz); Jeffrey M. Nolan (Nolan Associates); and William F. Cole, William R. Cotton, Dale R. Marcum, and Patrick O. Shires (Cotton, Shires Associates, Inc.). We also thank the many residents of the study area, who cooperated in providing access to private property and in sharing their observations of earthquake effects.

## REFERENCES CITED

- Aydin, Atilla, Johnson, A.M., and Fleming, R.W., in press, Coseismic right-lateral and left-lateral surface rupture and landsliding along the San Andreas and Sargent fault zones during the earthquake, in Ponti, D.J., ed., *The Loma Prieta, California, earthquake of October 17, 1989—ground ruptures*: U.S. Geological Survey Professional Paper 1551-D.
- Baum, R.L., Johnson, A.M., and Fleming, R.W., 1988, Measurement of slope deformation using quadrilaterals: U.S. Geological Survey Bulletin 1842-B, p. B1-B23.
- Beroza, G.C., 1991, Near-source modeling of the Loma Prieta earthquake; evidence for heterogeneous slip and implications for earthquake hazard: *Seismological Society of America Bulletin*, v. 81, no. 5, p. 1603-1621.
- Brown, W.M., III, 1988, Historical setting of the storm; perspectives on population, development, and damaging rainstorms in the San Francisco Bay region, in Ellen, S.D., and Wieczorek, G.F., eds., 1988, *Landslides, floods, and marine effects of the storm of January 3-5, 1982, in the San Francisco Bay region, California*: U.S. Geological Survey Professional Paper 1434, p. 7-15.
- Brumbaugh, Robert, 1990, Santa Cruz well history survey: Santa Cruz, Calif., report to Santa Cruz County Planning Department, 22 p.
- Carey, E.P., 1906, The great fault of California and the San Francisco earthquake, April 18, 1906: *Journal of Geography*, v. 5, no. 7, p. 289-301.
- Clark, J.C., Brabb, E.E., and McLaughlin, R.J., 1989, Geologic map and structure sections of the Laurel 7 1/2' Quadrangle, Santa Clara and Santa Cruz counties, California: U.S. Geological Survey Open-File Map 89-676, 31 p., scale 1:24,000, 2 sheets.
- Cole, W.J., Marcum, D.R., Shires, P.O., and Clark, B.R., 1991, Investigation of landsliding triggered by the Loma Prieta earthquake and evaluation of analysis methods: final technical report to U.S. Geological Survey under contract 14-08-0001-G1860, 33 p.
- Cooper-Clark and Associates, 1975, Preliminary map of landslide deposits in Santa Cruz County, California, in *Seismic safety element: Santa Cruz, Calif.*, Santa Cruz County Planning Department, scale 1:62,500.
- Cotton, W.M., 1990, Highway 17 deformation, stop 6 of Schwartz, D.P., and Ponti, D.J., eds., *Field guide to neotectonics of the San Andreas fault system, Santa Cruz Mountains, in light of the 1989 Loma Prieta earthquake*: U.S. Geological Survey Open-File Report 90-274, p. 31-32.
- Ellen, S.D., and Wieczorek, G.F., eds., 1988, *Landslides, floods, and marine effects of the storm of January 3-5, 1982, in the San Francisco Bay region, California*: U.S. Geological Survey Professional Paper 1434, 310 p.
- Ellen, S.D., Wieczorek, G.F., Brown, W.M., III, and Herd, D.G., 1988, Introduction, in Ellen, S.D., and Wieczorek, G.F., eds., 1988, *Landslides, floods, and marine effects of the storm of January 3-5, 1982, in the San Francisco Bay region, California*: U.S. Geological Survey Professional Paper 1434, p. 1-5.
- Griggs, G.B., Rosenbloom, N.A., and Marshall, J.S., 1990, Investigation and monitoring of ground cracking and landslides initiated by the October 17, 1989 Loma Prieta earthquake: Santa Cruz, Calif., Gary B. Griggs and Associates, 210 p.
- Jordan, D.S., ed., 1907, *The California earthquake of 1906*: San Francisco, A.M. Robertson, 360 p.
- Keefer, D.K., 1984, Landslides caused by earthquakes: *Geological Society of America Bulletin*, v. 95, no. 4, p. 406-421.
- Keefer, D.K., ed., 1991, *Geologic hazards in the Summit Ridge area of the Santa Cruz Mountains, Santa Cruz County, California, evaluated in response to the October 17, 1989, Loma Prieta earthquake; report of the Technical Advisory Group*: U.S. Geological Survey Open-File Report 91-618, 427 p.
- Keefer, D.K., Wilson, R.C., Mark, R.K., Brabb, E.E., Brown, W.M., III, Ellen, S.D., Harp, E.L., Wieczorek, G.F., Alger, C.S., and Zarkin, R.S., 1987, Real-time landslide warning during heavy rainfall: *Science*, v. 238, no. 4829, p. 921-925.
- Lawson, A.C., chairman, 1908, *The California earthquake of April 18, 1906; report of the State Earthquake Investigation Commission*: Carnegie Institution of Washington, Publication 87, 2 v.
- Manson, M.W., Keefer, D.K., and McKittrick, M.A., compilers, 1991, *Landslides and other geologic features in the Santa Cruz Mountains, California, resulting from the Loma Prieta earthquake of October 17, 1989*: California Division of Mines and Geology, Open-File Report 91-08, 45 p.
- Marshall, G.A., Stein, R.S., and Thatcher, Wayne, 1991, Faulting geometry and slip from coseismic elevation changes; the 18 October, 1989 Loma Prieta, California, earthquake: *Seismological Society of America Bulletin*, v. 81, no. 5, p. 1660-1693.
- Marshall, J.S., 1990, History of landsliding associated with prior earthquakes in the Santa Cruz Mountains, app. c of Griggs, G.B., Rosenbloom, N.A., and Marshall, J.S., 1990, *Investigation and monitoring of ground cracking and landslides initiated by the October 17, 1989 Loma Prieta earthquake*: Santa Cruz, Calif., Gary B. Griggs and Associates, unpaginated.
- Marshall, J.S., and Griggs, G.B., 1991, Ground crack monitoring program—December 1990–July 1991: report to U.S. Army Corps of Engineers, 14 p.
- McLaughlin, R.J., Clark, J.C., Brabb, E.E., and Helley, E.J., 1991, Geologic map and structure sections of the Los Gatos 7 1/2' Quadrangle, Santa Clara and Santa Cruz Counties, California: U.S. Geological Survey Open-File Report 91-593, 48 p., scale 1:24,000, 3 sheets.

- Nolan, J.M., in press. Paleoseismic investigation of a coseismic ground crack from the 1989 Loma Prieta earthquake, in Ponti, D.J., ed., *The Loma Prieta, California, earthquake of October 17, 1989—ground ruptures*: U.S. Geological Survey Professional Paper 1551-D.
- Patten, P.B., 1969, *Oh, that reminds me...*: Felton, Calif., Big Trees Press, 189 p.
- Payne, S.M., 1978, *A howling wilderness, a history of the Summit Road area of the Santa Cruz Mountains 1850-1906*: Santa Cruz, Calif., Loma Prieta, 156 p.
- Plafker, George, and Galloway, J.P., eds., 1989, *Lessons learned from the Loma Prieta, California, earthquake of October 17, 1989*: U.S. Geological Survey Circular 1045, 48 p.
- Ponti, D.J., Prentice, C.S., Schwartz, D.P., and Wells, R.E., 1990, *Mornil Road surface fractures associated with the 1906 and 1989 earthquakes*, stop 5 of Schwartz, D.P. and Ponti, D.J., eds., *Field guide to neotectonics of the San Andreas fault system, Santa Cruz Mountains, in light of the 1989 Loma Prieta earthquake*: U.S. Geological Survey Open-File Report 90-274, p. 23-30.
- Ponti, D.J., and Wells, R.E., 1991, *Off-fault ground ruptures in the Santa Cruz Mountains, California: ridge-top spreading versus tectonic extension during the 1989 Loma Prieta earthquake*: *Seismological Society of America Bulletin*, v. 81, no. 5, p. 1480-1510.
- , in press, *Surface ruptures produced by the earthquake: nature, origin, and hazard implications*, in Ponti, D.J., ed., *The Loma Prieta, California, earthquake of October 17, 1989—ground ruptures*: U.S. Geological Survey Professional Paper 1551-D.
- Rantz, S.E., 1971, *Mean annual precipitation and precipitation depth-duration-frequency data for the San Francisco Bay region, California*: U.S. Geological Survey Open-File Report, 23 p.
- Seed, R.B., Dickenson, S.E., Reimer, M.F., Bray, J.D., Sitar, Nicholas, Mitchell, J.K., Idriss, I.M., Kayen, R.E., Kropp, A.L., Harder, L.F., Jr., and Power, M.S., 1990, *Preliminary report on the principal geotechnical aspects of the October 17, 1989 Loma Prieta earthquake*: Berkeley, University of California, Earthquake Engineering Research Center Report UCB/EERC-90/05, 137 p.
- Shakal, A.F., Huang, M.J., Reichle, M.S., Ventura, C., Cao, T., Sherburne, R.W., Savage, M., Darragh, R.B., and Peterson, C., 1989, *CSMIP strong-motion records from the Santa Cruz Mountains (Loma Prieta), California earthquake of 17 October 1989*: California Division of Mines and Geology, Office of Strong Motion Studies, Report OSMS 89-06, 196 p.
- Spittler, T.E., and Harp, E.L., compilers, 1990, *Preliminary map of landslide features and coseismic fissures, in the Summit Road area of the Santa Cruz Mountains, triggered by the Loma Prieta earthquake of October 17, 1989*: U.S. Geological Survey Open-File Report 90-688, 31 p., scale 1:4,800, 3 sheets.
- U.S. Geological Survey, 1990, *The next big earthquake in the Bay Area may come sooner than you think*: Menlo Park, Calif., 23 p.
- U.S. Geological Survey staff, 1989, *Preliminary map of fractures formed in the Summit Road-Skyland Ridge area during the Loma Prieta, California, earthquake of October 17, 1989*: U.S. Geological Survey Open-File Report 89-686, scale 1:12,000.
- Varnes, D.J., 1978, *Slope movement types and processes*, in Schuster, R.L., and Krizek, R.J., eds., *Landslides—analysis and control*: U.S. National Academy of Sciences Transportation Research Board Special Report 176, p. 11-33.
- Wesnowsky, S.G., 1986, *Earthquakes, Quaternary faults, and seismic hazards of California*: *Journal of Geophysical Research*, v. 91, no. B12, p. 12587-12631.
- Wieczorek, G.F., Harp, E.L., Mark, R.K., and Bhattacharyya, A.K., 1988, *Debris flows and other landslides in San Mateo, Santa Cruz, Contra Costa, Alameda, Napa, Solano, Sonoma, Lake, and Yolo Counties, and factors influencing debris-flow distribution*, in Ellen, S.D., and Wieczorek, G.F., eds., 1988, *Landslides, floods, and marine effects of the storm of January 3-5, 1982, in the San Francisco Bay region, California*: U.S. Geological Survey Professional Paper 1434, p. 133-161.
- William Cotton and Associates, Inc., 1990, *Schultheis Road and Villa Del Monte areas geotechnical exploration Santa Cruz County, California*: Los Gatos, Calif., 2 v.
- Working Group on California Earthquake Probabilities, 1990, *Probabilities of large earthquakes in the San Francisco Bay region, California*: U.S. Geological Survey Circular 1053, 51 p.
- Young, J.V., 1979, *Ghost towns of the Santa Cruz Mountains*: Santa Cruz, Calif., Paper Vision Press, 342 p.
- Youd, T.L., and Hoose, S.N., 1978, *Historic ground failures in northern California triggered by earthquakes*: U.S. Geological Survey Professional Paper 993, 177 p.

THE LOMA PRIETA, CALIFORNIA, EARTHQUAKE OF OCTOBER 17, 1989:  
STRONG GROUND MOTION AND GROUND FAILURE

LANDSLIDES

ORIGIN OF FRACTURES TRIGGERED BY THE EARTHQUAKE  
IN THE SUMMIT RIDGE AND SKYLAND RIDGE AREAS  
AND THEIR RELATION TO LANDSLIDES

By Edwin L. Harp,  
U.S. Geological Survey

CONTENTS

	Page
Abstract .....	C129
Introduction .....	129
Geologic setting .....	130
Methods of fracture mapping and determination of origin .....	132
Criteria for discriminating fracture origins .....	132
Fractures related to landslide movement .....	132
Fracture orientation .....	132
Variation in trend .....	132
Displacement magnitude .....	133
Sense of relative displacement .....	133
Fractures related to regional structure .....	133
Fracture orientation .....	133
Trends of displacement vectors and sense of relative displacement .....	134
Displacement magnitude .....	135
Fractures related to both landslide movement and regional structure .....	135
Tranbarger fracture zone .....	135
Church fracture zone .....	136
Interpretation of fracture patterns .....	136
Effect of regional structure on landslides .....	136
Upper Morrell Road landslide .....	136
Villa Del Monte landslide .....	137
Other examples and summary .....	137
Similarity of fracture patterns to those produced in other earthquakes .....	138
The 1986 North Palm Springs, California, earthquake .....	138
The 1980 El Asnam, Algeria, earthquake .....	138
Summary .....	142
References cited .....	143

sional, and components of left-lateral slip were more common than those of right-lateral slip.

Fractures primarily related to landslide movement and those primarily related to regional structure were discriminated on the basis of orientation, variation in trends, displacement magnitude, sense of relative displacement, and spatial relation to existing geomorphic features. Fractures related primarily to landslide movement varied more widely in azimuthal trend and dip and had greater maximum displacements than those related primarily to regional structure. Interaction between landslide boundaries and structurally controlled fractures is evident in that the regional-structural trend (N. 30°–80° W.) is reflected in the shapes of some of the landslides reactivated by the earthquake. Several landslide headscarps that formed along structurally controlled discontinuities paralleled the regional-structural trend, and the landslide boundaries showed asymmetries imposed by regional structure.

The distributed off-fault fractures caused by the earthquake are similar to the fractures triggered by other recent earthquakes. For example, the 1986 North Palm Springs, Calif., and 1980 El Asnam, Algeria, earthquakes generated extensive off-fault fractures and landslides. Fracture patterns, extensional graben features, and landslide formation related to distributed horizontal shear, gravitational effects, and uplift-induced extension during the 1980 El Asnam earthquake suggest a useful qualitative model for similar features produced during the 1989 Loma Prieta earthquake.

ABSTRACT

The 1989 Loma Prieta earthquake generated a complex zone of distributed fractures related to both landslide movement and regional structure, such as bedding, joints, and faults, within a 3- by 10-km area primarily on the southwest flank of Summit Ridge in Santa Cruz County adjacent to the San Andreas fault zone. Instead of predominantly left stepping, right-lateral fractures confined to the mapped trace of the fault, these fractures were primarily exten-

INTRODUCTION

Initial efforts to locate a surface rupture from the 1989 Loma Prieta earthquake were frustrated largely by the confusing pattern of landslide-related fractures and numerous other ground cracks that displayed features generally considered to be uncharacteristic of the San Andreas fault. Instead of predominantly left stepping, right-lateral fractures confined to the mapped trace of the fault, fractures

were distributed throughout a wide zone southwest of the fault, along the crests of Summit and Skyline Ridges (fig. 1), approximately 3 km wide transverse to the ridgecrest by 10 km long parallel to the ridge, approximately between Hutchinson Road and Skyland Ridge (see pl. 4; fig. 1). Instead of the expected primarily right-lateral displacements, most fractures were primarily extensional, and components of left-lateral slip were more common than those of right-lateral slip.

This paper presents the fracture pattern produced by the earthquake in the Summit Ridge and Skyland Ridge areas (see pl. 4), discriminates fractures related to landslide movement and those related to regional structure (bedding, faults, joints), and discusses the relations between the existing structural fabric and the landslides generated by the earthquake.

**GEOLOGIC SETTING**

The geology of Summit Ridge itself is dominated by three units of Tertiary age: the Butano Sandstone, San

Lorenzo Formation, and Vaqueros Sandstone. All of these units consist of weakly cemented sandstone, siltstone, mudstone, and shale. According to the most recent geologic mapping in the study area (Clark and others, 1989, with landslide boundaries revised by R.J. McLaughlin and J.C. Clark, unpub. data, 1990; McLaughlin and others, 1991), the overall trend of bedding and other regional structure is northwest-southeastward. Bedding in the study area typically strikes N. 30°–80° W. The rocks are intensely folded, and dips are typically steep. Locally, the rocks dip southwest or northeast, are vertical, or are overturned to the northeast (fig. 2).

Several major geologic structures pass through the study area (fig. 2). The Laurel anticline trends approximately N. 45° W. through the south flank of Summit Ridge and is truncated by the Butano fault approximately 1.4 km southeast of the California Highway 17-Summit Road intersection. This fault, which diverges from the San Andreas fault 800 m northwest of the Old San Jose Road-Summit Road intersection, traverses the Summit Ridge area with local strikes of N. 60°–75° W. The Summit syncline trends N. 60°–65° W. and extends approximately 300 m west of

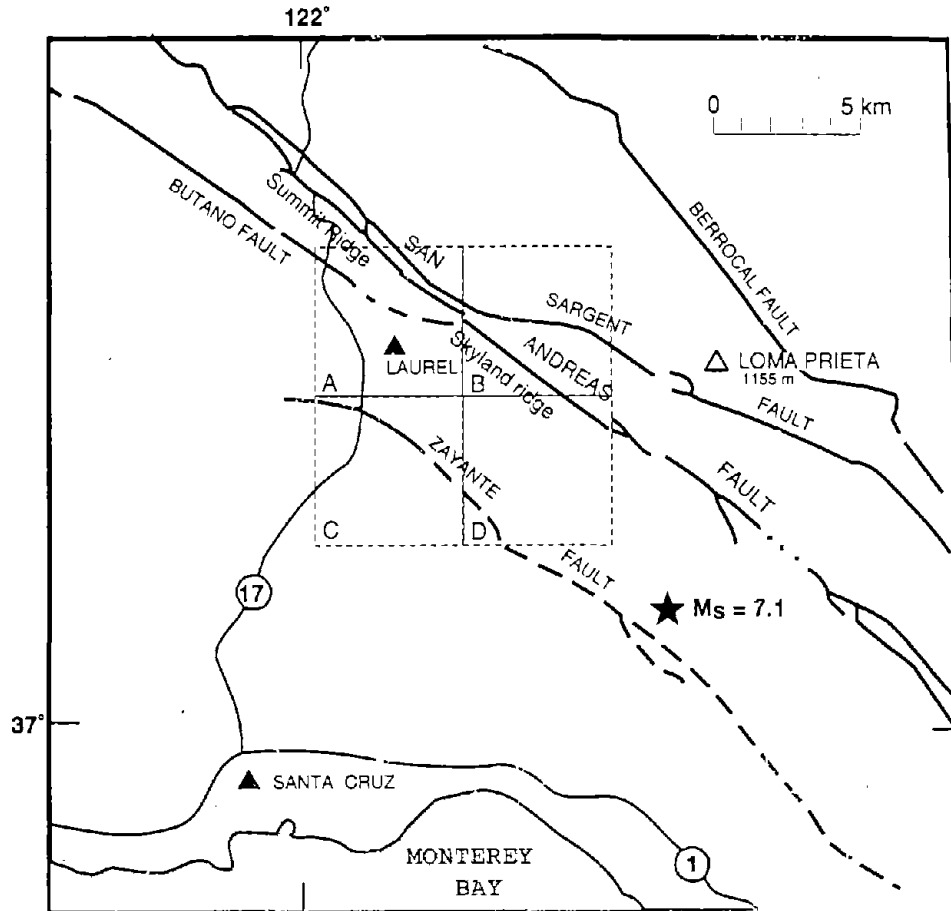


Figure 1.—Loma Prieta area, Calif., showing locations of major faults (dashed where inferred, dotted where concealed) and of study area in the Santa Cruz Mountains where widespread landsliding and coseismic ground fractures were generated by 1989 Loma Prieta earthquake. Star, epicenter.

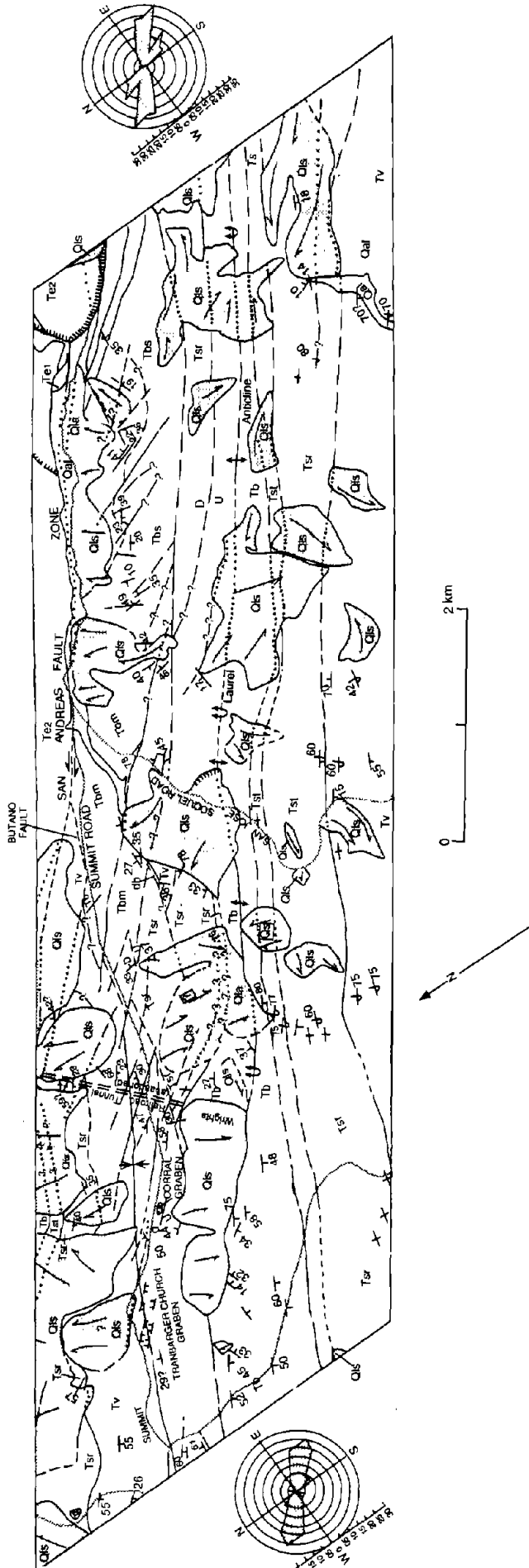


Figure 2.—Summit Ridge and Skyland Ridge areas, Calif., showing local geology, regional structure, and trends of fractures generated by 1989 Loma Prieta earthquake.

Morrell Road, where the synclinal axis is truncated by an unnamed fault trending N. 45° W. that is inferred to offset the Butano fault left laterally (fig. 2; McLaughlin and others, 1991). In the Villa Del Monte and Morrell Road areas, several faults striking approximately N. 45° W. extend across the Butano fault and the Summit syncline. Most of these faults are shorter than 1 km in mapped length and appear to offset structures little or not at all.

Several grabens are present near the crest of Summit Ridge (see pl. 4A; fig. 2); they are subparallel to the ridge and have a local relief of 1.5 to 6 m across their boundaries. Renewed displacement occurred on parts of graben boundaries during the earthquake, as evidenced by fractures with vertical displacements of from several centimeters to as much as 30 cm. Three of the most conspicuous grabens are near Summit Road (see pl. 4A; fig. 2); the westernmost of these is about 60 m southeast of Old Summit Road and about 750 m east of California Highway 17. This graben (Tranbarger graben, pl. 4A; fig. 2) is part of the extended Tranbarger fracture zone in the Old Santa Cruz Highway area. There, earthquake-induced fractures formed on both margins near its northwest limit, where it is approximately 15 m wide. To the southwest, the graben increases in width to approximately 60 m within a horizontal distance of 100 m. Measured vertical displacements during the earthquake ranged from 2.5 to 15 cm (Spittler and Harp, 1990).

Another visible graben along Summit Road lies adjacent to and southwest of a 430-m-long fracture (Church ruptures of Ponti and Wells, 1990) that extends southeastward from the Melody Lane-Summit Road intersection (see pl. 4A; fig. 2), crossing Summit Road twice. The long fracture along the northeastern margin of this graben is the only significant earthquake-induced fracture associated with it. Its maximum displacement is about 0.3 m (Spittler and Harp, 1990). As discussed below in the subsection entitled "Church Fracture Zone," no single origin is obvious for this feature.

Beginning at the Summit Road-Old Santa Cruz Highway intersection, a 30- to 50-m-wide graben extends approximately 250 m southeastward along the southwest side of Summit Road; it trends N. 45° W., diverging from the trend of Summit Road by about 5°. Both southwest- and northeast-facing scarps formed here on fractures (Corral graben, pl. 4A; fig. 2) triggered by the earthquake, with vertical displacements ranging from 5 to 36 cm (Spittler and Harp, 1990). Within this graben, earthquake-induced fractures did not wholly coincide with the graben margins but also formed southwest- and northeast-facing scarps within the graben itself. These grabens and the fractures created within them during the earthquake

parallel the prevailing structural trends in this area (N. 40°–60° W.), as discussed below in the subsection entitled "Fractures Related to Regional Structure."

## METHODS OF FRACTURE MAPPING AND DETERMINATION OF ORIGIN

The fractures or ground cracks that formed in the Summit Ridge area as a result of the earthquake were mapped by a team of geologists from Federal, State, and county agencies, universities, and private consulting firms. The map of landslide-related and other coseismic fractures (see pl. 4) was derived from the original map by Spittler and Harp (1990), using 1:6,000-scale aerial photographs taken October 27, 1989. Outside of this coverage, mapping was done on enlargements of 1:24,000-scale U.S. Geological Survey topographic maps, 1:31,680-scale aerial photographs taken in June 1989, and 1:4,800-scale County of Santa Cruz planimetric maps.

The locations of features mapped from the 1:6,000-scale aerial photographs are accurate to within 10 m where vegetation is sparse and to within 10 to 50 m where vegetation is dense. Outside the coverage of the 1:6,000 aerial photographs, accuracy is diminished. Where distinctive and (or) topographic features are present, locations are accurate to within 20 to 50 m; where no such distinctive features exist and where tree cover is dense, accuracy is estimated at within 50 to 100 m.

Some fractures may have been missed during the mapping because of dense vegetation, poor access, and the obliteration of many features due to repair work before mapping could be completed. The purpose of plate 4 is to systematically document and interpret the landslide and other coseismic fractures and to display their distribution with a minimum of generalization. Because these features were plotted by hand and are not precisely surveyed at a large scale, such as 1:500 or larger, some generalization has necessarily been incorporated into the mapping. Therefore, plate 4 is useful as a reconnaissance tool and as a guide to subsequent geologic and geotechnical investigations but is insufficiently precise to serve as a map on which to base site-specific engineering or planning decisions.

The various distinguishing characteristics of fractures, such as orientation, continuity, and relation to geomorphic features, were used to discriminate their origins. The criteria described below were used to discriminate on plate 4 between fractures primarily related to landslide movement and those primarily related to regional structure, such as bedding, joints, or faults. A few major fractures and fracture zones are designated as related to both types of processes because evidently both landslide movement and regional structure significantly influenced their geometry.

Relatively small ground cracks, whether within or outside landslide boundaries, were not individually categorized. Ground-crack patterns were analyzed primarily with the data of Spittler and Harp (1990, pl. 5) and Wells (in press).

## CRITERIA FOR DISCRIMINATING FRACTURE ORIGINS

### FRACTURES RELATED TO LANDSLIDE MOVEMENT

The typical association of fractures showing different relative displacements and orientations within the various parts of a landslide is well documented (Varnes, 1978) and forms a basis for relating fractures to landslides or other causes. The relation of fractures to slope morphology and to each other is also important in such a determination. The large landslides in the Summit Ridge area and the fractures associated with them are described by Keefer and others (this chapter), along with a discussion of the general criteria for identifying such landslides. To facilitate the discussion of fracture origins, however, in the following sections I discuss the criteria used to discriminate between fractures related to landslide movement and those related to regional structure.

### FRACTURE ORIENTATION

The orientation and shape of a fracture are primarily important in evaluating its origin. As shown on plate 3 and in figure 1 of Keefer and others (this chapter), if the main (head) scarp and both flanks of a rotational slump or block slide are completely defined by fractures, these fractures describe a horseshoe-shaped arc opening in the downslope direction, although, as discussed by Keefer and others, the main scarps of block slides may be only gently curved or relatively straight. Therefore, in general, fractures related to main scarps may vary in trends within approximately 180° on a single landslide. For example, on the southwest flank of Summit Ridge, most major groups of fractures associated with landslides had trends that spanned this full range although the full range of possible trends was not observed on all individual landslides.

### VARIATION IN TREND

Fractures associated with the main scarps of landslides are typically arcuate or curved. If the main scarp or flanks are exceptionally long, however, these fractures may be relatively straight over much of their length. Most, but



not all, fractures associated with landslides in the Summit Ridge area were in zones that remained straight for less than 100 m; the most notable exceptions to this limit were associated with the largest landslides.

### DISPLACEMENT MAGNITUDE

Though not a distinguishing criterion, maximum displacements measured across fractures within landslides in the Summit Ridge area were commonly larger than across fractures unrelated to landslide movement. Fracture displacements outside of landslide boundaries were typically less than 50 cm, whereas those of more than 60 cm across individual cracks were not uncommon within landslides. Thus, both fractures related to landslide movement and those related to regional structure had displacements of less than 50 cm, whereas only fractures related to landslide movement commonly had displacements of more than 60 cm, probably reflecting a gravity-driven component of landslide displacement in addition to a shaking-induced component. Cumulative displacements across fracture zones within landslides were as large as 2.4 m.

### SENSE OF RELATIVE DISPLACEMENT

Within a landslide mass that has a completely developed main scarp and flanks, vertical, right-lateral, and left-lateral senses of displacements are all represented. In the Summit Ridge area, this was not the case for all landslides because within some landslides (specifically, the Upper Morrell Road and Bel Air Court landslides, pl. 4A, 4B), fractures defining the flanks of the landslides were not equally developed. Throughout the study area, however, displacements across fractures along landslide margins were relatively consistent—dextral along the right flanks and sinistral along the left flanks.

### FRACTURES RELATED TO REGIONAL STRUCTURE

The origins of the fractures in the Summit Ridge area unrelated to landslide movement is still in debate. Ponti and Wells (1991) attributed much of the displacement across such fractures to gravitational movement and suggested that displacement vectors are in the direction of regional or local slope. Cotton and others (in press) invoke bedding-plane slip to account for the largely extensional style of the displacements across fractures, and similar past deformation to account for the grabens, in the Summit Ridge area; they consider this deformation to be tectonic in origin. Aydin and others (in press) found right-lateral displacements with reverse slip-slip components in short discontinuous segments along both the Sargent and

the San Andreas fault zones. They consider the displacements within these segments to be kinematically compatible with the source mechanism of the earthquake, and the broad zone of distributed fractures on Summit Ridge to be tectonic but otherwise obscure in origin. Johnson and Fleming (1993) considered fractures in the Summit Ridge area unrelated to landslide movement to be extensional features formed within a zone of distributed right-lateral shear and the observed left-lateral displacements observed across such fractures to derive from rotation accompanying the distributed right-lateral deformation. They stated that this deformation is tectonic, consistent with the source mechanism of the earthquake, and that the displacements observed in the Summit Ridge area are probably typical for past earthquakes there. Regardless of their specific origin, most of these fractures are probably openings along bedding surfaces or along other structures trending parallel to bedding.

Extension was the predominant mode of displacement across the fractures related to regional structure throughout the study area. Even those fractures that displayed lateral and (or) vertical offset generally lacked slickensides or surficial ridges of disturbed ground ("mole tracks"), which are created primarily by shear. Although both left- and right-lateral displacements occurred, left-lateral displacements were more common.

### FRACTURE ORIENTATION

In addition to their unrelatedness to any recognizable landslides, the principal criteria for identifying fractures related to regional structure were an absence of curvature and a limited variation in orientation parallel to regional structure, in contrast to the wide variation in orientation characteristic of the fractures related to landslide movement. Most fractures in the Summit Ridge area outside the boundaries of well-defined landslides parallel or nearly parallel bedding, as shown in figure 2. Most of these fractures and most bedding surfaces trend and strike in the range N. 30°–80° W. As previously stated, the trends of fractures related to landslide movement varied much more widely than those of fractures related to regional structure. The rose diagrams shown in figures 2, 3A, and 3B plot the cumulative trends of fractures related to regional structure in the northwest and southeast halves, respectively, of the study area (see pl. 4). Most fractures in the northwest half of the study area along Summit Ridge (figs. 2, 3A) trend approximately N. 45° W., whereas those in the southeast half of the study area along Skyland Ridge (figs. 2, 3B) show an additional clustering of trends around N. 15°–20° W., as well as a maximum trend of N. 45° W., reflecting a more northerly trend of regional structure and strike of bedding in parts of the Skyland Ridge area than in the Summit Ridge area.

### TRENDS OF DISPLACEMENT VECTORS AND SENSE OF RELATIVE DISPLACEMENT

The trends of displacement vectors and their sense of relative displacement were inconclusive in discriminating between fractures related to landslide movement and those related to regional structure. Instead, these criteria were supplemental to more deterministic data on orientation, fracture straightness, and proximity to topographic features. The rose diagrams in figures 3C and 3D plot the

trends of displacement vectors across fractures outside landslide boundaries in the northwest and southwest halves, respectively, of the study area (see pl. 4; fig. 2). The trends of displacement vectors across fractures in the northwest half of the study area (fig. 3C) show maximums that are slightly counterclockwise from perpendicularity to the maximums in figure 3A. Comparison of figures 3A and 3C reveals the mostly extensional style of relative displacement (normal to the maximum trend) with a small component of sinistral displacement across fractures in

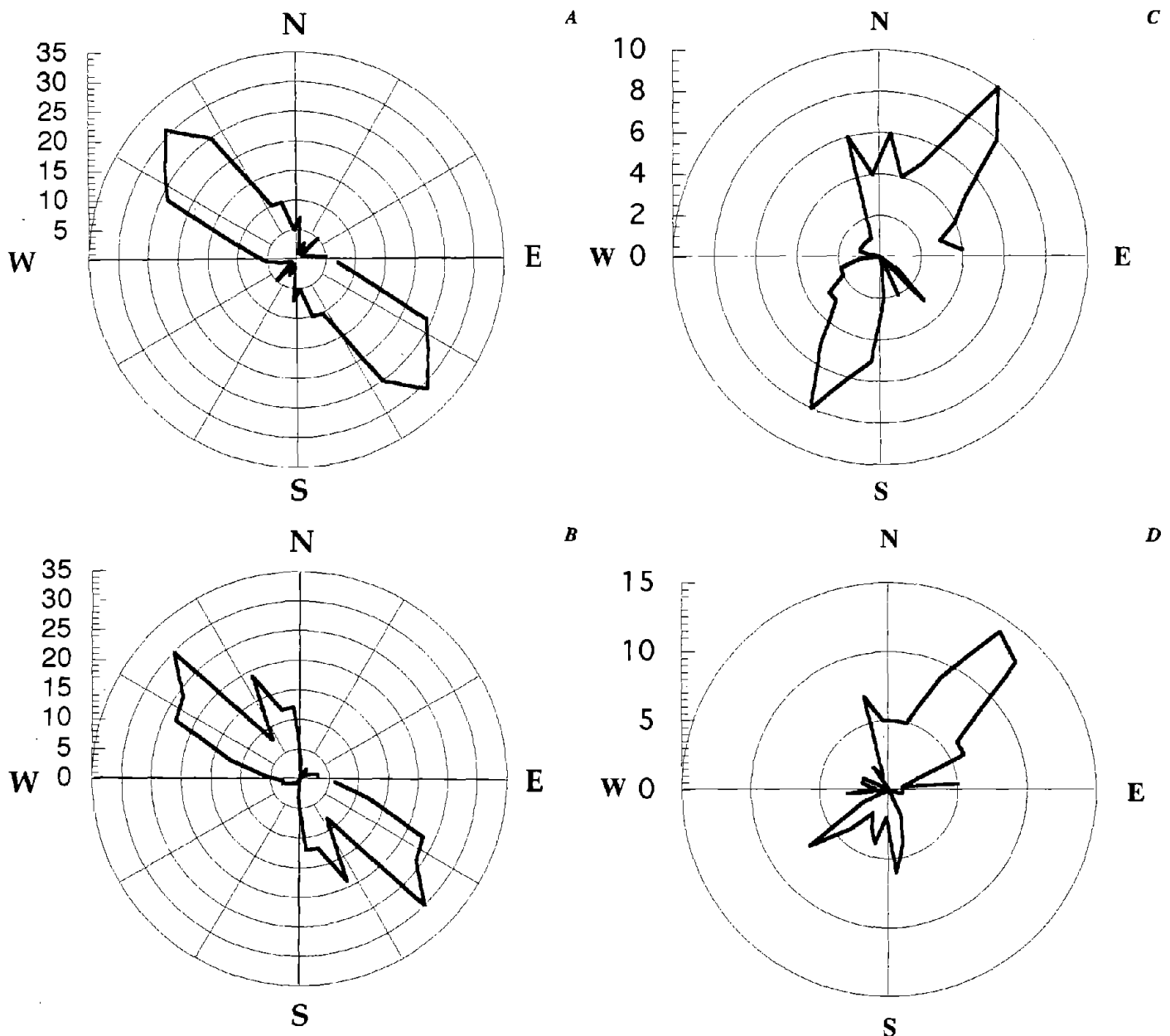


Figure 3.—Rose diagrams showing cumulative trends of (A, B), and trends of displacement vectors across (C, D), fractures inferred to be related to regional structure in northwest (A, C) and southeast (B, D) halves of study area (see fig. 2). Values on ordinate axis are numbers of fractures and correspond to radial length. Azimuth interval, 5°. Data from Spittler and Harp (1990) and Wells (in press).

the northwest half of the study area; comparison of figures 3B and 3D reveals similar relations in the trends of displacement vectors across fractures in the southeast half of the study area (see pl. 4; fig. 2).

As stated above, the sense of relative displacement across fractures was not a criterion in discriminating between fractures related to landslide movement and those related to regional structure. Both landslides and other structurally controlled processes affected fractures, producing relative vertical displacements that were down on the downslope side. Conversely, some fractures with upslope sides displaced relatively downward were found within landslide masses. Such fractures can be common within landslides just below the main-scarp area where an extensional domain exists or, in places where large displacements have occurred, within the toe region of a landslide, where compression commonly results in differential vertical deformation. Because displacements within landslide masses were relatively small during the earthquake, creating little evidence of compressional-toe formation, most long, straight fractures parallel to the regional-structural trend (especially those with upslope-facing scarps) were interpreted to be related to regional structure, even if they occurred within a recognizable landslide body.

#### DISPLACEMENT MAGNITUDE

The magnitudes of displacement across fractures outside landslide boundaries were generally lower than of those across fractures within landslides. As stated above, displacements across fractures related to regional structure were observed to be generally less than 50 cm, whereas those of more than 60 cm across individual fractures within landslide masses were not uncommon. Displacements across a few fractures related to regional structure were more than 1.0 m, but most displacements of more than 60 cm were across fractures related to landslide movement.

#### FRACTURES RELATED TO BOTH LANDSLIDE MOVEMENT AND REGIONAL STRUCTURE

The criteria described in the previous subsections allowed interpretation of the overall geometries of most fracture zones in the Summit Ridge area and enabled discrimination between fractures related to landslide movement and those related to regional structure. Several of the longest fracture zones within the Summit Ridge area, however, may be related to both landslide movement and regional structure, suggesting a possible interaction between the structural fabric of the study area and landslide processes during the earthquake.

#### TRANBARGER FRACTURE ZONE

The Tranbarger fracture zone, which received much attention during the first few days after the earthquake, crossed Summit Road 640 m east of California Highway 17 (loc. A, pl. 4A). It extended approximately 670 m along an average trend of N. 55° W. that changed locally to slightly west of north where the fracture crossed Old Summit Road (see pl. 4A; U.S. Geological Survey staff, 1989).

This fracture and several other approximately parallel fractures to the southwest formed a zone approximately 200 m wide along Summit Road (loc. B, pl. 4A). To the southeast, this fracture zone was approximately 120 m wide at Old Summit Road and less than 30 m wide at a point 200 m farther southeast. The fracture zone widened southeastward from this point to 120 m and ended near Old Santa Cruz Highway (loc. C, pl. 4A). The average trend of this somewhat discontinuous fracture zone was N. 45° W. It extended for more than 1,200 m and was thus the longest such zone in the Summit Ridge area. The trends of individual fractures in the zone ranged from N. 10° W. to N. 65° W. Near the northwest limit of this fracture zone, vertical displacements across fractures were generally less than 13 cm and were consistently southwest side down. Southeast of Old Summit Road, the zone was less complex in terms of magnitudes and senses of displacements. There, several grabenlike fractures formed. Farther southeast, upslope- and downslope-facing scarps faced away from each other, creating a horst. Still farther southeast, near the end of the zone, was another set of narrow grabenlike fractures. Vertical displacements on these fractures ranged from 5 to 60 cm and averaged 15 cm. Extension across the fractures in this set was typically 15 cm, and horizontal shear displacements typically sinistral and ranged from 2.5 to 80 cm in magnitude.

The trend of the Tranbarger fracture zone paralleled the regional trend of bedding. This trend, and the left-lateral shear displacements along fractures not suitably oriented with respect to the slope to be lateral shears of a landslide, suggest deformation along regional structure. The grabenlike fractures, however, also suggest a zone of extension developing along the main scarp of a large landslide; the sinistral shear displacements were small in comparison with the vertical displacements in most places. Thus, the 1,200-m-long fracture zone could well be the main scarp of a landslide affecting much of the southwest slope of Summit Ridge. Because the fractures within this zone formed along the regional-structural trend, their origin is thus ambiguous: It is unclear whether they simply formed along bedding planes due to seismic shaking, whether they indicate graben formation due to extension of the ridgecrest, or whether they formed in response to landslide movement along a large main scarp parallel to regional structure.

### CHURCH FRACTURE ZONE

Another long fracture approximately parallel to the regional-structural trend extended for approximately 430 m southeastward along Summit Road from near the Melody Lane-Summit Road intersection (loc. D, pl. 4A). This fracture intersects Summit Road approximately 200 m from the northwest end of the fracture. Southeastward from there, the fracture runs along the southwest edge of Summit Road for approximately 60 m and then recrosses Summit Road and parallels the road for an additional 140 m. The overall trend of this fracture is N. 40° W., and its trend ranges locally from N. 15° to 80° W. Throughout most of its length the fracture is a single discontinuity, with vertical displacements of as much as 30 cm, down to the southwest (downslope).

Like the Tranbarger fracture zone, the Church fracture zone has most of the characteristics of a ground crack opening along the regional-structural trend; however, it also has characteristics of the main scarp of a large landslide. Unlike the Tranbarger fracture zone, the sense of vertical displacement across the Church fracture zone is consistently downslope side down except in a few localities near its northwest and southeast ends, where small (max 2.5 cm) vertical displacements occurred that were upslope side down.

Ponti and Wells (1991) interpreted the displacements across this fracture as deformation along bedding on the northeast limb of the Summit syncline, the axis of which trends N. 60°–65° W. They suggested that this fracture, as well as others in the vicinity, may reflect slip along bedding surfaces because beds on both limbs of the syncline appear to move toward the center of the syncline. They furthermore suggested that movement of beds toward the syncline center may be due to ridge spreading caused by lateral movement of underlying mudstone units, allowing gravitational relaxation of the syncline.

Although the above model is consistent with vertical displacements of this fracture along its length, other fractures on the southwest limb of the syncline (loc. E, pl. 4A) have southwest-facing scarps, indicating movement of material in the opposite direction, away from the synclinal center. Although some fractures in this vicinity have northeast-facing scarps, other nearby fractures not obviously related to landslide movement have southwest-facing scarps.

A trench dug across the Church fracture zone at a locality on the southwest side of Summit Road (see Nolan and Weber, this chapter) showed that the fracture dips 45°–63° SW. Data from this trench, as well as surface data, suggest that this fracture could be the main scarp of a large deep-seated landslide involving much of the southwest slope of Summit Ridge. If both this fracture and those constituting the Tranbarger fracture zone are related to landslide movement, then this fracture along Summit

Road would be a main scarp along the ridgetop, and the Tranbarger fracture zone would be a zone of internal scarps downslope and within a large landslide that includes most of the southwest flank of Summit Ridge between California Highway 17 and Old Santa Cruz Highway. In fact, the Church fracture zone crosses Summit Ridge at its northwest end, occupying a position slightly to the north and downslope of the crest of Summit Ridge at this point. For a landslide scarp to occupy a position on the opposite side of a ridgetop from the slope toward which it is inclined is not uncommon where bedding surfaces or other structure has a similar inclination. According to the geologic map (McLaughlin and others, 1991), bedding in this area dips southwest. For the Church fracture zone to be the scarp of a deep-seated landslide, however, its failure surface would have to depart from the geometry of the Summit Ridge syncline in its lower reaches.

In addition, the Church fracture zone may be related to a fault mapped in approximately the same place and with the same overall trend (fig. 2; McLaughlin and others, 1991). The fault as mapped extends beyond the present fracture zone approximately 0.3 km farther northwestward and slightly more than 1 km farther southeastward. At present, however, the origin of the Church fracture zone is still uncertain, and any one or, possibly, all of these origins may have contributed to its formation.

### INTERPRETATION OF FRACTURE PATTERNS

The fractures on Summit Ridge created by the earthquake revealed a complex interaction between landslide processes as triggered by the earthquake and preexisting regional structure, such as bedding surfaces, joints, and faults. The fractures related to landslide movement evidently are superimposed on and, therefore, postdate the network of regional structural features.

### EFFECT OF REGIONAL STRUCTURE ON LANDSLIDES

The spacing and orientation of regional structure within the study area (see pl. 4) and generalized from McLaughlin and others (1991) evidently affected the shape and position of many of the margins of the larger landslides. Several examples of this effect are discussed below.

#### UPPER MORRELL ROAD LANDSLIDE

The Upper Morrell Road landslide, on the south flank of Summit Ridge approximately 370 m east of Taylor Gulch, shows a strong influence of regional structure on

the position and shape of the fractures forming the landslide margins. The fractures forming the main scarp and the flanks of the landslide are asymmetric (loc. F, pl. 4B), and fractures forming the left flank of the landslide parallel the regional-structural trend (N. 55°–60° W.) for as much as 240 m.

The fractures forming the right flank (looking downslope) of this landslide curved to the southwest from the main-scarp area and trended approximately N. 20° E. where they crossed Morrell Road. At that point, they were predominantly right lateral, with approximately 60 cm of horizontal displacement and 15 to 25 cm of vertical displacement, down to the southeast. Approximately 23 m to the southwest along this fracture zone, its trend abruptly swung clockwise to N. 60° W. (loc. G, pl. 4B), parallel to regional structure. Immediately west of this change in trend, the fracture was predominantly extensional, and several upslope-facing scarp segments were present, with maximum displacements of 5 cm. At this change in trend, the fracture zone ceased to exhibit the characteristics of right-lateral shear along the flank of a landslide and took on the attributes (largely extensional displacements, fractures parallel to regional structure and bedding, and upslope-facing scarps well downslope from graben-forming areas of the Upper Morrell Road landslide) of fractures related to regional structure.

#### VILLA DEL MONTE LANDSLIDE

Several fracture zones in the Villa Del Monte area seemed to be related to both landslide movement and regional structure. For example, near the junction of Skyview Terrace and Bel Air Court, a fracture zone trending N. 50° W. formed part of an internal landslide scarp (loc. H, pl. 4B). Similarly to the Upper Morrell Road landslide, this fracture zone, forming the left flank of the internal landslide, paralleled the regional-structural trend. The right flank of the fracture zone curved counterclockwise to the southwest, trending about N. 20° E.

Near the junction of Sunset Drive and Evergreen Lane, as well as immediately to the north, are several fractures that parallel the regional-structural trend but also resemble fractures forming the main scarp of a large, deep-seated landslide. This fracture zone trends approximately N. 65° W., but one fracture (near loc. I, pl. 4A) curves counterclockwise, trending N. 45° E., as displacements change from predominantly extensional to primarily dextral. This change in trend and the displacements along this fracture are common features of the transition from the main scarp to the right flank of a landslide.

One effect of the regional system of discontinuities on the shape of landslides along the south flank of Summit Ridge is a consistent asymmetry in their horizontal dimensions. Generally, the right flanks are more clearly de-

finied by fractures than are the left margins. Examples are the Upper Morrell Road landslide (see pl. 4B), the Burrell landslide (loc. H, pl. 4B), and the Villa Del Monte landslide (loc. I, pl. 4A). Because the left flanks of the landslides on the south side of Summit Ridge more nearly parallel the regional-structural trend, the fractures forming these flanks generally occur along previously existing structural discontinuities rather than propagating through unbroken ground, and generally are extensional rather than dominantly shear, as is more typical in the flanks of a landslide.

#### OTHER EXAMPLES AND SUMMARY

Many fractures that approximately parallel the regional-structural trend extend across landslide boundaries or through landslides, evidently affecting the shapes of the landslides. For example, a N. 50° W.-trending fracture related to regional structure cuts through one of the main scarps in the Burrell landslide (loc. H, pl. 4B) and continues into the landslide. Similarly, a N. 50°–67° W.-trending fracture cuts across the Taylor Gulch landslide (loc. J, pl. 4B). Finally, a set of N. 60° W.-striking fractures related to regional structure cut through the northwest part of the main scarp and the right flank of the Stetson Road landslide (loc. K, pl. 4D).

As these examples show, the pattern of fractures triggered by the earthquake on the southwest slopes of Summit and Skyland Ridges reveals an interaction between landslides triggered by the earthquake and a regional system of structural discontinuities, most likely bedding surfaces and faults subparallel to bedding. This interaction between landslide movement and regional structure takes two forms. One form of interaction involves the influence of the spacing and orientation of fractures related to regional structure on the position and shape of fractures forming landslide boundaries. This form of interaction also imparts an asymmetry, in that fractures outlining the left flanks of landslides commonly are poorly formed in comparison with those outlining the right flanks. In several places, the left flanks of landslides that formed along fractures which parallel the regional-structural trend were long and straight, whereas those forming the right flanks were arcuate. Another form of interaction involves the cross-cutting of landslides by fractures related to regional structure, with little apparent effect on the landslide shape.

Thus, in the 1989 Loma Prieta earthquake, a wide zone of distributed coseismic fractures and landslides was triggered to the southwest and approximately parallel to the mapped trace of the San Andreas fault. The pattern of landslides and fractures resulted from a complex interaction between strong shaking, fault movement, geologic structure, and gravitational slope movement. The 1989 Loma Prieta earthquake is not unique, however, in pro-

ducing such a complex pattern of fractures and slope failures within its epicentral area. Other recent earthquakes have also triggered complex patterns of surface deformation that are difficult to interpret.

### **SIMILARITY OF FRACTURE PATTERNS TO THOSE PRODUCED IN OTHER EARTHQUAKES**

The pattern of fractures formed on the southwest slopes of Summit and Skyland ridges by the 1989 Loma Prieta earthquake is similar to those produced in other recent earthquakes: The 1986 Palm Springs, Calif., and the 1980 El Asnam, Algeria, earthquakes both produced extensive zones of distributed fractures and reactivated landslides along and near the traces of the causative faults. We discuss these earthquakes here to provide a basis of comparison for evaluating the possible origins of the fractures in the Summit Ridge area and their relation to landslides triggered by the 1989 Loma Prieta earthquake.

#### **THE 1986 NORTH PALM SPRINGS, CALIFORNIA, EARTHQUAKE**

The July 8, 1986, North Palm Springs, Calif., earthquake ( $M_L=5.9$ ) produced an extensive network of fractures within a diffuse zone along both sides of the Banning fault, which dips about  $50^\circ$  N. in this area. The fracture zone extended 8.6 km along the fault and 90 to 300 m wide. Although discontinuous fractures and landslides were most abundant, and displacements greatest, where slopes were steepest within this fracture zone, gentle slopes and nearly level ground were also cracked. Extension and small (several millimeters) right-lateral offsets were the most common type of displacements. The fractures on nearly level ground were probably related to fault slip rather than to slope movement. Intensely fractured ground along ridgecrests was also a common feature within the fracture zone (Morton and others, 1989).

Many of the fractures within the diffuse zone along the Banning fault were interpreted to have been caused by shallow gravitational slope displacements (landslides) induced by the seismic shaking. The distribution of the fractures with respect to the fault trace, however, indicated that these fractures did not result from strong shaking alone. Morton and others (1989) concluded that this anomalous fracture zone formed from a combination of strong ground shaking, gravitational effects, and a localized surficial response to static shear strain induced near the fault trace by rupture at depth. Their model, based on elastic-dislocation theory, predicted that the surface fractures not caused by slope movements extended no deeper

than 100 m and that the fault rupture at depth extended only to within 4 km of the surface and was not connected to the surface fractures.

Similarities between the 1986 Palm Springs earthquake and the 1989 Loma Prieta earthquake are (1) the respective source mechanisms, which were both right lateral with a thrust component; and (2) the presence of discontinuous fracture zones away from the fault traces that showed dominantly extensional displacement. Also, many landslides were triggered within this diffuse zone of fractures, creating difficulties for geologists seeking to discriminate between fractures outlining the slope failures and other fractures due to shaking or faulting.

Differences between the fracture pattern created by the 1986 North Palm Springs earthquake and that created by the 1989 Loma Prieta earthquake were (1) shear displacements across fractures that were dominantly right lateral in the 1986 earthquake as opposed to dominantly left lateral in the 1989 earthquake, and (2) the presence of fractures and slope failures on both sides of the Banning fault in the 1986 earthquake. In the Summit Ridge area, most observed ground cracks were confined to the southwest side of the ridge or, at least, to the hanging wall (with respect to the thrust component of the Loma Prieta source mechanism) of the San Andreas fault zone, whereas the diffuse zone of fractures originating from the 1986 earthquake extended across the Banning fault trace.

In summary, both the 1986 North Palm Springs earthquake and the 1989 Loma Prieta earthquake formed broad zones of complex fractures as a result of strong ground shaking, gravitational effects, and fault rupture at depth. Differences existed as to the dominant sense of shear across fractures and the distribution of fracture zones with respect to the fault traces.

#### **THE 1980 EL ASNAM, ALGERIA, EARTHQUAKE**

A recent earthquake showing possibly even more similarities to the 1989 Loma Prieta earthquake in producing off-fault ground cracks was the October 10, 1980, El Asnam, Algeria, earthquake ( $M_S=7.3$ ). Cotton and others (1990 and in press) also pointed out the similarities between the landslides and off-fault fractures caused by these two earthquakes.

The 1980 El Asnam earthquake generated 40 km of primary surface rupture that ranged in trend from N.  $45^\circ$  to  $80^\circ$  E. (fig. 4). The primary rupture was somewhat discontinuous over this 40 km, but distances between individual fractures in the rupture zone generally were less than 100 m. The surface fault displacement was predominantly thrusting, with some left-lateral slip in the southern part of the fault trace (fig. 4; Philip and Meghraoui, 1983; Sorriso-Valvo, 1986). The source mechanisms indicated a dip of approximately  $50^\circ$  N. (Ouyed and others, 1981).

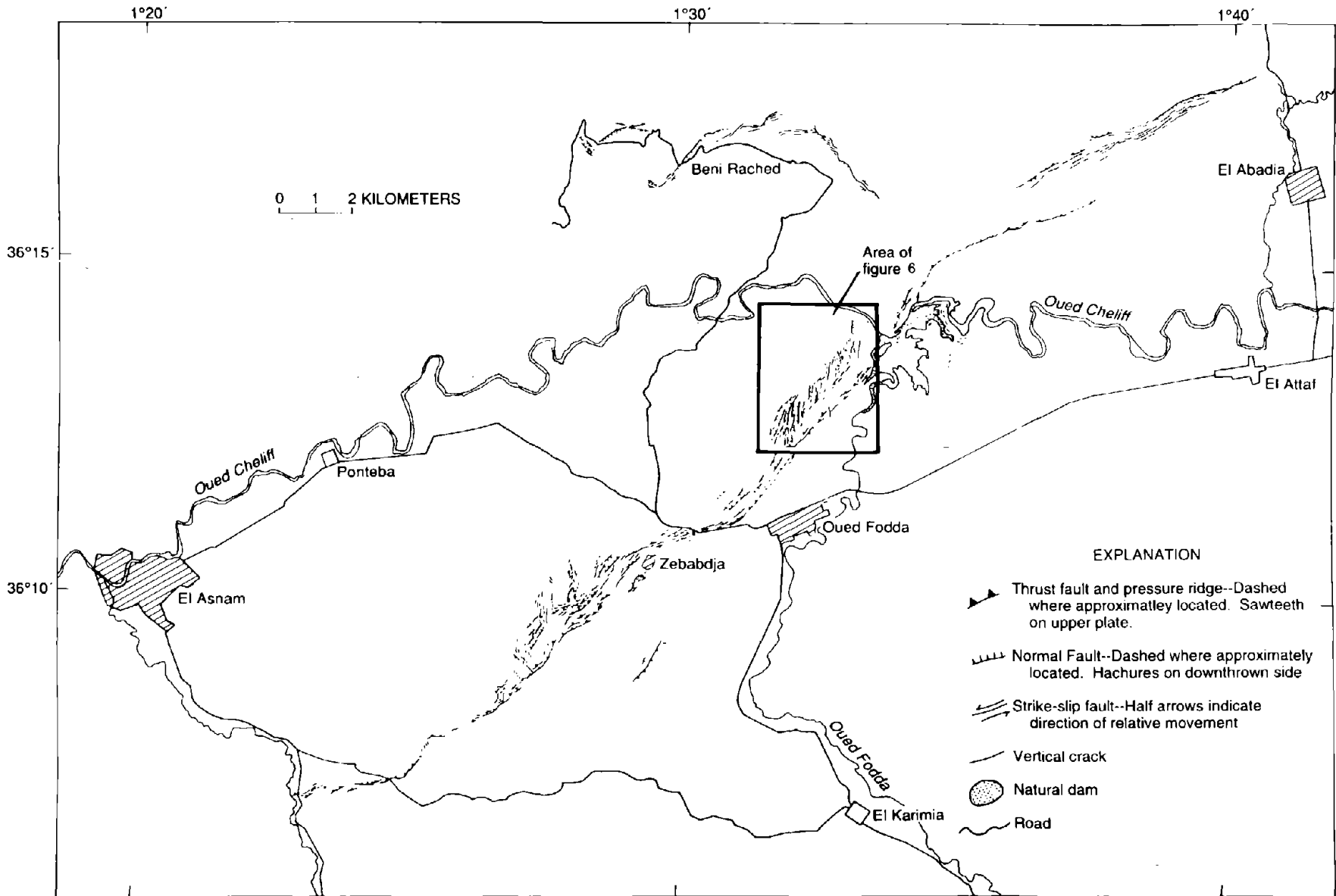


Figure 4.—El Asnam area, Algeria, showing ground cracks from the October 10, 1980, earthquake (after Philip and Meghraoui, 1983).

Few fractures formed south of the fault trace, on the foot-wall; however, along the hanging wall near the main trace, various compressional and extensional fractures and landslides (rotational slumps) formed in a zone as much as 1 km wide.

Several large rotational slumps were created where the surface of the hanging wall near the thrust fault was uplifted and folded. Landslide scarps formed immediately adjacent and parallel to the thrust fault and in the hanging wall as it was uplifted and extended by folding (fig. 5).

Compressional features were related to deformation at the leading edge of the thrust fault and to the regional stress field associated with it. Pressure ridges south of, or in front of, the thrust fault were observed where the fault became imbricate. Extension fractures perpendicular to the fault trace and parallel to the inferred regional direction of maximum principal stress were found primarily on the hanging-wall side. Extension fractures parallel to the fault trace occurred both as simple extension cracks

with little relative displacement and as large grabens (figs. 5, 6).

The patterns of fractures and landslides produced by the 1980 El Asnam and 1989 Loma Prieta earthquakes are similar in the spatial relations of landslides and extension fractures/grabens. Both earthquakes had thrusting source mechanisms and strike-slip displacement components. Also, most of the off-fault fractures and landslides generated by the earthquakes were confined to the hanging walls of the respective faults, and hundreds of discontinuous extension fractures were created, with little vertical or horizontal shear and orientations subparallel to the main fracture zones.

Unlike the 1989 Loma Prieta earthquake, the 1980 El Asnam earthquake produced an extensive echelon graben field at a high angle to the main fault (fig. 7). These grabens are oriented with their long dimensions at an angle of approximately  $35^\circ$  to the fault trace. The echelon pattern was right stepping, consistent with extensional dis-

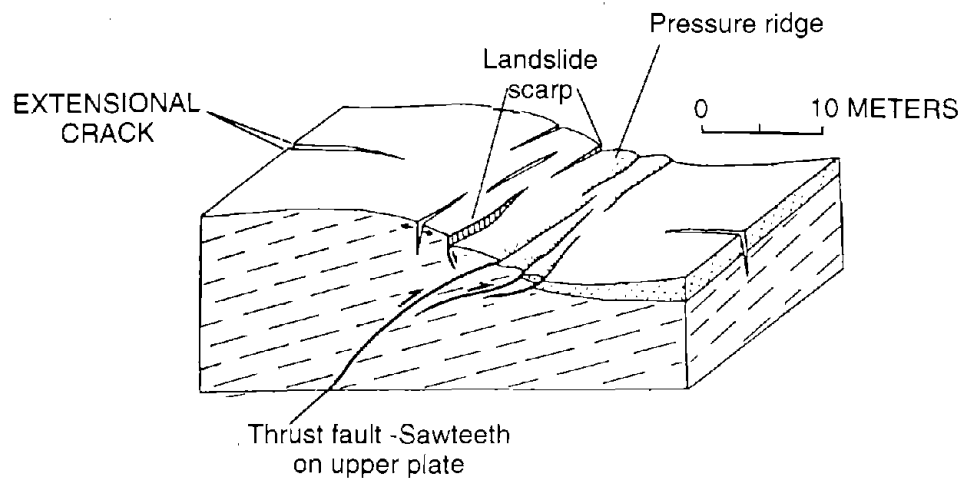


Figure 5.—Block diagram illustrating relation of pressure ridges, extension fractures, and slump scarps to main fault break in 1980 El Asnam earthquake (from Philip and Meghraoui, 1983).

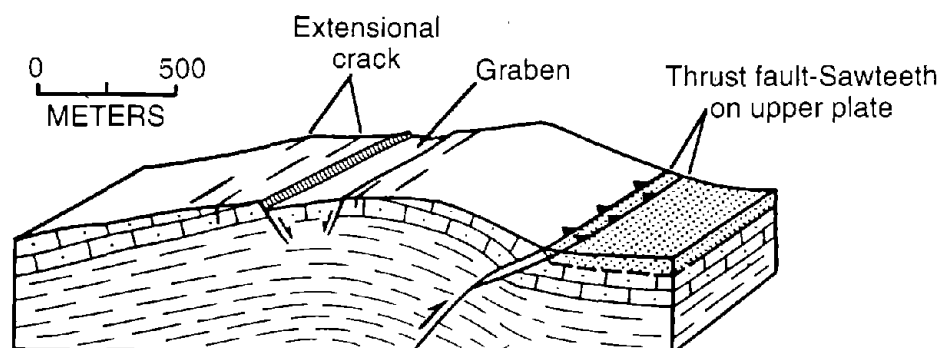


Figure 6.—Block diagram illustrating relation of graben features to main fault break in 1980 El Asnam earthquake (from Philip and Meghraoui, 1983).



placement within a sinistral shear zone. Philip and Meghraoui (1983) observed that displacements across individual graben scarps had horizontal right-lateral components, and they interpreted this echelon zone as due to distributed left-lateral deformation within a 1-km-wide zone northwest of the main fault. They interpreted the right-lateral displacements as due to small counterclockwise rotations of structural elements within the graben zone. Vertical displacements forming the grabens occurred

in response to extension generated by uplift and arching at the surface within the hanging wall of the thrust fault.

Although the 1989 Loma Prieta earthquake produced no such extensive echelon graben fields, horizontal displacements opposite in sense to those of the main fault within this zone in the 1980 El Asnam earthquake have been interpreted similarly to those horizontal displacements opposite in sense to that of the fault source in the 1989 Loma Prieta earthquake (Johnson and Fleming, 1993).

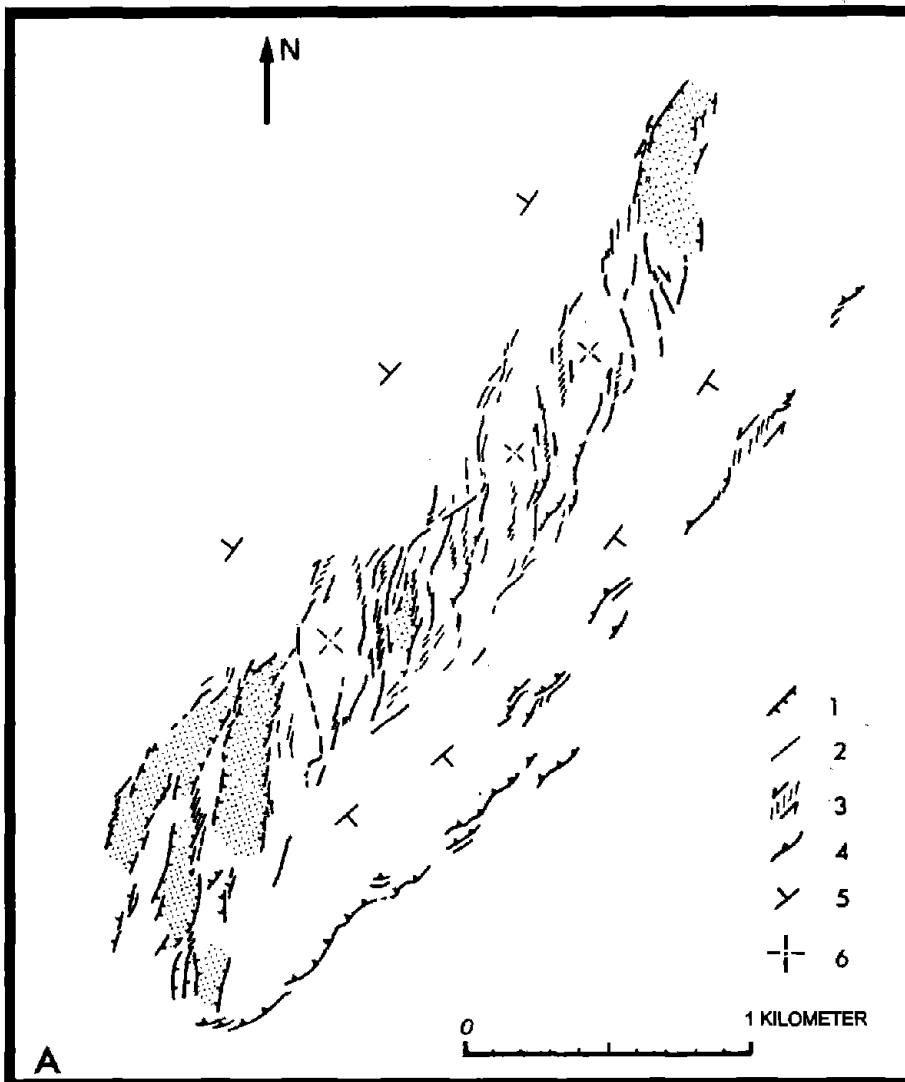


Figure 7.—Features of the 1980 El Asnam, Algeria, earthquake. *A*, Part of main fault trace (see fig. 4 for location), showing echelon graben features aligned at an angle of approximately  $35^\circ$  to fault trace. Right-lateral displacements at graben margins are due to rotation of structural elements within this zone. 1, normal faults, dashed where uncertain, hachures on downthrown side; 2, extension cracks, dashed where uncertain; 3, echelon cracks; 4, thrust faults and pressure ridges, sawteeth on upthrown side; 5, attitude of bedding planes; 6, horizontal stratification. Shaded areas denote downfaulted areas in graben. *B*, Block diagram illustrating relation of echelon graben features to fault and to sense of horizontal shear in this part of rupture zone (from Philip and Meghraoui, 1983).

The fault slip associated with the 1989 Loma Prieta earthquake had subequal components of strike slip and thrusting, whereas that of the 1980 El Asnam earthquake was primarily thrusting, and the senses of strike-slip motion on the two faults were opposite. Bedding in near-surface rocks of the El Asnam area is subparallel to the ground surface and directly reflects the deformation of this and similar past earthquakes, whereas bedding in the Summit Ridge area is more highly deformed. Finally, the 1980 El Asnam earthquake produced a conspicuous surface fault rupture, with surface offsets commonly of more than 2 m and regional uplift of greater than 6 m, whereas the 1989 Loma Prieta earthquake produced little, if any, primary fault rupture on a single trace or narrow zone at the ground surface and a maximum regional uplift of only about 56 cm (Anderson, 1990).

Despite the obvious differences between these two earthquakes, the patterns of surface fracturing and landslide generation have many similarities. Both earthquakes triggered landslides and extension fractures that were concentrated on the hanging walls of the respective fault zones, and both earthquakes produced zones of distributed shear and extension. Johnson and Fleming (1993) interpreted the dominantly left-lateral slip within the Summit Ridge and Skyland Ridge areas as due to rotation between structural blocks responding to right-lateral shear across a wide zone rather than a narrow zone or single fault trace. Their model portrays the San Andreas fault within these areas as a wide zone with horizontal right-lateral deformation distributed completely across it, forming extension fractures that subsequently rotate clockwise and produce predominantly left-lateral shear displacements along structural elements within this zone. They maintained that the fractures unrelated to landslide movement within the Summit Ridge area that formed during the 1989 Loma Prieta earthquake are tectonic and consistent with the source mechanism of the earthquake, and that this deformation is probably typical of movement on the San Andreas fault in this area.

Philip and Meghraoui (1983) similarly interpreted the horizontal right-lateral displacements along graben margins in the central part of the El Asnam rupture zone as due to rotation of structural elements within the echelon graben field, which was itself a result of left-lateral deformation over a wide zone.

In the 1980 El Asnam earthquake, much of the graben formation and many of the extension fractures were probably related to regional and local uplift, which was a maximum of 6 m. According to the model of Johnson and Fleming (1993), the fractures produced by the 1989 Loma Prieta earthquake were probably due to distributed horizontal deformation rather than to regional uplift, which was comparatively small.

Alternatively, Ponti and Wells (1990) attributed most of the extensional deformation across fractures in the Sum-

mit Ridge and Skyland Ridge areas to gravitational spreading. They contended that the displacement vectors across individual fractures generally parallel the regional or local slope direction and that the displacements, which are largely extensional, are governed by gravity-induced downslope movement.

Cotton and others (in press) build a case for bedding-plane slip as the origin for many of the fractures in the Summit Ridge area. They argue that the fractures caused by the 1989 Loma Prieta earthquake and previous earthquakes in this area formed by slip along bedding planes which have undergone flexing due to compression and uplift from the reverse-slip component of the earthquake source mechanism. They also attribute much of the extension across fractures to stretching created by uplift and compression-generated folding.

The models of Ponti and Wells (1990), Johnson and Fleming (1993), and Cotton and others (in press) are all probably applicable in respective proportions. Distributed right-lateral shear across a wide zone, gravitational spreading, and bedding-plane slip may all have been active to a greater or lesser degree and have interacted while also being subjected to deformation by landslides generated by the earthquake. I expect that other such complex patterns will have to be studied from future earthquakes before the relative merits of such models can be properly evaluated.

## SUMMARY

The mapping of fractures triggered by the 1989 Loma Prieta earthquake revealed a complex pattern that was inconsistent with the pattern previously expected from ground rupture within the San Andreas fault zone. The fractures were widely distributed on the southwest side of Summit Ridge within a broad zone, approximately 2.4 km wide by 8.0 km long, extending from near the California Highway 17-Summit Road intersection to Skyland Ridge.

The fracture pattern indicated that many landslides were triggered or reactivated by the earthquake and that fractures unrelated to landslide movement paralleled the regional trend of bedding or other structures. On the basis of the orientation, sense and magnitude of displacement, relation to adjacent landforms, and degree of curvature, most fractures were characterized as related to either landslide movement or regional structure.

The influence of regional structure was apparent in the trend and shape of many landslide margins. The main scarps of several large landslides formed along discontinuities that are part of the regional structure—probably mostly bedding surfaces. Many of the large landslides were distinctly asymmetric in that many right flanks were arcuate where they connected to their main scarps, whereas left flanks were typically straight, parallel to regional structure, and nonarcuate at points of intersection

with main scarps. Some fractures related to regional structure extended across landslide margins and through landslides with little deviation.

Two of the longest fracture zones—the Tranbarger fracture zone and the Church fracture zone—have many of the characteristics of landslide main scarps and may be associated with a landslide that involves much of the southwest flank of Summit Ridge; yet these fracture zones also formed parallel to the regional-structural trend and may have originated along bedding surfaces.

The 1989 Loma Prieta earthquake was similar to other recent earthquakes producing off-fault fractures and triggering landslides near the causative faults. Both the 1986 North Palm Springs, Calif., and 1980 El Asnam, Algeria, earthquakes produced extensive off-fault fractures and landslides. Extensional grabens and landslides were generated by the 1980 El Asnam earthquake, a thrusting event with accompanying left-lateral shear displacement; and the relations between distributed horizontal shear, fracture patterns, and landslide movements in that earthquake appear analogous to those in the Summit Ridge area associated with the 1989 Loma Prieta earthquake. Regional uplift in the 1989 Loma Prieta earthquake was small in comparison with that in the 1980 El Asnam earthquake and probably does not account for much of the extensional deformation in the Summit Ridge and Skyland Ridge areas.

## REFERENCES CITED

- Anderson, R.S., 1990, Evolution of the northern Santa Cruz Mountains by advection of crust past a San Andreas fault bend: *Science*, v. 249, no. 4967, p. 397–401.
- Aydin, Attila, Johnson, A.M., and Fleming, R.W., in press, Coseismic right- and left-lateral surface ruptures and landsliding along the San Andreas and Sargent fault zones during the earthquake, in Ponti, D.J., ed., *The Loma Prieta, California, earthquake of October 17, 1989—ground ruptures*: U.S. Geological Survey Professional Paper 1551–D.
- Clark, J.C., Brabb, E.E., and McLaughlin, R.J., 1989, Geologic map and structure sections of the Laurel 7 1/2' Quadrangle, Santa Clara and Santa Cruz counties, California: U.S. Geological Survey Open-File Map 89–676, 31 p., scale 1:24,000, 2 sheets.
- Cotton, W.R., Fowler, W.L., and Van Velsor, J.E., 1990, Coseismic bedding plane faults and ground fissures associated with the Loma Prieta earthquake of 17 October 1989, in McNutt, S.R., and Sydnor, R.H., eds., *The Loma Prieta (Santa Cruz Mountains), California, earthquake of 17 October 1989*: California Division of Mines and Geology Special Publication 104, p. 95–104.
- Cotton, W.R., Hardin, B.C., and Smelser, M.G., in press, Origin and characteristics of coseismic ground fissures associated with the earthquake, in Ponti, D.J., ed., *The Loma Prieta, California, earthquake of October 17, 1989—ground ruptures*: U.S. Geological Survey Professional Paper 1551–D.
- Johnson, A.M., and Fleming, R.W., 1993, Formation of left-lateral fractures within the Summit Ridge shear zone, 1989 Loma Prieta, California, earthquake: *Journal of Geophysical Research*, v. 98, no. B12, p. 21823–21837.
- McLaughlin, R.J., Clark, J.C., Brabb, E. E., and Helley, E. J., 1991, Geologic map and structure sections of the Los Gatos 7 1/2' Quadrangle, Santa Clara and Santa Cruz counties, California: U.S. Geological Survey Open-File Report 91–593, 48 p., scale 1:24,000, 3 sheets.
- Morton, D.M., Campbell, R.H., Jibson, R.W., Wesson, R.L., and Nicholson, Craig, 1989, Ground fractures and landslides produced by the North Palm Springs, California, earthquake of July 8, 1986, in Sadler, P.M., and Morton, D.M., eds., *Landslides in a semi-arid environment with emphasis on the inland valleys of southern California*: Riverside, Calif., Inland Geological Society, p. 183–196.
- Ouyed, Merzouk, Meghraoui, Mustapha, Cisternos, Armando, Deschamps, Anne, Dorel, Jacques, Frechet, Julien, Gaulon, Roland, Hatzfield, Denis, and Philip, Herve, 1981, Seismotectonics of the El Asnam earthquake: *Nature*, v. 292, no. 5818, p. 26–31.
- Philip, Herve, and Meghraoui, Mustapha, 1983, Structural analysis and interpretation of the surface deformations of the El Asnam earthquake of October 10, 1980: *Tectonics*, v. 2, no. 1, p. 17–49.
- Ponti, D.J., and Wells, R. E., 1990, Origin of surface ruptures that formed in the Santa Cruz Mountains, California, during the Loma Prieta earthquake [abs.]: *Seismological Research Letters*, v. 41, no. 1, p. 17.
- , 1991, Off-fault ground ruptures in the Santa Cruz Mountains, California: ridge-top spreading versus tectonic extension during the 1989 Loma Prieta earthquake: *Seismological Society of America Bulletin*, v. 81, no. 5, p. 1480–1510.
- Sorriso-Valvo, Marino, 1986, Landslide activity in the area of the El Asnam 1980 earthquake (Algeria): *Geologia Applicata e Idrogeologia*, v. 21, no. 2, p. 291–304.
- Spittler, T. E., and Harp, E. L., compilers, 1990, Preliminary map of landslide features and coseismic fissures in the Summit Road area of the Santa Cruz Mountains, triggered by the Loma Prieta earthquake of October 17, 1989: U.S. Geological Survey Open-File Report 90–688, 31 p., scale 1:4,800, 3 sheets.
- Varnes, D.J., 1978, Slope movement types and processes, in Schuster, R.L., and Krizek, R.J., eds., *Landslides—analysis and control*: U.S. National Academy of Sciences, Transportation Research Board Special Report 176, p. 11–33.
- Wells, R.E., in press, Surface ruptures produced by the earthquake; their characteristics, origin, and hazard implications, in Ponti, D.J., ed., *The Loma Prieta, California, earthquake of October 17, 1989—ground ruptures*: U.S. Geological Survey Professional Paper 1551–D.
- U.S. Geological Survey staff, 1989, Preliminary map of fractures formed in the Summit Road-Skyland Ridge area during the Loma Prieta, California, earthquake of October 17, 1989: U.S. Geological Survey Open-File Report 89–686, scale 1:12,000.

1 2 3 4 5 6 7 8 9 10 11 12 13 14 15 16 17 18 19 20 21 22 23 24 25 26 27 28 29 30 31 32 33 34 35 36 37 38 39 40 41 42 43 44 45 46 47 48 49 50 51 52 53 54 55 56 57 58 59 60 61 62 63 64 65 66 67 68 69 70 71 72 73 74 75 76 77 78 79 80 81 82 83 84 85 86 87 88 89 90 91 92 93 94 95 96 97 98 99 100

THE LOMA PRIETA, CALIFORNIA, EARTHQUAKE OF OCTOBER 17, 1989:  
STRONG GROUND MOTION AND GROUND FAILURE

LANDSLIDES

EVALUATION OF COSEISMIC GROUND CRACKING ACCOMPANYING  
THE EARTHQUAKE:  
TRENCHING STUDIES AND CASE HISTORIES

By Jeffrey M. Nolan, Nolan Associates; and  
Gerald E. Weber, University of California, Santa Cruz

CONTENTS

	Page
Abstract .....	C145
Introduction .....	145
Trenching investigations .....	147
Trench 1 .....	147
Trench 2 .....	150
Summary of case histories .....	152
Case history 1: Preearthquake investigation for Loma Prieta Elementary School .....	153
Case history 2: Postearthquake investigation for a family residence .....	156
Case history 3: Postearthquake investigation at Robinwood Ridge .....	156
Case histories: Discussion and conclusions .....	161
General conclusions .....	162
References cited .....	162

ABSTRACT

Although the 1989 Loma Prieta earthquake, centered in Santa Cruz County, Calif., was associated with little observable fault-related surface rupture, it caused abundant coseismic ground cracking throughout the epicentral region. Many homes and other structures in the Santa Cruz Mountains were damaged by ground cracking through their foundations. The purpose of this study is to assess the level of risk associated with this phenomenon and to determine effective means for mitigating the hazard to structures. The study included geologic trenching investigations of two ground-crack systems, using paleoseismic techniques, and a case-history review of geologic-hazard reports for sites that sustained ground cracking.

Geologic trenching across two separate ground cracks revealed well-defined, southwest-dipping shear or slip surfaces associated with normal displacement during the earthquake. In trench 1, earliest Holocene  $^{14}\text{C}$  ages from the basal part of a colluvial wedge on the downdropped side of the shear indicate that slip on this shear surface has been ongoing throughout the Holocene. Evidence for four separate movement episodes are recorded in the stratigraphic section for approximately the past 2,000 years.

Trench 2, located across a ground crack clearly associated with a reactivated landslide, revealed a moderately dipping slip surface overlain by landslide debris, with a small colluvial wedge at the head of the landslide mass. A  $^{14}\text{C}$  age on soil from the basal part of the colluvial wedge indicates initial formation of this landslide about 3.2 ka. The wedge records three additional movements within about the past 2,000 years, including the 1989 Loma Prieta earthquake.

To supplement our trenching studies, we reviewed all geologic-hazard studies on file with the Santa Cruz County Planning Department for the Summit Ridge area of the Santa Cruz Mountains, the area of most severe damage. Trench logs in the 24 reports we selected for study indicated that most large ground cracks (those with more than about 5 cm of displacement) could have been identified in advance by appropriate geologic investigation; however, small ground cracks (those with less than 3–5 cm of displacement) were not so predictable.

We conclude that the geologic hazard due to ground cracking in the Summit Ridge area is moderate but may be reducible to a relatively low level by appropriate site investigations and project design. Comparison of the geomorphic features in the Summit Ridge area with those reported by researchers in other seismically active regions shows that ground cracking may represent a significant geologic hazard in many other localities.

INTRODUCTION

The 1989 Loma Prieta earthquake was associated with right-lateral, reverse-oblique slip on a steeply southwest dipping fault surface that is part of the San Andreas fault system (fig. 1; Dietz and Ellsworth, 1990). The earthquake was associated with little, if any, ground surface rupture attributable to slip on this fault surface (Aydin and others, 1990). Extensive coseismic ground cracking, however, occurred throughout the epicentral region, especially on ridgecrests and steep slopes in the Santa Cruz Mountains (Ponti and Wells, 1991). The geologic hazard

associated with these ground cracks was clearly demonstrated by the damage caused to roads and structures. Where the ground cracks intercepted buildings, the structures commonly were severely damaged or destroyed.

Similar ground cracking has been observed in other large earthquakes, including more severe ground cracking in the same area of the Santa Cruz Mountains during the great 1906 San Francisco earthquake (Lawson, 1908) and ground deformation associated with the 1980 El Asnam, Algeria, earthquake (Philip and Meghraoui, 1983) or the 1980 Irpinia, Italy, earthquake (Cotecchia, 1982). The purpose of this study is to determine whether the ground-cracking hazard observed in the 1989 Loma Prieta earthquake can be mitigated by appropriate geologic site investigations and (or) project design. The study therefore focuses on the predictability of ground-crack locations, displacement magnitudes, and frequency of occurrence, without necessarily determining the mechanisms of the

ground cracking. Our research pursued two avenues of investigation: (1) a geologic trenching investigation of two ground cracks to study the structures responsible for the ground cracks and to evaluate their movement histories, and (2) a case-history study that included a review of all geologic-hazard reports on file with the County of Santa Cruz through November 1990. In all, 24 of these reports included trenching investigations and were therefore selected for detailed study.

In addition to assessing the geologic hazard associated with ground cracks, the trenching studies also provide insight into the seismic history of the study area. In contrast to standard paleoseismic studies, the movement histories derived from coseismic ground cracks record the recurrence of a certain intensity of seismic shaking, rather than movements on a specific fault, and therefore elucidate a different aspect of the seismic record from what is normally seen.

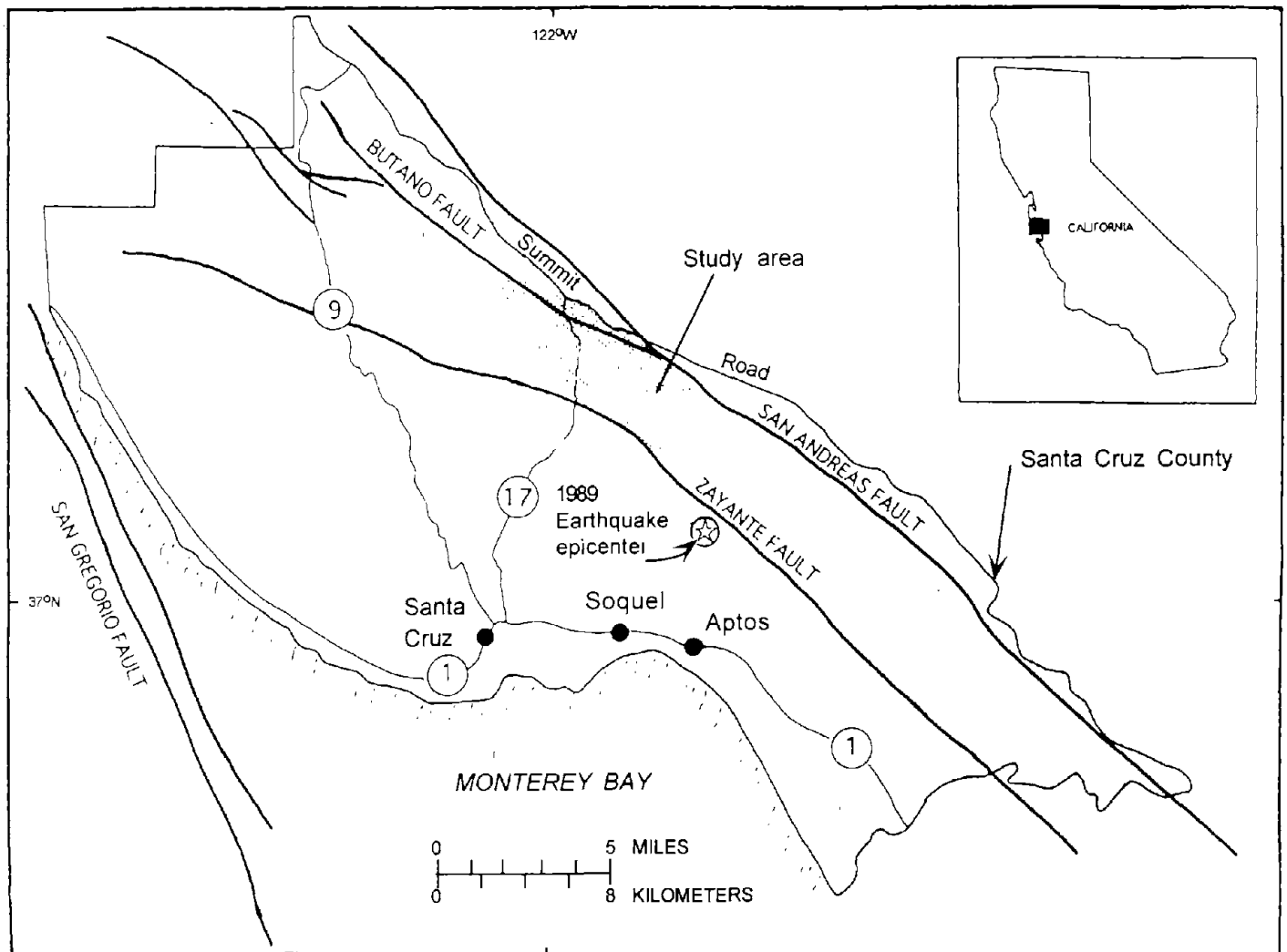


Figure 1.—Loma Prieta area, Calif., showing locations of study area (shaded) and major faults.

Large ground cracks produced by the 1989 Loma Prieta earthquake were commonly associated with recognizable older scarps, an indication of previous movements on structures in the same localities. Such structures had, in fact, been identified before the earthquake, both on photointerpretative maps (Sarna-Wojcicki and others, 1975) and in geologic trenching investigations of linear topographic features in the Summit Ridge area (Foxy, Nielsen, and Associates, 1988; Rogers E. Johnson and Associates, 1988). These structures were formerly interpreted as recently active faults. This section summarizes the results of a trenching investigation of two ground cracks formed by the earthquake; a more complete discussion of the trenching investigations summarized here was presented by Nolan (1992). The  $^{14}\text{C}$  ages of samples from trenches 1 and 2 cited in the following discussions are listed in table 1.

## TRENCH 1

### DESCRIPTION OF TRENCH SITE

Trench 1 was excavated across a 1989 ground crack that occurred along a 10-m-high, 0.5-km-long, northwest-trending scarp along Summit Road, approximately 1.4 km southeast of California Highway 17 (see pl. 5). The trench extends across a topographic basin formed on the downdropped side of the scarp. Surface topography at the trench has been altered slightly by grading for an old alignment of Summit Road.

Measurements in two places along the ground crack yield a consistent slip direction of S.  $32^\circ$  W. and a net slip magnitude of 21 to 24 cm. The 1989 ground crack showed approximately 18 cm of vertical separation and 12 cm of horizontal separation where it crossed the trench. Bedrock in the vicinity is the Vaqueros Sandstone, a sequence of thick-bedded, fine- to medium-grained arkosic sandstone with shale interbeds (McLaughlin and others, 1991). The trench site lies on the southwest-dipping limb of a synclinal fold aligned with Summit Ridge.

### DESCRIPTION OF TRENCH EXPOSURE

The trench revealed Vaqueros Sandstone and shale offset in a normal sense by a southwest-dipping shear surface, possibly aligned with bedding (fig. 2). A sequence of colluvial deposits, 3.6 m thick, overlies the downdropped block. The shear surface is a sharply defined parting lined with a 3- to 4-mm-thick layer of gray clay and a band of iron oxide staining. Slickensides observed on the shear surface have rakes of  $76^\circ$ – $77^\circ$  SE. Movement therefore is dominantly normal, dip slip, with a slight left-lateral component.

The sedimentary deposits overlying the Vaqueros Sandstone bedrock on the downdropped block are entirely colluvial, except for some artificial fill at the surface. The colluvium is deposited in a closed depression that evolved because of multiple offsets on the shear surface in the trench.

## SUMMARY OF MOVEMENT HISTORY

The long-term displacement history on the shear surface in trench 1 is recorded by the colluvial deposits overlying the downdropped block (fig. 2). Deposition of colluvium began approximately 10 ka, as indicated by concordant  $^{14}\text{C}$  ages on charcoal from the basal part of the colluvial wedge (samples CAMS 838, CAMS 839, table 1; see fig. 2 for locations). The colluvium shown on the trench log is divided into two units, older and younger colluvium, on the basis of the occurrence of a buried soil horizon at the top of the older colluvium.

Four discrete displacements are recorded by the most recent colluvial deposits. Although earlier events are likely to have occurred, they are not preserved as discrete stratigraphic offsets in the sedimentary record. The first recorded episode of movement offset the uppermost layer of older colluvium (unit 4, fig. 2). Cumulative vertical separation on the two shears that offset the base of this layer is about 0.4 m, but total throw during the displacement event(s) may be obscured by later ground cracking and (or) subsequent soil-forming processes. This movement was followed by the deposition of unit 3. The shears that offset unit 4 extend into unit 3, indicating some secondary movement, but do not visibly offset the unit 3/4 contact, indicating that unit 3 postdates most of the observed displacement of unit 4. A  $^{14}\text{C}$  age of  $1,400 \pm 180$  yr B.P. (sample CAMS 843, table 1) on soil from the upper part of unit 3 (fig. 2) indicates a latest date for the first recorded episode of movement. A tentative date for this event of about 2 ka was estimated by considering average sedimentation rates in the colluvial section (Nolan, 1992).

The second recorded episode of movement consisted of the displacement of unit 3, followed by the deposition of unit 2. A  $^{14}\text{C}$  age of  $450 \pm 90$  yr B.P. (sample CAMS 842, table 1) on charcoal from a backfilled older ground crack that penetrates unit 3 indicates a latest date for this event. The third and fourth episodes of movement are recorded in the offset of unit 2. The upper and lower contacts of unit 2 both show a cumulative offset of 0.6 m from corresponding sedimentary deposits on the footwall block (unit 1). Because only 0.2 m of this offset is attributable to the 1989 ground crack, this age implies an earlier event(s) constituting about 0.4 m of throw. This earlier event was probably the 1906 San Francisco earthquake, on the basis of indirect evidence (Nolan, 1992, p. 39). Cumulative

Table 1.—<sup>14</sup>C ages of samples from trenches 1 and 2

[Charcoal samples were pretreated by washing in 0.1N HCl to remove carbonates, washing three to four times in 0.1N NaOH until the solution remained translucent (to remove humic acid), and reacidifying in 0.1N HCl. Soil fraction (density less than 2.0 mg/mL), primarily charcoal, was separated from bulk dried soil by using a solution of sodium polytungstate; the floated material was visually inspected for root hairs and washed once in 0.1N HCl (samples were deemed too small for repeated washing).  $\delta^{13}\text{C}$  values from Stuiver and Polach (1977). Ages calculated using Libby half-life of 5.568 yr, according to the conventions of Stuiver and Polach.  $\pm$ , range of precision. Do., ditto]

Sample	Material	$\delta^{13}\text{C}$	$\delta^{14}\text{C}$	$\pm$	Age	$\pm$
					(yr B.P.)	
CAMS 838	Charcoal-----	-25	-710.2	8.6	9950	240
CAMS 839	---Do.-----	-25	-712.2	3.9	10000	110
CAMS 841	---Do.-----	-25	-3.9	.7	< 130	---
CAMS 842	---Do.-----	-25	-53.9	10.2	450	90
CAMS 843	Low-density soil fraction----	-25	-160	18.2	1400	180
CAMS 845	---Do.-----	-25	-325.9	11.9	3170	150
CAMS 1240	---Do.-----	-25	-220.5	13.0	2000	140

throw on the base of the younger colluvial section is 1.2 m, indicating that the initial offset of unit 3 also consisted of 0.6 m of throw.

Evidence for repeated past displacements on the shear surface identified in the trench is unequivocal, although the precise timing of such displacements is only loosely constrained by analytic ages. The evidence indicates two recent movements (in 1989 and 1906), preceded by only two previous episodes of movement in approximately the past 2,000 years. The average recurrence interval for these events is therefore longer than the commonly cited recurrence intervals for major seismic events on the adjacent section of the San Andreas fault: 201 to 281 years for 1906-type events and 88 to 100 years for  $M=7$  earthquakes (Working Group on California Earthquake Probabilities, 1990). Each of the earlier recorded movements may consist of more than one individual movement; in fact, the 1989 and (inferred) 1906 events presently appear as a single stratigraphic offset. Also, events associated with small stratigraphic displacements may have occurred more frequently, but they left little record. A <sup>14</sup>C age of 450±90 yr B.P. on a piece of charcoal lodged in a 1-cm-wide backfilled ground crack may indicate such an event. Each of the episodes of movement discussed above, however, is defined by a relatively large, discrete stratigraphic offset separated by long time periods, indicating a particular event or a series of closely timed events. These relations are incompatible with a history consisting only of more frequent, small displacement events.

We cannot be certain that all the displacements on the shear surface are associated with earthquakes. If the main shear surface in this trench is associated with a landslide, movement could be triggered by intense or prolonged rainfall. Thus, we cannot place upper limits on potential displacements. Nevertheless, information from the trench demonstrates that movements in the past few thousand years have been episodic and have involved limited, incremental displacements. The displacements observed in 1989 and postulated for 1906 (0.2 and 0.4 m, respectively) provide a realistic range for coseismic offsets, because these events probably represent the upper limit of ground shaking intensity and duration in this locality.

## TRENCH 2

### DESCRIPTION OF TRENCH SITE

Trench 2 was excavated across 1989 ground cracks that outlined the head of a preexisting landslide mass in the Burrell landslide, on the southwest flank of Summit Ridge (see pl. 5). The ground crack around this mass showed 7 to 10 cm of horizontal extension and a few centimeters of vertical separation. The trench site is underlain by the mudstone unit of the Butano Sandstone (Clark and others, 1989), a sequence of dark-gray, thin-bedded, nodular mudstone with interbedded arkosic sandstone. Bedding was not visible in the trench. The site is approximately 200 m southwest of the mapped trace of the San Andreas fault (see pl. 5).



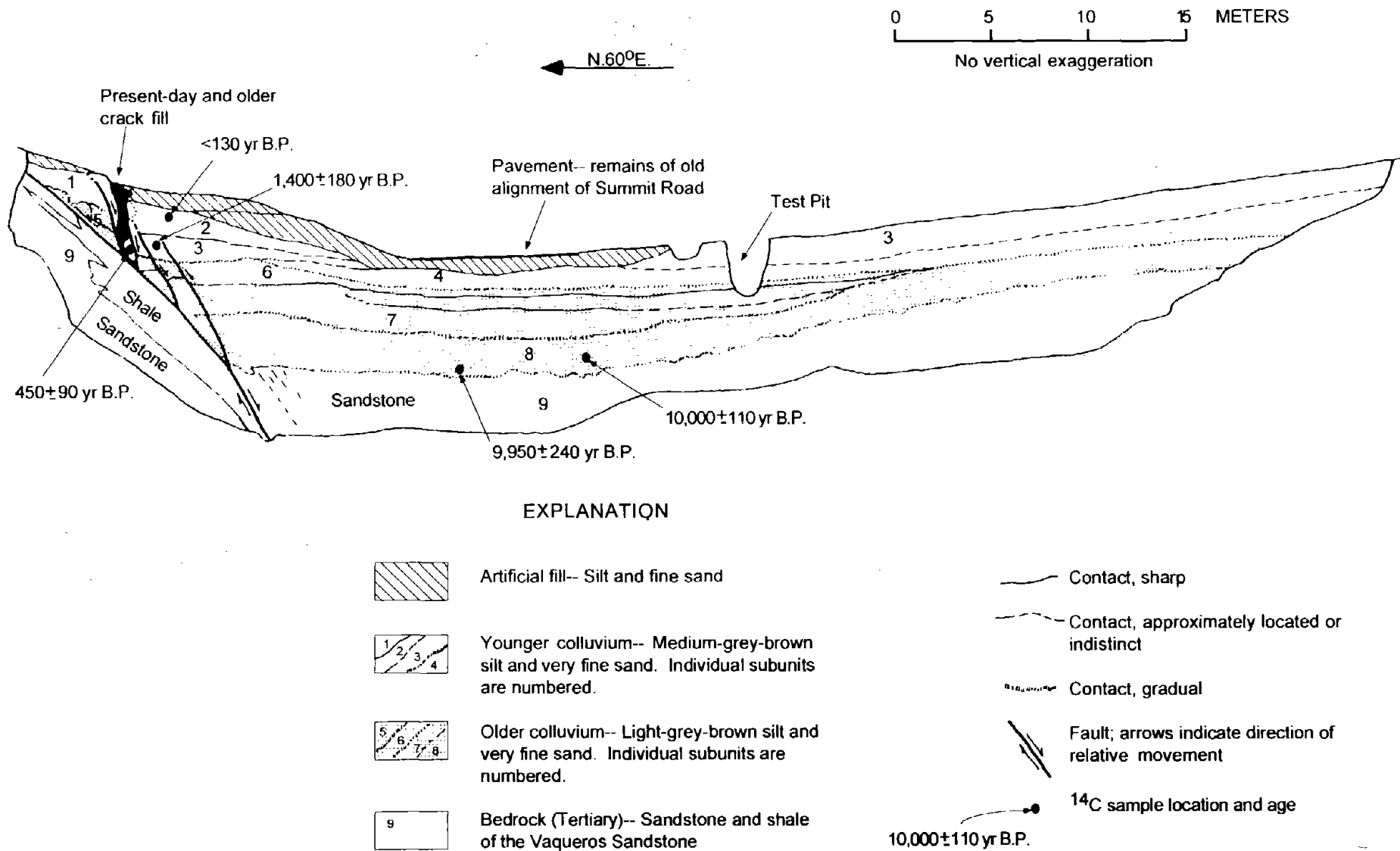


Figure 2.—Log of trench 1, which was excavated across a ground crack along base of a 0.5-km-long, northwest-trending scarp at summit of the Santa Cruz Mountains. Trench exposed a southwest-dipping slip surface and a 4-m-thick colluvial wedge overlying downdropped block. Earliest Holocene  $^{14}\text{C}$  ages on soil from basal part of colluvium and offset stratigraphic layers indicate that movement on this slip surface has been ongoing throughout the Holocene, including at least three discrete events in the past approximately 2,000 years.

### DESCRIPTION OF TRENCH EXPOSURE

The trench exposed a shear surface dipping 32° SW. and striking approximately N. 40° W. (fig. 3). Bedrock below the shear surface is dark-gray shale. Above the shear surface, bedrock consists of broken and disaggregated sandstone and shale that we interpreted as landslide debris (unit 8, fig. 3). Overlying this bedrock debris is a wedge of colluvial sedimentary deposits at the base of the landslide scarp (units 1–7, fig. 3). These colluvial sedimentary deposits consist of fine-grained sand and silt and varying amounts of pebble- to cobble-size, angular clasts of sandstone and siltstone.

### SUMMARY OF MOVEMENT HISTORY

The colluvial wedge is offset by a steeply dipping slip surface that branches upward from the main slip surface (A, fig. 3). This slip surface is moderately well defined at the base of the colluvial section, where it offsets units 6 and 7, but is visible only as a flexure in the coarser grained overlying units (fig. 3). The amount of flexure of unit 4, about 0.5 m, was estimated by comparing the flexured bed with the smoothly concave modern depositional surface; the estimated flexure is comparable to the amount of discrete offset on unit 7. Comparison of the geometry of unit 2 with the present surface profile shows about 0.2 m of flexure, about half as much as for unit 4, indicating that the total displacement of 0.5 m at the base of the section (units 6, 7) is due to at least two separate events. The upper surface of unit 1 shows no flexure and no ground cracks or other evidence for movement on this slip surface in 1989. These observations therefore suggest at least two pre-1989 movements of about 20 to 30 cm each after the initial landslide movement.

Displacement due to movement during the 1989 Loma Prieta earthquake occurred southwest of the colluvial wedge (slip surface B, fig. 3). Movement occurred on a fracture surface that shows a cumulative displacement (vertical separation) on a sandstone/shale contact of 24 cm. This displacement is larger than the 1989 vertical separation measured at this locality, indicating earlier movement(s), the timing of which is unconstrained.

A  $^{14}\text{C}$  age of  $3,170 \pm 150$  yr B.P. (sample CAMS 845, table 1) on soil from the basal part of unit 7 (fig. 3), approximately 6 to 10 cm above bedrock, dates the onset of colluvial deposition and thus approximates the date of the original landslide movement. This age is compatible with the state of preservation of the surficial landslide features.

A second soil sample from unit 3 (fig. 3) yielded a  $^{14}\text{C}$  age of  $2,000 \pm 140$  yr B.P. (sample CAMS 1240, table 1). The upper surface of unit 3 conforms to the geometry of overlying beds (unit 2) and therefore postdates the ini-

tial displacement of units 4 through 6, although it is unclear whether unit 3 was deposited entirely after the initial displacement of unit 4 or whether the lower part of unit 3 was already in place at the time of the initial movement. Nevertheless, this age suggests that the initial offset of units 4 through 6 occurred shortly before 2 ka. The second movement that offset unit 2 occurred after 2 ka. No information regarding the timing of earlier events on the fracture reactivated by the 1989 earthquake is available.

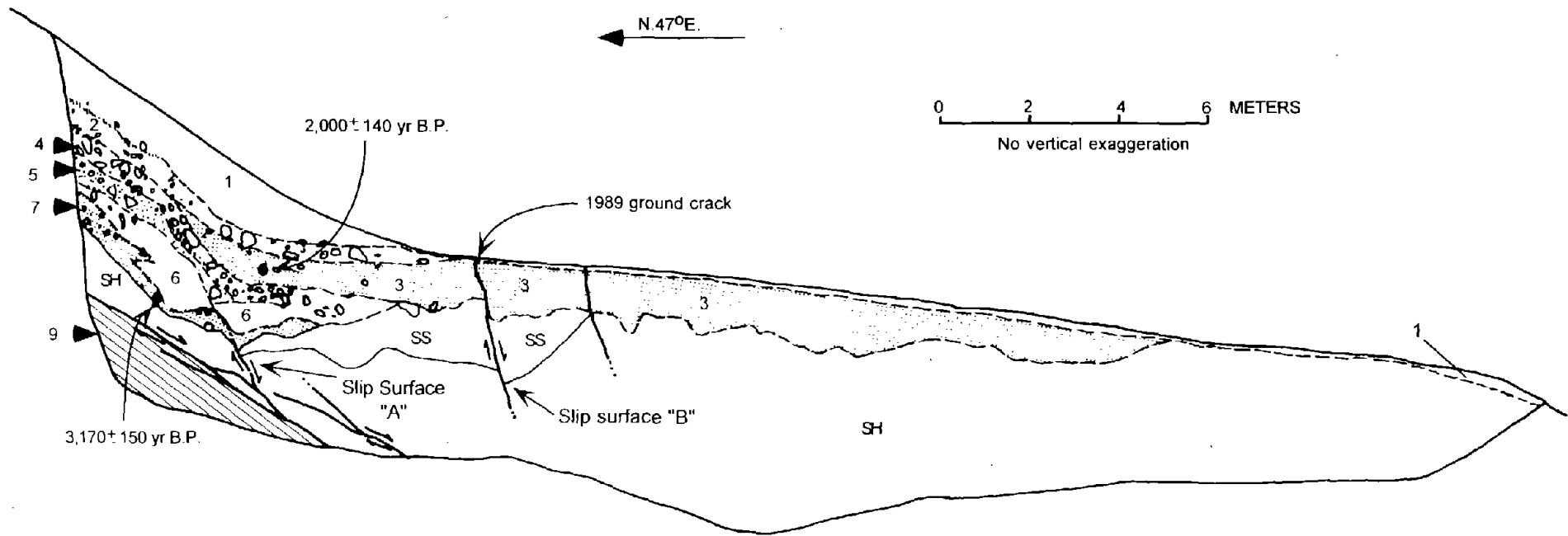
On the basis of these observations, we conclude that the Burrell landslide has been reactivated at least three times since its initial failure, including the movement in 1989. This number of movements is a minimum because each episode of offset preserved in the stratigraphic record could have been produced by more than one movement on the shear surface and because some displacement events may have left no record in the part of the landslide examined in the trench. Cumulative throw on shear surfaces in the trench in the past 3,000 years (after the initial landslide formation) has been less than 1 m.

### SUMMARY OF CASE HISTORIES

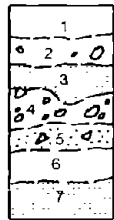
This section presents the results of a case-history study of coseismic ground cracking caused by the 1989 Loma Prieta earthquake. The purpose of this study was to evaluate whether the ground-cracking hazard posed to future development in the epicentral region can be mitigated by appropriate geologic investigation before site development. Specifically, we examined existing geologic-hazard investigations of damaged properties to answer two questions: (1) Can the locations of future coseismic ground cracks be reliably predicted; and (2) where potential ground-crack locations cannot be avoided, can probable displacements be constrained to provide mitigating design parameters?

We reviewed all geologic-hazard reports on the Summit Ridge area of the Santa Cruz Mountains filed with the County of Santa Cruz before mid-November 1990. These reports were prepared by private consultants for properties in steeply sloping terrain or in State-delineated hazard zones surrounding active or potentially active faults (Alquist-Priolo Special Studies Zones). Reports examined included those completed both before and after the earthquake. These reports were of varying quality, reflecting the varied backgrounds and experience of the geologists preparing them.

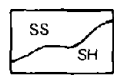
Of a total of 81 available reports, 23 included records of subsurface (trench) exposures and were thus selected for more detailed review. One additional geologic report, conducted for Loma Prieta Elementary School on the north side of Summit Road in Santa Clara County, was included in our review because its geologic setting is identical to that of adjacent parts of Santa Cruz County. The proper-



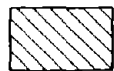
EXPLANATION



Colluvium-- Grey-brown fine sand and silt, with varying amounts of pebble- to cobble-size, angular clasts of sandstone and shale. Individual subunits are numbered



Landslide debris derived from the Butano Sandstone-- Sandstone (SS) and shale (SH), sheared and broken



Bedrock (Tertiary)-- Shale of the Butano Sandstone

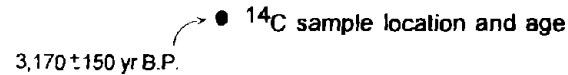
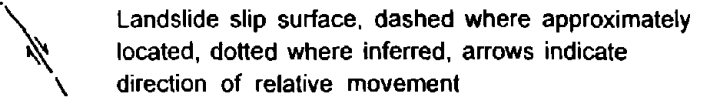
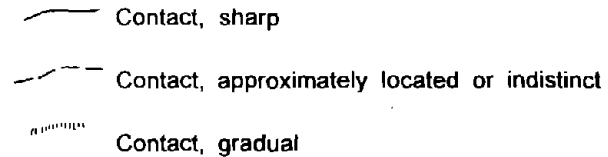


Figure 3.—Log of trench 2, which was excavated across a ground crack following crown of a preexisting landslide mass. Offset of layers within colluvial wedge at head of landslide and 1989 ground-cracks indicate that at least three reactivations of this landslide have taken place in the past approximately 2,000 years.

ties for which these reports were prepared are listed in table 2, and the locations of all 24 sites are shown on plate 5. All reports are on file with the County of Santa Cruz by assessor's parcel number (APN, table 2) and are available to the public.

Most of the reviewed reports contained either clear or probable evidence of ground cracking that predated the 1989 Loma Prieta earthquake; of the 24 reports reviewed, 14 contained definite evidence of previous ground cracking, 5 contained probable evidence for previous ground cracking, 3 were indeterminate, and 2 contained no evidence of previous ground cracking. Those sites considered to show definite evidence for previous ground cracking are those where relations shown in the trench logs require previous movements or where the author(s) specifically stated that previous movement was indicated by the exposure. The evidence for previous movement includes older ground cracks backfilled with surface sedimentary deposits, 1989 fissures that connected to shear surfaces with much larger stratigraphic separations at depth, and slip-parallel shear fabrics too well developed to have formed entirely in the recent slip event.

The "probable" category was applied to sites where information included in the trench logs or in the report text indicated previous ground-cracking episodes, although such information was not discussed by the author(s). The "indeterminate" category was applied to sites where information on the trench log was uninterpretable or judged to be incomplete. Of the two reports that contained no evidence for previous ground cracking, one omitted any trenches dug to intercept existing ground cracks or surface lineaments, and the other stated that no evidence of preexisting ground cracking existed where the cracks caused by the 1989 Loma Prieta earthquake crossed the trench, although the relations depicted in one trench indicated that preexisting cracks were present nearby.

The following sections review three case histories chosen to illustrate the type of subsurface relations observed in trenches and to describe the associations between subsurface expression and displacements during the 1989 Loma Prieta earthquake. We note, however, that our conclusions are based on the entire data base, rather than on only the three case histories presented here. These case histories include one preearthquake investigation for Loma Prieta Elementary School and two postearthquake studies of residential properties. The figures accompanying this part of the paper are reproduced from the originals.

#### **CASE HISTORY 1: PREEARTHQUAKE INVESTIGATION FOR LOMA PRIETA ELEMENTARY SCHOOL**

Geologic investigations for Loma Prieta Elementary School were mandated by the Office of the California

State Architect, as directed by the Alquist-Priolo Act, to evaluate the potential ground-rupture hazard due to faulting. The school is located on the northeast side of Summit Road, approximately 4 km east of California Highway 17 (case history 1, pl. 5). The investigation (Rogers E. Johnson and Associates, 1989) (loc. 24, table 2) consisted of more than 360 m of backhoe trenching.

Bedrock in the area is the Vaqueros Sandstone, a sequence of fine- to medium-grained sandstone with lesser interbedded shale and mudstone, of Oligocene and early Miocene age. The school site was extensively graded before construction, and so Quaternary deposits had been stripped from many of the areas trenched, leaving no datum with which to evaluate fault activity. Thus, several of the faults identified in the trenches could not be evaluated with regard to Holocene activity.

The locations of the school buildings and trenches, and of faults with demonstrable offset of Quaternary strata, are shown in figure 4. Pregrading aerial photographs of the site show a set of northeast-trending ridges and valleys approximately parallel to the nearby San Andreas fault. The identified faults coincide with topographic breaks that follow the margins or axes of valleys that existed before grading for the school.

Logs of trenches 3 and 4 are shown in figure 5. Trench 3 shows a colluvium-filled basin formed by downdropping and rotation of bedrock blocks along two well-defined slip surfaces. No slickensides were noted along these slip surfaces, although consistent normal separations on strata were observed. Both slip surfaces showed evidence for more than one episode of movement, as indicated by increasing stratigraphic separation on successively older layers.  $^{14}\text{C}$  ages on disseminated carbon from soil samples indicate that approximately 0.75 m of normal separation has occurred on the easternmost slip surface during the past 4.7 to 2.0 ka. This trench was discussed in more detail by Rogers E. Johnson and Associates (1989).

The log of trench 4 (fig. 5) depicts a type of subsurface expression of ground cracking common in the Summit Ridge area. The zone of offset is not marked by any clearly recognizable shear surface but, instead, by a near-vertical, indistinct contact between weathered bedrock and colluvium. The absence of a well-defined slip surface is due to extensional movement that produces open cracks without mechanical reduction of materials along the parting surface. In this trench, the contrast between weathered bedrock and colluvium is subtle, and the offset was not recognized during the initial trench logging. This exposure highlights the caution that must be exercised when examining subsurface exposures of extensional ground cracking.

Displacement of the ground surface during the 1989 Loma Prieta earthquake occurred along the trend of the slip surface recognized in the middle of trench 3 (fig. 4). This deformation was not uniform along the projected surface fault trace but was greatest in the vicinity of class-

Table 2.—*Sites of properties where geologic-hazard reports were selected for detailed review*

[All reports are public information on file with the County of Santa Cruz by assessor's parcel number (APN). Evidence for previous ground movement: D, definite; I, indeterminate; N, none; NGC, no ground cracks; P, probable. Do., ditto]

Locality (pl.6)	APN	Address	Previous Movement	Consultant
<b>Postearthquake Reports</b>				
1	97-101-32	25295 Old San Jose Road	N	Applied Soil Mechanics.
2	96-271-09	24620 Miller Road	D	Upp Geotechnology.
3	96-291-07	23430 Sunset Drive	I	J.W. Leonard, C.E.
4	96-131-36	23080 Summit Road	P	Jo Crosby and Associates.
5	96-151-13	23700 Morrell Cut Off	D	William Cotton and Associates.
6	96-311-23	23484 Bel Aire Ct.	I	Jo Crosby and Associates.
7	98-281-12	25200 Adams Road	P	Michelucci and Associates.
8	98-151-04	15052 Stetson Road	I	Geoforensics.
9	98-271-11	25734 Adams Road	D	Robertson Geotechnical.
10	97-161-03	25507 Old San Jose Road	NGC	Freeman-Kern Associates.
11	96-292-34	23048 Evergreen Lane	D	Upp Geotechnology.
12	97-071-20	16000 Redwood Lodge Road	P	Hydro-Geo Consultants.
13	96-283-06	18338 Las Cumbres	D	William Cotton and Associates.
14	96-382-04	22494 Citation Drive	D	Geoforensics.
15	96-131-22	23136 Summit Road	D	Foxx-Nielsen and Associates.
16	96-111-01	23201 Old Santa Cruz Highway	D	Pacific Geotechnical.
17	97-231-09	16010 Stetson Road	D	G.E. Weber and Associates.
18	97-231-10	16020 & 16060 Stetson Road	D	Do.
	97-231-11			
19	97-231-12	16026 & 16044 Stetson Road	D	Do.
	97-231-13			
20	96-061-11	17774 Old Summit Road	D	Do.
<b>Preearthquake Reports</b>				
21	96-281-13	23426 Sunset Road	P	K.W. Price.
22	96-121-21	Schultheis Road	P	G.E. Weber and Associates.
23	95-021-21	Summit Road	D	JCP Engineers.
24	Santa Clara County	23845 Summit Road (Loma Prieta School).	D	Rogers E. Johnson and Associates (1988).

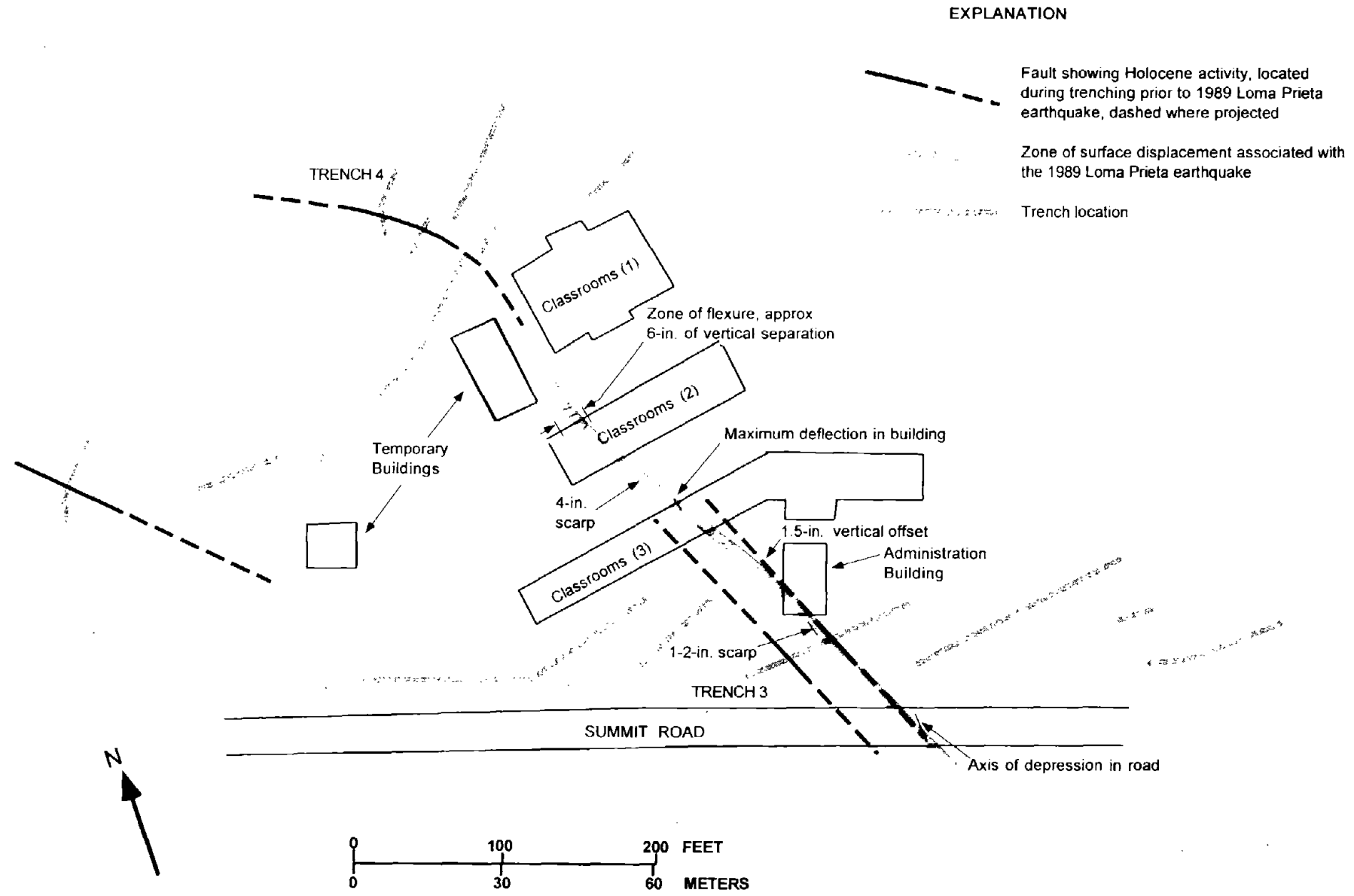


Figure 4.—Simplified site plan for Loma Prieta Elementary School, showing locations of paleoseismic trenches excavated before 1989 Loma Prieta earthquake, suspected active faults identified in trenches, and ground displacement that occurred during the earthquake. Modified from Rogers E. Johnson and Associates (1989).

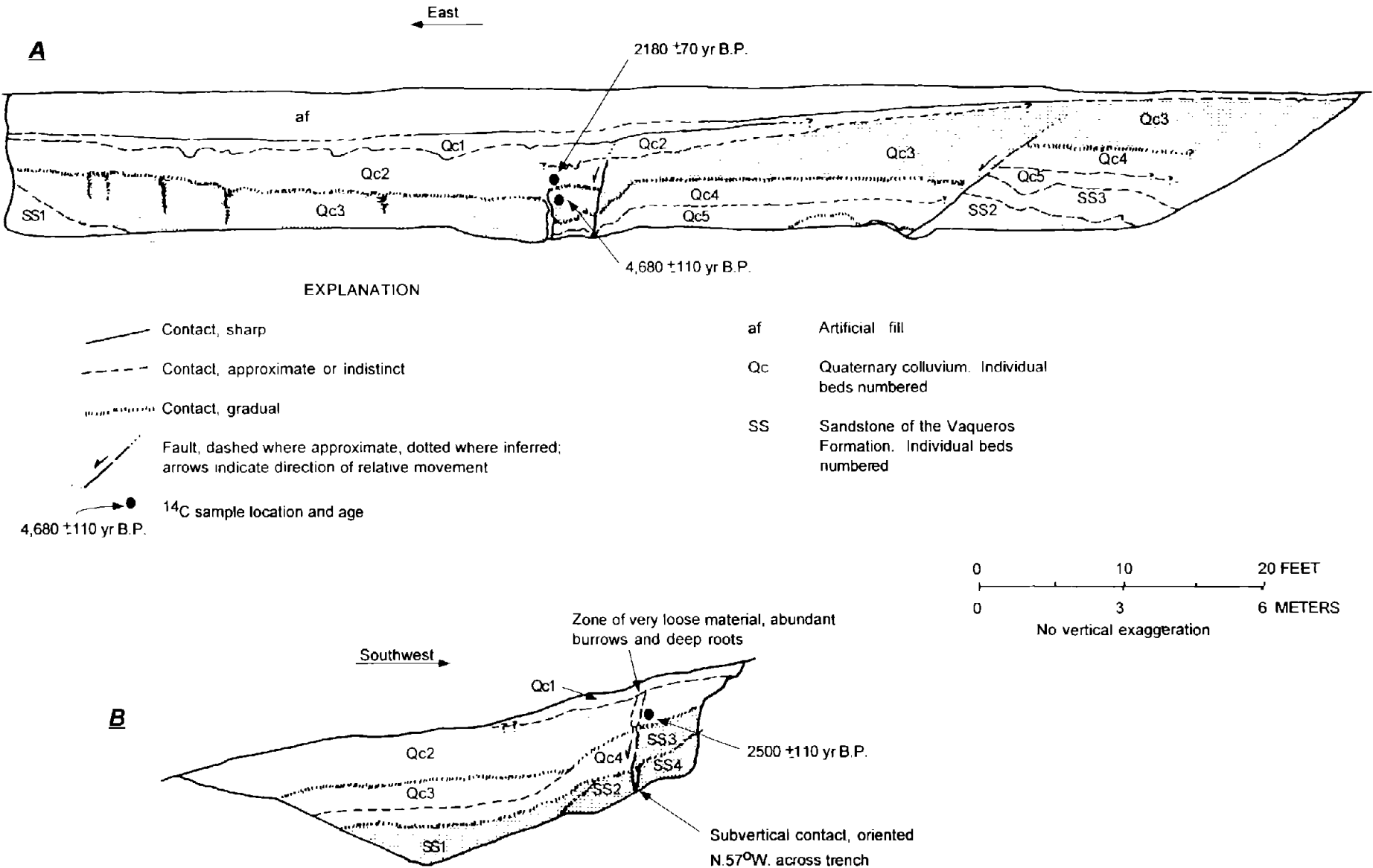


Figure 5.—Logs of trenches 3 (A) and 4 (B), showing evidence for active faulting found during preearthquake trenching investigation. Fault in center of trench 3 was reactivated during 1989 Loma Prieta earthquake, causing as much as 15 cm of down-to-the-northeast displacement under classroom unit 2. Modified from Rogers E. Johnson and Associates (1989).

room building 2 and decreased to the northwest and southeast. The deformation occurred as flexure of the ground surface, northeast side down, probably as a result of normal slip at depth. Maximum vertical displacement was approximately 15 cm across a zone of flexure about 3 m wide.

As a result of the geologic investigation, the consultant recommended that the school site be abandoned. This recommendation, however, was not followed by the school board, and so the school was in use, though not in session, when the earthquake struck. The administration building and classroom units 2 and 3 were moderately to severely damaged by ground cracking, but no structural collapse took place. The school was subsequently abandoned.

### CASE HISTORY 2: POSTEARTHQUAKE INVESTIGATION FOR A FAMILY RESIDENCE

Weber and Associates (1990a) investigated the site of a single-family residence near the intersection of Summit Road and California Highway 17 (see pl. 5; loc. 20, table 2). The house and property were severely damaged by strong seismic shaking and a broad, arcuate zone of ground cracking (fig. 6). The ground cracks had extensional displacements of 3 to 30 cm and southwest-side-down vertical separations of as much as 25 cm, reflecting movement of the earth materials toward the steep-walled drainage on the southwest.

Trenches 5B and 6 (fig. 7) were excavated across the ground cracks. In trench 5B, the ground cracks coincided with a large, colluvium-filled graben formed by normal displacement on bounding slip surfaces, indicating a history of displacement at this site. Previous episodes of movement were also indicated by trench 6, where 1989 ground cracks were associated with larger displacements of bedrock stratigraphy and soil horizons, as well as older generations of infilled ground cracks (fig. 7).

In trench 5B, a 6-in.-wide ground crack at the surface could not be traced into the subsurface (fig. 7). The subsurface material here (unit 2) is a massive, very loose silty sand that evidently accommodated extension as distributed shear throughout, rather than as the single open crack seen at the surface. Similar behavior was observed in loose, granular sediment in other case-history localities. The disappearance of ground cracks, even very large ones, at shallow depth should not therefore be taken as conclusive evidence that no deeper seated failure has occurred. This point is particularly important at sites where the potential for catastrophic slope failure is being evaluated. In more cohesive materials, such as those in trench 6, surficial cracks generally persist at depth (fig. 7).

Trench 5A is a northward continuation of trench 5B (figs. 6, 7). A second colluvium-filled basin was exposed in this trench. Although no ground cracks were observed at the surface in this locality (except for a few cracks due

to fill failure under the driveway), careful inspection of slip surfaces exposed in the trench revealed 3 to 6 mm of extension across shear surface a (fig. 7) that was not visible at the surface.

The processes responsible for forming and filling the colluvial basin in trench 5A began approximately 6 ka, as indicated by a  $^{14}\text{C}$  age on a bulk soil sample from the base of unit 2 (fig. 7). Like the Loma Prieta Elementary School site, this parcel was graded to form a level pad before development. Historical aerial photographs and old topographic maps, however, indicate a preexisting ridge through the central part of the site, corresponding to the bedrock high between the two grabens. The axes of the adjacent topographic troughs coincide with basins identified in the trenches.

Although one of the smaller ground cracks ruptured the foundation, the home on this site was destroyed primarily by seismic shaking. The ground-crack system trending through trenches 5B and 6 was considered particularly dangerous because the cracks dip toward a steep slope (50- to 80-percent gradient) and could therefore facilitate landsliding, with potentially catastrophic displacements.

### CASE HISTORY 3: POSTEARTHQUAKE INVESTIGATION AT ROBINWOOD RIDGE

Robinwood Ridge is a long, narrow, northwest-trending ridge in the southeastern part of the study area (case history 3, pl. 5). Five contiguous parcels were investigated by G.E. Weber and Associates, Inc. (loc. 17, table 2), covering a 0.5-km-long stretch of the ridgetop. The investigation included 12 trenches totaling about 150 m in length. The complete geologic maps and trench logs are too voluminous to reproduce here, but a small part of the mapped area (fig. 8) and two trench logs (fig. 9) are included for illustrative purposes. Observations in all the trenches are summarized below.

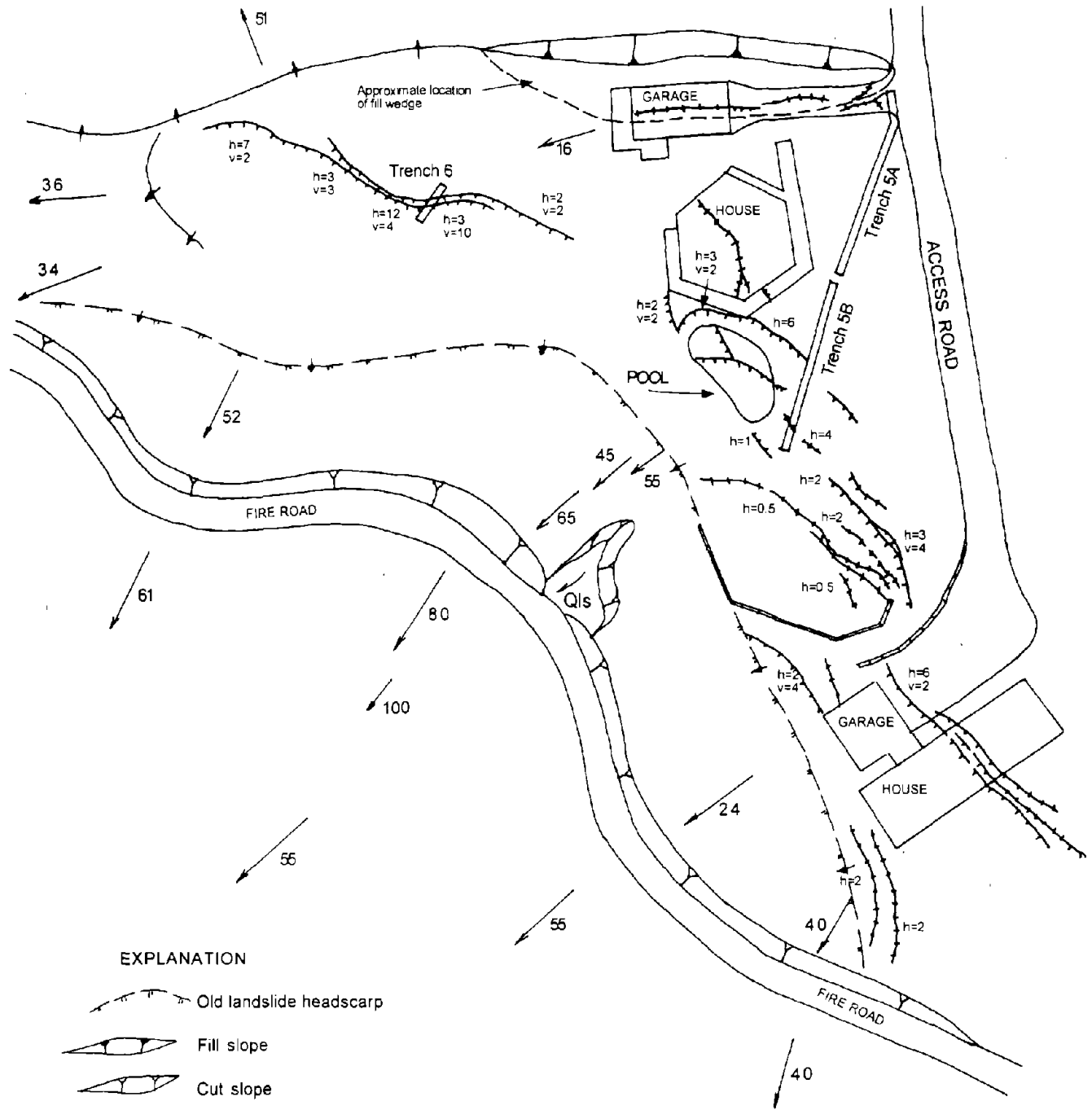
In general, 1989 ground cracks were associated with evidence of previous episodes of movement in the subsurface, commonly expressed as zones of fine, parallel, discontinuous fractures or shears that form a "shear fabric," with a grain parallel to the recent ground cracks. The shear fabric is commonly accompanied by older, infilled ground cracks that appear as thick, continuous veins or thin, discontinuous stringers of darker fill material. There may be little or no observable displacement of stratigraphic markers where the movement is primarily extensional, but large vertical separations occur elsewhere. The log of

Figure 6.—Area of case history 2 (see pl. 5 for location), showing pattern and dimensions of ground cracking that occurred during 1989 Loma Prieta earthquake. Trenches across ground-cracks showed evidence for many previous episodes of ground cracking in the same places. From G.E. Weber and Associates (1990a).

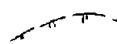
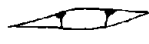

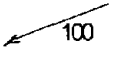
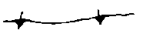
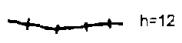
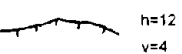

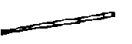



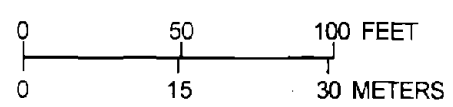
EVALUATION OF COSEISMIC GROUND CRACKING ACCOMPANYING THE EARTHQUAKE

C157



EXPLANATION

-  Old landslide headscarp
-  Fill slope
-  Cut slope
-  Slope direction and grade in percent
-  Top of steep slope
-  h=12 Crack showing only horizontal movement, width in inches
-  h=12  
v=4 Crack showing horizontal and vertical separation, separations shown in inches
-  Qls Landslide, of Quaternary age, arrow indicates direction of movement
-  Retaining wall
-  Trench location



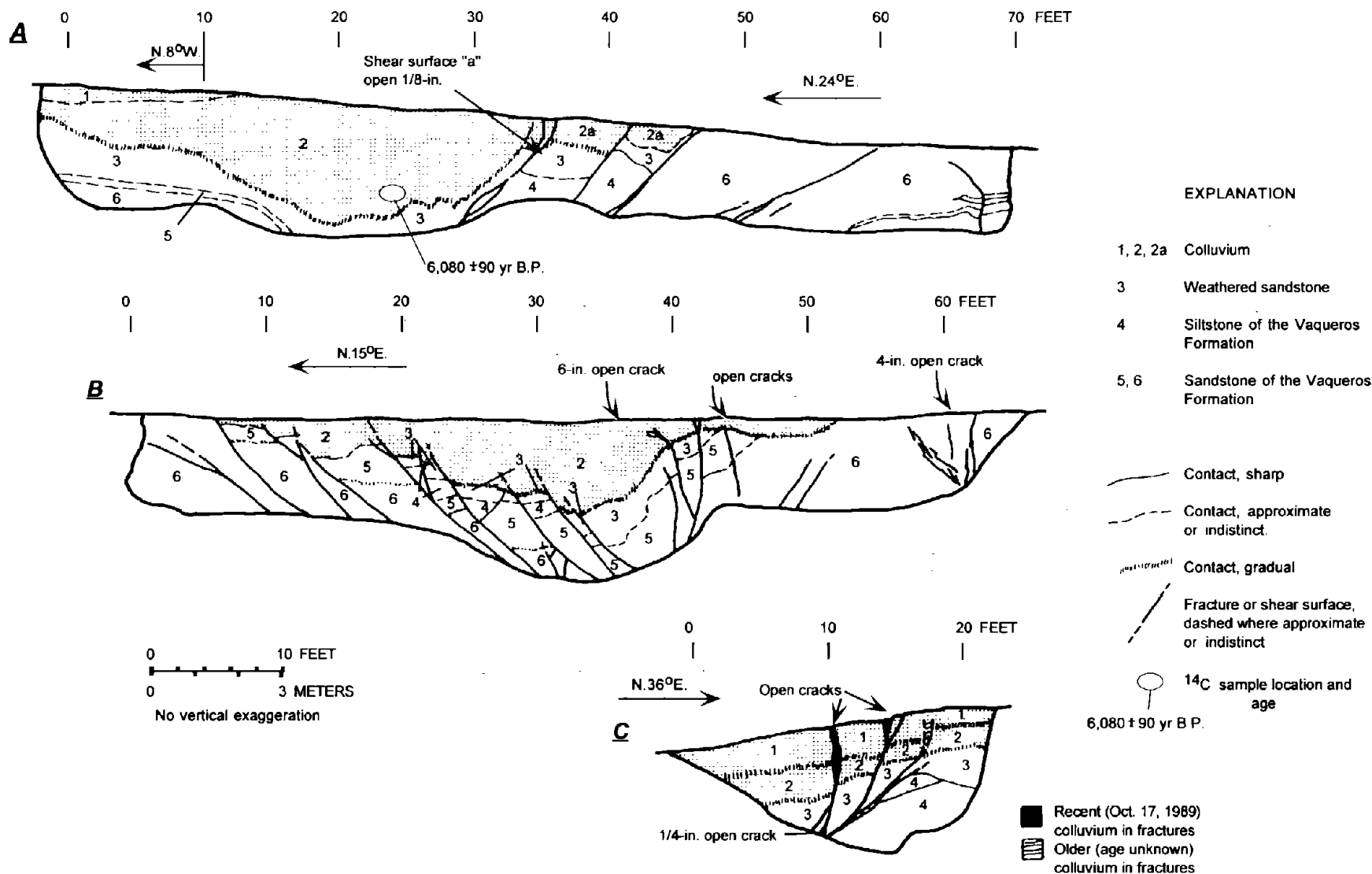


Figure 7.—Logs of trenches 5A (A), 5B (B), and 6 (C) across area of major ground cracks. A, Trench 5A crosses a colluvium-filled graben that was not perceptibly reactivated in 1989. B, Trench 5B shows a second colluvium-filled graben where ground cracks cross trench, indicating many previous episodes of ground cracking in the same place. C, Trench 6 shows bedrock and soil offsets much larger than 1989 displacements, clear evidence for earlier episodes of movement. From G.E. Weber and Associates (1990a).

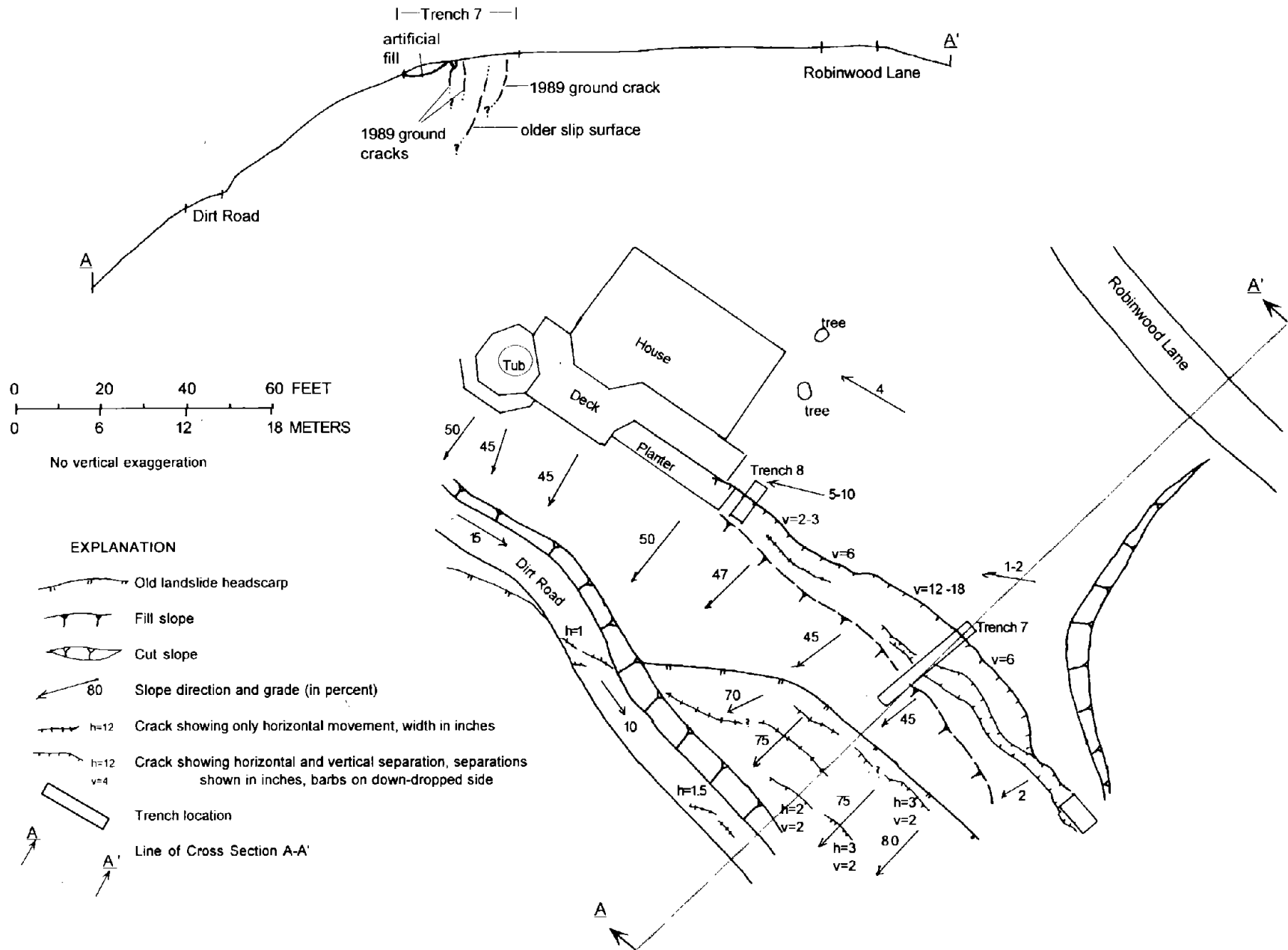
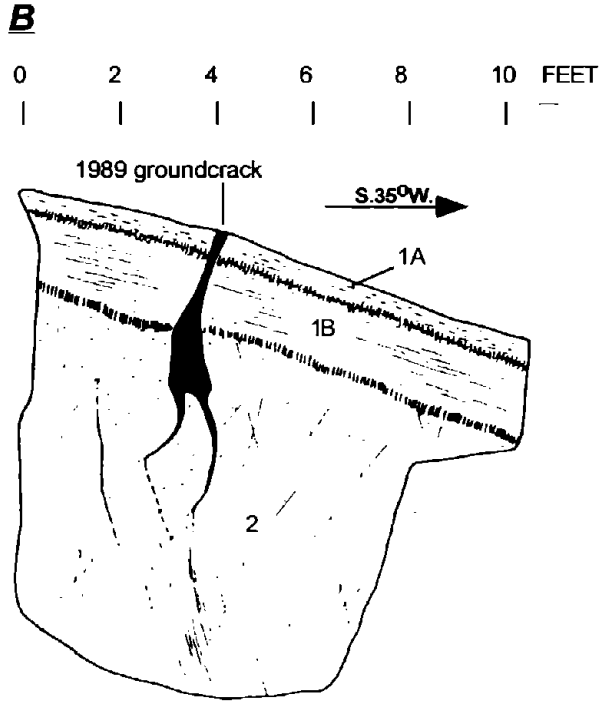
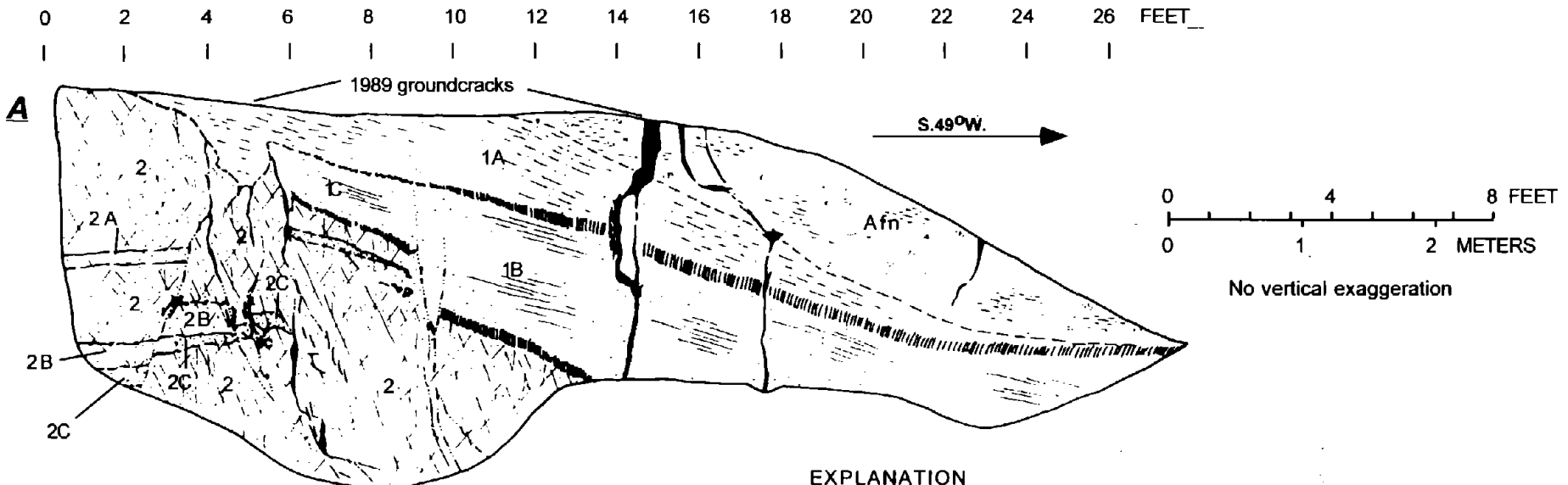


Figure 8.—Area of case history 3 (see pl. 5 for location), at the crest of a narrow, steep-sided ridge, and cross section A-A'. Ground cracking occurred continuously along crest and southwest facing flank of ridge for a distance of more than 0.5 km. A total of 12 trenches across this series of cracks revealed evidence for multiple earlier movements on 1989 ground cracks but also several previous ground cracks that were not reactivated by 1989 Loma Prieta earthquake. From G.E. Weber and Associates (1990b).



**EXPLANATION**

- Afn Artificial fill, composed of mixed native soils
  - 1A Unit 1A— Very dark-brown to black, very fine to fine sandy silt with trace of clay
  - 1B Unit 1B— Dark-yellowish-brown to dark-brown, grading downward from sand and clay with trace of silt to clayey fine sand. Subangular blocky to prismatic peds, moderately thick clay films.
  - 1C Unit 1C— Brown to dark-brown, grading downward from sandy clay to fine sand with some clay. Thin clay films.
  - 2 Unit 2— Light- to medium-olive brown (moist) or pale-yellow or light-yellowish-brown (dry), fine-grained to very fine grained sandstone, generally massive, with two dark-greyish-brown, fine grained sandstone layers (units 3A, 3C) and one white to light-yellow, fine grained sandstone layer (unit 3B).
- Contact, sharp
  - Contact, approximate or indistinct
  - Contact, gradual
  - Poorly defined slip surface with no observed parting or gouge, defined by offset stratigraphy
  - Open crack, shown to scale where possible
  - Shear fabric in sandstone

Figure 9.—Logs of trenches 7 (A) and 8 (B), showing ground cracks caused by surface-parallel slip of a relatively loose, surficial soil layer. Relatively large ground crack in trench 8 was not accompanied by evidence of pre-1989 displacements, a relatively rare observation. From G.E. Weber and Associates (1990b).

C160

LANDSLIDES

trench 7 (fig. 9) shows features associated with both types of movement. At the northeast end of the trench (near the 4-ft marker along the scale) is a zone characterized mainly by extensional deformation. The lower contact of unit 1A is not displaced across this zone but appears to be subsiding into a small graben created by extension. At the same time, several of the larger ground cracks mapped in the section curve abruptly into a ground-surface parallel orientation toward the bottom of the trench. These relations suggest formation of the graben by translation of a near-surface layer moving approximately parallel to the ground surface. Infilled older fissures show that several episodes of movement have occurred.

In contrast to this zone of extensional deformation, a large, discrete, vertical displacement of soil horizon B (units 1B, 1C) was also observed (at 8 ft along the scale). Unit 1B is a well-developed argillic horizon that was partly stripped from the footwall after being offset; unit 1C is a relict of the partly stripped soil horizon B. No movement occurred on this slip surface during the 1989 Loma Prieta earthquake.

Some ground cracks crossed by the trenches were not observed in the subsurface, nor was any visible evidence of earlier episodes of ground cracking found at these localities. Such areas were associated only with smaller cracks showing less than 2.5 to 5 cm of total displacement in relatively loose, granular materials. In contrast, at some other localities where clear evidence for large, older ground cracks existed, no visible ground cracking occurred during the 1989 Loma Prieta earthquake.

In contrast to trench 7 and the other trenches included in the review, the crack observed in trench 8 (fig. 9) exhibits a large displacement at the surface (15 cm), yet any evidence for earlier movement would probably not have been observed, had trenching been conducted at this site before the earthquake. The slight shear fabric depicted in the trench log (fig. 9) is weakly expressed and could have formed in the most recent event. The geometry of the ground crack indicates that it results from nearly surface parallel slip (downhill translation) of the shallow weathered sandstone, rather than deep-seated offset. This type of failure appears to be associated with sites underlain by loose sand and was not observed at hard-bedrock sites. The adjacent residence was thrown off its foundation by shaking but was not damaged by ground cracking.

## CASE HISTORIES: DISCUSSION AND CONCLUSIONS

The preceding case histories were selected to provide a brief overview of the types of subsurface expression associated with ground cracks caused by the 1989 Loma Prieta earthquake. On the basis of our review of these and other sites, we conclude as follows.

1. With few exceptions, ground cracks exhibiting large displacements resulting from the earthquake (more than 3–5 cm of extension and (or) more than 1–3 cm of vertical displacement) showed clear evidence of earlier episodes of movement in the subsurface. Therefore, using appropriate investigative techniques, including geologic trenching of prospective sites, a site can be selected with a low potential for large-scale ground cracks. Ground cracks exhibiting smaller earthquake-related displacements were commonly, but not necessarily, associated with subsurface evidence of earlier episodes of movement. Therefore, the predictive reliability for small-scale cracks is lower.
2. Not all ground cracks with earlier displacements observed in the subsurface were reactivated by the earthquake. Therefore, the ground-cracking pattern resulting from the earthquake cannot, by itself, be used to evaluate the potential for future displacement.
3. Areas of repeated large-scale ground displacements, even those not reactivated during the earthquake, are commonly associated with visible topographic expressions.

Precise predictions of displacement are probably impossible at most localities, except in the sense that areas not characterized by older ground cracks are unlikely to undergo displacements of more than 3 to 5 cm. Newmark (1965) described a method of quantifying seismically induced displacement of a soil mass, using the time-acceleration history of the seismic event; his method is now commonly used to estimate landslide displacements during earthquakes (Wilson and Keefer, 1983, 1985; Keefer, 1991). According to Newmark, displacement is proportional to the intensity and duration of shaking above a certain minimum shaking threshold. Therefore, the displacements observed during the most intense expectable earthquakes are probably reasonable upper bounds for predicted displacements. Although data on displacements in identical ground-crack systems in 1989 and 1906 are sparse, they suggest that movement on ground cracks was greater in 1906 than in 1989 (for example, trench 1; Prentice and Schwartz, 1991). This information, which is consistent with the greater intensity and duration of the 1906 earthquake, indicates that the 1906 displacements may be a reasonable upper limit for coseismic offset in the study area.

In some places, the magnitude of past displacements can be deduced from the geologic record exposed in the trench, such as in trenches 1 and 2. Where ground cracks connect to preexisting shear surfaces that dip downslope in steep terrain (for example, at locs. 2, 3, pl. 5), we assume that the shear surfaces can initiate landsliding with catastrophic displacements.

These conclusions indicate that a thorough subsurface investigation is prudent at any site located in an area with an elevated risk of coseismic ground cracking, such as on narrow-crested and (or) steep-sided ridges, or in areas of earlier landsliding. Such studies can identify building sites

free of past large-scale ground cracks and thus significantly lower the potential for future, large-scale displacement during earthquakes. Because smaller ground cracks are not so predictable, such investigations must be augmented by foundation design to accommodate small-scale displacements.

These evaluations must be integrated with a full geologic evaluation of the site because other site characteristics may complicate the analysis. A comparison between trenches 1 and 2 (figs. 2, 3) suggests that the potential for initiation of large-scale ground cracks at new sites is probably higher for reactivated landslides than for other types of ground-crack systems. Therefore, evaluation of a site on a preexisting landslide mass should be sensitive to the potential internal mechanics of the landslide mass.

## GENERAL CONCLUSIONS

The results of both the trenching and case-history studies indicate that the ground cracks observed after the 1989 Loma Prieta earthquake are recurrent phenomena which can be located according to recognizable surficial geologic features, including topographic lineaments, preexisting landslide masses, and preexisting shear surfaces. Trenches 1 and 2 both show evidence for two prehistoric episodes of movement during approximately the past 2,000 years, with additional movement in 1989 and, probably, 1906 in trench 1. The movement histories in these two trenches are compatible and may describe the same two prehistoric events. These data suggest major events, or groups of events, probably seismic, with a recurrence interval of about 1,000 years. We emphasize that these displacement histories record only "events," which are not necessarily linked only to seismic events or to every earthquake on the San Andreas fault.

The recurrence interval for episodes of movement indicated by the trenching data is significantly longer than the approximately 100- to 300-year recurrence intervals cited for various events on the adjacent segment of the San Andreas fault. The ground cracking may occur only with very specific seismic events, and so multisegment ruptures like the 1906 San Francisco earthquake or reverse-oblique events like the 1989 Loma Prieta earthquake may be much rarer than the brief historical record would suggest.

The results of our case-history review clearly indicate that appropriate geologic site investigations, in conjunction with site engineering, can significantly reduce the hazards posed to development by coseismic ground cracking. Where the ground cracking results from ridgetop spreading, potential ground-crack locations can be identified with confidence; where the ground cracking is due to landslide reactivation, predictive reliability may be less. Discrimination between these two types of ground crack-

ing depends on correct geomorphologic evaluation of the site. This observation underscores the importance of a complete geologic characterization of a prospective building site, rather than relying simply on trenching.

The ground cracking recognized in the Santa Cruz Mountains may also be a significant geologic hazard in other areas. Not only are examples of coseismic ground cracking known from other earthquakes (Cotecchia, 1982; Philip and Meghraoui, 1983), but also abundant geomorphic evidence for ridgetop spreading has been observed in many seismically active regions throughout the world (Jahn, 1964; Beck, 1968; Radbruch-Hall and others, 1976; Mahr, 1977; Radbruch-Hall, 1978; Bovis, 1982). In the Summit Ridge area, preearthquake geologic mapping identified many large preexisting landslides on the flanks of the ridge (Cooper-Clark and Associates, 1975). These large, complex landslides, which commonly display relatively subtle morphology, were previously assumed to be ancient and inactive. Many of these preexisting landslides were reactivated during the 1989 Loma Prieta earthquake and may be viewed as active features that are evolving as a result of relatively regular, incremental displacements, coseismic or not. These observations highlight geologic hazards that may apply to any seismically active region of the world.

Local, regional, or State agencies must decide whether or not the hazard reduction afforded by geologic site investigations is sufficient to permit development. The results of this study, however, indicate that the cumulative risk to development posed by coseismic ground cracking can be significantly reduced by appropriate investigation and design.

## REFERENCES CITED

- Aydin, Atilla, Johnson, A.M., and Fleming, R.W., 1990, Field evidence for right-lateral/reverse tectonic surface rupture along the San Andreas/Sargent fault systems associated with the 1989 Loma Prieta earthquake [abs.]: *Eos (American Geophysical Union Transactions)*, v. 71, no. 43, p. 1460.
- Beck, A.C., 1968, Gravity faulting as a mechanism of topographic adjustment: *New Zealand Journal of Geology and Geophysics*, v. 11, no. 1, p. 191-199.
- Bovis, M.J., 1982, Uphill-facing (antislope) scarps in the Coast Mountains, Southwest British Columbia: *Geological Society of America Bulletin*, v. 93, no. 8, p. 804-812.
- Clark, J.C., Brabb, E.E., and McLaughlin, R.J., 1989, Geologic map and structure sections of the Laurel 7 1/2' Quadrangle, Santa Clara and Santa Cruz counties, California: U.S. Geological Survey Open-File Map 89-679, 31 p., scale 1:24,000, 2 sheets.
- Cooper-Clark and Associates, 1975, Preliminary map of landslide deposits in Santa Cruz County, California: Santa Cruz, Calif., Santa Cruz County Planning Department, scale 1:62,500.
- Cotecchia, Vincenzo, 1982, Phenomena of ground instability produced by the earthquake of November 23, 1980 in Southern Italy: *International Association of Engineering Geology International Congress*, 4th, New Delhi, 1982, Proceedings, v. 8, p. 151-164.

- Dietz, L.D., and Ellsworth, W.L., 1990, The October 17, 1989 Loma Prieta, California, earthquake and its aftershocks; geometry of the sequence from high-resolution locations: *Geophysical Research Letters*, v. 17, no. 9, p. 1417-1420.
- Foxx, Nielsen, and Associates, 1988, Geologic fault investigation, lands of Donna Hines, Summit Road, Santa Cruz County, California: Santa Cruz, Calif. 32 p., 3 sheets.
- G.E. Weber and Associates, 1990a, Geologic hazards evaluation for the Almaneih property, 17774 Old Summit Road, Los Gatos, Santa Cruz County, California: Watsonville, Calif., 39 p., 3 sheets.
- 1990b, Geologic hazards investigation, Gartner property, 16010 Stetson Road, APN 097-231-09, Santa Cruz County, California: Watsonville, Calif., 35 p., 2 sheets.
- Jahn, Alfred, 1964, Slopes morphological features resulting from gravitation: *Zeitschrift für Geomorphologie*, supp. v. 5, p. 59-72.
- Keefer, D.K., ed., 1991, Geologic hazards in the Summit Ridge area of the Santa Cruz Mountains, Santa Cruz County, California, evaluated in response to the October 17, 1989, Loma Prieta earthquake; report of the Technical Advisory Group: U.S. Geological Survey Open-File Report 91-618, 427 p.
- Lawson, A.C., chairman, 1908, The California earthquake of April 18, 1906; report of the State Earthquake Investigation Commission: Carnegie Institution of Washington Publication 87, 2 v.
- Mahr, Tibor, 1977, Deep-reaching gravitational deformations of high mountain slopes: *International Association of Engineering Geology Bulletin*, no. 16, p. 121-127.
- McLaughlin, R.J., Clark, J.C., Brabb, E.E., and Helley, E.J., 1991, Geologic map and structure sections of the Los Gatos 7 1/2' Quadrangle, Santa Clara and Santa Cruz counties, California: U.S. Geological Survey Open-File Report 91-593, 48 p., scale 1:24,000, 3 sheets.
- Newmark, N.M., 1965, Effects of earthquakes on dams and embankments: *Geotechnique*, v. 15, no. 2, p. 139-160.
- Nielsen, Foxx, and Associates, 1988, Geologic fault investigation, lands of Donna Hines, Summit Road, Santa Cruz County, California: Santa Cruz, Calif. 32 p., 3 sheets.
- Nolan, J.M., 1992, An evaluation of coseismic ground-cracking accompanying the October 17, 1989 Loma Prieta, California earthquake; paleoseismic studies and case histories: Santa Cruz, University of California, M.S. thesis, 87 p., 8 sheets.
- Phillip, Herve, and Meghraoui, Mustapha, 1983, Structural analysis and interpretation of the surface deformations of the El Asnam earthquake of October 10, 1980: *Tectonics*, v. 2, no. 1, p. 17-49.
- Ponti, D.J., and Wells, R.E., 1991, Off-fault ground ruptures in the Santa Cruz Mountains, California; ridge-top spreading vs. tectonic extension during the 1989 Loma Prieta earthquake: *Seismological Society of America Bulletin*, v. 81, no. 5, p. 1480-1510.
- Prentice, C.S., and Schwartz, D.P., 1991, Reevaluation of 1906 surface faulting, geomorphic expression, and seismic hazard along the San Andreas fault in the southern Santa Cruz Mountains: *Seismological Society of America Bulletin*, v. 81, no. 5, p. 1424-1479.
- Radbruch-Hall, D.H., 1978, Gravitational creep of rock masses on slopes, chap. 17 of Voight, Barry, ed., *Rockslides and avalanches*, 1. Natural phenomena (Developments in Geotechnical Engineering, v. 14A): Amsterdam, Elsevier, p. 607-657.
- Radbruch-Hall, D.H., Varnes, D.J., and Savage, W.Z., 1976, Gravitational spreading of steep sided ridges ("Sackung") in western United States: *International Association of Engineering Geology Bulletin*, no. 14, p. 23-35.
- Rogers E. Johnson and Associates, 1988, Fault investigation report, Loma Prieta Elementary School, Santa Clara County, California (phases 1 and 2): Santa Cruz, Calif. 28 p., 4 sheets.
- Sarna-Wojcicki, A.M., Pampeyan, E.G., and Hall, T.N., 1975, Map showing recently active breaks along the San Andreas fault between the central Santa Cruz Mountains and the northern Gabilan Range, California: U.S. Geological Survey Miscellaneous Field Studies Map MF-650, scale 1:24,000, 2 sheets.
- Stuiver, Minze, and Polach, H.A., 1977, Discussion: reporting of <sup>14</sup>C data: *Radiocarbon*, v. 19, no. 3, p. 355-363.
- Wilson, R.C., and Keefer, D.K., 1983, Dynamic analysis of a slope failure from the 6 August 1979 Coyote Lake, California, earthquake: *Seismological Society of America Bulletin*, v. 73, no. 3, p. 863-877.
- 1985, Predicting areal limits of earthquake-induced landsliding, in Ziony, J.I., ed., *Earthquake hazards in the Los Angeles region— an earth-science perspective*: U.S. Geological Survey Professional Paper 1360, p. 317-494.
- Working Group on California Earthquake Probabilities, 1990, Probabilities of large earthquakes in the San Francisco Bay region, California: U.S. Geological Survey Circular 1053, 51 p.

1000

1000



THE LOMA PRIETA, CALIFORNIA, EARTHQUAKE OF OCTOBER 17, 1989:  
STRONG GROUND MOTION AND GROUND FAILURE

LANDSLIDES

ANALYSIS OF EARTHQUAKE-REACTIVATED LANDSLIDES IN  
THE EPICENTRAL REGION, CENTRAL SANTA CRUZ MOUNTAINS,  
CALIFORNIA

By William F. Cole, Dale R. Marcum, and Patrick O. Shires,  
Cotton, Shires and Associates, Inc.;  
and  
Bruce R. Clark,  
Leighton and Associates, Inc.

CONTENTS

	Page
Abstract .....	C165
Introduction .....	165
Topographic and geologic setting .....	166
Central Santa Cruz Mountains .....	166
Preexisting "ancient" landslides .....	166
Landslide characterization .....	169
Site selection .....	169
Summary of subsurface conditions .....	169
Regolith detachments .....	169
Structural control on deeper failures .....	172
Key parameters in slope-stability analysis .....	172
Landslide geometry and ground-water conditions .....	172
Earthquake ground motions .....	173
Unit weight and shear strength .....	174
Methods of analysis .....	175
Pseudostatic method .....	175
Cumulative-displacement method .....	175
Results .....	176
Pseudostatic analysis .....	176
Cumulative-displacement analysis .....	177
Sensitivity analysis .....	177
Conclusions .....	181
Acknowledgments .....	183
References cited .....	183
Appendix: Description of landslide sites .....	184
Lower Schultheis Road West landslide .....	184
Ditullio landslide .....	185

ABSTRACT

The reactivation of large landslides during the 1989 Loma Prieta earthquake provided a unique opportunity to evaluate the seismic stability of preexisting landslides and to test the dynamic slope-stability methods currently used in geotechnical practice. For this study, we characterize two reactivated landslides, using the investigative techniques of geologic mapping, subsurface logging and sam-

pling, and laboratory direct shear testing developed over decades of landslide investigation. We then compare actual landslide behavior during the earthquake with the results of several analytical methods, and test the sensitivity of key parameters in the calculations.

Results of both pseudostatic and cumulative-displacement analyses are less conservative than what actually occurred at the two landslide sites during the earthquake. We obtain a relatively high pseudostatic factor of safety of 1.1, using minimum shear strengths from direct shear tests and a seismic coefficient of 0.20. Cumulative-displacement calculations yield displacements within an order of magnitude of the 33 to 61 cm of displacement measured in the two landslides, generally lower than the actual field displacements.

Comparisons with actual measured landslide displacements show that the stability analyses are highly sensitive to the angle of internal friction, a parameter that is difficult to determine accurately in the laboratory. Backanalysis of the shear strength of the basal rupture surface for static stability can help define a realistic range of friction angles. The cumulative-displacement analyses are also sensitive to the acceleration-time history of ground motion at the two landslide sites. Models of earthquake-triggered landslide failure could be refined by using more rigorous physical models, but the resulting displacement calculations will not improve until earthquake ground motions at landslide sites can be better characterized.

INTRODUCTION

The combination of existing slope failures and a history of seismic ground shaking has led to the current practice of incorporating both static and seismic loading conditions into slope-stability studies in California. Although the analytical techniques and models used for static-

loading conditions have been standardized, uncertainty exists among practicing engineers and geologists regarding the accuracy of the seismic analytical methods. For typical residential- and commercial-development investigations, earthquake loading is simulated by applying a seismic coefficient to a static-limit-equilibrium calculation. The value of this coefficient is selected on the basis of experience and judgment; therefore, the values chosen to be appropriate for particular sites by various workers commonly differ. State-of-the-art slope-stability-analytical methods have been modified and used by scientists at the U.S. Geological Survey to predict hillslope behavior during earthquakes (Wieczorek and others, 1985; Wilson and Keefer, 1985); however, the ability of available analytical methods to predict the occurrence and amount of displacement of earthquake-triggered landslides is not well established. Very few case studies of actual earthquake-triggered landslides have been published as of this writing (1993) (for example, Clark and others, 1979; Wilson and Keefer, 1983; Keefer, 1991; Jibson and Keefer, 1993).

The 1989  $M=7.0$  Loma Prieta earthquake caused discrete ground cracking in the preexisting-landslide terrane of the central Santa Cruz Mountains. Much of this ground cracking occurred along preearthquake landslide boundaries, suggesting reactivation of old bedrock landslides in the region and providing an opportunity to compare the actual seismic stability of old landslides with the results of analyses for dynamic slope stability as currently conducted in geotechnical practice.

## TOPOGRAPHIC AND GEOLOGIC SETTING

### CENTRAL SANTA CRUZ MOUNTAINS

The Santa Cruz Mountains are part of the northern Coast Ranges of California. This rugged mountain range forms the spine of the San Francisco peninsula, extending approximately 135 km northwestward from the Pajaro River in the south to near the community of South San Francisco in the north (fig. 1). Elevations of ridgecrests range from about 450 to 1,150 m above mean sea level.

The study area lies between about 8 and 19 km south of the community of Los Gatos at elevations of 280 to 340 m (fig. 1). The landslides chosen for study occurred in an area that underwent particularly intense ground cracking during the earthquake (fig. 2). The two sites selected for detailed study are situated 10 to 13 km northwest of the 1989 main-shock epicenter.

The study area, which is from 1.5 to 3.0 km southwest of the mapped trace (that is, probable 1906 surface rupture) of the San Andreas fault zone, is underlain by tightly folded Eocene, Oligocene, and Miocene sedimentary rocks

(fig. 2). This Tertiary bedrock section consists of relatively soft, poorly indurated, marine clastic sedimentary rocks, about 7,600 m thick (Clark, 1981). In the study area, the rocks have been strongly folded and locally overturned into a series of northwest-southeast-trending anticlines and synclines. Specific Tertiary bedrock formations underlying the study areas are the Butano Sandstone, Vaqueiros Sandstone, and San Lorenzo Formation.

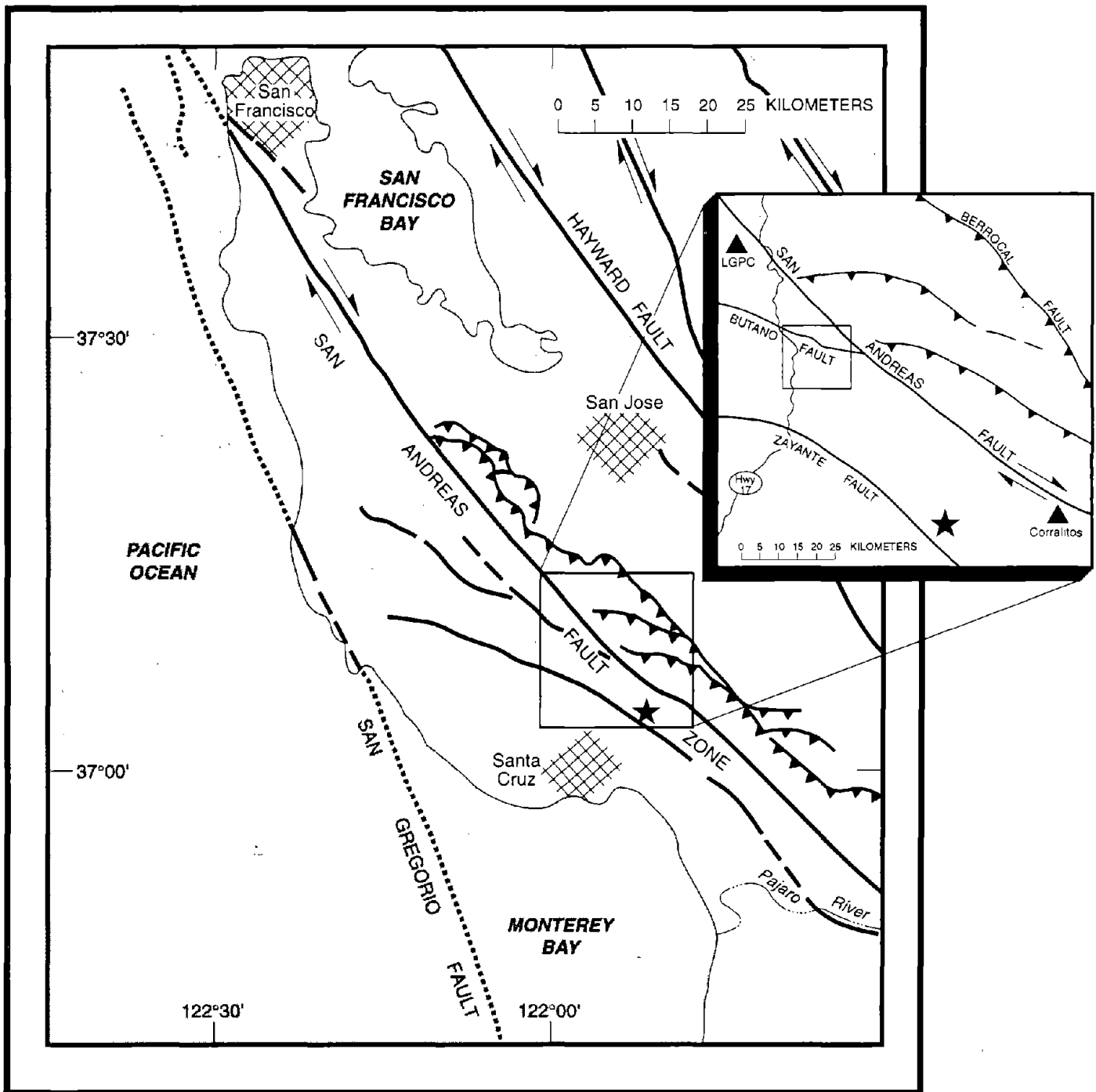
### PREEXISTING "ANCIENT" LANDSLIDES

The study area encompasses a widespread landslide terrane. In general, the geomorphology of this terrane is characterized by "stepped" topography, including very steep, curved scarps, flat-lying benches, and steep-walled, deeply incised creek canyons. Typically, several sequences of scarps with intervening flat-lying benches form the slope face between the ridgetops and creek canyons. Geomorphic features range in appearance from relatively fresh to subdued, strongly suggesting periodic movement of individual landslides within a large landslide complex. The large areal extent of these landslides and multiple scarps suggest large cumulative displacements of these features.

"Ancient landslides" are defined here to be landslides that originated thousands to tens of thousands of years ago, although the most recent movement may have been only years or decades ago. Indeed, geomorphic and subsurface geologic data suggest periodic and episodic reactivation of these landslides. Although the exact date of landslide initiation in the study area is unknown, other landslide complexes in California are associated with Pleistocene glacial and climatic changes during the past 100,000 years (Stout, 1969).

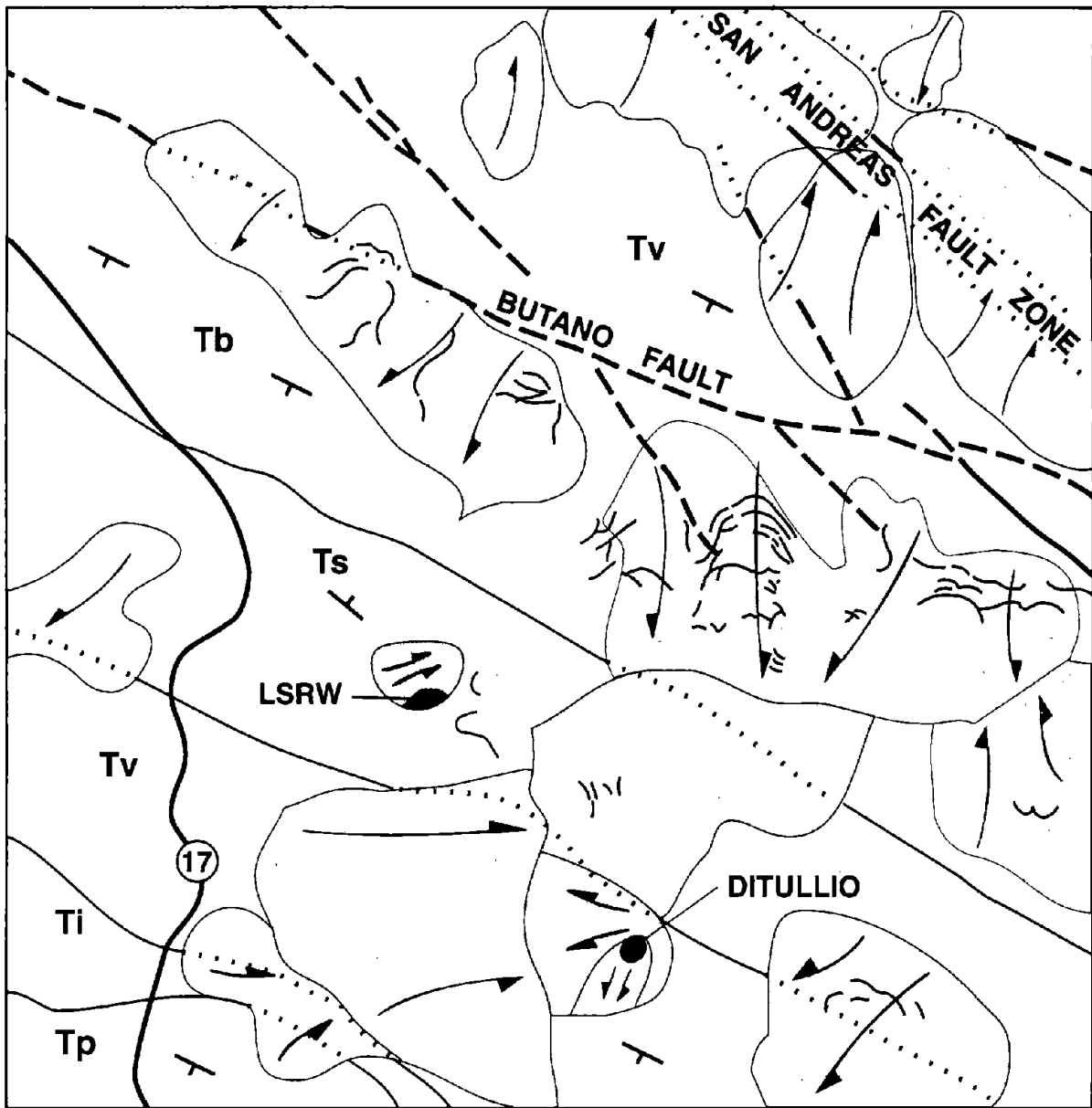
The landslide masses are composed of weak earth materials derived from fractured, folded, and faulted Tertiary sedimentary rocks that have been subjected to periods of intense rainfall, ground-water fluctuations, and strong earthquake shaking. The sedimentary rocks consist primarily of fine-grained, thin-bedded, highly fractured shale, claystone, and siltstone that contain numerous shears, fractures, and other discontinuities. The resulting permeability of the near-surface materials enables them to collect, transmit, and store water from various sources (for example, rainfall, runoff, and lateral ground-water flow).

Figure 1.—San Francisco Bay region, Calif., showing location of study area (small shaded box), major faults (dashed where approximately located, dotted where concealed; half-arrows indicate direction of relative movement) and thrust faults (sawteeth on upper plate), and epicenter of 1989 Loma Prieta earthquake (star). Triangles, strong-motion-recording stations used in this study; LGPC, Los Gatos Presentation Center station.



EXPLANATION

- Fault-** Dashed where approximately located; dotted where concealed. Half arrows indicate direction of relative movement.
- Thrust fault-** Sawteeth on upper plate
- Strong motion recording station-** LGPC, Los Gatos Presentation Center
- ★** 1989 Loma Prieta earthquake epicenter



EXPLANATION

TERTIARY BEDROCK UNITS

- Tp** Purisima Formation
- Ti** Lambert Shale
- Tv** Vaqueros Sandstone
- Ts** San Lorenzo Formation
- Tb** Butano Sandstone

- Preexisting landslide- Half arrows indicate direction of downslope movement. Reactivated-landslide study site
- 1989 coseismic ground fissures
- Contact- Dotted where concealed
- Strike and dip of bedding
- Fault- Approximately located; dotted where concealed.

## LANDSLIDE CHARACTERIZATION

### SITE SELECTION

A general reconnaissance of more than 50 large earthquake triggered or reactivated landslides was performed after the 1989 Loma Prieta earthquake. Of the landslide sites, approximately 20 were selected for more rigorous inspection. Early inspections focused on identifying landslides that met the following criteria: (1) deep-seated failures that involved bedrock materials, (2) a well-defined pattern of ground cracks and surface displacements indicating probable reactivation of the basal rupture surface, (3) location within preexisting landslides or landslide complexes, and (4) terrain amenable to detailed surface and subsurface investigation and not so steep or heavily vegetated as to prevent drill-rig access. We also preferred sites where ground water was anticipated to be deeper than several meters, so that a geologist could safely enter and log large-diameter boreholes without the need for dewatering. Shallow ground water prevented full characterization of landslide parameters at 4 of the 20 selected sites.

Many of the earthquake-activated landslides appear to have been only partially mobilized, without shear failure along the entire basal rupture surface. The pattern of surface deformation at several sites, however, indicated that some landslides had been fully mobilized by the earthquake. Two of these landslides, here referred to as the Lower Schultheis Road West and Ditullio landslides, were characterized by a combination of field mapping and subsurface exploration. Large-diameter boreholes were excavated and logged by a geologist descending into the borehole to directly observe and sample landslide rupture-surface materials. Geologic and geotechnical conditions, deformational features, and the investigative procedures used at each site were described in detail by Cole and others (1991).

### SUMMARY OF SUBSURFACE CONDITIONS

The preexisting-landslide masses are composed of three distinguishable rock and soil materials: (1) regolith, (2) sparsely to highly fractured bedrock units, and (3) clay shear and gouge material, including landslide rupture surfaces.

1. The regolith consists of oxidized and fractured rock and soil derived from the underlying bedrock that have been subjected to seismic shaking, cyclic changes in groundwater levels, and other weathering processes. Regolith at the landslide sites contains angular, weathered, gravel- to boulder-size sandstone and siltstone fragments in a matrix of clayey silt to silty sand. The upper approximately 4 m of regolith typically is a plastic silty clay.
2. Displaced sedimentary bedrock sequences of the San Lorenzo Formation are present at depth in the Lower Schultheis Road West and Ditullio landslides; the bedrock is highly fractured and oxidized above major shear surfaces at 7.3- and 18-m depth, respectively (figs. 3, 4). Below these shear surfaces, the bedrock is less fractured, denser, and relatively unoxidized. Interbedded sandstone and siltstone are present at the Lower Schultheis Road West landslide, and massive sandstone at the Ditullio landslide.
3. Thin seams of clayey gouge occur in the regolith and fractured bedrock at several landslide sites explored in the study area. The gouge is generally a wet silty clay with a soft to firm consistency and medium to high plasticity. The gouge seams are commonly from about 1 to 10 cm thick. Polished surfaces were observed in many of these seams. At the Lower Schultheis Road West landslide, several continuous and discontinuous gouge zones are present at 4- and 7-m depth. Thicker gouge zones are present within, and at the base of, the regolith. A relatively thin seam of gouge forms the contact between highly fractured rock and underlying unfractured rock. At the Ditullio landslide, a 2- to 5-cm-thick gouge seam separates oxidized, fractured rock from underlying unfractured rock at about 18-m depth; this gouge seam is associated with a zone of crushed siltstone and sandstone, as much as about 80 cm thick (fig. 3).

The results of subsurface exploration indicate that the reactivated landslides occurred within preexisting landslide masses that are characterized by relatively coherent, rather than disrupted, landslide materials. Complex, shallow perched ground water and both shallow and deep preexisting rupture surfaces were penetrated. The shallow shear surfaces typically were observed at the base of the regolith at 5- to 15-m depth, and deeper shears were penetrated within the underlying fractured sedimentary bedrock. The primary geologic controls on these shear surfaces appear to be the regolith-bedrock contact and adversely oriented bedding planes and fractures in the bedrock.

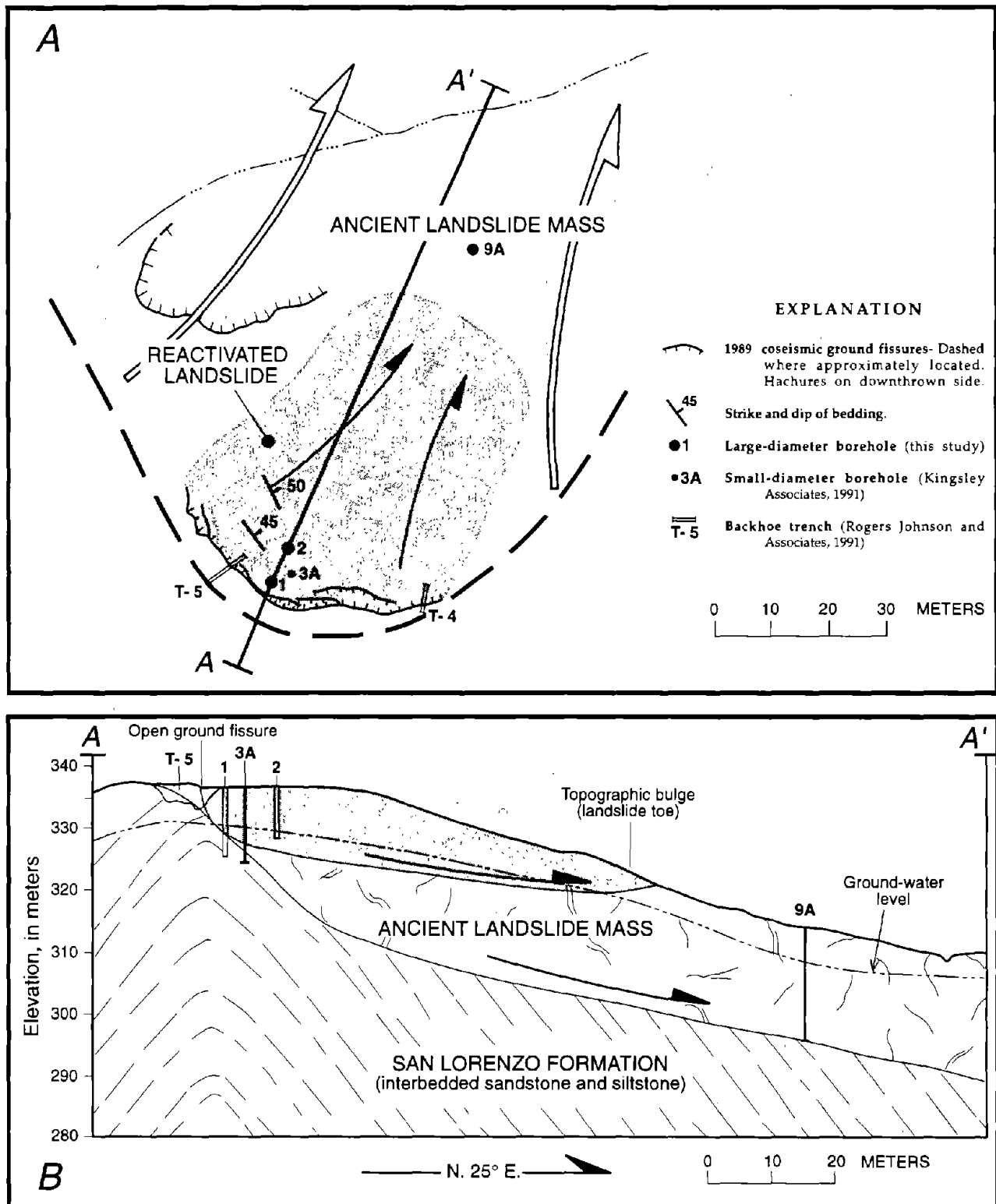
### REGOLITH DETACHMENT

On the basis of our downhole observations, the contact between overlying, oxidized regolith and underlying, unoxidized bedrock was commonly a well-developed shear

Figure 2.—Geologic map of study area (see fig. 1 for location), showing locations of Lower Schultheis Road West (LSRW) and Ditullio landslides discussed in text. Geology from Clark and others (1989) and McLaughlin and others (1991); areas of preexisting landslides (shaded) from Cooper-Clark and Associates (1975) and this study; coseismic ground fissures from Spittler and Harp (1990).

contact. The base of the overlying regolith is generally at 5- to 15-m depth. The underlying bedrock, though part of a larger, ancient landslide mass, typically is unoxidized (or only locally oxidized) and closely fractured. The ob-

served shear contact separating the two units is a saturated, clay-rich, soft, plastic gouge ranging from approximately 2 to 5 cm in thickness. At one of the landslides we explored but do not analyze here, a sheared water well



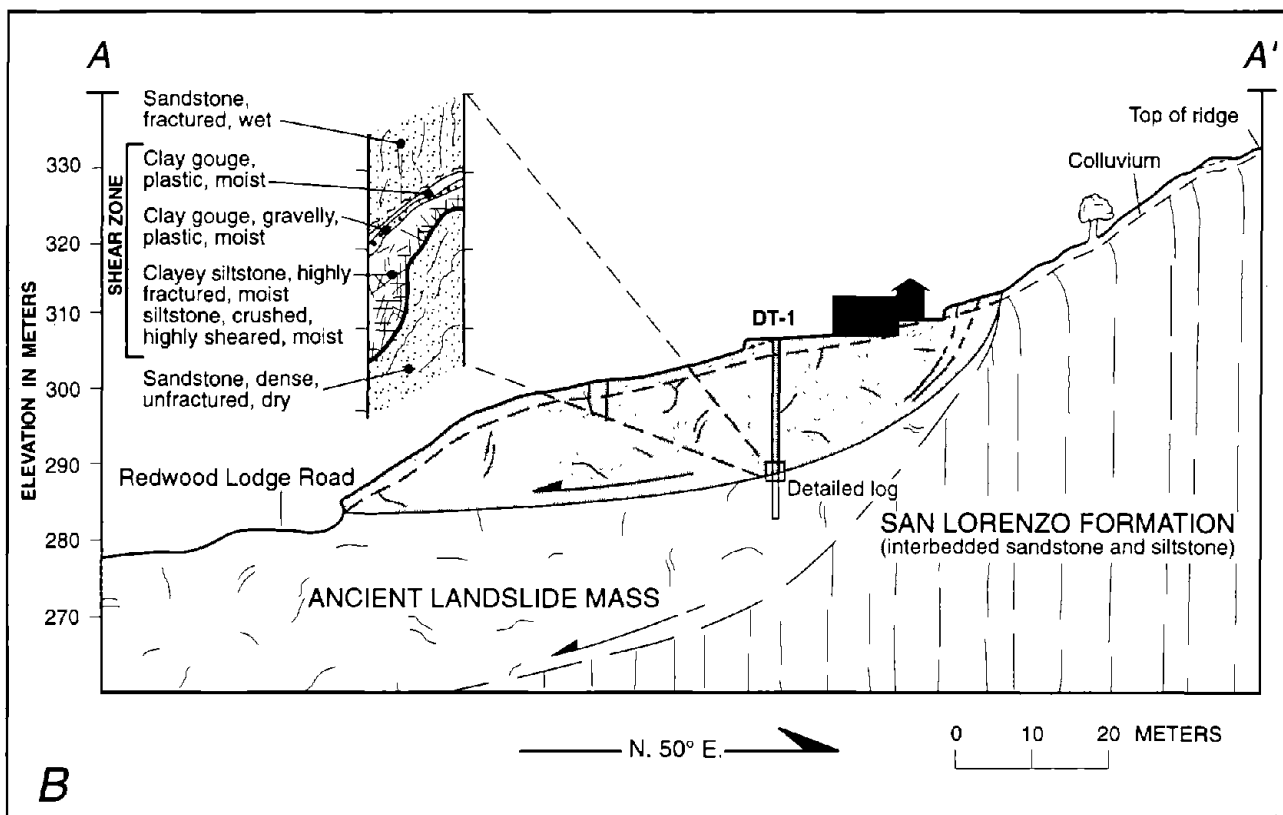
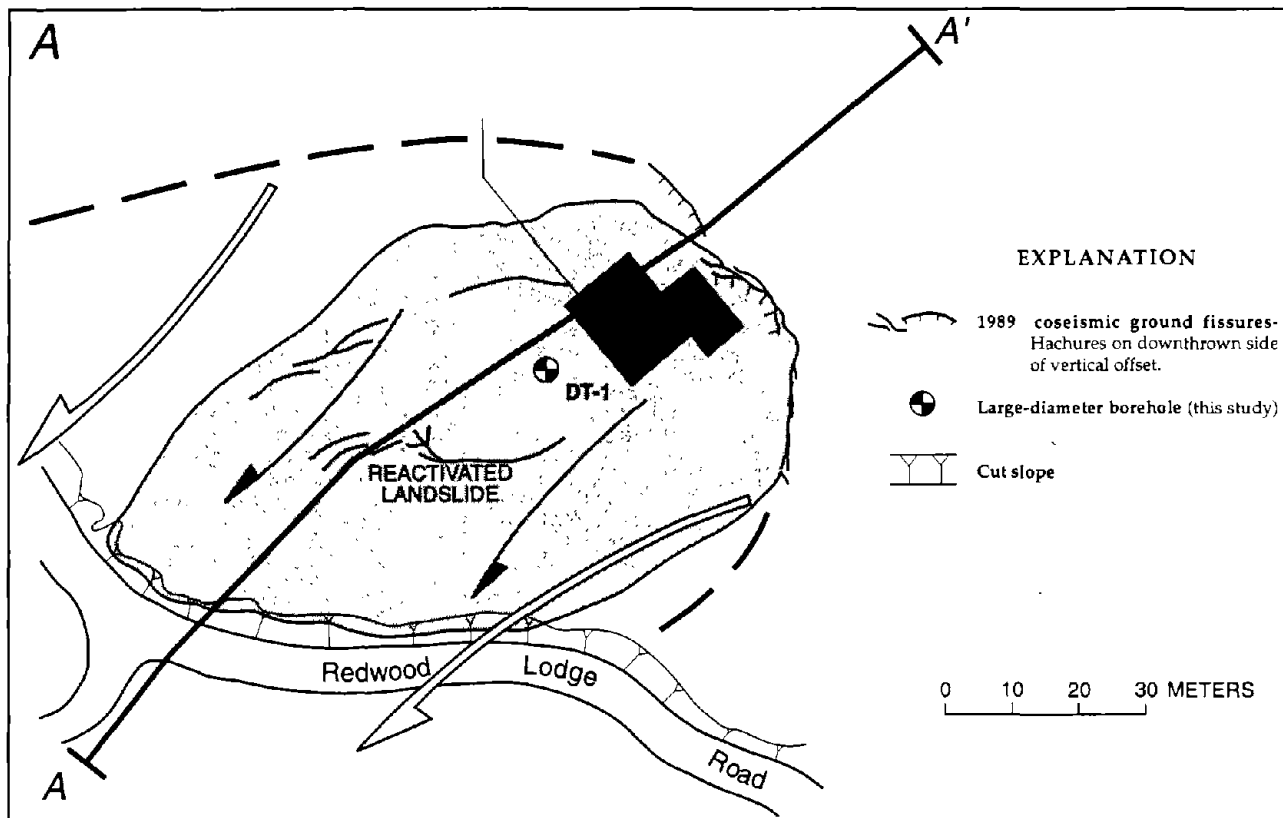


Figure 4.—Simplified geologic map (A) and cross section (B) of Ditullio landslide (see fig. 2 for location). Half-arrows indicate direction of downslope movement.

provided a piercing point on the reactivated rupture surface. A large-diameter borehole adjacent to the well revealed that this rupture surface coincided with the regolith-bedrock contact.

Although the geomorphology of the area is best explained by the presence of deep-seated landsliding, logging of large-diameter borings revealed that shallow landslide debris was much more disrupted than the deeper landslide material. The degree of development and fresh appearance of the shears separating the regolith from the underlying rock suggests that the Loma Prieta landsliding event mobilized these shears and that they had been mobilized frequently in the past as well.

#### STRUCTURAL CONTROL ON DEEPER FAILURES

Bedding-plane shears were observed at the Lower Schultheis Road West landslide and in trenches excavated in the headscarps of other landslides in the study area (Cotton and others, 1991; Keefer, 1991). An interpretation that old landslides failed repeatedly along a preexisting bedding-plane shear is supported by the difference in physical characteristics between the overlying landslide debris and underlying bedrock at the Lower Schultheis Road West landslide (fig. 4). Regional geologic data suggest that the upslope parts of several other landslides may be underlain by bedding planes dipping steeply downslope.

For the landslides to have fully failed in the past, the basal surfaces must eventually break out to the slope surface, whereas the bedding planes likely remain steeply dipping. Therefore, rupture surfaces that coincide with bedding planes in the upslope (headward) parts of a landslide mass dip less steeply than these bedding planes beneath much of the landslide mass. The presence of steeply dipping bedding planes could help to explain how many slope failures from the 1989 Loma Prieta earthquake were restricted to only the steeply dipping, upslope components of the landslides. Many of these landslides, however, do not appear to have been influenced by dip-slope conditions (D.K. Keefer, oral commun., 1992); thus, the limited movement of the landslides must be explained by other mechanisms.

Subsurface geologic evidence does not demonstrate conclusively whether the landslides were caused originally by seismic activity or by excessive water during wetter climatic conditions, or by some combination of these two mechanisms. Subsurface exposures, however, confirm the presence of multiple rupture surfaces of quite different geometry and stratigraphic position, arguing for the existence for multiple rupturing events since the landslides first formed. The deep-seated rupture surfaces that incorporated relatively fresh bedrock into the landslide mass

also involved a much greater volume of the slope than the shallow ruptures observed at the regolith-bedrock contact. Such massive failures must have been generated by an event quite different in magnitude from the 1989 Loma Prieta earthquake. The largest measured displacements in this earthquake were less than 3 m (Keefer, 1991). Thus, it apparently reactivated only shallow segments of relatively small areal extent within deep-seated, large preexisting landslide masses.

### KEY PARAMETERS IN SLOPE-STABILITY ANALYSIS

The key parameters in slope-stability analysis include landslide geometry, generally analyzed as a representative cross section; ground-water levels or pore-water pressures acting on the landslide, generally considered as a phreatic surface; the intensity of earthquake ground motion at the site, typically inputted in the form of a single seismic coefficient or an appropriate acceleration-time history; the unit weights of the landslide materials; and an average shear strength along the basal rupture surface.

#### LANDSLIDE GEOMETRY AND GROUND-WATER CONDITIONS

The geometry and ground-water parameters were determined directly from field measurements. Geologic cross sections were carefully constructed through the landslides on the basis of field measurements. Establishing that a landslide had actually moved downslope, in contrast to simply forming a scarp by settlement of loose graben debris, required careful examination but could be verified by the presence of sheared flanks or compressional-toe areas. Determining landslide depth is complicated by the fact that multiple shear surfaces were observed in boreholes penetrating the preexisting-landslide masses. In the absence of well-defined subsurface piercing points, the selection of which of the multiple shear surfaces was reactivated involves careful correlation between borehole logs and surface deformational features, as well as reasonable assumptions regarding landslide behavior. Only one well-developed shear surface was penetrated in the Ditullio landslide, thus making the determination of landslide depth straightforward. The selection of the activated Lower Schultheis Road West landslide rupture surface was based on the fresh appearance and continuity of the regolith-bedrock contact, correlation with the headscarp fissures and downslope zone of compression, and observations from other similar types of landslides in the study area.



The ground-water levels shown on the cross sections (figs. 3, 4) were those penetrated during subsurface exploration. Because the 1989 Loma Prieta earthquake occurred near the beginning of the 1989–90 rainy season during a period of prolonged drought, the conditions in boreholes are believed to represent ground-water conditions immediately before the earthquake. We realize that changes in water-well levels and surface streamflow after the earthquake suggest that trapped ground water may have been freed by fracturing during the earthquake and that water levels may have dropped significantly (Rojstaczer and Wolf, 1992). However, perched water in the analyzed landslides is unlikely to exit through new fractures extending into the landslide debris. Furthermore, we know of no reports or evidence of ground water flowing to the surface from within these small landslide masses after the earthquake. Nonetheless, we performed sensitivity analyses to test the effects of changing ground-water levels on the stability analyses (see subsection below entitled "Sensitivity Analysis").

## EARTHQUAKE GROUND MOTIONS

Earthquake ground motions can be entered into the displacement calculations from published maps (K.L. Lee, unpub. data, 1977; Makdisi and Seed, 1977; Hynes-Griffin and Franklin, 1984; Lin and Whitman, 1986), as well as directly from acceleration-time histories recorded on strong-motion instruments located near the study area. We used data from the Corralitos station, part of the California Division of Mines and Geology's California Strong Motion Instrumentation Program (CSMIP), and the Los Gatos Presentation Center station (LGPC, fig. 1), operated by the Charles F. Richter Seismological Laboratory of the University of California, Santa Cruz. The Corralitos and LGPC stations are approximately 7 and 19 km, respectively, from the epicenter (fig. 1).

The intensity of ground motion at a particular site is influenced by several factors, including earthquake magnitude, epicentral distance, local geologic structure, source and rupture mechanism of the earthquake, wave-interference effects, geotechnical site conditions, and topographic amplification. The selection of appropriate acceleration-time histories for seismic stability is generally problematic because most landslide sites are at great distances from actual recording stations and the conditions at these sites generally differ from those at the recording stations. The large magnitude and complex rupture mechanism of the 1989 Loma Prieta earthquake, in combination with extremely irregular topographic conditions, indicate that ground motion in the study area may have varied considerably. Thus, selection of appropriate ground-motion parameters at the landslide sites involved an assessment of the site conditions at the two closest recording stations

(fig. 1). Several studies indicate that the earthquake had a strong azimuthal effect on ground motion (Beroza, 1991; Steidl and others, 1991; Wald and others, 1991). The earthquake ruptured bilaterally, and so the region northwest of the epicenter (including the LGPC station and both landslide sites) was influenced by northwest-propagating rupture, whereas the region southeast of the epicenter (including the Corralitos station) was more affected by southeast-propagating rupture (table 1). Furthermore, rupture was predominately reverse slip to the northwest of the hypocenter and predominately strike slip to the southeast. According to Wald and others, the bilateral rupture resulted in a larger overall stress drop and correspondingly higher ground motion to the northwest of the epicenter, and lower ground motion directly updip of the hypocenter near the Corralitos station. Campbell (1991) suggested that the northwest-trending geologic structure may explain the higher ground motion and lower attenuation rate northwest of the epicenter.

The Corralitos station (fig. 1) recorded a peak horizontal ground acceleration,  $k_{\max}$ , of 0.63 g (California Division of Mines and Geology, 1990), whereas the LGPC station appears to have recorded a  $k_{\max}$  value of greater than 1.00 g (off scale). Because the recorder was not firmly anchored to the floor and an apparent baseline offset occurred during the strong ground shaking, seismologists have cautioned that the data from the LGPC station may not be a reliable indicator of the actual ground motion at this site (Karen McNally, oral commun., 1991). For the purposes of our analysis, however, the baseline correction for this offset (approx 0.03 g north-south), was considered insignificant relative to the  $k_{\max}$  value. The amplitude of long-period waves on the corrected acceleration-time history for the LGPC station is similar to the modified record from the Corralitos station scaled to 1.00 g (fig. 5).

The site conditions at the LGPC station (fig. 1) are thought to more closely resemble those at the landslide sites than do those at the Corralitos station because (1) the LGPC station and the landslide site are at similar distances from the San Andreas fault and the Loma Prieta epicenter, (2) topographic conditions at the LGPC station and the landslide sites are similar in terms of slope position and elevation, and (3) the LGPC station is located along the same azimuth from the epicenter (320°) as the two landslide sites. In the absence of recorded data in the immediate vicinity of the landslide sites and because of very high ground motions in the surrounding region, the acceleration-time history of the LGPC station was selected initially to represent "bedrock" ground motions at the landslide sites during the earthquake. We also used the Corralitos station record, both unscaled ( $k_{\max}=0.63$  g) and scaled ( $k_{\max}=1.00$  g), to test the sensitivity of the calculations to ground motion (see subsection below entitled "Sensitivity Analysis").

Table 1.—Distance of two strong-motion stations used in this study from earthquake and landslide features

[The Lower Schultheis Road West and Ditullio landslides are about 12 and 11 km, respectively, northwest (az 320°) of the epicenter of the 1989 Loma Prieta earthquake. Both landslides are about 2 km southwest of the Loma Prieta rupture zone, as measured from the San Andreas fault zone]

Strong-Motion station (fig. 1)	Distance (km) to:				
	Loma Prieta epicenter (azimuth)	San Andreas fault	Loma Prieta rupture zone	Lower Schultheis Road West landslide (elev., 335 m)	Ditullio landslide (elev., 351 m)
Corralitos (elev., 320 m).	7.0 (080°)	0.3	0.3	16.4	15.9
Los Gatos Presentation Center (elev., 366 m).	19.0 (320°)	1.4	1.5	7.0	8.2

### UNIT WEIGHT AND SHEAR STRENGTH

Moisture content and density were determined in the laboratory on selected undisturbed samples of the landslide mass by measuring the weight and volume of material collected and sealed in brass tubes. For the Lower Schultheis Road West landslide, we identified two geotechnical units in the landslide mass. The soil (upper unit) has a moist unit weight of  $2.06 \text{ g/cm}^3$  and a saturated unit weight of  $2.16 \text{ g/cm}^3$ ; the regolith (lower unit) has a moist unit weight of  $1.96 \text{ g/cm}^3$  and a saturated unit weight of  $2.08 \text{ g/cm}^3$ . For the Ditullio landslide, only one geotechnical unit was identified, with a moist unit weight of  $1.92 \text{ g/cm}^3$ .

Shear strengths were determined initially by laboratory measurements on samples collected from subsurface rupture zones. Backcalculations were subsequently performed under static-loading conditions for comparison with the laboratory results. Collecting representative and oriented samples of landslide rupture surfaces is a difficult task. To obtain the best possible samples, we collected tube samples of the landslide rupture surfaces from large-diameter boreholes. At each sample location, a geologist hand-excavated a horizontal shelf into the landslide material several centimeters above and parallel to the shear surface. Tube samples were pushed and driven through the landslide debris, through the shear surface, and into the underlying materials. The samples were sealed and transported to our laboratories for various direct shear tests (consolidated drained and consolidated undrained, peak, and residual) on "undisturbed" and remolded samples.

Because of the rapid failure of the landslides, we chose consolidated-undrained ("quick") direct shear tests, rather than triaxial strength testing, to represent the loading con-

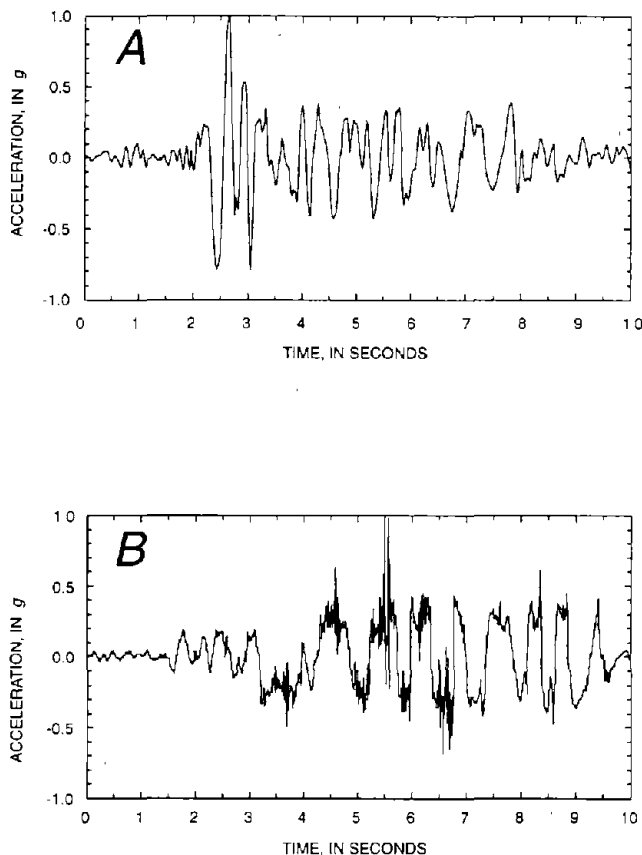


Figure 5.—Corrected north-south component of motion on strong-motion records of October 17, 1989, main shock from California Division of Mines and Geology station at Corralitos (A) and University of California, Santa Cruz, station at Los Gatos Presentation Center (B) (see fig. 1 for locations). Record in figure 5A is scaled to 1.0 g.

ditions imposed by the earthquake. Although some drainage can occur during direct shear testing, the permeability of the gouge material from these landslides is very low, and the sample does not have sufficient time to drain during the relatively rapid test. Triaxial tests can measure pore pressures, but shear surfaces must be oriented at an angle to the sample axis to avoid stresses perpendicular to the shear surface. In addition, direct shear tests can be performed on relatively short samples, whereas triaxial samples must be about twice as long as the diameter. Thus, the triaxial procedure requires a longer sample, which involves more disturbance during sampling and is difficult where thin, soft gouge material lies between hard, brittle rock. We favor direct shear tests over triaxial tests for these reasons and because they offer the best chance for shearing the actual rupture surface in a similar mode of failure to that in the landslide.

The residual shear strengths measured in direct shear tests are approximately 70 to 75 percent of the peak values. This result approximates the reduction to 80 percent of peak shear strength estimated by Makdisi and Seed (1977) and recommended by Hynes-Griffin and Franklin (1984), owing to cyclic-loading effects. Therefore, we used the residual shear strengths to characterize the cyclic strength of the basal rupture surfaces. Two measures of residual shear strength, lower-bound and average or "best fit" curves, were drawn by linear regression through the data points (fig. 6). The shear-strength parameters, in terms of angle of internal friction ( $\phi$ ) and cohesion ( $c$ ), that describe the lower-bound and best-fit values are  $\phi=25^\circ$ ,  $c=0$  kg/cm<sup>2</sup> and  $\phi=24^\circ$ ,  $c=0.22$  kg/cm<sup>2</sup>, respectively.

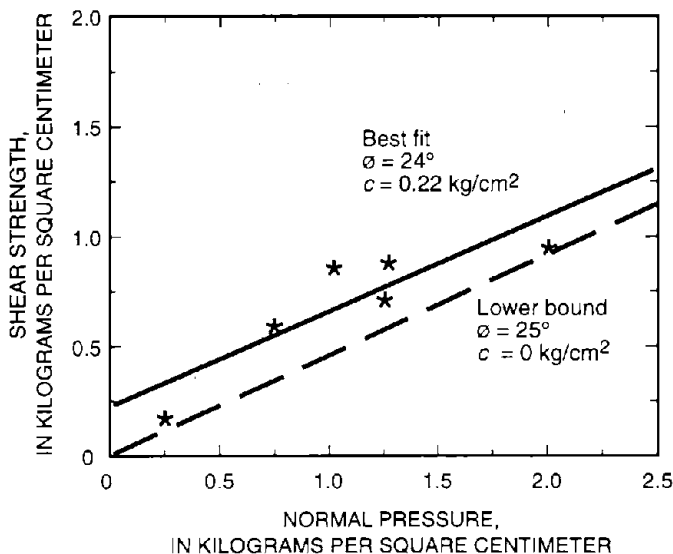


Figure 6.—Residual shear strength versus normal pressure in laboratory consolidated-undrained tests on landslide rupture surface material.

## METHODS OF ANALYSIS

### PSEUDOSTATIC METHOD

Pseudostatic analysis is a standard method of assessing seismic slope stability in the geotechnical industry. This method involves analyzing landslides by using a traditional method of limit-equilibrium-stability analysis, such as Spencer's or Bishop's method (Chowdhury, 1978; Huang, 1983). In addition to the static forces acting on the landslide body, a static force proportional to the weight of the landslide mass is then added as a permanent horizontal force to simulate the dynamic force of the earthquake. The magnitude of this force is the product of the weight of the landslide body and a seismic yield coefficient,  $k$ .

The  $k$  value significantly affects the results of the pseudostatic analysis, yet traditionally it has been arbitrarily chosen on the basis of experience and judgment. Lambe and Whitman (1969) stated that  $k$  values of 0.1 to 0.2 are commonly assumed. K.L. Lee (unpub. data, 1977) indicated that the  $k$  value may fall in a somewhat broader range of 0.05–0.25. Chowdhury (1978) suggested that  $k$  values of 0.10 to 0.15 are typically used in the United States, whereas Huang (1983) suggested a  $k$  value of 0.27 for design in western California. A  $k$  value of 0.15 is currently required by the California Division of Safety of Dams for analysis of earthfill dams. In California,  $k$  values of more than 0.20 are rarely used in practical design for residential and commercial sites. The diversity in chosen  $k$  values reflects the uncertainty that engineers have with regard to the pseudostatic approach and the selection of design-level earthquakes.

### CUMULATIVE-DISPLACEMENT METHOD

As recognized by many previous workers, the pseudostatic method of analysis has some significant limitations. Newmark (1965) noted that the transitory vibrations of earthquake ground motions could cause the factor of safety (FS) of a slope to temporarily drop below 1 several times during a seismic event. An accurate pseudostatic analysis of this situation would indicate failure. However, if the drop in the FS value is so transient that the induced deformations are small and the slope is essentially unchanged, then the term "failure" may not accurately describe the actual condition of the slope.

A method of measuring incremental displacements of the slope during an earthquake was developed by Newmark (1965) as an alternative to the pseudostatic approach for earth embankments. Commonly referred to as "Newmark analysis," "cumulative-displacement analysis," "permanent-deformation analysis," and "sliding-block analysis,"

this method sums the downslope movements of the landslide during each cycle of high acceleration to compute a cumulative displacement. Thus, this method evaluates performance rather than stability. The magnitude of the computed displacement can be used to assess the degree of damage. For example, if the displacements are several meters, deformation of the slope probably will be heavy; conversely, if the computed displacements are less than a few centimeters, deformation of the slope will be slight. This method requires a complete acceleration-time history as input, as well as a value for the yield acceleration ( $k_y$ ) of the landslide, defined as the ground acceleration required to bring the FS value to 1 in a pseudostatic analysis.

A basic assumption of the cumulative-displacement method is that the landslide mass behaves as a rigid body and can be modeled as a friction block on an inclined plane. Under static conditions, the block rests on the inclined plane without sliding. As the inclined plane is shaken, the block moves with the plane (without slipping) until the acceleration of the plane exceeds the  $k_y$  value of the friction surface, at which point the block begins to slide. When the acceleration of the plane decreases below the  $k_y$  value, the block continues to move because of momentum but decelerates because of friction until movement stops. The amount of displacement of the block is a function of the elapsed time while the  $k_y$  value was exceeded and the magnitude by which the  $k_y$  value was exceeded by the shaking. The displacement of the block during an acceleration pulse is then calculated by integrating the area under the velocity curve. Additional displacements caused by subsequent pulses of shaking above the  $k_y$  value are summed to give the cumulative displacement of the block.

For design problems, investigators wishing to estimate landslide displacements commonly use published curves or graphs of the integrated displacements determined for historical earthquakes of different magnitudes by previous workers, such as Makdisi and Seed (1977) or Hynes-Griffin and Franklin (1984). These curves were constructed by double-integrating acceleration-time histories as a function of the  $k_y$  value. Makdisi and Seed integrated the average acceleration-time histories calculated for embankments of varying heights that had been subjected to a range of earthquake-induced base accelerations. Hynes-Griffin and Franklin integrated the horizontal components of 348 actual and 6 synthetic earthquake acceleration-time histories. The investigator typically enters a curve with the  $k_y$  value of the landslide and the expected peak ground acceleration, and arrives at an estimate of the landslide displacement. Although these curves are relatively simple to use, they are by no means consistent with each other. A comparison of several widely used curves by Jibson (1993) demonstrated that the displacements estimated from different curves can vary by a factor of as much as 100.

Another method of using cumulative displacement during design to predict landslide movement is to select an actual earthquake acceleration-time history that could affect the site. The part of the acceleration record above the  $k_y$  value is then double-integrated to arrive at a displacement estimate. For this study, we chose to use the largest-amplitude seismic record in the study area and a convenient computer program, DISPLMT (Houston and others, 1987), to carry out the computations. The effects of using various seismic records are discussed in the subsection below entitled "Sensitivity Analysis."

## RESULTS

In our analysis of the Lower Schultheis Road West and Ditullio landslides, we approached the seismic-stability problem in two different ways. First, we calculated the pseudostatic stability and predicted displacements, using the parameters measured during our site investigation. For a typical geotechnical site investigation, either the best-fit or lowest shear strength determined from laboratory measurements would be used. This approach actually represented a hindcast, because accelerograph records from the 1989 Loma Prieta earthquake (unavailable for a true prediction before the earthquake) were used rather than a record already on file before the earthquake. Second, we tested the sensitivity of the displacement results to reasonable variations in the shear-strength parameters. We analyzed the FS and  $k_y$  values by Spencer's method with the computer program PCSTABL developed at Purdue University (Carpenter, 1985).

### PSEUDOSTATIC ANALYSIS

The pseudostatic FS and  $k_y$  values for the Lower Schultheis Road and Ditullio landslides, calculated from the laboratory-determined residual shear strengths, are listed in table 2.

FS values of about 1.1 are calculated for both sites if the lower-bound residual shear strengths and a relatively high  $k_y$  value (that is, 0.20  $g$ ) are used. In current geotechnical practice, an FS value of 1.1 is generally considered acceptable for the seismic stability of engineered slopes. Because the shear strengths used represent residual, rather than peak, values, some geotechnical practitioners would consider this analysis to be overly conservative. In practice, the best-fit, rather than the lower-bound, strengths might have been selected. These best-fit strengths would have resulted in computed FS values of 1.2 to 1.4, indicating considerable stability of both slopes under dynamic loading. Thus, our results demonstrate that, using the laboratory-determined residual shear strengths, the pseudostatic

Table 2.—Pseudostatic factors of safety (FS) and yield coefficients ( $k_y$ ) in the Lower Schultheis Road West and Ditullio landslides, calculated from laboratory-determined residual shear strengths

	FS for $k_y=0.20$	$k_y$ (g) for FS=1.0
Lower Schultheis Road West landslide		
Lower-bound shear strength .....	1.1	0.23
Best-fit shear strength .....	1.4	.35
Ditullio landslide		
Lower-bound shear strength .....	1.1	0.22
Best-fit shear strength .....	1.2	.30

analysis would not have predicted the slope failures even if the lower-bound values were used. However, the FS value drops below 1.0 when a  $k_y$  value of about 0.25 g is used.

### CUMULATIVE-DISPLACEMENT ANALYSIS

To estimate the displacements, we first used the curves of Makdisi and Seed (1977) and Hynes-Griffin and Franklin (1984), and then double-integrated a record from the 1989 Loma Prieta earthquake. The curves were entered with the  $k_y$  values calculated by the pseudostatic method, using  $k_{max}=1.0$  g. Makdisi and Seed presented upper- and lower-bound curves for  $M=6.5$ , 7.5, and 8.5 earthquakes. Upper- and lower-bound curves were interpolated for a theoretical  $M=7.0$  event. The  $k_y$  values listed in table 3 are derived from an interpreted geometric-mean curve drawn between the upper- and lower-bound  $M=7.0$  curves. Hynes-Griffin and Franklin presented mean,  $\text{mean} \pm 1\sigma$ , and upper-bound curves; the results listed in table 3 are from their mean curve.

Table 3 shows that the curves of Makdisi and Seed (1977) predict displacements in reasonable agreement with those measured after the earthquake, using the lower-bound residual shear strengths to characterize the landslide rupture surface. If the best-fit residual shear strengths are used, the predicted displacements are too low but are still within the same order of magnitude as those observed. The displacements calculated using the mean curve of Hynes-Griffin and Franklin (1984) underpredict the displacements by almost an order of magnitude, using the lower-bound residual shear strengths.

The results of the double-integrated acceleration-time history for the LGPC station, using the computer program DISPLMT of Houston and others (1987), are also listed

in table 3. The  $k_y$  value can be inputted as a constant, as a function of time, or as a function of displacement. Uphill movements of the landslide block are accounted for by assuming a relation between the upslope and downslope  $k_y$  values and the static FS value. Most accelerograms are asymmetric, and the program accounts for this feature by calculating displacements twice, assuming that each side acts downslope, and averaging the results. For simplicity, a constant  $k_y$  value was used.

The cumulative-displacement method predicts landslide displacements within an order of magnitude of the measured displacements, using the curves of Makdisi and Seed (1977). The curves of Hynes-Griffin and Franklin (1984) and the integrated record from the LGPC station (fig. 1) both predict displacements within the range of those measured, but only when the lower-bound residual shear strengths are used. When the best-fit residual shear strengths are used (corresponding to  $k_y=0.30-0.35$  g), the predicted displacements are an order of magnitude less than those observed and an order of magnitude less than those calculated using  $k_y=0.22-0.23$  g. This result indicates that the displacements calculated by integrating the record from the LGPC station are highly sensitive to the  $k_y$  value and thus highly sensitive to the shear strengths chosen for the landslide rupture surface. The results of cumulative-displacement calculations for the two reactivated landslides, using five different analytical methods, are listed in table 4. The method of K.L. Lee (unpub. data, 1977) produces the most conservative results. However, the median displacements from all methods range from 10 to 100 cm for  $k_{max}=1.00$  g, which is as close as we should expect from the level of uncertainty in the  $k_y$  value and shear-strength parameters, and the sensitivity of the predicted displacements to these measurements.

### SENSITIVITY ANALYSIS

The sensitivity of the calculated displacements to variations in both shear strength and acceleration-time history is apparent from various analyses. The dependence on shear strength is of great concern because of the difficulty in obtaining well-constrained values. The shear strength of the rupture-surface materials can be calculated in two somewhat-independent ways: (1) by sampling and testing actual gouge materials in the laboratory and (2) by backanalyzing the landslide to determine the shear strengths required for failure.

We know that the present geometry of the landslide is stable under current ground-water conditions, which provides a minimum shear strength for the gouge. If we assume that the landslide would be unstable when ground water filled it to the surface, then a backanalysis of that saturated condition would provide a maximum shear strength for the gouge. An argument can be made that this

Table 3.—*Seismic yield coefficients ( $k_y$ ) and displacements in the Lower Schultheis Road West and Ditullio landslides, calculated from laboratory-determined residual shear strengths*

[All values assume a peak horizontal ground acceleration of 1.0 g. Shear-strengths:  $\phi=25^\circ$ ,  $c=0$  kg/cm<sup>2</sup> for lower-bound values and  $\phi=24^\circ$ ,  $c=0.22$  kg/cm<sup>2</sup> for best-fit values, where  $\phi$  is the angle of internal friction and  $c$  is the cohesion. Mean 1, geometric mean from Makdisi and Seed (1977); mean 2, mean from Hynes-Griffin and Franklin (1984), with displacements below 10 cm not plotted]

	$k_y$ (g) for FS=1.0	Displacement (cm)			
		Mean 1	Mean 2	Program DISPLMT Actual	
Lower Schultheis Road West landslide					
Lower-bound shear strength.....	0.23	36	10	23	61
Best-fit shear strength.....	.35	17	<10	1	61
Ditullio landslide					
Lower-bound shear strength.....	0.22	38	10	29	33-57 (avg 45)
Best-fit shear strength.....	.30	24	<10	3	33-57 (avg 45)

assumption is reasonable on the basis of the widespread presence of shallow slope failures within this terrain in the general vicinity during periods of very heavy rainfall. We have no evidence that the Lower Schultheis Road West or Ditullio landslide failed statically during recent years; however, we know that laboratory shear strengths generally are at the high end of the range. Thus, these two approaches can give us some confidence about the range of shear strengths that should be considered for these two reactivated landslides.

Representative samples of the material from rupture zones are generally available only if a geologist retrieves them by hand from within a large excavation, such as a trench or large-diameter borehole. Rupture zones are seldom captured intact in drill-core samples because they are softer and more clay rich than the surrounding rock. During coring, the gouge materials are commonly destroyed by small amounts of relative movement between the core segments above and below the shear surface, and the gouge can be washed away by circulating fluid.

When a sample is tested in the laboratory, precautions are needed to prevent disturbance of the gouge. Direct shear testing is generally favored because the thin rupture zone can be aligned with the shear surface to ensure that the gouge material itself is tested, rather than the harder rock above or below the rupture zone. As a result of the uncertainties associated with laboratory results, it is not uncommon during postfailure landslide studies to discover that laboratory-determined shear strengths overestimate the strengths computed for the landslide surface from backanalyses of landslide stability.

Backanalyses for stability also need to be evaluated carefully. A backanalysis based on a seismic failure is a circular argument, because we test our ability to predict seismic failure from independent measurements of key parameters, including shear strength and seismic ground motion. However, if we backanalyze a static (that is, ground-water driven) failure, we gain some insight into the range of possible shear strengths of the rupture-surface materials.

We backanalyzed the Lower Schultheis Road West and Ditullio landslides under static conditions to determine a reasonable range of shear strengths for examination in our sensitivity analysis. The backanalyses assume that the landslides failed under static conditions at some time in the past and that the rupture surfaces had reached their residual strengths (that is,  $c=0$ ). The range of  $\phi$  values that would satisfy the backanalysis for possible ground-water levels is plotted in figure 7. This range was the basis for selecting angles of  $17^\circ$ – $25^\circ$  in our cumulative-displacement analyses.

Cumulative displacements as a function of the angle of internal friction,  $\phi$ , and the yield acceleration,  $k_y$ , of the two reactivated landslides for a peak horizontal ground acceleration of 1.00 g are plotted in figure 8, which shows the results using the curves of K.L. Lee (unpub. data, 1977), Makdisi and Seed (1977), Hynes-Griffin and Franklin (1984), and Lin and Whitman (1986), as well as from the program DISPLMT using the Corralitos and LGPC station (fig. 1) records scaled to  $k_{max}=1.0$  g.

Figure 8 demonstrates that the displacements calculated by all five methods are sensitive to the chosen  $\phi$  value.

Table 4.—Summary of cumulative-displacement results using five analytical methods for the Lower Schultheis Road West and Ditullio landslides

[ $k_y$ , seismic yield coefficient;  $k_{max}$ , peak horizontal ground acceleration;  $M$ , earthquake magnitude; static FS, static factor of safety (3.6 for Lower Schultheis Road West landslide, 2.9 for Ditullio landslide); LSRW, Lower Schultheis Road West. Shear strengths for Lower Schultheis Road West landslide:  $\phi=25^\circ$ ,  $c=0$  kg/cm<sup>2</sup>,  $k_y=0.23$  g for lower-bound values and  $\phi=24^\circ$ ,  $c=0.22$  kg/cm<sup>2</sup>,  $k_y=0.35$  g for best-fit values, where  $\phi$  is the angle of internal friction and  $c$  is the cohesion. Shear strengths for Ditullio landslide:  $\phi=25^\circ$ ,  $c=0$  kg/cm<sup>2</sup>,  $k_y=0.23$  g for lower-bound values and  $\phi=24^\circ$ ,  $c=0.22$  kg/cm<sup>2</sup>,  $k_y=0.30$  g for best-fit values]

Analytical method	Input parameter	Value	Predicted displacements (cm)			
			Ditullio landslide		LSRW landslide	
			Lower bound	Best fit	Lower bound	Best fit
Program DISPLMT (Houston and others, 1987): Double integration of accelerations above $k_y$ (average of two runs with accelerations inverted).	Corralitos station record ( $k_{max}=0.63$ g)	Average of two runs	5	3	4	3
	Corralitos station record ( $k_{max}=1.00$ g)	-----	35	4	49	6
	Station LGPC record ( $k_{max}=1.00$ g)	-----	29	3	23	1
Makdisi and Seed (1977), with Keefer and others (1991) for $M = 7.0$ .	$k_y$ , $k_{max}=1.00$ g, $M = 7.0$	Upper bound -----	82	50	76	40
		Lower bound -----	15	9	14	6
		Geometric mean ----	37	22	35	17
K.L. Lee (unpub. data, 1977) -----	$k_y$ , $k_{max}=1.00$ g, $M = 7.1$	Upper bound -----	179	97	160	68
		Lower bound -----	45	24	40	17
		Geometric mean ----	77	42	69	29
Lin and Whitman (1986): Provides expected values, implying not especially conservative values.	$k_y$ , $k_{max}=1.00$ g, subsurface conditions	Mixed sites -----	84	42	77	29
		Deep-cohesionless-soil and stiff-soil sites.	67	34	62	22
		Rock sites -----	42	21	38	14
Hynes-Griffin and Franklin (1984)	$k_y$ , $k_{max}=1.00$ g, confidence level	Upper bound -----	73	47	68	37
		Mean ? -----	21	12	19	<10
		Mean -----	11	<10	10	<10
Field measurements -----	-----	-----	33-57 (avg 45)		61	

The curves of K.L. Lee (unpub. data, 1977) and Lin and Whitman (1986) are the most conservative, yielding predicted displacements near or slightly greater than the ob-

served displacements when lower-bound laboratory shear strengths ( $c=0$ ,  $\phi=25^\circ$ ) are used. The other methods predict displacements lower than the observed displacements

under the same conditions. However, these results also indicate that the laboratory shear strengths generally predict displacements lower than those actually measured for a seismic event as large as the 1989 Loma Prieta earthquake. The two program DISPLMT analyses for each landslide provide the clearest examples: The best comparison of predicted-to-observed displacements are for  $\phi=18^\circ-22^\circ$  for the Lower Schultheis Road West landslide and  $\phi=21^\circ-24^\circ$  for the Ditullio landslide. Use of the lower-bound laboratory shear strengths leads to predicted displacements that are about two-thirds less than those measured on the Lower Schultheis Road West landslide and about one-half less than those measured on the Ditullio landslide. The program DISPLMT results for the Corralitos and LGPC

station (fig. 1) records also differ markedly, demonstrating that displacements calculated by using integration methods depend heavily on the selected acceleration-time history.

Although we believe that ground motion at the landslide sites was much greater than that recorded at the Corralitos strong-motion station (fig. 1), we also calculated displacements by using the unscaled acceleration-time history at this station to determine the sensitivity of the results to this seismic record. Cumulative displacements calculated using five analytical methods for  $k_{\max}=0.63 g$  are plotted as a function of  $\phi$  value in figure 9. A comparison of figures 8 and 9 demonstrates the importance of the acceleration-time history and peak ground acceleration on the calculations. Using the scaled Corralitos station record ( $k_{\max}=1.00 g$ ), the measured displacements correspond relatively well to those calculated from the program DISPLMT; however, the unscaled Corralitos station record ( $k_{\max}=0.63 g$ ) yields significantly smaller displacements for the same shear strengths.

The displacements that can be calculated for an  $M=7.0$  earthquake, using the three curves of Makdisi and Seed (1977) and Hynes-Griffin and Franklin (1984) for the Lower Schultheis Road West landslide, are plotted in figure 10. Because of the bilateral rupture, the 1989 Loma Prieta earthquake was of considerably shorter duration than most other earthquakes of similar magnitude. Therefore, we might expect the measured displacements to fall in the lower part of the range of calculated displacements. Figure 10 shows, however, that they do so only for the smallest  $\phi$  values. If we assume that the appropriate  $\phi$  value should be about  $21^\circ$ , then the measured displacements fall in the middle of the range of displacements in the data sets of both Makdisi and Seed (1977) and Hynes-Griffin and Franklin (1984).

In summary, the mean to upper-bound curves for the four chart methods, as well as the DISPLMT integration method, appear to predict displacements that are within an order of magnitude of the displacements measured on the two reactivated landslides when a  $k_{\max}$  value of  $1.00 g$  is used in conjunction with low shear strengths. It is remarkable, however, how broad the range of calculated displacements can be for an earthquake of a specific size. Adaptation of specific strong-motion records to the actual field conditions at a particular site, to account for the effects of attenuation, distance, topography, or directivity, is subject to uncertainties that can change the predicted displacements by a factor of at least 3. For example, the displacements calculated using the unscaled Corralitos and LGPC station records scaled to the same peak acceleration ( $k_{\max}=1.00 g$ ) vary by a factor of as much as 2 (fig. 8). At this time, it is unclear how the specific record should be chosen or scaled (if at all) for local conditions.

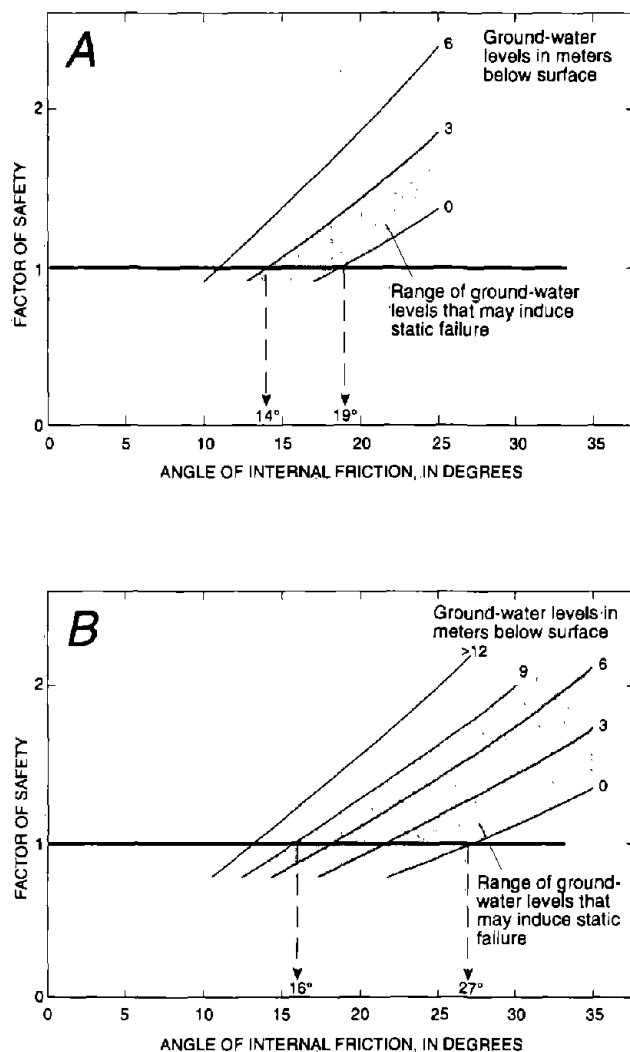


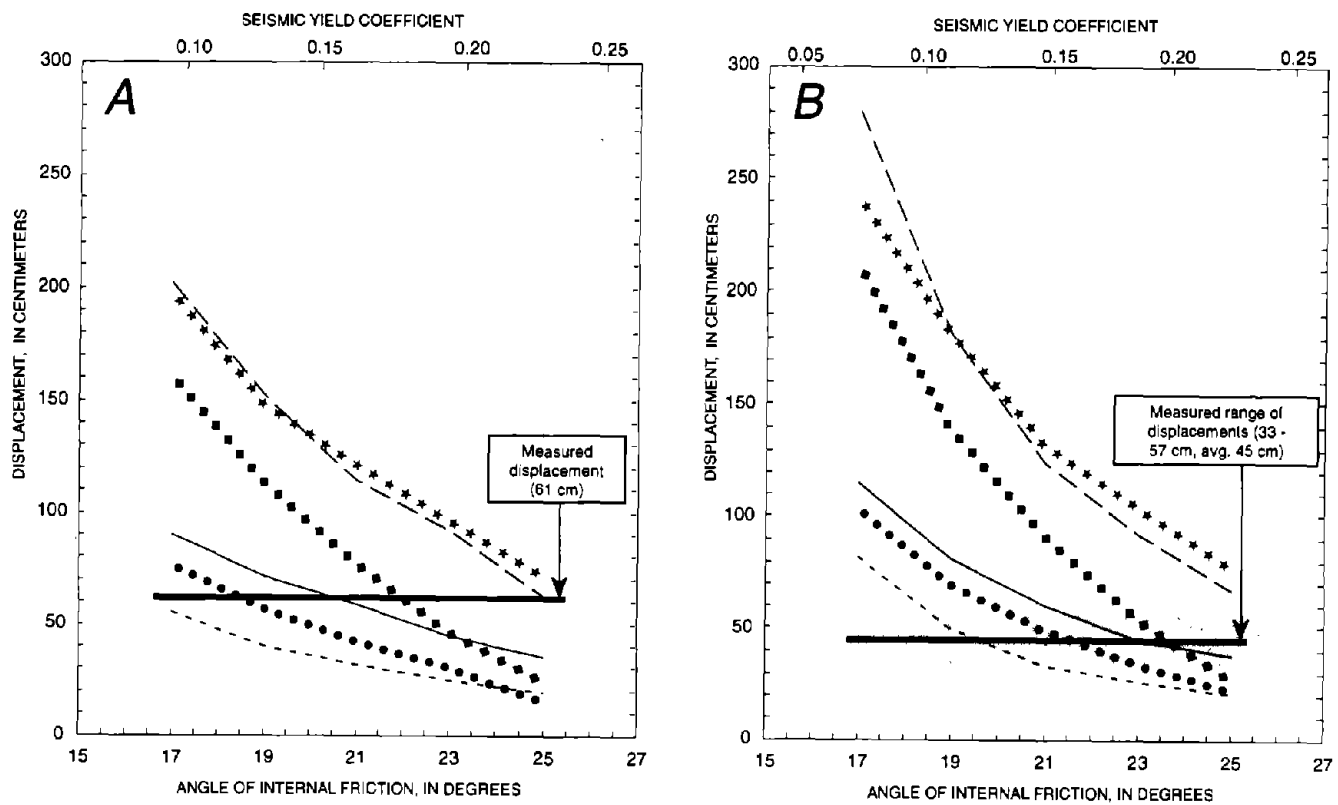
Figure 7.—Factor of safety versus shear strength (expressed as angle of internal friction) at various ground-water levels in Lower Schultheis Road West (A) and Ditullio (B) landslides (see fig. 2 for locations).



## CONCLUSIONS

1. **Preexisting landslides commonly were only partially reactivated.** The pattern of ground cracking within preexisting ancient landslides indicates that only part of many preexisting landslides were mobilized by the ground motion from the 1989 Loma Prieta earthquake. In many places, ground cracks coincided with preexisting-landslide boundaries, even where these boundaries were relatively subdued. The absence of ground cracks displaying shear movement on the flanks of many of these landslides was interpreted to reflect mobilization of only the upslope segments of the basal rupture surfaces of the landslides during earthquake shaking.

2. **Seismic-displacement calculations are highly sensitive to selected yield coefficients and shear strengths.** The results of the cumulative-displacement analyses indicate that calculated displacements are highly sensitive to the seismic yield coefficient, which is a function of the shear strength of the basal rupture surface. The determination of a representative strength across the basal rupture surface, therefore, is crucial to the success of the analysis. Sampling and testing of thin shear surfaces separating hard-rock strata is difficult, and standard "small diameter" exploration methods have a very low probability of allowing identification, adequate sampling, and preservation of thin rupture surfaces. Direct observation and careful hand extraction of oriented samples from large excavations



### EXPLANATION

- |         |   |     |  |
|---------|---|-----|--|
| ••••    | Program DISPLMT (Houston and others, 1987), scaled Corralitos Station record  | —   | Mean for theoretical $M=7.0$ earthquake (Makdisi and Seed, 1977) |
| ♦♦♦♦    | Program DISPLMT (Houston and others, 1987), unscaled Los Gatos Presentation Center Station record, $k_{max} = 1.00 g$ | *** | Geometric mean (K.L. Lee, unpublished data, 1977)                |
| - - - - | Mean $\pm 1\sigma$ (Hynes-Griffin and Franklin, 1984)   | —   | Stiff soils or deep cohesionless soils (Lin and Whitman, 1986)   |

Figure 8.—Predicted displacement versus shear strength (expressed as angle of internal friction) calculated by five cumulative-displacement methods, using records from stations at Corralitos and Los Gatos Presentation Center (see fig. 1 for locations), assuming a peak horizontal ground acceleration of 1.0 g. A, Lower Schultheis Road West landslide. B, Ditullio landslide.

(trenches or large-diameter boreholes) are recommended to observe the landslide geometry and collect the appropriate materials for testing.

3. **Laboratory strengths may be too high to accurately predict stability and displacements.** The pseudostatic method of analysis incorrectly predicted the stability of the Lower Schultheis Road West and Ditullio landslides, using lower-bound laboratory shear strengths and a seismic yield coefficient of 0.20, but would have predicted the failures if a higher seismic yield coefficient had been used. The magnitudes of the deformations on the Lower Schultheis Road West and Ditullio landslides generally were underestimated, using various cumulative-displacement methods and laboratory shear strengths.
4. **Backanalyzed shear strengths can be used to improve the accuracy of calculated cumulative displacements.** Backanalyses give a range of reasonable shear strengths for landslide rupture materials in the form of a range of angles of internal friction of 17°–25°. Backanalyzed shear strengths can be used with laboratory results to better estimate the average shear strength of the basal rupture surface. In this study, use of an angle of internal friction of about 21° produces displacements that generally are consistent with measured displacements, and appears to correctly predict the onset of instability when using the pseudostatic analysis.

5. **Ground-water levels significantly influence slope stability.** Despite a prolonged, 4-year-long drought, shallow ground water was present in many of the landslides investigated. Ground-water zones appear to be perched on impermeable rupture surfaces. Laboratory results indicate high angles of internal friction and relatively low cohesion. The presence of higher ground-water levels in the landslides before the earthquake would have increased the landslide displacements. Measurements of ground-water levels are important to make in the field and to include in calculations.
6. **Displacement calculations are also sensitive to the selected acceleration-time history.** The range of displacements calculated from published compilations of earthquake records is clear testimony to the degree of sensitivity to this parameter. Because the effect of the long-period part of the seismic record is significant, the peak ground acceleration, though important, may not be as critical as other factors, such as duration of shaking, attenuation with distance from the source, and seismic focusing effects (including topographic amplification and directivity). Seismic-stability analyses should be based on more than one seismic record whenever practical.

This study emphasizes that available methods of cumulative-displacement analysis are useful, but investigators should select variables with care so as not to underesti-

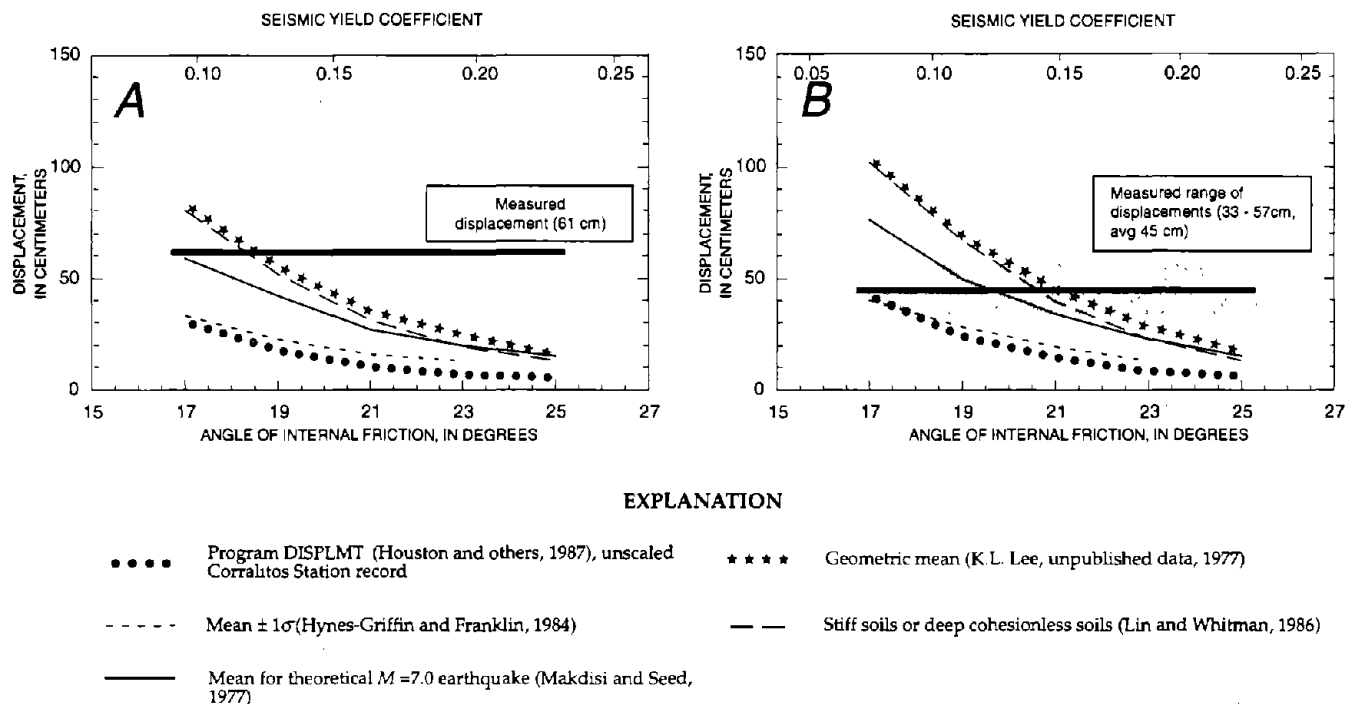
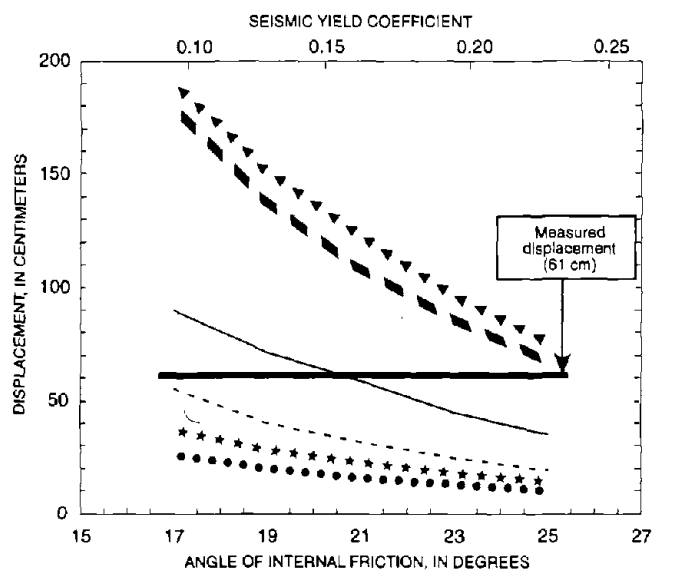


Figure 9.—Predicted displacement versus shear strength (expressed as angle of internal friction) calculated by five cumulative-displacement methods, using peak horizontal ground acceleration of 0.63 g from station at Corralitos (see fig. 1 for location). A, Lower Schultheis Road West landslide. B, Ditullio landslide.

mate the stability of preexisting landslides. With a thorough characterization of landslide geometry, local geologic conditions, and engineering properties, and a selection of conservative strength parameters for the basal rupture surfaces, existing analytical techniques are sufficient for order-of-magnitude predictions when the lowest laboratory shear strengths are used.

## ACKNOWLEDGMENTS

This research was partly supported by U.S. Geological Survey grant 14-08-0001-G1860, Cotton, Shires and Associates, Inc., and Leighton and Associates, Inc. We thank Randy Jibson, Dave Keefer, and Ray Wilson for their thorough and provocative reviews. We also thank Phil Buchiarelli, Chester Burrous, and Rick Lozinsky for assisting with this study.



### EXPLANATION

- ▲▲▲ Upper bound (Hynes-Griffin and Franklin, 1984)
- Mean  $\pm 1\sigma$  (Hynes-Griffin and Franklin, 1984) Deviation
- Mean (Hynes-Griffin and Franklin, 1984)
- ▲▲▲ Upper bound for theoretical  $M=7.0$  earthquake (Makdisi and Seed, 1977)
- Mean for theoretical  $M=7.0$  earthquake (Makdisi and Seed, 1977)
- \*\*\* Lower bound for theoretical  $M=7.0$  earthquake (Makdisi and Seed, 1977)

Figure 10.—Predicted displacement versus shear strength (expressed as angle of internal friction) calculated by two cumulative-displacement methods for Lower Schultheis Road West landslide (see fig. 2 for location).

## REFERENCES CITED

- Beroza, G.C., 1991, Near-source modeling of the Loma Prieta earthquake; evidence for heterogeneous slip and implications for earthquake hazard: *Seismological Society of America Bulletin*, v. 81, no. 5, p. 1603-1621.
- California Division of Mines and Geology, 1990, Second interim set of processed strong-motion records from the Santa Cruz Mountains (Loma Prieta), California earthquake of 17 October 1989: California Strong Motion Instrumentation Program Report OSMS 90-01.
- Campbell, K.W., 1991, An empirical analysis of peak horizontal acceleration for the Loma Prieta earthquake of 18 October 1989: *Seismological Society of America Bulletin*, v. 81, no. 5, p. 1838-1858.
- Carpenter, J.R., 1985, Final report, STABL5—the Spencer method of slices; Joint Highway Research Project: Lafayette, Ind., Purdue University report on project C-36-36L, file 6-14-12, 26 p.
- Chowdhury, R.N., 1978, *Slope analysis*: Amsterdam, Elsevier, 423 p.
- Clark, B.R., Leighton, F.B., Cann, L.R., and Gaffey, J.T., 1979, Surficial landslides triggered by seismic shaking, San Fernando earthquake of 1971: final technical report to U.S. Geological Survey under contract 14-08-001-16810, 42 p.
- Clark, J.C., 1981, Stratigraphy, paleontology, and geology of the central Santa Cruz Mountains, California Coast Ranges: U.S. Geological Survey Professional Paper 1168, 51 p.
- Clark, J.C., Brabb, E.E., and McLaughlin, R.J., 1989, Geologic map and structure sections of the Laurel 7-1/2' Quadrangle, Santa Clara and Santa Cruz counties, California: U.S. Geological Survey Open-File Map 89-676, 31 p., scale 1:24,000, 2 sheets.
- Cole, W.F., Marcum, D.R., Shires, P.O., and Clark, B.R., 1991, Investigation of landsliding triggered by the Loma Prieta earthquake and evaluation of analysis methods: final technical report to U.S. Geological Survey under contract 14-08-0001-G1860, 120 p.
- Cooper-Clark and Associates, 1975, Preliminary map of landslide deposits in Santa Cruz County, California: Mountain View, Calif., scale 1:24,000.
- Cotton, W.R., Hardin, B., and Smelser, M.G., 1991, Coseismic bedding plane faults and ground fissures associated with the Loma Prieta Earthquake: final technical report to U.S. Geological Survey under contract 14-08-0001-G1829, 23 p.
- Houston, S.L., Houston, W.N., and Padilla, J.M., 1987, Microcomputer-aided evaluation of earthquake-induced permanent slope displacement: *Microcomputers in Civil Engineering*, no. 2, p. 207-222.
- Huang, Y.H., 1983, *Stability analysis of earth slopes*: New York, Van Nostrand Reinhold, 305 p.
- Hynes-Griffin, M.E., and Franklin, A.G., 1984, Rationalizing the seismic method: Vicksburg, Miss., U.S. Army Corp of Engineers, Waterways Experiment Station Miscellaneous Paper GL-84-13, 37 p.
- Jibson, R.W., 1993, Predicting earthquake-induced landslide displacements using Newmark's sliding block analysis: Washington, D.C., National Research Council Transportation Research Record 1411, p. 9-17.
- Jibson, R.W., and Keefer, D.K., 1993, Analysis of the seismic origin of landslides; examples from the New Madrid seismic zone: *Geological Society of America Bulletin*, v. 105, no. 4, p. 521-536.
- Keefer, D.K., ed., 1991, Geologic hazards in the Summit Ridge area of the Santa Cruz Mountains, Santa Cruz County, California, evaluated in response to the October 17, 1989, Loma Prieta earthquake; report of the Technical Advisory Group: U.S. Geological Survey Open-File Report 91-618, 427 p.
- Kingsley Associates, 1991, Geologic hazard report, Frank Deak property: Monterey, California, 28 p.
- Lambe, T.W., and Whitman, R.V., 1969, *Soil mechanics*: New York: John Wiley and Sons, 553 p.
- Lin, J.S., and Whitman, R.V., 1986, Earthquake induced displacements

- of sliding blocks: *Journal of Geotechnical Engineering*, v. 112, no. 1, p. 44–59.
- Makdisi, F.I., and Seed, H.B., 1977, A simplified procedure for estimating earthquake-induced deformations in dams and embankments: Berkeley, University of California, Earthquake Engineering Research Center Report UCB/EERC-77/19, 33 p.
- McLaughlin, R.J., Clark, J.C., Brabb, E.E., and Helley, E.J., 1991, Geologic map and structure sections of the Los Gatos 7-1/2' Quadrangle, Santa Clara and Santa Cruz counties, California: U.S. Geological Survey Open-File Map 91-593, 48 p., scale 1:24,000, 3 sheets.
- Newmark, N.M., 1965, Effects of earthquakes on dams and embankments: *Geotechnique*, v. 15, no. 2, p. 139–160.
- Rogers E. Johnson and Associates, 1991, Geologic investigation, Frank Deak property: Santa Cruz, Calif., report G91036–26, 65 p.
- Rojstaczer, S.A., and Wolf, S.C., 1992, Permeability changes associated with large earthquakes—an example from Loma Prieta, California: *Geology*, v. 20, no. 3, p. 211–214.
- Spittler, T.E., and Harp, E.L., compilers, 1990, Preliminary map of landslide and coseismic fissures triggered by the Loma Prieta Earthquake of October 17, 1989: California Division of Mines and Geology Open-File Report 90-6, scale 1:4,800.
- Steidl, J.H., Archuleta, R.J., and Hartzell, S.H., 1991, Rupture history of the 1989 Loma Prieta, California, earthquake: *Seismological Society of America Bulletin*, v. 81, no. 5, p. 1573–1602.
- Stout, M.L., 1969, Radiocarbon dating of landslides in southern California and engineering geology implications, in Schumm, S.A., and Bradley, W.C., eds., *United State contributions to Quaternary research*: Geological Society of America Special Paper 123, p. 167–179.
- Terwilliger, V.J., and Waldron, L.J., 1991, Effects of root reinforcement on soil-slip patterns in the Transverse Ranges of southern California: *Geological Society of America Bulletin*, v. 103, no. 6, p. 775–785.
- Wald, D.J., Helmsberger, D.V., and Heaton, T.H., 1991, Rupture model of the 1989 Loma Prieta earthquake from the inversion of strong-motion and broadband teleseismic data: *Seismological Society of America Bulletin*, v. 81, no. 5, p. 1540–1572.
- Wieczorek, G.F., Wilson, R.C., and Harp, E.L., 1985, Map showing slope stability during earthquakes in San Mateo County, California: U.S. Geological Survey Miscellaneous Investigation Series Map I-1257-E, scale 1:62,500.
- Wilson, R.C., and Keefer, D.K., 1983, Dynamic analysis of a slope failure from the 6 August 1979 Coyote Lake, California, earthquake: *Seismological Society of America Bulletin*, v. 73, no. 3, p. 863–877.
- , 1985, Predicting areal limits of earthquake-induced landsliding, in Ziony, J.I., ed., *Evaluating earthquake hazards in the Los Angeles region—an earth-science perspective*: U.S. Geological Survey Professional Paper 1360, p. 317–345.

## APPENDIX: DESCRIPTION OF LANDSLIDE SITES

The two reactivated landslides discussed in this paper were chosen from an initial group of more than 50 relatively large landslides in the study area. Detailed surface and subsurface data were collected from five of these landslides. This appendix provides descriptions of the two landslides discussed above. More complete descriptions of these sites, as well as two additional sites, including maps,

cross sections, borehole logs, and laboratory procedures, were presented by Cole and others (1991).

## LOWER SCHULTHEIS ROAD WEST LANDSLIDE

### LOCATION AND SCOPE OF INVESTIGATION

The site of the Lower Schultheis Road West landslide, referred to as “Upper Laurel” by Cole and others (1991), is near Laurel, Calif., along the north-facing flank of an east-west-trending spur ridge (fig. 2) that is underlain at depth by siltstone and sandstone of the San Lorenzo Formation. A surveyed topographic map of the entire 7.7-ha parcel was provided by the property owner. Surface mapping and profiling of the landslide was performed at a scale of 1:240, using a semi-total-station (STS) survey instrument for horizontal and vertical control. Two large-diameter boreholes, LD-1 and LD-2 (fig. 3), were excavated and logged to 11.3- and 8.5-m depth, respectively.

### SURFACE CONDITIONS

The geomorphology of the ridge and adjacent valley indicate that a large, ancient landslide underlies most of the north-facing hillside. A system of arcuate ground fissures near the ridge crest indicates that the earthquake reactivated a part of this preexisting landslide. The system of cracks defines a graben that follows the ridge crest for approximately 60 m before curving downslope to form a broad arc (fig. 4). The head of the reactivated landslide mass was downthrown about 25 cm and offset laterally about 61 cm. No ground deformation was observed along the probable lateral margins. The probable toe of the landslide is indicated by a zone of compression coinciding with a slight topographic bulge. The reactivated landslide appears to be about 61 m wide by 76 m long. The total area of the reactivated landslide is approximately 0.4 ha.

### SUBSURFACE CONDITIONS

The two large-diameter boreholes, LD-1 and LD-2 (fig. 3), were located 4.6 and 12.2 m, respectively, downslope from the headscarp crack. Both boreholes penetrated a near-horizontal, well-developed shear surface at 4.9-m depth; this shear surface separates overlying, oxidized regolith from underlying, unoxidized fractured rock. A deeper, steeply dipping shear surface was penetrated in borehole LD-1 at 7.3-m depth; this deeper shear surface is a sheared siltstone interbed within massive sandstone that separates the overlying fractured rock from dense, relatively intact rock. The shallower shear surface appeared

to be thicker, more moist, and generally better developed than the deeper shear surface within more indurated rock.

Subsurface data indicate that the earthquake did not reactivate the uppermost part of the preexisting landslide mass. Trenches excavated by Rogers E. Johnson and Associates (1991) demonstrate that the deeper (7.3 m deep) rupture surface exposed in borehole LD-1 (fig. 3) extends along a 30° plane to the ridge crest and passes undisturbed beneath the 1989 graben that forms the upslope boundary of the 1989 reactivated landslide (fig. 4). The reactivated headscarp (1989 graben) is 5.9 m downslope from the intersection of the buried slide surface with the present ground surface. The slide surface at this point is 3.2 m deep. Thus, the earthquake apparently failed to reactivate an upper wedge of preexisting landslide material. (The deeper shear surface is a bedding-plane fault that probably formed during folding of an underlying bedrock anticline; the shallower shear surface exposed in boreholes LD-1 and LD-2 was not exposed in the trenches.) Rogers E. Johnson and Associates found a similar relation between a buried rupture surface and an arcuate, 1989 earthquake-triggered landslide headscarp in the same vicinity. The preexisting rupture surface forming the base of the dormant wedge of preexisting-landslide material may have acquired more cohesion over time, owing to root reinforcement and clay development during pedogenesis. The associated increase in shear strength may have helped to maintain stability in the shallow (upper 3 m) part of the landslide. The maximum thickness of the stable wedge coincides with the approximate base of significant roots, suggesting that root reinforcement could have increased resistance to sliding in this wedge. Terwilliger and Waldron (1991) discussed the role of root reinforcement on the stability of shallow landslides.

Ground water was penetrated in the two large-diameter boreholes, as well as in boreholes drilled by Kingsley Associates (1991). Isolated zones of ground water were perched on impermeable shear surfaces. Significant amounts of ground water also were penetrated below the deepest shear surface (8–10 m below the ground surface).

## DITULLIO LANDSLIDE

### LOCATION AND SCOPE OF INVESTIGATION

The site of the Ditullio landslide is on Redwood Lodge Road, about 1.2 km southeast of the Lower Schultheis

Road West landslide. The Ditullio landslide is near the top of a southwest-facing slope within and near the southern margin of a previously mapped, very large landslide complex (fig. 2). The Ditullio landslide is 92 to 122 m long by 76 m wide, covering an area of about 0.6 to 0.8 ha. Surface mapping and profiling of the landslide was performed at a scale of 1:240, using an STS survey instrument for horizontal and vertical control.

### SURFACE CONDITIONS

The headscarp is characterized by echelon and parallel fissures that form a 76-m-long, arcuate zone of ground cracks. Individual cracks within this zone indicate 0.3 to 0.6 m of extension and 0.3 m of vertical downdropping. The zone coincides with the apparent headscarp of an ancient landslide. The locations of the toes of both the ancient and 1989 landslides are unknown; however, this ancient landslide probably is part of a landslide complex that extends about 350 m downslope to the creek.

Several linear, echelon cracks that extend 52 m downslope from the scarp along the probable north boundary of the landslide may represent shearing along its right flank; however, these cracks could also be due to settlement of a septic leachfield. No evidence of offset or deformation was observed along the left flank. The earthquake-triggered landslide does not appear to cross Redwood Lodge Road, located 61 to 92 m downslope from the headscarp (fig. 3).

### SUBSURFACE CONDITIONS

A large-diameter borehole, DT-1 (fig. 4), was located about 40 m downslope from the headscarp cracks. Borehole DT-1, which was drilled and downhole logged to 22.5-m depth, exposed a well-developed, slickensided shear surface at about 18-m depth. The gradational oxidized-unoxidized contact is at 20.7-m depth; however, oxidized sandstone bedrock immediately below the landslide plane is very dense. Figure 4, which includes a detailed log of the landslide rupture surface, illustrates the relation between the 1989 reactivation, the underlying ancient landslide material, and deeper bedrock structure.

No ground water was penetrated in borehole DT-1, even after remaining open for 12 days.

